Title

BIS-(PENTAMETHYLCYCLOPENTADIENYL) YTTERBIUM AS AN ELECTRON TRANSFER REAGENT TOWARD ORGANIC AND ORGANO-TRANSITION METAL COMPOUNDS

Author

Boncella, J.M.

Publication Date

1984-09-01

Lawrence Berkeley Laboratory
UNIVERSITY OF CALIFORNIA

Materials & Molecular Research Division

BIS-(PENTAMETHYLCYCLOPENTADIENYL) YTTERBIUM AS AN ELECTRON TRANSFER REAGENT TOWARD ORGANIC AND ORGANO-TRANSITION METAL COMPOUNDS

J.M. Boncella
(Ph.D. Thesis)

September 1984

Prepared for the U.S. Department of Energy under Contract DE-AC03-76SF00098

DISCLAIMER

LBL-18387

BIS-(PENTAMETHYLCYCLOPENTADIENYL) YTTERBIUM AS AN ELECTRON TRANSFER REAGENT TOWARD ORGANIC AND ORGANO-TRANSITION METAL COMPOUNDS

James Matthew Boncella

Ph.D. Thesis

Lawrence Berkeley Laboratory
University of California
Berkeley, California 94720

September 1984

This work was supported by the Director, Office of Energy Research, Office of Basic Energy Sciences, Chemical Sciences Division of the U.S. Department of Energy under Contract No. DE-AC03-76SF00098.

LBL-18387

James Matthew Boncella

Bis-(Pentamethylcyclopentadienyl) Ytterbium as an Electron Transfer Reagent Toward Organic and Organo-Transition Metal Compounds

Abstract

The complex $(C_5Me_5)_2Yb^{\cdot}OEt_2$ reduces dimeric, metal-metal bonded transition metal carbonyl complexes to form complexes which contain $(C_5Me_5)_2Yb(III)$ groups and transition metal carbonyl anions as contact ion-pairs. When the products of these reactions are isolated from noncoordinating solvents, they have dimeric structures in which two transition metal fragments are linked to two $(C_5Me_5)_2Yb(III)$ groups by way of four Yb-OC-M_t bridges. Variable temperature ^1H NMR and crossover reaction studies indicate that the Yb-O bonds of the Yb-OC-M_t bridges are labile in hydrocarbon solution.

The mononuclear complexes $(C_5H_4R)M(CO)_2$ (M=Co, R=Me, $SiMe_3$, H; M=Rh; R=H) react with $(C_5Me_5)_2Yb^{\cdot}OEt_2$ to give the novel cluster compound $[(C_5Me_5)_2Yb(III)]_2[(\mu_3\text{-}OC)_4M_3(C_5H_4R)_2]$. Each μ_3-OC group in this complex is bound to $(C_5Me_5)_2Yb(III)$ via O and two M_t atoms via C. The trinuclear transition metal dianion contains the first example of a six coordinate planar transition metal atom. More electron rich complexes such as $(C_5H_5)Co(CO)PMe_3$ behave as Lewis bases toward $(C_5Me_5)_2Yb^{\cdot}OEt_2$ and form coordination complexes such as $[(C_5Me_5)_2Yb(II)][(\mu_2\text{-}OC)CoPMe_3(C_5H_5)]_2$.

Reaction of $(C_5Me_5)_2Yb^{\cdot}OEt_2$ with 2,2'-bipyridine or 2,2'-bipyrimidine gives the complexes $(C_5Me_5)_2Yb(bipy)$ and $[(C_5Me_5)_2Yb]_2bipm$. These materials are best formulated as complexes

which contain $(C_5Me_5)_2Yb(III)$ and the heterocyclic radical anion. Variable temperature magnetic susceptibility studies show that the Yb(III) ions and the radical anions are antiferromagnetically coupled, and that the bipm complex contains a Yb(III) ion and a Yb(II) ion. Phenylacetylene reacts with $(C_5Me_5)_2M^{\cdot}OEt_2$ (M=Eu, Yb) to form the complexes $(C_5Me_5)_4Yb_3$ $(\mu_2\text{-}C{\equiv}CPh)_4$ and $(C_5Me_5)_2Eu_2$ $(\mu_2\text{-}C{\equiv}CPh)_2(THF)_4$. The Yb complex is a mixed valence (Yb(III)-Yb(II)-Yb(III) complex. The Eu complex remains divalent, a reflection of the weaker reducing power of Eu(II) relative to Yb(II).

Some reaction chemistry of $[(Me_3Si)_2N]_2Yb(OEt_2)_2$ was also explored. The ether may be removed from $[(Me_3Si)_2N]_2Yb(OEt_2)_2$ by evaporating a toluene soluion at 80°C. The base-free complex, $\{[(Me_3Si)_2N]_2Yb\}_2$, reacts with two equivalents of HC_5Me_5 to give the complex $(C_5Me_5)_2Yb[HN(SiMe_3)_2]$. Toluene displaces $HN(SiMe_3)_2$ from $(C_5Me_5)_2Yb[HN(SiMe_3)_2]$ to form the base-free metallocene $(C_5Me_5)_2Yb$. The complex $\{[(Me_3Si)_2N]_2Yb\}_2$ also reacts with Lewis acids such as $AlMe_3$ to give $[(Me_3Si)_2N]_2Yb(AlMe_3)_2$ in which the Al atoms are bound to the N atoms, and methyl groups bridge between the two metals.

RA Andersen

Acknowledgements

There are many people who have helped make my stay at Berkeley a rewarding and enjoyable experience. The work described herein was carried out under the direction of Dick Andersen whose guidance and scientific insight provided an exciting atomsphere for research, and whose friendship provided many adventuresome hours at the Cat, the Rose and Brennan's.

I wish to thank Fred Hollander for performing the X-ray crystal structures of the Mn, Fe, Co, and Ybbipy compounds as well as for all the help that he gave me in solving the other structures described here.

The members of the Andersen research group have been good friends and fun to work with. In particular I wish to thank the following people for their support and friendship: Don Tilley, Peter Edwards, John Arenivar, Roy Planalp, John Brennan, Steve Stults, Dave Berg, Carol Burns, Nicki Rutherford, and Joanne Stewart. I also wish to thank E. J. Wucherer, Al Del Paggio, and Guy Rosenthal for making life a little bit more fun.

Finally, I wish to thank my wife Linda whose love, support, and patience has made the last four years most enjoyable. I also wish to thank Linda for typing this manuscript.

This work was supported by the Director, Office of Energy Research, Office of Basic Energy Sciences, Chemical Sciences Division of the U. S. Department of Energy under Contract No. DE-AC03-76SF00098.

Table of Contents

Introduction

The first organometallic complexes of the lanthanide elements that were synthesized were the trivalent complexes $(C_5H_5)_3Ln$.[1a] Since this original preparation, most research in this area has focused on compounds in the trivalent oxidation state. Very little chemistry of divalent lanthanide complexes has been published despite the fact that the divalent oxidation states of europium, ytterbium and samarium are all stable enough to form isolable compounds.

For many years, the stability of the divalent oxidation states of lanthanide ions has been attributed to the presence or approach to either a half-filled or filled 4f valence shell in the 2^+ oxidation state.[2] Table (I) contains a list of lanthanide elements whose divalent

Table I.) Isolable Molecular Dihalides of the Lanthanide Elements.[3]

Element	Atomic Config. of 2^+ Oxidation State	MX_2 X =	$E°(V)$ $M^{3+}+e^- \rightarrow M^{2+}$	3rd Ionization Pot. (EV)
Nd	f^4	Cl,Br,I	-	22.09
Sm	f^6	F,Cl,Br,I	-1.5	23.40
Eu	f^7	F,Cl,Br,I	-0.35	24.91
Dy	f^{10}	Cl,Br,I	-	22.93
Tm	f^{13}	Cl,Br,I	-2.3	23.68
Yb	f^{14}	F,Cl,Br,I	-1.1	25.02

halides have been isolated as discrete molecular compounds. The class

of conducting diiodides and monohalides have been omitted since they are better described as $M^{3+}(e^-I_2^-)$ or $M^{3+}(e^-{}_2X^-)$. As can be seen from Table (I) the old explanation very nicely explains the stability of Eu^{2+}, Yb^{2+}, Sm^{2+}, and Tm^{2+} as well as their relative stabilities (as judged by their oxidation potential) i.e., $Eu^{2+}>Sm^{2+}$ and $Yb^{2+}>Tm^{2+}$. The existence of Nd^{2+} and Dy^{2+} compounds does not follow from this explanation.

A new explanation of the stabilities of divalent lanthanide atoms has been proposed by Johnson[3-5] which accounts for the stabilities of all the divalent lanthanide ions. The measured crystal field splittings for lanthanide complexes are small (ca. hundreds of cm^{-1}) indicating that the 4f electrons of these ions do not interact strongly with the ligands surrounding them. Thus, unlike transition metal ions the stability of the divalent oxidation state should correlate rather well with the third ionization potential (I_3) of the metals, and it does.[3] In the lanthanide series, I_3 increases as expected from La to Eu, then drops sharply at Gd and increases again to Yb. The increase in I_3 is due to the increasing nuclear charge, and the drop at Gd is due to the loss of exchange energy at the $f^7(Eu^{2+})$ vs. $f^8(Gd^{2+})$ electronic configurations.[5] There is also a drop in I_3 from Dy^{2+} to Er^{2+} and a leveling off of I_3 from Pr^{2+} to Pm^{2+}. The drop in I_3 at the $1/4$ and $3/4$ filled shell are surprising, but are explained by considering the m_l values of the electrons being ionized. Electron-electron repulsion is larger for electrons which have opposite signs of m_l.[3,6] Thus ionizing an electron from an ion for which the remaining electrons have the same sign will give a larger ionization energy than if the remaining electrons are of opposite sign. For example Pr^{2+} (f^3) has m_l = 3, 2, and 1 while Pm^{2+} (f^5) has m_l = 3, 2, 0, -1. The ionization of Pr^{2+} will

be higher in energy than that of Pm^{2+} because Pm^{2+} loses the electron with $M_l = -1$, and therefore Pr^{2+} is more stable. A similar argument follows for the ions Dy^{2+}, Ho^{2+} and Er^{2+}.[3] It must be stressed once again that the above argument holds because the ligand field associated with lanthanide complexes is very small.

The explanation proposed by Johnson not only explains the observed stabilities of the various Ln^{2+} ions, but also suggests that the chemistry of the lanthanide ions may differ from one element to the next. Thus, if reactions which involve a change in the oxidation state of the metal ion are considered, the chemistry of the lanthanide elements should differ markedly from one to another. This is in stark contrast to conventional thinking about lanthanide ions which says that the chemical properties of these ions do not change much from one element to the next. It is therefore the goal of this research to explore some of the redox chemistry associated with divalent lanthanide complexes in order to define whatever differences exist between different elements.

Complexes of Yb^{2+} and Eu^{2+} have been considered during this research because they are the most readily prepared divalent lanthanide ions. The preparation of the diiodides of Eu and Yb is easily accomplished by mixing liquid ammonia solutions of the metals with NH_4I. Removal of excess ammonia then provides base free MI_2 complexes which are convenient starting materials for the preparation of all the complexes prepared in this research.

The first divalent organolanthanide complexes to be prepared were $(C_5H_5)_2M$ (M=Yb, Eu) which were prepared by reacting the diene C_5H_6 with the metal dissolved in liquid ammonia.[7] The complex $(C_5H_5)_2Yb{\cdot}THF$ was

first synthesized by reduction of $(C_5H_5)_2YbCl$ using sodium metal.[8] Other divalent complexes of the type $(RC_5H_4)ML_2$ are listed in Table (II).

Table II.) Some Divalent Cyclopentadienyl Lanthanide Complexes.

Compound	Ligand	Reference
$(C_5H_5)_2YbL_2$	THF, L_2=DME	7b, 8, 9
$(MeC_5H_5)_2YbL_2$	THF	10
$(Me_3SiC_5H_4)_2YbL_2$	THF, L_2=TMED	11
$(C_5H_5)_2Yb$	a	7a,b
$(Me_3SiC_5H_4)_2Yb$	a	11
$(C_5H_5)_2SmL$	THF	12
$(C_5H_5)_2Eu$	a	7

DME=1,2-dimethoxyethane; TMED=N,N',N'',N'''-tetramethylethylenediamine, a.) Isolated base free.

All of the Yb complexes in Table (II) are diamagnetic having f^{14} electronic configurations as expected for Yb(II) complexes.

One reason why the chemistry of these molecules has not been studied in much detail is because with the exception of $(Me_3SiC_5H_4)_2Yb{\cdot}L_2$ they are all insoluble in hydrocarbon solvents. Evidently, they lose L via the equilibrium in eqn (1), (page 5) and form the insoluble base free materials. The insolubility of these complexes is due to their

$$RC_5H_4)_2YbL \qquad (RC_5H_4)_2Yb + L \qquad (1)$$

polymeric nature. Bis(cyclopentadienyl)ytterbium has been shown to be isostructural with $(C_5H_5)_2Ca$ and $(C_5H_5)_2Sr$[7]; $Ca(C_5H_5)_2$ has a polymeric structure in which the C_5H_5 groups undergo η^5, η^3 and η^1 bonding to the Ca ion. Similarly, the structure of $(MeC_5H_4)_2Yb(THF)_2$ is polymeric with C_5H_4Me groups bridging two ytterbium atoms by η^5 bonding to both atoms.

The problem with solubility has been solved by replacing the C_5H_5 groups with C_5Me_5 groups. Table(III) contains a list of various divalent $(C_5Me_5)_2ML$ complexes which have been described more recently.

Table III.) Some Divalent Pentamethylcyclopentadienyl Lanthanide Complexes.

Compound	Ligand	Reference
$(C_5Me_5)_2Yb^{\bullet}L$	THF,OEt_2	13
$(C_5Me_5)_2YbL_2$	py,THF,dmpm,DME	14,15,16
$(C_5Me_5)_2EuL$	THF	13
$(C_5Me_5)_2EuL_2$	L_2=(THF,Et_2O),Bpy	13
$(C_5Me_5)_2SmL$	Et_2O	17
$(C_5Me_5)_2SmL_2$	THF	18

py=pyridine; dmpm=1,2-bis(dimethylphosphino)methane; Bpy=2,2'-bipyridine

One advantage that the C_5Me_5 ligand has over the C_5H_5 ligand is that it

imparts hydrocarbon solubility and crystallizability to its complexes. All the complexes listed in Table (III) are hydrocarbon soluble, and because of the steric bulk of the C_5Me_5 ligands, they do not form polymers.

Although no quantitative studies on the relative binding strengths of the ligands in Table(III) have been done, qualitatively the $(C_5Me_5)_2Yb\cdot L$ complexes behave as hard Lewis acids as do all lanthanide complexes, and the relative ligand affinity for $(C_5Me_5)_2Yb$ is Py>>THF>Et_2O≈dmpm.[19] There is no evidence for the binding of CO, olefins, or acetylenes to $(C_5Me_5)_2Yb$. Likewise, $(C_5Me_5)_2Yb\cdot OEt_2$ does not react with molecular hydrogen.[19]

Another bulky ligand which has been successfully employed to stabilize divalent ytterbium complexes, and one that affords hydrocarbon soluble complexes, is the hexamethyldisilylamido ligand $(Me_3Si)_2N^-$. Reaction of two equivalents of $NaN(SiMe_3)_2$ with one equivalent of YbI_2 in diethyl ether affords the complex $[(Me_3Si)_2N]_2Yb(OEt_2)_2$.[20] The diethyl ether in this complex may be displaced by dmpm, dmpe (1,2-bis(dimethylphosphino) ethane), and diphos (1,2-bis(diphenylphosphino)-ethane).[21] If the complex is dissolved in pentane in the presence of NaI, the anionic complex $NaYb[N(SiMe_3)_2]_3$ is the only product isolated.[20] When the parent $[(Me_3Si)_2N]_2Yb(OEt_2)_2$ is dissolved in hydrocarbons, the orange solid gives red solutions. Thus, both divalent complexes $(C_5Me_5)_2Yb\cdot OEt_2$ and $[(Me_3Si)_2N]_2Yb\cdot L$ have their coordinated ether molecules displaced by other donor ligands L. The coordination chemistry of the bis(hexamethyldisilylamido)ytterbium complexes indicates that they also behave as class A[22] or hard[23] Lewis acids.

Of the complexes found in Table(III) $(C_5Me_5)_2Yb\cdot OEt_2$ has been

studied rather extensively with regard to reactions in which it is oxidized.[29] Reaction of $(C_5Me_5)_2Yb{\cdot}OEt_2$ with AgI or $AgOOCCF_3$ results in formation of the trivalent $(C_5Me_5)_2YbX$ (where $X=I^-$ or CF_3COO^-). Similarly, the complexes $(C_5Me_5)_2YbX{\cdot}L$ can be prepared by reaction of $(C_5Me_5)_2Yb{\cdot}L$ with alkyl halides or $YbCl_3$. Experimentally, it is easy to determine if the divalent ytterbium complex has been oxidized since Yb(II) has an f^{14} electronic configuration and all of its complexes are diamagnetic, while those of Yb(III) are f^{13} and paramagnetic. Proton NMR spectroscopy is useful in distinguishing between Yb(II) and Yb(III) complexes because of the line widths and chemical shifts of the Yb(III) complexes.

The amount of structural information which may be obtained from the ^1H NMR spectra of Yb(III) complexes is severely limited due to the line widths. The ability of $(C_5Me_5)_2Yb$(III) complexes to crystallize well is extremely important, since single crystal X-ray diffraction studies are the prime method of structural characterization for these paramagnetic molecules. It has been shown that because the bonding in lanthanide complexes is primarily ionic in nature, and changes in the averaged metal-carbon bond lengths of $(C_5R_5)_2Ln$ complexes are due solely to changes in the ionic radius of the metal ion.[24] Table (IV) shows the results of several structural studies which have been carried out on some di- and trivalent $(C_5Me_5)_2Yb$ complexes.

Table IV.) Bonding Parameters of Some Di- and Trivalent $(C_5Me_5)_2Yb$ Complexes.

Compound	$M-C_{ave}$ Bond Lgth Å	Effective Metal Ion Radius Å	C_5M_5 Radius Å	Ref.
$(C_5Me_5)_2Yb(Py)_2$	2.74(4)	1.14	1.60	14
$(C_5Me_5)_2Yb(THF)$	2.66(2)	1.08	1.58	13
$(C_5Me_5)_2Yb(S_2CNEt_2)$	2.63(3)	.985	1.64	32
$[(C_5Me_5)_2YbTHF][Co(CO)_4]$	2.596(2)	.985	1.61	27
$[(C_5Me_5)_2Yb]_2[Fe_3(CO)_{11}]$	2.57(1)	.985	1.59	28
$[Li(OEt_2)_2][(C_5Me_5)_2YbCl_2]$	2.611(4)	.985	1.63	33
$[(C_5Me_5)_2Yb][AlCl_4]$	2.584(5)	.985	1.60	33

Examination of the table clearly shows that di- and trivalent ytterbium complexes are easily distinguished by crystallographic methods.

The ability of divalent ytterbium complexes to function as hydrocarbon soluble one electron reducing agents and hard Lewis acids is a unique property of these complexes. It was shown some years ago that hard Lewis acids will form complexes with binuclear metal carbonyl complexes by bonding to the oxygen atom of a bridging CO group.[25a-f] Trivalent lanthanide complexes have been shown to form similar complexes.[26] One of the best known reactions of transition metal carbonyl dimers is their reductive cleavage with alkali metals to form the monomeric transition metal carbonyl anions. The complex $(C_5Me_5)_2Yb{\cdot}OEt_2$ has been shown to behave as both a reducing agent and a

Lewis acid toward transition metal carbonyl dimers. When $(C_5Me_5)_2Yb^{\cdot}OEt_2$ is mixed with $Co_2(CO)_8$ or $Fe_3(CO)_{12}$, the products which result are contact ion pairs of the formula $[(C_5Me_5)_2Yb(III)(\mu_2\text{-}OC)M(CO)_x]$ which contain Yb-O-C-M bridging groups.[27,28]

Other work has shown that lanthanide metal powders which have been activated with $HgCl_2$ also reduce transition metal carbonyl dimers to form the complexes $[Ln(III)(THF)_x][(\mu_2\text{-}OC)M(CO)_x]_3$.[29] These complexes also contain Ln-O-C-M interactions. Other complexes which are not as well characterized which have Ln-O-C-M interactions result from the interaction of transition metal carbonyl anions and $(C_5H_5)_2LnCl$[30] or $Hg[M(CO)_x]_2$ with Ln metal powders.[31]

Complexes which have Ln-O-C-M interactions might serve as models for the activation of carbon monoxide. Therefore, the chemistry of the complexes which result from the reaction of $(C_5Me_5)_2Yb^{\cdot}OEt_2$ and metal carbonyl complexes will be studied. In addition, it is useful to define the effect which substitution of carbonyl ligands for other ligands will have on the ability of $(C_5Me_5)_2Yb^{\cdot}OEt_2$ to behave as a reductant. The observation that alkyl halides oxidize $(C_5Me_5)_2Yb^{\cdot}OEt_2$ suggests that it might be possible to transfer electrons into reducible organic molecules. Finally, the bewildering array of Lewis acid-base equilibria which are observed in the chemistry of $[(Me_3Si)_2N]_2Yb^{\cdot}(OEt_2)_2$ must be more fully understood if the redox chemistry of this species is to be understood.

References

1.) Birmingham, J. M.; Wilkinson, G. W. J. Am. Chem. Soc. **1956**, 78, 42.

2.) Cotton, F. A. ; Wilkinson, G. "Advanced Inorganic Chemistry", 4th ed., Wiley-Interscience: New York, **1980**, pp. 981-1004.

3.) Johnson, D. A., "Some Thermodynamic Aspects of Inorganic Chemistry", 2nd ed., Cambridge University Press: Cambridge, **1982**, pp. 158-168.

4.) Johnson, D. A. in "Adv in Inorganic Chemistry and Radiochemistry", Emeleus, H. J. and Sharpe, A. G., eds., Academic Press: New York, **1977**, 20, p.1.

5.) Johnson, D. A. J. Chem. Educ., **1980**, 57, 475.

6.) Blake, A. B. J. Chem. Educ. **1981**, 58, 393.

7.) a) Fischer, E.O.; Fischer, H. J. Organomet. Chem., **1965**, 3, 181. b) Deacon, G. B.; Doplick, A. J.; Tuong, T. D. Polyhedron, **1982**, 1, 423.

8.) Calderazzo, F.; Pappalardo, R.; Losi, S. J. Inorg. Nucl. Chem., **1966**, 28, 987.

9.) Deacon, G. B.; Mackinnon, P. I.; Hambley, T. W.; Taylor, J. C. J. Organomet. Chem., **1983**, 259, 91.

10.) Zinnen, H. A.; Pluth, J. J.; Evans, W. J. J. Chem. Soc., Chem. Commun., **1980**, 810.

11.) Lappert, M. F.; Yarrow, P. I.; Atwood, J. L.; Shakir, R.; Holton, J. J. Chem. Soc., Chem. Commun., **1980**, 987.

12.) Watt, G. W.; Gillow, E. W. J. Am. Chem. Soc., **1969**, 91, 775.

13.) Tilley, T. D.; Andersen, R. A.; Spencer, B.; Ruben, H.; Zalkin, A.; Templeton, D. H. Inorg. Chem. **1980**, 19, 2999.

14.) Tilley, T. D.; Andersen, R. A.; Spencer, B.; Zalkin, A. Inorg. Chem., **1982**, 21, 2647.

15.) Tilley, T. D.; Andersen, R. A.; Zalkin, A. Inorg. Chem., **1983**, 22, 856.

16.) Watson, P. L. J. Chem. Soc., Chem. Commun., **1980**, 652.

17.) Watson, P. L., Personal Communication.

18.) Evans, W. J.; Bloom, I.; Hunter, W. E.; Atwood, J. L. J. Am. Chem. Soc. **1981**, 103, 6507.

19.) Tilley T. D., PhD Thesis. University of California, Berkeley, California, U.S.A. 1982.

20.) Tilley, T. D.; Andersen, R. A.; Zalkin, A. Inorg. Chem. 1984.

21.) Tilley, T. D.; Andersen, R. A.; Zalkin, A. J. Am. Chem. Soc., 1982, 104, 3725.

22.) Ahrland, S.; Chatt, J.; Davies, N. R. Q. Rev., Chem. Soc. 1958, 12, 265.

23.) Pearson, R. G. J. Am. Chem. Soc. 1963, 85, 3533.

24.) Raymond, K. N.; Eigenbrot, C. W., Jr. Acc. Chem. Res. 1980, 13, 276.

25.) a) Shriver, D. F. J. Organomet. Chem. 1975, 94, 159; Acc. Chem. Res. 1970, 3, 231. b) Nelson, N. J.; Kime, N. E.; Shriver, D. F. J. Am. Chem. Soc. 1969, 91, 5173. c) Alich, A.; Nelson, N. J.; Strope, D.; Shriver, D. F. Inorg. Chem. 1972, 11, 2976. d) Shriver, D. F.; Alich, A. Ibid. 1972, 11, 2984. e) Kristoff, J. S.; Shriver, D. F. Ibid. 1974, 13, 499.

26.) Onaka, S.; Eurwichi, N. J. Organomet. Chem. 1979, 173, 77.

27.) Tilley, T. D.; Andersen, R. A. J. Chem. Soc., Chem. Commun. 1981, 985.

28.) Tilley, T. D.; Andersen, R. A. J. Am. Chem. Soc. 1982, 104, 1772.

29.) Pasynskii, A. A.; Eremenko, I. L.; Suleimanov, G. Z.; Nuriev, Yu.; Beletskaya, I. P.; Shklover, V. E.; Struchkov, Yu. T. J. Organomet. Chem. 1984, 266, 45.

30.) Crease, A. E.; Legdins, P. J. Chem. Soc., Dalton. Trans. 1973, 501.

31.) a) Deacon, G. B.; Koplick, A. I. Inorg. Nucl. Chem. Lett. 1979, 13, 263. b) Suleimanov, G. Z., et. al. Dokl. Akad. Nauk. SSSR. 1982, 265, 896.

32.) Tilley, T. D.; Andersen, R. A.; Zalkin, A.; Templeton, D. H. Inorg. Chem. 1982, 21, 2644.

33.) Watson, P. L.; Whitney, J. F.; Harlow, R. L. Inorg. Chem., 1981, 20, 3271.

Chapter 1

Reactions of Bis(pentamethylcyclopentadienyl)ytterbium with Transition Metal Carbonyl Complexes

Reactions with Transition Metal Carbonyl Dimers

It has been shown that $(C_5Me_5)_2Yb{\cdot}OEt_2$ can be employed as a single electron transfer reagent toward the transition metal carbonyl complexes $Co_2(CO)_8$ and $Fe_3(CO)_{12}$.[1a,b] Since both of these molecules contain CO groups which bridge between both metal centers, and are strong enough Lewis bases to coordinate to AlR_3 compounds, it was of interest to see if these electron transfer reactions could be extended to complexes which do not contain CO bridging groups. It was also of interest to see what effect substitution of some of the CO groups by other groups such as cyclopentadienyl, and trialkylphosphines would have on these reactions.

Reaction of two equivalents of $(C_5Me_5)_2Yb{\cdot}OEt_2$ with one equivalent of the transition metal carbonyl dimers $M_2(CO)_{10}$ (M=Mn, Re) or $Cp_2M_2(CO)_x$ (M=Fe, Ru, x=4; M=Mo, x=6) results in reductive cleavage of the metal–metal bond and formation of complexes having the stoichiometries $[(C_5Me_5)_2Yb(III)][M(CO)_5]$ (M=Mn, Re) and $[(C_5Me_5)_2Yb(III)][CpM(CO)_x]$ (M=Fe, Ru, x=2; M=Mo, x=3), respectively. These reactions are rapid at room temperature and in most cases the reaction is complete within minutes. The notable exception is the reaction between $(C_5Me_5)_2Yb{\cdot}OEt_2$ and $(C_5Me_5)_2Fe_2(CO)_4$ which is not

Table I. ^{1}H NMR Data For $[(C_5Me_5)_2Yb(III)][M(CO)_xL]$ Compounds at 30°C.

Compound	Color	^{1}H NMR	Reference
$[(C_5Me_5)_2Yb(III)][Mn(CO)_5]$	Blue	δ8.75($\nu_{1/2}$=47Hz)	this work
$[(C_5Me_5)_2Yb(III)][Re(CO)_5]$	Red	δ9.56($\nu_{1/2}$=110Hz)	this work
$\{[(C_5Me_5)_2Yb(III)][(Me_3SiC_5H_4)Mo(CO)_3]\}_2$	Blue	δ7.55($\nu_{1/2}$=34Hz, 13.2H); δ8.27($\nu_{1/2}$=34Hz, 30H); δ8.98($\nu_{1/2}$=34Hz,13.2H); δ25.30(9H); δ25.58(7.92H); δ32.05($\nu_{1/2}$=21Hz, 2.0H); δ33.50($\nu_{1/2}$=21Hz, 1.76H); δ34.63(2.0H); δ34.80(1.76H)	this work
$\{[(C_5Me_5)_2Yb(III)][(C_5H_5)Mo(CO)_3]\}_2$	Blue	δ8.16($\nu_{1/2}$=62Hz, 30H); δ32.85($\nu_{1/2}$=10Hz, 5H)	this work
$\{[(C_5Me_5)_2Yb(III)][(C_5H_5)Mo(CO)_3]\}_2$ at -74°C		δ12.21($\nu_{1/2}$=100Hz, 30H); δ46.57($\nu_{1/2}$=28Hz, 2H); δ48.43($\nu_{1/2}$=28Hz, 3H)	this work
$\{[(C_5Me_5)_2Yb(III)][(C_5H_5)Fe(CO)_2]\}_2$	Black	δ8.09($\nu_{1/2}$=36Hz, 30H); δ35.23($\nu_{1/2}$=13Hz, 5H)	this work

Table I (cont.)

Compound	Color	^{1}H NMR	Reference
$\{[(C_5Me_5)_2Yb(III)][(MeC_5H_4)Fe(CO)_2]\}_2$	Black	δ7.91($\nu_{1/2}$=45Hz, 30H); δ38.52($\nu_{1/2}$=7.8Hz, 3H); δ40.31($\nu_{1/2}$=8.6Hz, 2H); δ44.19($\nu_{1/2}$=11Hz, 2H)	this work
$\{[(C_5Me_5)_2Yb(III)][(Me_3SiC_5H_4)Fe(CO)_2)]\}_2$	Black	δ8.01($\nu_{1/2}$=37Hz, 30H); δ19.45($\nu_{1/2}$=10Hz, 9H); δ32.33($\nu_{1/2}$=12Hz, 2H); δ50.21($\nu_{1/2}$=3Hz, 2H)	this work
$[(C_5Me_5)_2Yb(III)py][(Me_3SiC_5H_4)Fe(CO)_2]$	Red	δ4.46($\nu_{1/2}$=20Hz, 30H); δ6.30($\nu_{1/2}$=6.5Hz, 9H); δ9.92($\nu_{1/2}$=7.0Hz, 2H); δ10.24($\nu_{1/2}$=7.4Hz, 2H)	this work
$\{[(C_5Me_5)_2Yb(III)][(Me_3SiC_5H_4)Ru(CO)_2]\}_2$	Purple	δ8.27($\nu_{1/2}$=41Hz, 30H); δ19.55($\nu_{1/2}$=7.4Hz, 9H); δ31.87($\nu_{1/2}$=10Hz, 2H); δ43.80($\nu_{1/2}$=9.4Hz, 2H).	this work

complete after several days. The Mn and Re compounds are only sparingly soluble in aromatic hydrocarbons and virtually insoluble in aliphatic hydrocarbons. The solubility of the Fe, Ru and Mo complexes is dependent upon the substituents on the cyclopentadienyl ring bound to the transition metal. The $Me_3SiC_5H_4$ derivatives are the most soluble, and readily crystallize in all cases.

All of the complexes are paramagnetic as judged by the chemical shifts and line widths of the peaks in their ^1H NMR spectra. Their ^1H NMR spectra are given in Table (I). Figures 1 and 2 show plots of $1/\chi_M$ vs. T for the ytterbium-manganese and ytterbium-iron compounds, respectively. Both of these complexes follow Curie-Weiss behavior from 5 to ca. 20K and from ca. 100 to 300K. The effective magnetic moments Table (II) for these complexes are consistent with the complexes containing trivalent ytterbium. The reason that two linear regions in the $1/\chi_M$ vs. T curves are observed is because ytterbium(III) is an f^{13} ion which has a $^2F_{7/2}$ ground state. This energy level is split into at most three levels by the crystal field ($\Gamma_6, \Gamma_7, \Gamma_8$) which for lanthanide ions is usually on the order of hundreds of cm^{-1}.[2a,b] At low temperature, only the ground state is populated. At higher temperatures thermal population of the first excited state causes curvature of the plot until kT is larger than the separation of the two levels. Once this occurs, a second linear region is observed. A third linear region is predicted, and evidently thermal population of this level does not occur to 300K and hence it is not observed. The qualitative result that the ytterbium center has transferred an electron to the metal carbonyl substrate is indisputable.

The infrared spectra in the ν-CO region for the set of complexes

Figure 1. Plot of $1/x_M$ vs. T for $[(C_5Me_5)_2Yb(III)][Mn(CO)_5] \cdot {}^1/_4$ PhMe

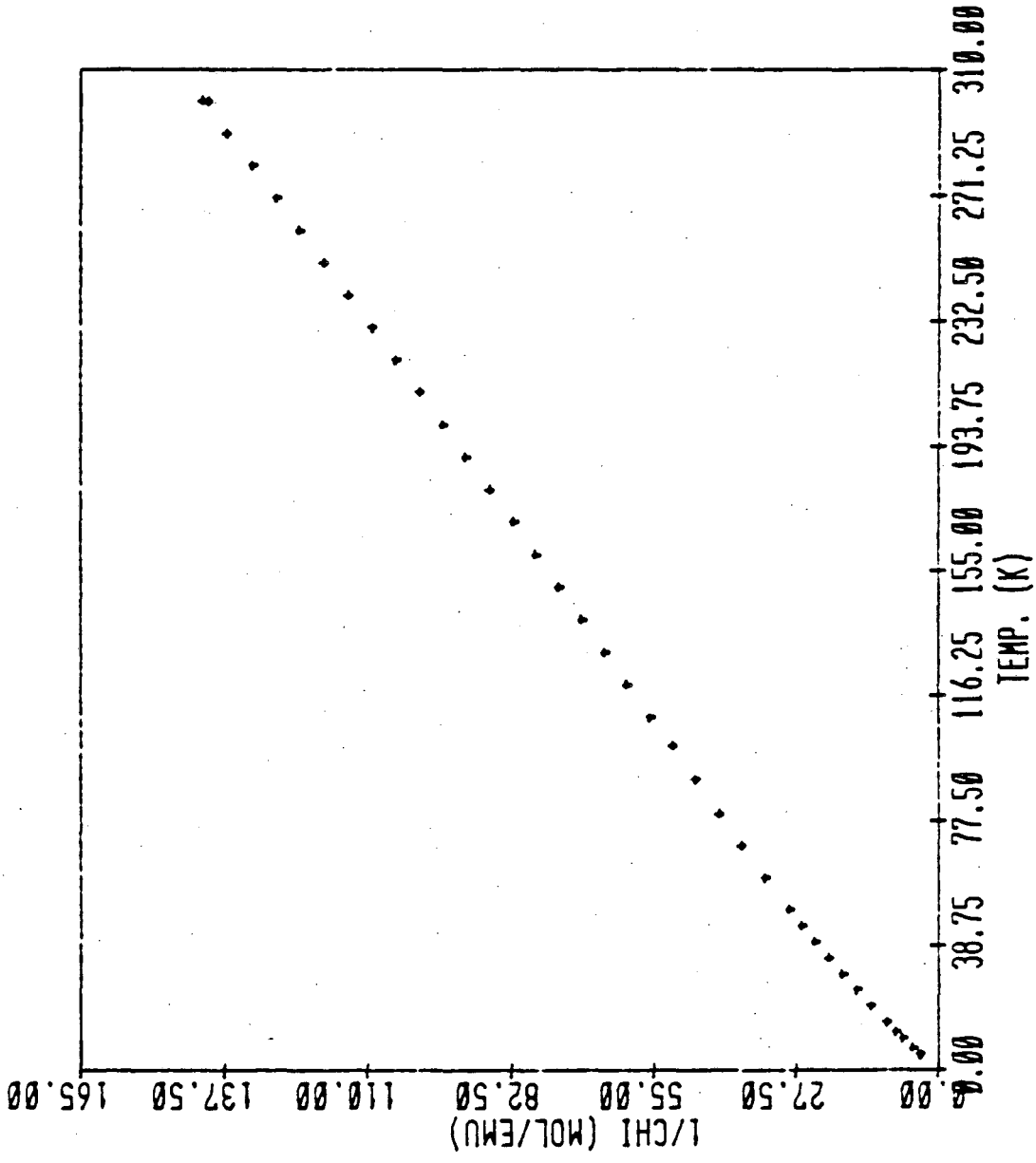

Figure 2. Plot of $^{1}/\chi_{M}$ vs. T for $[(C_5Me_5)_2Yb(III)](\mu_2\text{-}OC)_2Fe(C_5H_4Me)_2$

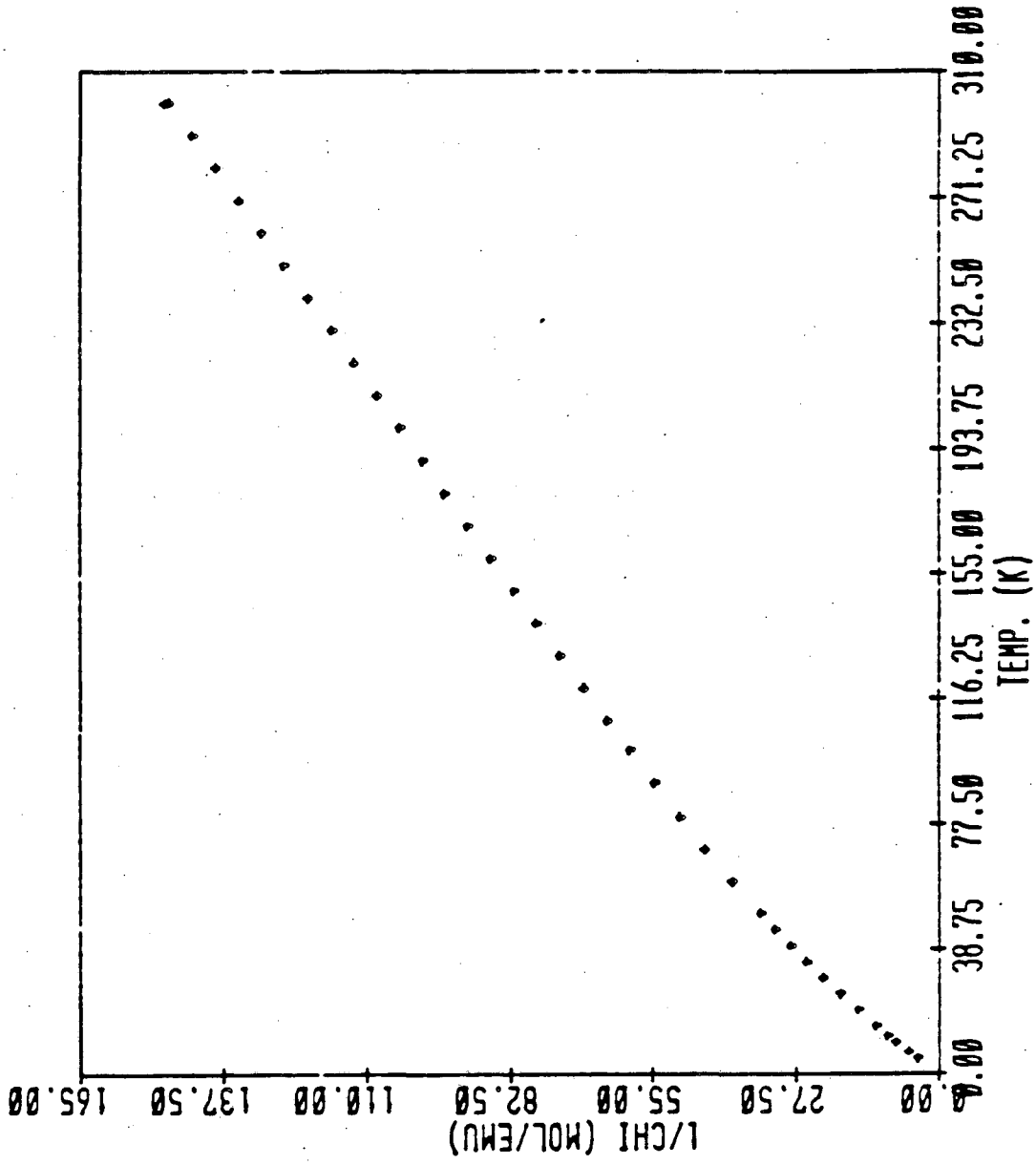

Table II. Magnetic Data for $[(C_5Me_5)_2Yb(II)][Mn(CO)_5]$ and $\{[(C_5Me_5)_2Yb(III)][(MeC_5H_4)Fe(CO)_2]\}_2$ Fit to $\chi_M = C_M(T-\theta)^{-1}$

Compound	Temp Range(K)	C_M	θ(K)	μ_{eff}(B.M.)
$[(C_5Me_5)_2Yb(III)][Mn(CO)_5]$	5-20	1.58(2)	-0.69(18)	3.57(2)
	80-300	2.225(5)	-13.46(51)	4.237(5)
$\{[(C_5Me_5)_2Yb(III)][(MeC_5H_4)Fe(CO)_2]\}_2$	5-25	1.28(1)	-0.50(10)	3.21(2)
	90-290	2.267(4)	-33.78(39)	4.276(4)
$[(C_5Me_5)_2Yb(III)]_2[(Me_3SiC_5H_4)_2Co_3(CO)_4]$	5-30	2.64(2)	-1.05(16)	4.61(2)
	100-300	3.067(6)	-14.50(46)	4.973(5)

Table III.) ν-CO for $[(C_5Me_5)_2YbM(CO)_xL]_2$ Compounds

Compound	Medium	Obsd Bands	Reference
$[(C_5Me_5)_2Yb(III)][Mn(CO)_5]$	THF	2030w,2010m,1934s,1903s, 1770s	this work
	Nujol	1965s,1937sh,1928sh,1882m, 1840s,1775s	
	cyclohexane	1984m,1962s,1955s,1945m, 1778m,1762s,1750m,1728m	
$[(C_5Me_5)_2Yb(III)][Re(CO)_5]$	Nujol	1982sh,1972s,1950s,1945sh, 1785sh,1770sh,1750Br,s	this work
$[(C_5Me_5)_2Yb(III)THF][Co(CO)_4]$	THF	2025m,1935s,1885w,1736s	this work
	methylcyclohexane	2015s,1975s,1960sh,1945s, 1930s,1825sh, 1810s, 1780s,1715Br,s	
$\{[(C_5Me_5)_2Yb(III)][(Me_3SiC_5H_4)Mo(CO)_3]\}_2$	cyclohexane	1944s,1730s,1680s,	this work
	PhMe	1935s,1730s,1685s,	
	THF	1927s,1828s,1625s	

Table III. (cont.)

Compound	Medium	Obsd Bands	Reference
$\{[(C_5Me_5)_2Yb(III)][(C_5H_5)Mo(CO)_3]\}_2$	cyclohexane	1940s,1729s,1680s	this work
	Nujol	1940s,1725s,1680s	
$\{[(C_5Me_5)_2Yb(III)][(C_5H_5)Fe(CO)_2]\}_2$	Nujol	1800s,1740s	
$\{[(C_5Me_5)_2Yb(III)][(MeC_5H_4)Fe(CO)_2]\}_2$	cyclohexane	1787s,1723s	this work
	Nujol	1784s,1723s	
$\{[(C_5Me_5)_2Yb(III)][Me_3SiC_5H_4)Fe(CO)_2]\}_2$	cyclohexane	1795s,1732s	this work
$[(C_5Me_5)_2Yb(III)py][(Me_3SiC_5H_4)Fe(CO)_2]$	Nujol	1970s,1678s	this work
$\{[(C_5Me_5)_2Yb(III)][(C_5Me_5)Fe(CO)]\}_2$	Nujol	1760s,1695s	this work
$\{[(C_5Me_5)_2Yb(III)][(Me_3SiC_5H_4)Ru(CO)_2]\}_2$	Nujol	1815s,1730s	this work
$LiMn(CO)_5$	THF	1895s,1861s	3

Table III. (cont.)

Compound	Medium	Obsd Bands	Reference
$NaMn(CO)_5$	THF	1902s,1897s,1875s,1862s, 1829s	3
$KMn(CO)_5$	THF	1896s,1862s,1830m	4
$Mg(py)_4[Mn(CO)_5]_2$	PhMe	2031w,1928s,1904s,1721s	5
$(n\text{-}Bu_4N)(C_5H_5)Fe(CO)_2$	THF	1865s,1788s	4
$(Et_4N)(C_5H_4)Fe(CO)_2(AlPh_3)$	Nujol	2012w,1960w,1940s,1920wsh, 1871s,1843w	6
$Li(C_5H_5)Fe(CO)_2$	THF	1884s,1869s,1812s,1788w, 1750s	7
$Na(C_5H_5)Fe(CO)_2$	THF	1877s,1862m,1806s,1786m, 1770m	8
$K(C_5H_5)Fe(CO)_2$	THF	1868s,1792s,1772s	7
$Mg[(C_5H_5)Fe(CO)_2]_2$	THF	2010w,1941w,1916s,1883s 1852s,1712s	5, 7, 9

Table III. (cont.)

Compound	Medium	Obsd Bands	Reference
$Na(C_5H_5)Mo(CO)_3$	THF	1899s,1796s,1743m	10
$K(C_5H_5)Mo(CO)_3$	THF	1897s,1798s,1748m	10
$PPn(C_5H_5)Mo(CO)_3$	THF	1896s,1780s	10
$Mg(THF)_4[(C_5H_5)Mo(CO)_3)]_2$	THF	1912s,1815s,1680s	9
$Mg(py)_4[(C_5H_5)Mo(CO)_3]_2$	Nujol	1918s,1828s,1667s	5
$Mn(py)_4[(C_5H_5)Mo(CO)_3]_2$	Nujol	1905s,1808s,1650s	11

obtained from the reaction of $(C_5Me_5)_2Yb{\cdot}OEt_2$ and transition metal carbonyl dimers are summarized in Table (III). One common feature of the spectra of all the ytterbium compounds is that they contain at least one low energy ν-CO bond. It is well known that when group 3B compounds such as AlR_3 form acid-base complexes with metal carbonyls the stretching frequency of the CO which bridges between the two metals in these complexes is lowered in energy by approximately $100cm^{-1}$.[22] The low energy ν-CO bands in the complexes studied here indicate that they all contain Yb-O-C-M linkages. Closer inspection of Table (III) reveals that the spectra of all the complexes are dependent upon the medium in which they are measured. In particular, the spectra of the complexes $[(C_5Me_5)_2Yb(III)][M(CO)_x]$ (M=Co, x=4; M=Mn, x=5) in THF have ony one low ν-CO band and either three or four bands in the terminal ν-CO region.

The infrared spectrum of the ytterbium-manganese complex is similar to that of $NaMn(CO)_5$ in THF (Table III). The infrared spectrum of $NaMn(CO)_5$ in THF has been interpreted as arising from either an equilibrium between solvent-separated and contact ion-pairs or a single contact ion-pair with local C_{2v} symmetry. The five line pattern for the ytterbium complex suggests a similar explanation. We cannot rigorously rule out an equilibrium between a solvent-separated and a contact ion-pair, but it is extremely unlikely since it requires that no THF be coordinated to the ytterbium atom in the contact ion pair, and also requires that the solvent-separated ion-pair have two of its three infrared active bands accidently degenerate with two of the bands of the contact ion-pair. Strong support for the existence of an ytterbium-manganese contact ion-pair having C_s symmetry is found by examining the infrared spectrum of the related complex $[(C_5Me_5)_2Yb(III){\cdot}THF][(\mu_2-$

$OC)Co(CO)_3]$ in THF (Table III). In the solid state, this molecule is a contact ion-pair in which the ytterbium atom is bonded to a carbonyl oxygen and tetrahydrofuran molecule as in I below. The infrared spectrum of this complex in THF has four absorptions with one in the bridging region as is expected for a structure of local C_s symmetry. The infrared spectrum of the ytterbium-manganese complex suggests an analogous structure as in II.

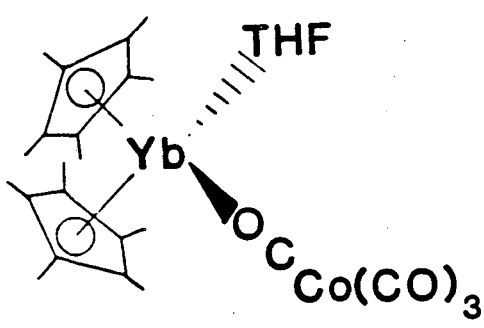

I

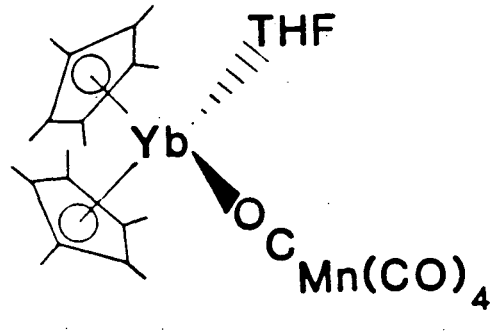

II

The infrared spectra of the ytterbium-manganese complex as well as the ytterbium-cobalt complex in non-polar solvents or in the solid are much more complex than in tetrahydrofuran. The large number of ν-CO bands cannot be rationalized unless other species are present in solution or in the solid. This is confirmed by the crystal and molecular structure of the manganese complex as will be discussed later.

The infrared spectra of the complexes $[(C_5Me_5)_2Yb(III)]$ $[(RC_5H_4)M(CO)_x]$ (M=Fe, Ru, x=2; M=Mo, x=3), though less complex than the spectra of the Mn, Re and Co complexes, also change depending upon the medium in which they are measured. The spectrum of the ytterbium-molybdenum complex in THF has three bands, one of which is in the ν-CO bridging region. This spectrum is similar to the spectra observed for

the complexes $Mg(L)_4[(C_5H_5Mo(CO)_3]_2$ or $[(C_5H_5)Mo(CO)_3]$ ($M=Na^+$, K^-) which have structures which are crystallographically determined to have one Mo-CO-Mg interaction per molybdenum atom (Table III). This suggests a structure for the ytterbium-molybdenum complex which is similar to the others we have seen for cobalt and manganese as in III. The spectrum of this complex, either dissolved in cyclohexane, or in toluene, also

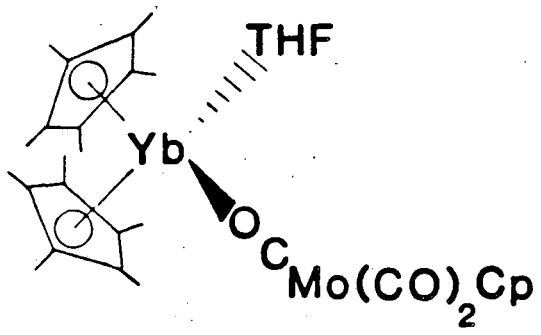

III

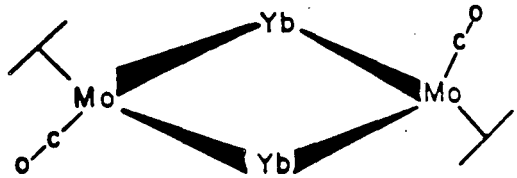

IV

contains three ν-CO bands. The difference is that two of these bands lie in the bridging ν-CO region whilst only one lies in the terminal region. This spectrum is consistent with a dimeric complex having the structure shown in IV for which it is predicted that the complex will have two bridging and one terminal ν-CO band under C_{2h} symmetry.

Since tetrahydrofuran solutions of the iron and ruthenium compounds were too air sensitive to obtain infrared spectra, a pyridine complex was synthesized and isolated. Addition of two equivalents of pyridine to the complex $\{[(C_5Me_5)_2Yb(III)][(Me_3SiC_5H_4)Fe(CO)_2]\}_2$ results in cleavage of the dimeric structure and formation of a complex having the stoichiometry $[(C_5Me_5)_2Yb(III)py][(Me_3SiC_5H_4)Fe(CO)_2]$. These bands are consistent with a structure in which one carbonyl group bridges the two metals and this complex has one terminal and one bridging ν-CO band

(Table III). This suggests once again that the complex has a structure in which the ytterbium is bound to one carbonyl oxygen atom and one pyridine molecule as in V. If the spectra of the iron-ytterbium complexes are measured in cyclohexane solution, or as Nujol mulls, two ν-CO bands in the bridging region are observed suggesting a centro-

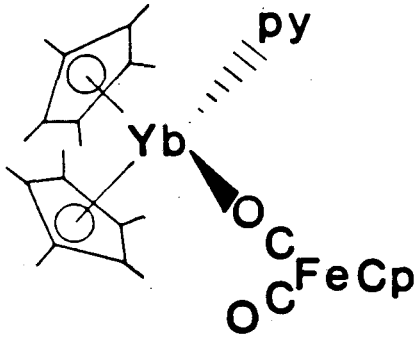

V

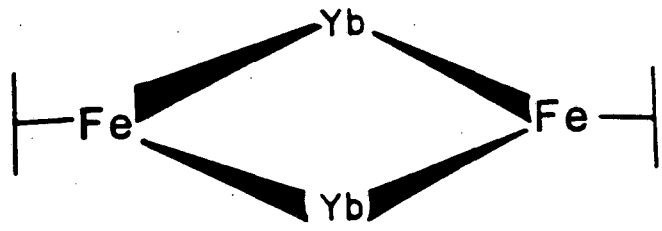

VI

symmetric dimeric structure shown in VI.

In general, when the ytterbium compounds in Table (III) are dissolved in a polar solvent such as THF an infrared spectrum results which is consistent with a structure which contains one CO group that bridges the ytterbium and transition metal atoms and the other coordination site on ytterbium is occupied by the THF molecule. When there is no base to coordinate to the ytterbium, the structure that results is a dimeric one in which two coordination sites on ytterbium are occupied by μ-CO groups.

Chemical Reactivity

One of the reactions molecules with μ-CO linking two metals in a linear fashion might be expected to undergo is reaction with hydrogen

resulting in CO bond cleavage. The complexes which result from reacting $(C_5Me_5)_2Yb{\cdot}OEt_2$ and transition metal carbonyl dimers containing linear μ-CO groups, but do not react with H_2 and/or carbon monoxide at pressures of 18atm and room temperature. They do, however, react with acids and hydride sources such as $LiEt_3BH$, but these reaction products have not been investigated since they could not be isolated.

One reaction which transition metal carbonyl anions undergo is the reaction with alkyl halides to give transition metal alkyl complexes. When the ytterbium-manganese complex, the ytterbium-molybdenum complex, and the ytterbium-iron complexes are reacted with methyl iodide in toluene three distinct modes of reactivity are observed. The ytterbium-manganese (or rhenium) complexes react with CH_3I to give $MeM(CO)_5$ and $(C_5Me_5)_2YbI$ (by infrared and mass spectrometry, respectively). The ytterbium-molybdenum complex reacts with CH_3I to give a mixture of $C_5H_5Mo(CO)_3Me$ and $C_5H_5Mo(CO)_3I$ by infrared spectroscopy. The ytterbium-iron complex reacts with CH_3I to give $[C_5H_5Fe(CO)_2]_2$ and $(C_5Me_5)_2YbI$ as the only observable products by infrared and mass spectrometry.

The observed reactivity of CH_3I indicates that there is an increasing amount of electron transfer character in the reaction in the series Mn, Mo, Fe. This is precisely the order which is observed in these anions when the counter-ion is an alkali metal such as sodium[12]; however, the difference between alkali metal ions as counter ions and $(C_5Me_5)_2Yb(III)$ is that the reaction always produces the metal alkyl in the alkali metal case, and this is not so in the Yb case.

One possible explanation for the observation that no metal alkyl product is observed in the $(C_5H_5)Fe(CO)_2^-$ case is that because the complexes are dimeric any electron transfer from the Fe center to give

$(C_5H_5)Fe(CO)_2^{\bullet}$ causes immediate coupling to the adjacent iron center to give $[(C_5H_5)Fe(CO)_2]_2^{-}$ which then transfers another electron to give the observed products.

X-Ray Crystallographic Studies

The infrared spectrum of the manganese-ytterbium complex in the solid state and in non-coordinating solvents indicated the possibility of either more than one species being present in the solid, or a very complicated solid state structure. In order to fully characterize the molecule, a single crystal X-ray diffraction study was performed. Figure 3 shows a stereopair view of a portion of the unit cell oblique to the ac plane. Only half of the b axis is shown. A full layer of the structure from 0 to 0.25 in y is shown. A portion of the y=0.5 layer shows how these layers pack in the unit cell.

Inspection of Figure 3 shows that the structure consists of layers of infinite, planar, polymeric sheets of the stoichiometry $[(C_5Me_5)_2Yb(III)(\mu_2\text{-}OC)_3Mn(CO)_2]_x$. Dimeric molecules of the formula $[(C_5Me_5)_2Yb(III)(\mu_2\text{-}OC)_2Mn(CO)_3]_2$ are packed between the polymeric sheets. The solvating toluene molecules fill regularly spaced voids in the network of dimers and polymer sheets.

Close inspection of the polymeric sheet reveals that it consists of essentially trigonal-bipyramidal $Mn(CO)_5$ groups that are each coordinated to three different $(Me_5C_5)_2Yb$ groups through their equatorial carbonyls. Each $(Me_5C_5)_2Yb$ cation is in turn coordinated only to the equatorial carbonyls of the $Mn(CO)_5$ units, and all the Mn and Yb atoms in the polymer are essentially coplanar. The largest

Figure 3. ORTEP Packing Diagram for $[(C_5Me_5)_2Yb(III)][Mn(CO)_5] \cdot {}^1/_4\,PhMe$

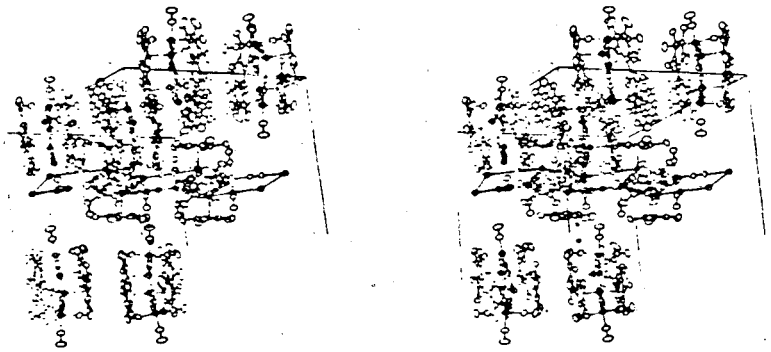

deviation of a metal atom from the least-squares plane through them is 0.065Å by Yb1.

The dimeric $[(C_5Me_5)_2Yb(III)(\mu_2\text{-}OC)_2Mn(CO)_3]_2$ units are disposed about the mirror plane at y=0 such that two ytterbium atoms lie in the mirror plane and the manganese atoms lie above and below the mirror plane. In addition, all four Me_5C_5 rings in the dimer are bisected by the mirror plane and are normal to it. The dimers pack in the ac plane at y=0 with the disordered toluene molecule filling the voids such that the overall composition of the crystal is $[(C_5Me_5)_2YbMn(CO)_5]_4[PhMe]$. The crystal structure, then, consists of alternate planar, polymeric sheets normal to b with dimers at 0, $1/2$, 1 etc. and the polymer at $1/4$, $3/4$, etc.

The very complex, though regular, crystal structure rationalizes in a general, though not in an analytic, fashion with the large number of C-O stretching frequencies observed in the spectrum of the solid. It also offers a rationalization for the complexity of the infrared spectrum in the ν-CO region in nonpolar solvents. The presence of oligomers and C_{2h} dimers, or dimers that do not have C_{2h} point symmetry in solution, is consistent with the observed spectra. The formation of dimers or other higher oligomers by the compound $[(C_5Me_5)_2Yb(III)THF][(\mu_2\text{-}OC)Co(CO)_3]$ is consistent with the complexity of its ν-CO IR spectrum in noncoordinating solvents (see Table III).

In the discussion that follows, the discrete dimeric and polymeric units will be described with respect to their individual stereochemistry. An ORTEP view of the dimeric units is shown in Figure 4, and a portion of the polymeric unit in Figure 5. Bond lengths and angles are found in Tables (IV) and (V), respectively. As alluded to

Figure 4. ORTEP of Dimeric Portion of $[(C_5Me_5)_2Yb(III)][Mn(CO)_5] \cdot PhMe$

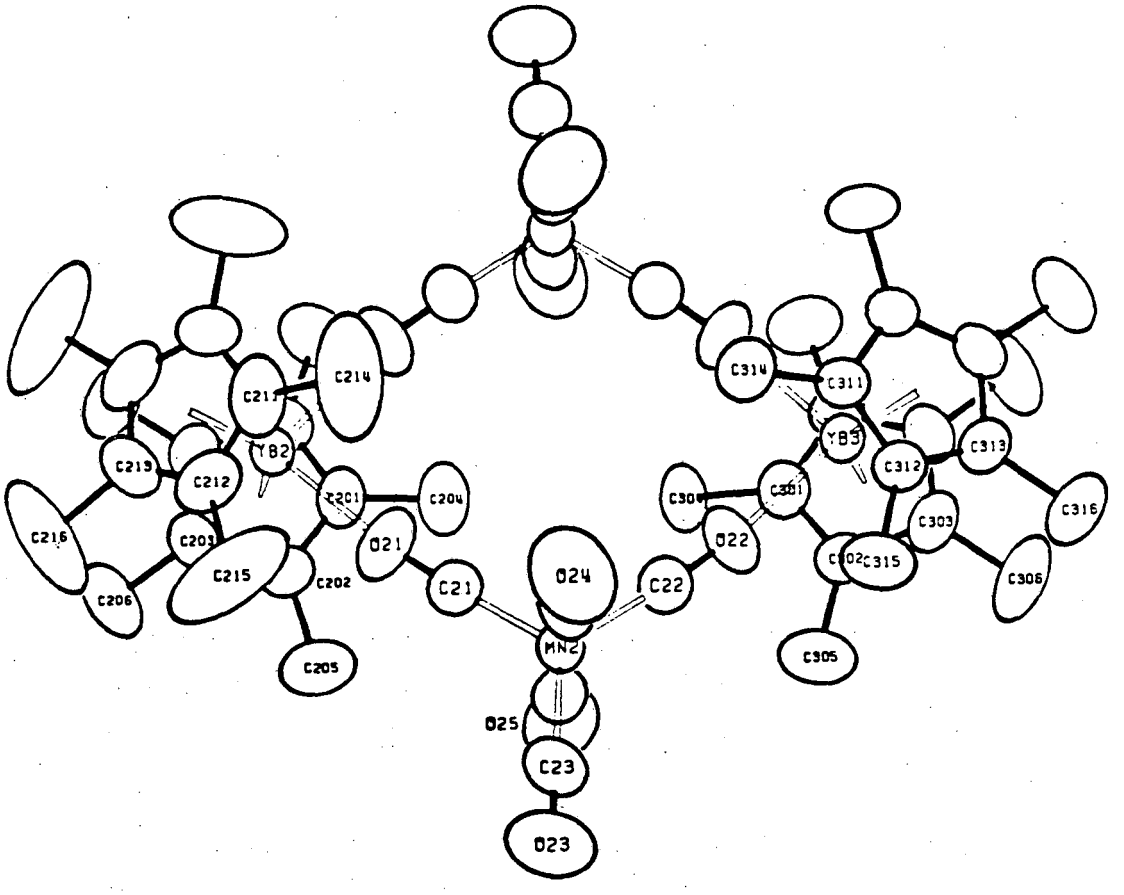

Figure 5. ORTEP of a Portion of the Polymer in $[(C_5Me_5)_2Yb(III)]$ $[Mn(CO)_5] \cdot \frac{1}{4}$ PhMe

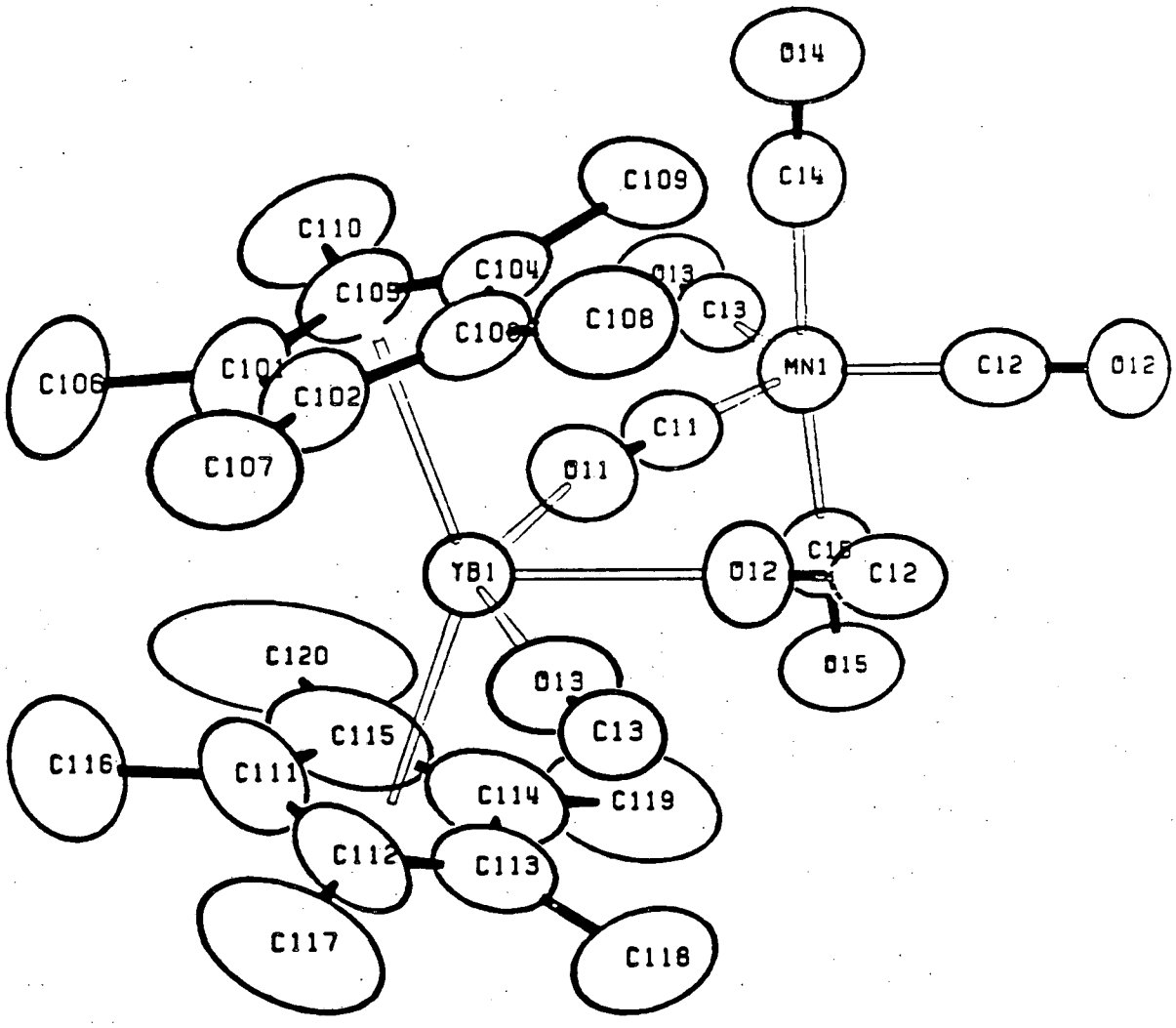

Table IV. Selected Bond Lengths (Å) for $[(C_5Me_5)_2Yb(III)][Mn(CO)_5]\cdot{}^1/_4\,PhMe$

Yb1-O11	2.401(5)	Mn1-C11	1.796(7)
Yb1-O12	2.349(4)	Mn1-C12	1.771(8)
Yb1-O13	2.417(5)	Mn1-C13	1.805(8)
Yb1-C101	2.607(6)	Mn1-C14	1.825(7)
Yb1-C102	2.584(6)	Mn1-C15	1.814(7)
Yb1-C103	2.578(6)	Mn1-O11	2.957(5)
Yb1-C104	2.599(6)	Mn1-O12	2.968(5)
Yb1-C105	2.590(6)	Mn1-O13	2.963(5)
Yb1-Cp11[a]	2.304	Mn1-O14	2.974(5)
Yb1-C111	2.610(7)	Mn1-O15	2.959(5)
Yb1-C112	2.612(7)	Mn2-C21	1.735(6)
Yb1-C113	2.571(7)	Mn2-C22	1.761(6)
Yb1-C114	2.564(7)	Mn2-C23	1.823(8)
Yb1-C115	2.577(7)	Mn2-C24	1.839(8)
Yb1-Cp12[a]	2.305	Mn2-C25	1.838(8)
Yb2-O21	2.268(4)	Mn2-O21	2.924(4)
Yb2-C201	2.551(7)	Mn2-O22	2.940(4)
Yb2-C202	2.576(5)	Mn2-O23	2.962(6)
Yb2-C203	2.599(5)	Mn2-O24	2.964(6)
Yb2-Cp21[b]	2.279	Mn2-O26	2.972(6)
Yb2-C211	2.560(9)	C11-O11	1.161(7)
Yb2-C212	2.565(6)	C12-O12	1.197(8)
Yb2-C213	2.563(5)	C13-O13	1.159(8)
Yb2-Cp22[b]	2.283	C14-O14	1.149(7)
Yb3-O22	2.273(4)	C15-O15	1.145(7)
Yb3-C301	2.582(8)	C21-O21	1.190(6)
Yb3-C302	2.582(5)	C22-O22	1.181(6)
Yb3-C303	2.590(5)	C23-O23	1.139(8)
Yb3-Cp31[b]	2.292	C24-O24	1.125(8)
Yb3-C311	2.554(7)	C25-O25	1.135(8)
Yb3-C312	2.572(5)		
Yb3-C313	2.591(5)		
Yb3-Cp32[b]	2.280		

[a] Centroid of the five carbons above. [b] Centroid of cyclopentadiene ring generated by the three carbons above.

Table V. Selected Bond Angles (deg) for $[(C_5Me_5)_2Yb(III)][Mn(CO)_5]\cdot 1/4\ PhMe$

Mn1-C11-O11	178.2(5)	C21-Mn2-C23	118.6(3)
Mn1-C12-O12	179.4(6)	C21-Mn2-C24	91.7(3)
Mn1-C13-O13	179.1(5)	C21-Mn2-C25	91.9(3)
Mn1-C14-O14	177.9(6)	C22-Mn2-C23	125.5(3)
Mn1-C15-O15	178.6(6)	C22-Mn2-C24	90.4(3)
Mn2-C21-O21	176.7(5)	C22-Mn2-C25	90.0(3)
Mn2-C22-O22	175.9(5)	C23-Mn2-C24	87.8(4)
Mn2-C23-O23	178.6(9)	C23-Mn2-C25	88.5(4)
Mn2-C24-O24	178.6(6)	C24-Mn2-C25	175.7(3)
Mn2-C25-O25	177.8(7)	O11-Yb1-O12	69.20(18)
Yb1-O11-C11	160.4(5)	O11-Yb1-O13	138.85(17)
Yb1-O12-C12	169.1(5)	O12-Yb1-O13	69.65(18)
Yb1-O13-C13	173.7(5)	Cp11[a]-Yb1-O11	95.8
Yb2-O21-C21	170.6(4)	Cp11-Yb1-O12	107.9
Yb3-O22-C22	172.5(4)	Cp11-Yb1-O13	96.7
C11-Mn1-C12	119.0(3)	Cp12-Yb1-O11	97.5
C11-Mn1-C13	115.2(3)	Cp12-Yb1-O12	108.7
C11-Mn1-C14	92.2(3)	Cp12-Yb1-O13	95.4
C11-Mn1-C15	91.5(3)	Cp11-Yb1-Cp12	143.4
C12-Mn1-C13	125.8(3)	O21-Yb2-O21	85.41(24)
C12-Mn1-C14	87.4(3)	O21-Yb2-Cp21	103.5
C12-Mn1-C15	87.8(3)	O21-Yb2-Cp22	102.9
C13-Mn1-C14	89.8(3)	Cp21-Yb2-Cp22	143.8
C13-Mn1-C15	91.7(3)	O22-Yb3-O22	85.85(22)
C14-Mn1-C15	174.9(3)	O22-Yb3-Cp31	103.1
C21-Mn2-C22	116.0(3)	O22-Yb3-Cp32	103.2
		Cp31-Yb3-Cp32	143.8

[a] Cp11, Cp12, etc. are the centroids of the ring carbons of the pentamethylcyclopentadiene ligands.

earlier, the Mn_2Yb_2 unit is not planar. The angle between the normals of the two planes defined by Yb2-Yb3-Mn2 and Yb2-Yb3-Mn2' is 15.2°. The plane defined by Yb2-Yb3-Mn2' is essentially coplanar with the equatorial carbonyl ligands on Mn2. The distortion of the dimeric unit from planarity may also be described by reference to the Mn2-Yb2-Mn2' and Mn2-Yb3-Mn2' planes, which form a dihedral angle of 11.8°. In addition, the dihedral angles formed by extension of the centroids of the Me_5C_5 rings CP21-CP31 and CP22-CP32 (see Table (IV) for the definition of these symbols) are 17.5° and 51.6°, respectively.

The average ytterbium-carbon length in the dimer is 2.574±0.013Å and the average ytterbium-centroid distance is 2.281±0.002Å. The centroid-Yb-centroid angle is 143.8°. These bond lengths are in the range found for other Yb(III) complexes in eight-coordination[1a,b,13] and significantly shorter (0.17 Å) than those found for a Yb(II) ion in eight-coordination.[14] The average ytterbium-oxygen bond length is 2.271±0.002Å, and the average O-Yb-O angle is 85.63±0.22°. The bond parameters in the dimer are very similar to those found in the polymer, even though the coordination number of ytterbium is nine in the latter, the only difference being their ytterbium-oxygen bond lengths. In the polymer the average ytterbium-carbon bond length is 2.589±0.015Å, the ytterbium-centroid distance is 2.304Å, the ytterbium-oxygen bond length is 2.389±0.027Å, and the average O-Yb-O angle is 69.43±0.006°.

The coordination geometries of the pentacarbonylmanganate fragment in the dimer and polymer are very similar, both being related to a trigonal bipyramid as found in $[Ni(phen)_3][Mn(CO)_5]_2$.[15a] The most important feature, perhaps, of the ytterbium-manganese complex is the carbonyl groups that bridge the ytterbium and manganese atoms. In the

dimer two equatorial carbonyl groups are bonded to two different ytterbium atoms, and in the polymer all three equatorial carbonyl groups are bonded to three ytterbium atoms. In the dimer the average Yb-O-C and Mn-C-O angles are 171.6 ± 0.9 and 176.3 ± 0.4°, respectively. In the polymer, these average angles are 167.7 ± 0.5 and 178.9 ± 0.3°.

The average terminal manganese-carbon bond lengths in the dimer and polymer are 1.833 ± 0.007 and 1.820±0.005Å, respectively, whereas the bridging manganese-carbon distances are 1.748 ± 0.013 and 1.791±0.013Å, respectively. These distances may be compared with the average terminal manganese to carbon (equatorial) distance in $Mn_2(CO)_{10}$ of 1.856±0.005Å[16] and in a number of anionic $Mn(CO)_5$ fragments that range from 1.78 to 1.82Å. In the ytterbium-manganese complex the shortened bridging manganese-carbon distance, relative to the terminal distance, is consistent with the view that electron transfer into a neutral $Mn(CO)_5$ frangment puts electron density into molecular orbitals that are C-O anti-bonding and Mn-C bonding. The carbon-oxygen bond lengths are also consistent with this view (Table IV), though these distances are not determined with high accuracy. The variations of the manganese-carbon and carbon-oxygen bond lengths suggest that the resonance structures VII

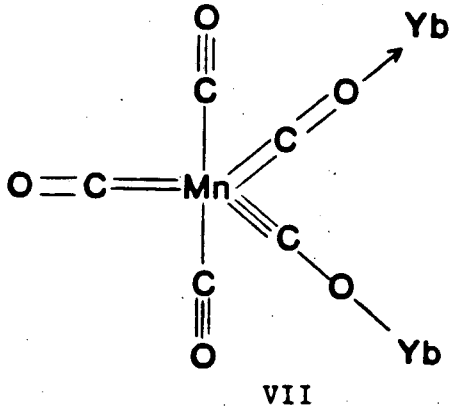

VII

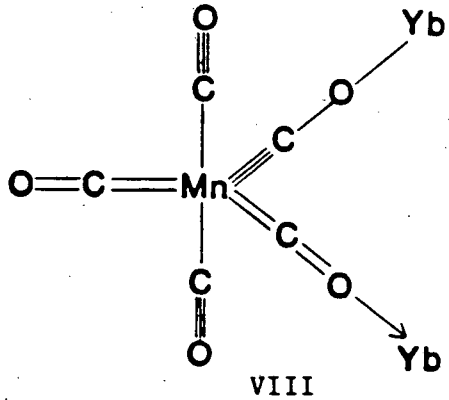

VIII

and VIII are important in the bonding in the contact ion-pair. Further, structures VII and VIII emphasize that contact ion-pair formation tends to localize electron density into the manganese-carbon bonds that are part of the Mn-CO-Yb interaction.

In order to confirm the postulate that the complex $\{[(Me_5C_5)_2Yb(III)][(RC_5H_4)Fe(CO)_2]\}_2$ is indeed a dimer as indicated by its infrared spectrum, a single crystal X-ray diffraction study was performed on the complex. An ORTEP drawing of $[(C_5Me_5)_2Yb(III)(\mu_2\text{-}OC)_2Fe(MeC_5H_4)]_2$ is shown in Figure 6. As can be seen, the MeC_5H_4 and the Me_5C_5 ligands are undergoing substantial thermal motion, which contributes to the large spread in the carbon-carbon bond lengths and angles. The $Yb_2Fe_2C_4O_4$ core, however, does not seem to be undergoing substantial thermal motion. Tables (VI) and (VII) list the bond lengths and bond angles.

The complex is a dimer, similar to that found in the dimeric portion of the electronically equivalent $[(Me_5C_5)_2Yb(III)(\mu\text{-}OC)_2Mn(CO)_3]_2$. Each of the carbonyl groups in the $(MeC_5H_4)Fe(CO)_2$ units is connected to the ytterbium atoms by way of an essentially linear Fe-CO-Yb interaction. The averaged Fe-C-O and Yb-O-C angles are 176.4±0.1° and 170.3±0.3°, respectively. The Yb_2Fe_2 unit is planar since the molecule has a crystallographic inversion center. The dihedral angle formed by the intersection of the Yb_2Fe_2 and YbO(1')O(2) planes is 6.1°, and between the Yb_2Fe_2 and FeC(1)C(2) planes is 5.5°. The plane defined by the FeC_2 atoms passes only 0.08Å from the inversion center at $\frac{1}{2}$, 0,0 but the YbO_2 plane is 0.37Å from the inversion center. Therefore, the bending direction for both planes is approximately parallel to the Fe-Fe vector. The angles formed by the MeC_5H_4 plane with the FeC_2 and Yb_2Fe_2

Figure 6. ORTEP of $\{(C_5Me_5)_2Yb(III)[\mu_2\text{-}OC)_2Fe(C_5H_4Me)\}_2$

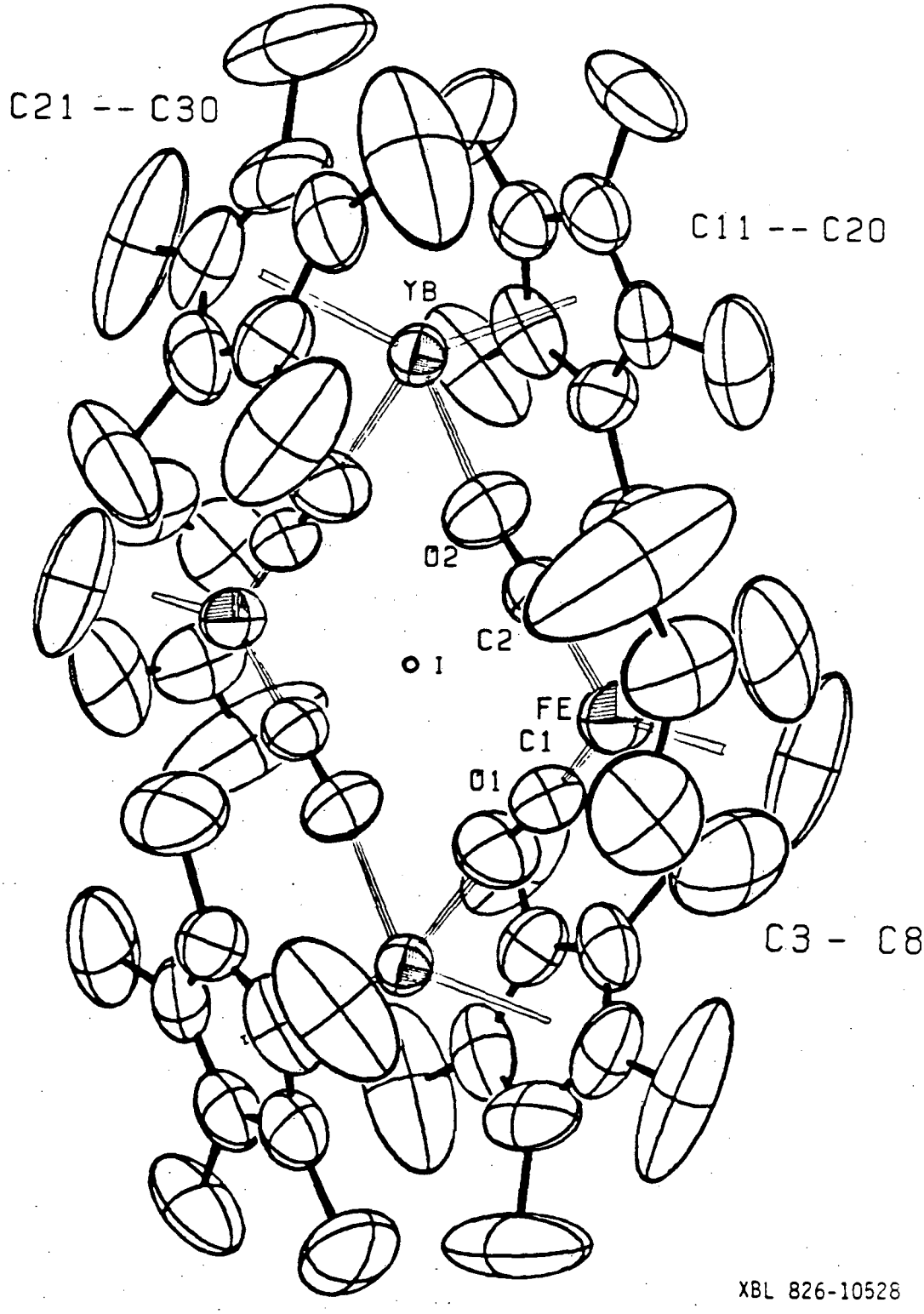

Table VI. Selected Bond Lengths (Å) for $\{[(C_5Me_5)_2Yb(III)][(\mu_2\text{-}OC)_2Fe(C_5H_4Me)]\}_2$

Yb-O1	2.228(4)	C3-C7	1.501(11)
Yb-O2	2.230(4)	C3-C4	1.374(13)
Yb-C11	2.565(5)	C4-C5	1.387(17)
Yb-C12	2.598(5)	C5-C6	1.353(17)
Yb-C13	2.609(5)	C6-C7	1.332(13)
Yb-C14	2.572(5)	C7-C8	1.415(11)
Yb-C15	2.545(5)	C11-C12	1.381(8)
Yb-Cp2*	2.290	C12-C13	1.409(8)
Yb-C21	2.577(6)	C13-C14	1.385(8)
Yb-C22	2.590(6)	C14-C15	1.414(9)
Yb-C23	2.590(5)	C15-C11	1.373(8)
Yb-C24	2.559(6)	C11-C16	1.547(9)
Yb-C25	2.567(6)	C12-C17	1.530(8)
Yb-Cp3*	2.296	C13-C18	1.540(9)
Fe-C1	1.669(6)	C14-C19	1.498(9)
Fe-C2	1.673(5)	C15-C20	1.549(8)
Fe-C3	2.106(7)	C21-C22	1.412(10)
Fe-C4	2.086(8)	C22-C23	1.358(9)
Fe-C5	2.089(8)	C23-C24	1.352(10)
Fe-C6	2.083(8)	C24-C25	1.336(11)
Fe-C7	2.120(6)	C25-C21	1.412(11)
Fe-Cp1*	1.733	C21-C26	1.466(10)
C1-O1	1.201(6)	C22-C27	1.521(9)
C2-O2	1.199(6)	C23-C28	1.488(9)
		C24-C29	1.517(11)
		C25-C30	1.519(10)

* Cp1, Cp2, and Cp3 are the centroids of the rings C3-C7, C11-C15, and C21-C25, respectively.

Table VII. Selected Bond Angles (deg) for $\{[(C_5Me_5)_2Yb(III)][(\mu_2\text{-}OC)_2Fe(C_5H_4Me)]\}_2$

O1'-Yb-O2	87.92(15)	C16-C11-C12	127.0(7)
O1'-Yb-Cp2*	105.0	C16-C11-C15	125.3(7)
O1'-Yb-Cp3*	103.0	C17-C12-C11	124.9(6)
O2-Yb-Cp2	104.9	C17-C12-C13	125.1(7)
O2-Yb-Cp3	104.2	C18-C13-C12	126.3(7)
Cp2-Yb-Cp3	140.0	C18-C13-C14	125.6(7)
C1-Fe-C2	87.80(23)	C19-C14-C13	123.3(8)
C1-Fe-Cp1*	135.5	C19-C14-C15	129.1(8)
C2-Fe-Cp1	136.7	C20-C15-C11	126.3(7)
Yb'-O1-C1	169.7(4)	C20-C15-C14	124.7(7)
Yb-O2-C2	170.8(4)	C25-C21-C22	105.0(6)
Fe-C1-O1	176.6(5)	C21-C22-C23	107.4(6)
Fe-C2-O2	176.2(4)	C22-C23-C24	109.7(6)
C7-C3-C4	106.1(9)	C23-C24-C25	108.7(7)
C3-C4-C5	107.5(11)	C24-C25-C21	109.1(7)
C4-C5-C6	109.9(12)	C26-C21-C22	125.5(11)
C5-C6-C7	110.7(13)	C26-C21-C25	129.3(11)
C6-C7-C3	105.7(9)	C27-C22-C21	125.2(8)
C3-C7-C8	131.9(13)	C27-C22-C23	127.1(8)
C6-C7-C8	122.2(14)	C28-C23-C22	124.9(8)
C15-C11-C12	107.6(5)	C28-C23-C24	125.3(8)
C11-C12-C13	108.9(5)	C29-C24-C23	126.0(11)
C12-C13-C14	107.3(5)	C29-C24-C25	125.2(11)
C13-C14-C15	107.2(5)	C30-C25-C21	122.6(12)
C14-C15-C11	109.0(5)	C30-C25-C24	127.6(12)

* Cp1, Cp2, and Cp3 are the centroids of the rings C3-C7, C11-C15, and C21-C25, respectively.

' Primed atoms are related to atoms in the asymmetric unit by the inversion center at $\frac{1}{2}$, 0, 0.

planes are 89.6° and 88.0°, respectively. The MeC_5H_4-rings are orientated so that C(7)C(8) are gauche relative to Fe-C(2), the C(2)FeCp(1)C(7) torsional angle being 34.3°. The Cp(1) and C(4) are eclipsed relative to Fe-C(1), the torsional angle being -0.5°. The Me_5C_5-rings are essentially staggered with respect to each other.

The coordination geometry about the ytterbium atom is pseudo-tetrahedral, defining the midpoint of the Me_5C_5-group as occupying one coordination site. The centroid-Yb-centroid and O-Yb-O angles are 140° and 87.92(15)°, respectively. The averaged Yb-O bond length of 2.229±0.001Å is similar to that found in the ytterbium-manganese complex of 2.277±0.002Å. The averaged Yb-C distance of 2.577±0.016Å and the averaged Yb-centroid distance is 2.293Å, again similar to that found in the ytterbium-manganese complex.

In the discussion that follows we will compare the metrical parameters of $[(Me_5C_5)_2Yb(III)(\mu\text{-}OC)_2Fe(MeC_5H_4)]_2$ with the related anion $[Et_4N][CpFe(CO)_2AlPh_3]$, which contains a direct Fe-Al bond, and with the electronically equivalent $[(Me_5C_5)_2Yb(III)(\mu\text{-}OC)_2Mn(CO)_3]_2$. The averaged Fe-C($MeC_5H_4$)bond length in the Yb-Fe complex of 2.097±0.013Å is identical within experimental error to that found in the Fe-Al compound of 2.097±0.003Å. These bond lengths are also identical to those found in <u>trans-</u> and <u>cis-</u> $Cp_2Fe_2(\mu\text{-}CO)_2(CO)_2$. The averaged Fe-C(CO) distance in the Yb-Fe compound of 1.671±0.002Å is shorter than that found in the Fe-Al compound (1.731±0.001Å) and the C-O bond length is longer, 1.200±0.001Å vs. 1.158±0.001Å, than that found in the Fe-Al compound. Thus, the carbon monoxide ligands in the Yb-Fe compound carries significantly more negative charge, relative to the Fe-Al compound, as suggested by the carbon monoxide stretching frequencies

(Table III). The bond length data suggest that the electronic structure of the Yb-Fe complex may be represented by the two resonance forms IX and X, and the Al-Fe complex by XI.

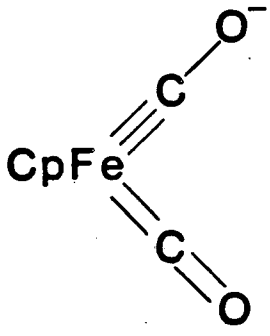

IX

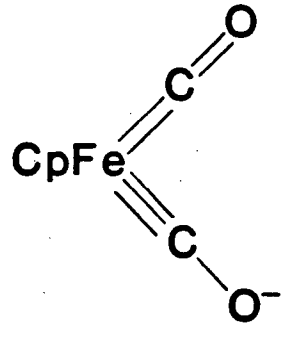

X

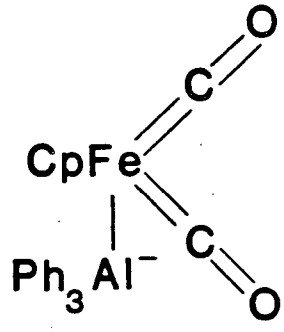

XI

The averaged, bridging Fe-C(CO) bond length of 1.671±0.002Å in the Yb-Fe complex is shorter (1.784±0.002Å) than that found for the Mn-C(CO) bond distance in the Yb-Mn complex. This is expected since the radius of iron is ca. 0.6Å smaller than that of manganese. Thus, the Yb-Fe and Yb-Mn dimers are very similar in a geometrical and electronic sense.

Examination of the ^1H NMR spectrum of $\{[(Me_5C_5)_2Yb(III)][Me_3SiC_5H_4Mo(CO)_3]\}_2$ (see Table I) reveals that there are two types of $Me_3SiC_5H_4$ and C_5Me_5 resonances. This is inconsistent with the C_{2h} structure which was proposed from the IR spectrum of the complex. In order to at least define the solid state structure of the complex a single crystal X-ray diffraction study was performed. The crystal structure of $\{[(Me_5C_5)_2Yb(III)][Me_3SiC_5H_4Mo(CO)_3]\}_2$ consists of crystallographically centrosymmetric dimers (see Figure 7 for an ORTEP drawing). The bond distances and angles for this compound can be found in Tables (VIII) and (IX), while the crystal data is found in the Experimental Section and tables of positional and thermal parameters are

Figure 7. ORTEP of $\{(C_5Me_5)_2Yb(III)(\mu_2\text{-}OC)_2Mo(CO)(C_5H_4SiMe_3)\}_2$

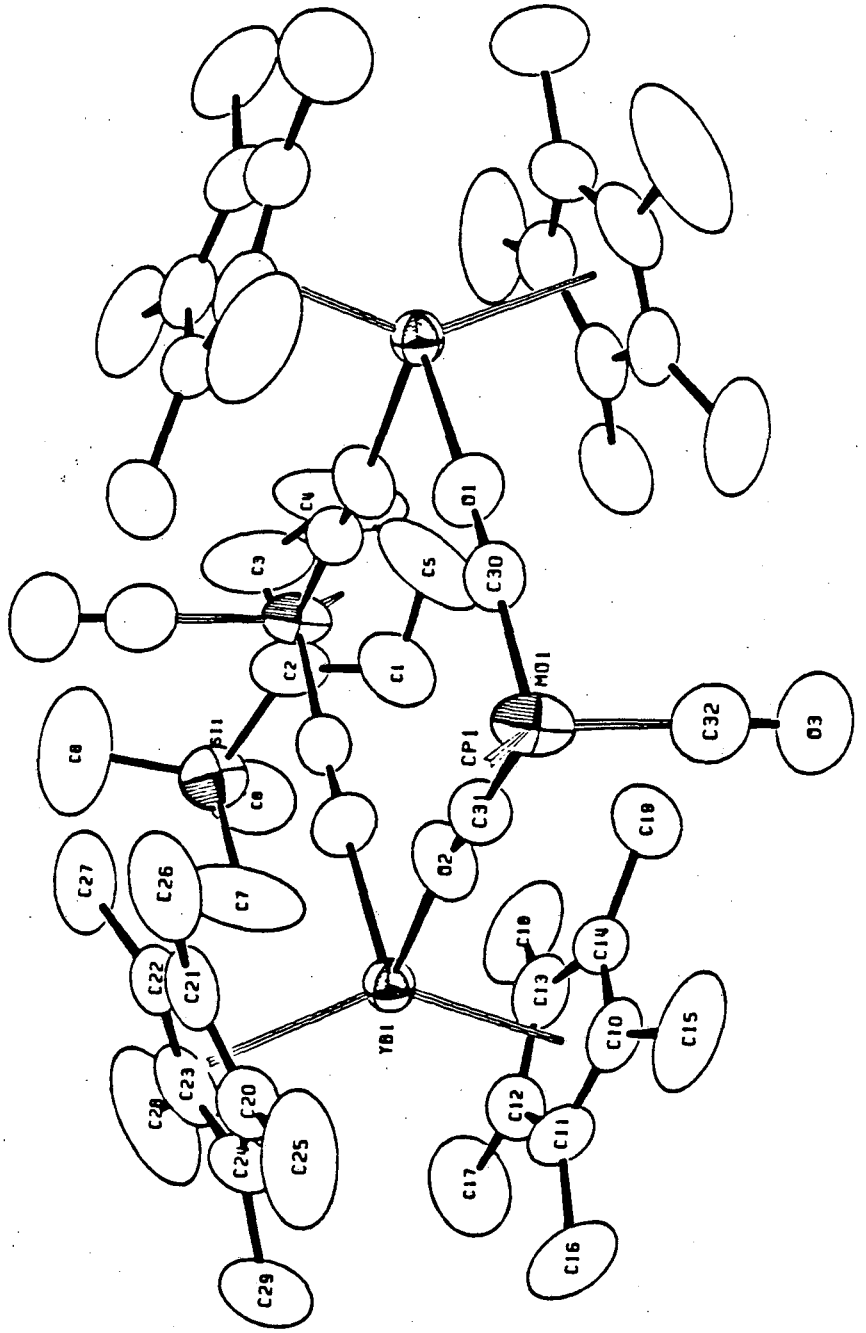

Table VIII. Selected Bond Lengths (Å)for $\{[(C_5Me_5)_2Yb(III)][(\mu_2\text{-}OC)_2Mo(CO)(C_5H_4SiMe_3)]\}_2$

Yb1-O1	2.245(3)	C2-C3	1.426(6)
Yb1-O2	2.245(3)	C3-C4	1.383(9)
Yb1-C10	2.581(4)	C4-C5	1.387(9)
Yb1-C11	2.596(4)	Si1-C2	1.858(4)
Yb1-C12	2.597(4)	Si1-C6	1.821(6)
Yb1-C13	2.581(4)	Si1-C7	1.834(6)
Yb1-C14	2.565(4)	Si1-C8	1.831(5)
Yb1-C111*	2.295(1)	C10-C11	1.369(5)
Yb1-C20	2.565(4)	C10-C14	1.391(5)
Yb1-C21	2.578(4)	C11-C12	1.409(5)
Yb1-C22	2.592(4)	C12-C13	1.403(6)
Yb1-C23	2.587(4)	C13-C14	1.410(6)
Yb1-C24	2.600(4)	C10-C15	1.517(5)
Yb1-C112*	2.296(1)	C11-C16	1.504(6)
Mo1-C1	2.369(4)	C12-C17	1.494(6)
Mo1-C2	2.377(4)	C13-C18	1.500(6)
Mo1-C3	2.383(4)	C14-C19	1.512(6)
Mo1-C4	2.377(6)	C20-C21	1.385(6)
Mo1-C5	2.387(5)	C20-C24	1.385(6)
Mo1-C101*	2.054(1)	C21-C22	1.376(6)
Mo1-C30	1.890(4)	C22-C23	1.405(6)
Mo1-C31	1.880(4)	C23-C24	1.417(6)
Mo1-C32	1.928(5)	C20-C25	1.490(6)
C30-O1	1.185(4)	C21-C26	1.508(6)
C31-O2	1.196(4)	C22-C27	1.511(6)
C32-O3	1.169(5)	C23-C28	1.507(6)
C1-C2	1.412(6)	C24-C29	1.475(6)
C1-C5	1.434(7)		

* C111, C112, and C101 are the centroids of the rings C10-C14, C20-C24, and C1-C5, respectively.

Table IX. Selected Bond Angles (deg) $\{[(C_5Me_5)_2Yb(III)][(\mu_2Mo(CO)(C_5H_4SiMe_3)]\}_2$

C2-Si1-C6	110.2(3)	C22-C23-C24	106.6(4)
C2-Si1-C7	109.71(23)	C23-C24-C20	107.8(4)
C2-Si1-C8	109.12(23)	C24-C20-C21	108.5(4)
C6-Si1-C7	110.0(4)	C24-C20-C25	125.0(5)
C6-Si1-C8	109.8(3)	C21-C20-C25	126.3(5)
C7-Si1-C8	108.0(3)	C20-C21-C26	127.6(5)
Si1-C2-C1	126.6(4)	C22-C21-C26	123.6(5)
Si1-C2-C3	127.6(4)	C21-C22-C27	127.5(6)
C1-C2-C3	105.7(5)	C23-C22-C27	123.7(5)
C2-C3-C4	109.6(6)	C22-C23-C28	126.6(6)
C3-C4-C5	108.9(6)	C24-C23-C28	126.3(6)
C4-C5-C1	107.3(6)	C23-C24-C29	124.9(6)
C5-C1-C2	108.6(5)	C20-C24-C29	126.5(6)
C14-C10-C11	109.1(4)	O1-Yb1-O2	88.26(10)
C10-C11-C12	108.4(4)	O1-Yb1-C111*	105.02(6)
C11-C12-C13	107.3(4)	O1-Yb1-C112*	104.89(6)
C12-C13-C14	107.6(4)	O2-Yb1-C111	102.55(6)
C13-C14-C10	107.6(4)	O2-Yb1-C112	103.47(6)
C15-C10-C11	123.5(5)	C111-Yb1-C112	140.56(1)
C15-C10-C14	127.2(5)	C30-Mo1-C31	83.21(15)
C16-C11-C10	125.1(5)	C30-Mo1-C32	89.33(17)
C16-C11-C12	125.6(5)	C30-Mo1-C101*	129.53(10)
C17-C12-C11	127.7(5)	C31-Mo1-C32	88.43(17)
C17-C12-C13	124.4(5)	C31-Mo1-C101	128.81(11)
C18-C13-C12	127.6(5)	C32-Mo1-C101	123.84(13)
C18-C13-C14	124.4(5)	Yb1-O1-C30	178.8(3)
C19-C14-C10	125.8(5)	Yb1-O2-C31	166.8(3)
C19-C14-C13	126.6(5)	Mo1-C30-O1	177.8(3)
C20-C21-C22	108.6(4)	Mo1-C31-O2	177.3(3)
C21-C22-C23	108.5(4)	Mo1-C32-O3	179.9(3)

* C111, C112, and C101 are the centroids of the rings C10-C14, C20-C24, and C1-C5, respectively.

found in Appendix (I).

The four metal atoms of this dimer are coplanar as imposed by the inversion center. The $Me_3SiC_5H_4$ rings are <u>trans</u> with respect to the plane defined by the metal atoms confirming the C_{2h} structure proposed from the ir of the complex. The four metal atoms are bridged by four CO groups by way of Mo-C-O-Yb interactions. The Yb-O-C bond angles are 166° and 178°, respectively, while the Mo-C-O bond angles are 178° and 177°. Thus, the carbonyl groups bridge the metal atoms in a linear fashion as in the Mn-Yb and Fe-Yb compounds.

The dihedral angle formed by the intersection of the Yb_2Mo_2 and YbO(1)O(2) planes is 1.6°, and between the Yb_2Mo_2 and MoC(3')C(3) planes is 1.9°. Thus the $Mo_2Yb_2(CO)_4$ core is very nearly planar. The angle between the $Me_3SiC_5H_4$ ring and the Mo_2Yb_2 plane is 56°. The $Me_3SiC_5H_4$ rings are canted so that the Me_3Si group fits into the slot between the two C_5Me_5 rings bound to ytterbium, and the Me_5C_5 rings are staggered with respect to one another.

The coordination geometry about ytterbium is pseudo-tetrahedral if the centroids of each of the C_5Me_5 rings are defined as occupying one coordination site. The oxygen atoms of the bridging carbonyl groups occupy the other coordination sites. The centroid-Yb-centroid angle and O(1)-Yb-O(2) angles of 140° and 88.3° are unexceptional. The Yb-C(ring) averaged bond length is 2.584±0.012Å and in the range found for $(C_5Me_5)_2Yb(III)$ complexes. The Yb-O(1,2) distances are 2.245(3)Å and are slightly shorter (0.03Å) than those found in the Fe-Yb on Mn-Yb complexes. Overall, the coordination geometry about ytterbium is identical to that in the Fe-Yb complex.

Comparison of the geometry of the complex $[nBu_4N^+][CpMo(CO)_3^-]$[17]

with $[(Me_5C_5)_2Yb(II)(\mu_2\text{-}OC)_2Mo(CO)(Me_3SiC_5H_4)]_2$ is revealing. The averaged Mo-C (Cp) distances are identical at 2.371±0.009Å in the ammonium salt and 2.379±0.007Å in the Yb complex. The $Mo\text{-}C_{(ave)}$ distance of 1.909±0.009Å in the ammonium complex is longer than the Mo-C bridging distance of 1.885±0.005Å in the Yb complex, and shorter than the terminal distance of 1.928(4)Å. The averaged C-O (bridging) distance of 1.191±0.005Å is longer than the $C\text{-}O_{(ave)}$ distance in the ammonium complex 1.176±0.006Å. The C-O terminal distance in the Yb complex is shorter at 1.169(5)Å. This pattern of bond length variations is similar to those observed in the complexes $[(C_5Me_5)_2Yb(III)\cdot THF][\mu_2\text{-}(OC)CO(CO)_3]$, $[(Me_5C_5)_2Yb(III)\mu_2\text{-}(CO)_2Mn(CO)_3]_2$ and $[(Me_5C_5)_2Yb(III)\mu_2(OC)_2FeC_5H_4Me]_2$.

Some conclusions can be formed from the structural studies of the Mn-Yb, Fe-Yb, and Mo-Yb complexes. The complexes tend to form dimeric structures giving the ytterbium atom a formal coordination number of eight. In the structure of the manganese complex, the ytterbium atom also increases its coordination number to nine by forming an infinite polymer. The polymerization is prevented in the case of molydenum and iron because of the presence of the cyclopentadienyl groups.

Coordination of the CO ligands to the ytterbium atom causes systematic changes in the metal carbon and carbon oxygen bond lengths. When compared to terminal CO groups, the bridging CO groups have shorter metal carbon and longer carbon oxygen bond lengths. A cautionary note must be added here, however. The data for all these structures was collected to a scattering angle of 45° in 2θ. This means that the CO bond lengths are close to the inherent resolution of the structure, and may not be meaningful. The metal carbon bond lengths are, however, more

trustworthy.

The observed distortions in the M-CO bonds as well as the lowered ir stretching frequencies would indicate that the C-O bond has been weakened. The lack of reactivity of these complexes with H_2 indicates that the weakening of the CO bond is not large enough to cause a drastic change in the observed chemical properties of the complexes. Although the chemical reactivities of these complexes have proven a disappointment, the iron and molybdenum complexes have shown some unexpected solution properties as are discussed below.

Variable Temperature NMR Studies

Variable temperature proton NMR studies of all the complexes reported here reveal that the proton chemical shifts follow a linear dependence of chemical shift vs. 1/T(K) as is expected for paramagnetic lanthanide complexes.[18] The ^1H NMR spectra of the iron complexes consist of resonances assignable to one type of RC_5H_4 resonance and one type of C_5Me_5 group in a 1:2 ratio from 100° to -80°C.

At room temperature the proton NMR spectrum of the complex $\{[(Me_5C_5)_2Yb(III)][Me_3SiC_5H_4Mo(CO)_3]\}_2$ has resonances assignable to two different kinds of $Me_3SiC_5H_4$ environments. These two sets of resonances have an area ratio of 0.88:1 (relative to one another). This complex also has three different C_5Me_5 environments which have an area ratio of 0.44:1.0:0.44 relative to one another (see Figures 8 and 9). When the Mo complex is heated to temperatures greater than 135°C resonances assignable to only one type of RC_5H_4 environment, and one type of Me_5C_5 environment are observed.

Figure 8. 250MHz ^{1}H NMR Spectrum of the C_5Me_5 Protons of $\{(C_5Me_5)_2Yb(III)(\mu_2\text{-}OC)_2Mo(CO)(C_5H_4SiMe_3)\}_2$

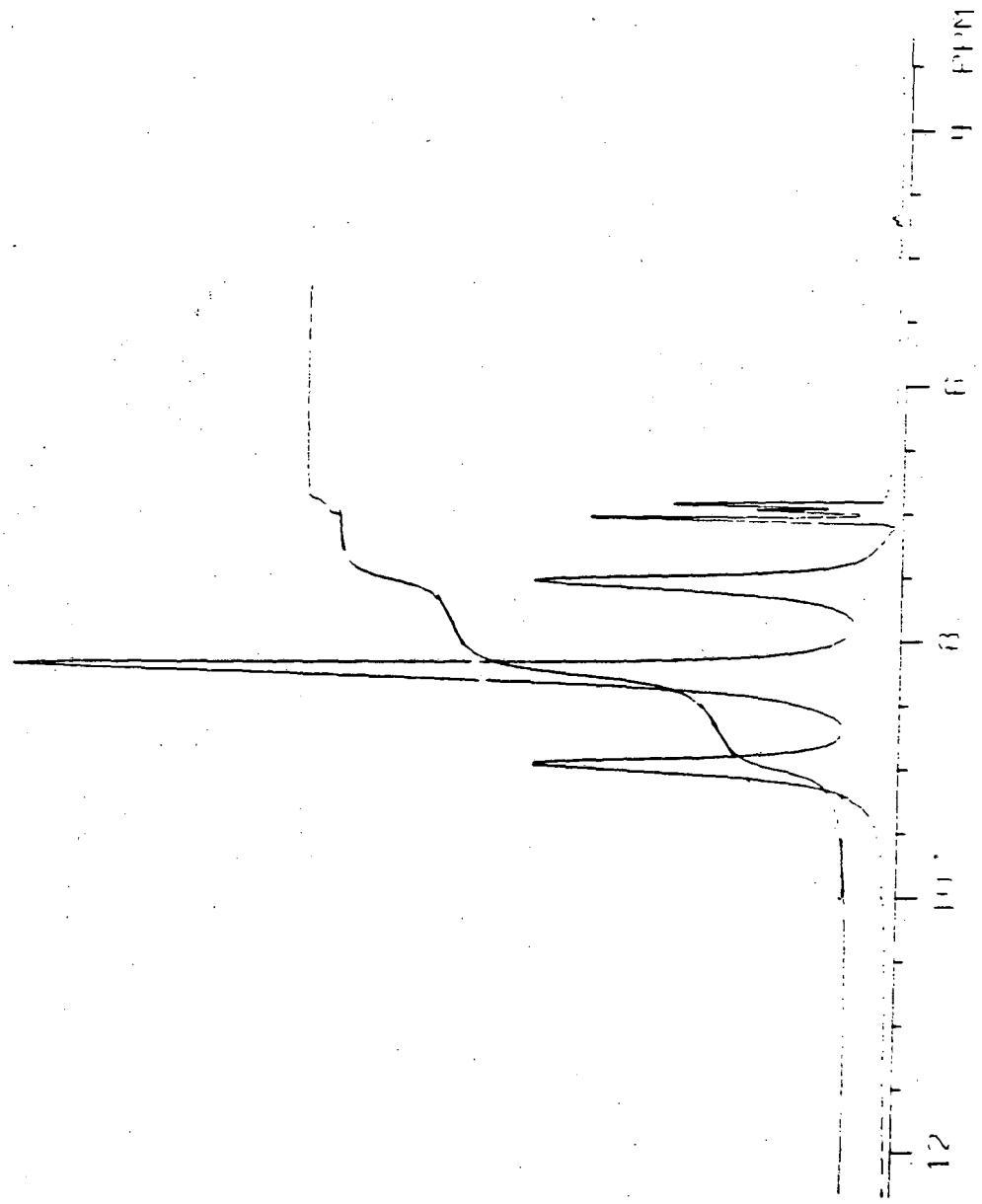

Figure 9. 250MHz ^{1}H NMR Spectrum of the $Me_3SiC_5H_4$ Protons of $\{(C_5Me_5)_2Yb(III)(\mu_2\text{-}OC)_2Mo(CO)(H_4C_5SiMe_3)\}_2$

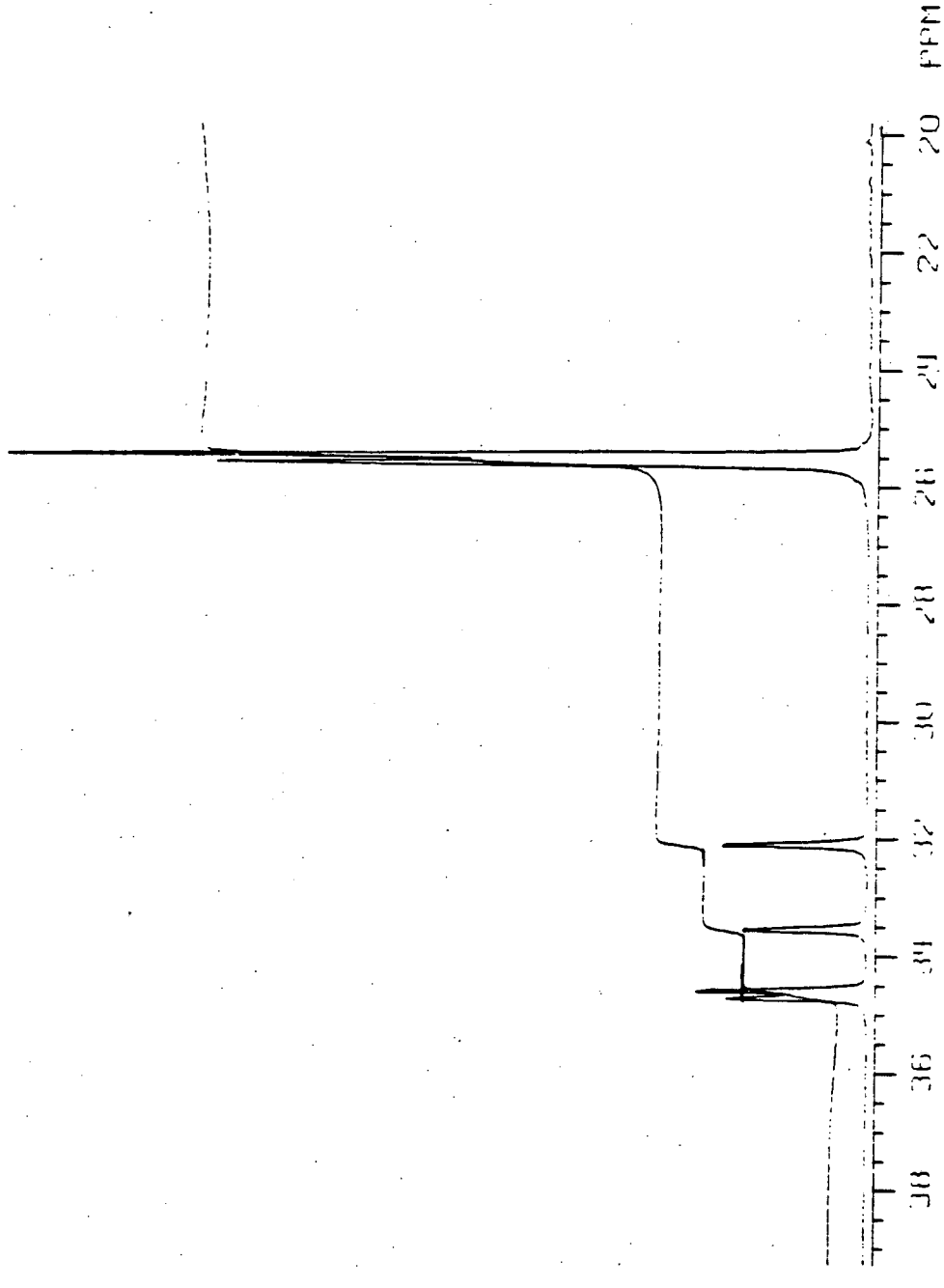

The Mo complexes exist in the solid state as centrosymmetric dimers having structure XII (see below). The ^1H NMR of such a complex should have one type of cyclopentadienyl group, and one type of pentamethylcyclopentadienyl group. We assign the larger area set of cyclopentadienyl resonances as well as the larger area single C_5Me_5 resonance to this complex. We assign the remaining resonances in the spectrum to XIII (see below) an isomer of compound XII. Isomer XIII differs from isomer XII in that the cyclopentadieynyl rings bonded to Mo are cis relative to the MoMo'YbYb' plane rather than trans.

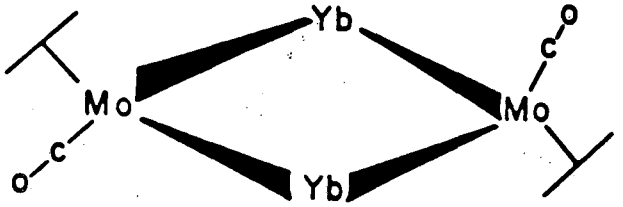

trans C2h - 55%

XII

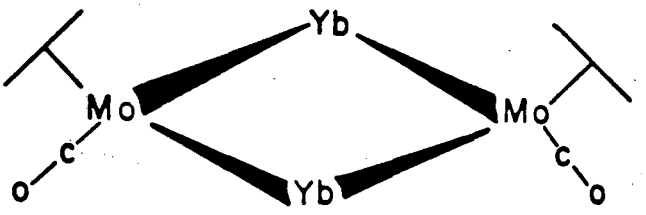

cis C2v - 45%

XIII

Integration of the areas of the peaks for the two compounds gives a value of ca. 55% trans to 45% cis in solution at any given time. Lowering the temperature does not change the cis-trans ratio. Raising the temperature to 135°C causes the cis-trans equilibrium to become fast on the NMR time scale, and only resonances due to one $Me_3SiC_5H_4$ environment and one C_5Me_5 environment are observed.

The simple two site exchange equation which is used to calculate the activation energy for this equilibrium is given by equation (1)[19]

$$\frac{\Delta G^{\ddagger}}{RT_c} = \ln(\sqrt{2}\ R/\pi\ Nh) + \ln(T_c/\delta\nu) \qquad (1)$$

where N is Avogadro's number, T_c is the temperature of coalescence, and $\delta\nu$ is the chemical shift difference of the two resonances in Hz at coalescence. The equation does not account for a difference in population of the two species which give rise to the coalescing peaks. In this case, the difference in population is 55:45 and disregarding this difference does not have a large effect on the calculated $\Delta G^{\ddagger}$. Measurement of $\delta\nu$ at T_c for paramagnetic complexes is accomplished by plotting the chemical shift vs. 1/T(K) at temperatures where the exchange is slow on the NMR timescale and extrapolating to the coalescence temperature.[20] This is shown in Figure 10 for one of the $Me_3SiC_5H_4$ proton resonances.

Unfortunately, the $\Delta G^{\ddagger}$ for the equilibrium could only be calculated from one set of $Me_3SiC_5H_4$ proton resonances. The reason for this is that the temperature dependence of the chemical shift for all of the other resonances in the complex causes the difference in chemical shift between each set of peaks to become smaller as the temperature is raised. Eventually, the difference in chemical shift in each pair becomes unobservable, and the resonances overlap before they can broaden and coalesce due to the exchange phenomenon. The two resonances which do broaden and coalesce due to the equilibrium between isomers, do so only because the difference in chemical shift between them becomes larger as the temperature is raised allowing them to broaden and coalesce at high temperatures. The $\Delta G^{\ddagger}$ calculated using equation (1), a $\delta\nu$ of 137Hz and T_c= 404K is found to be 19.3(1.0) kcal mol^{-1}. The large

Figure 10. Plot of δ vs. 1/T for One Set of $C_5H_4SiMe_3$ Protons of $\{(C_5Me_5)_2Yb(III)(\mu_2\text{-}OC)_2Mo(CO)(H_4C_5SiMe_3)\}_2$

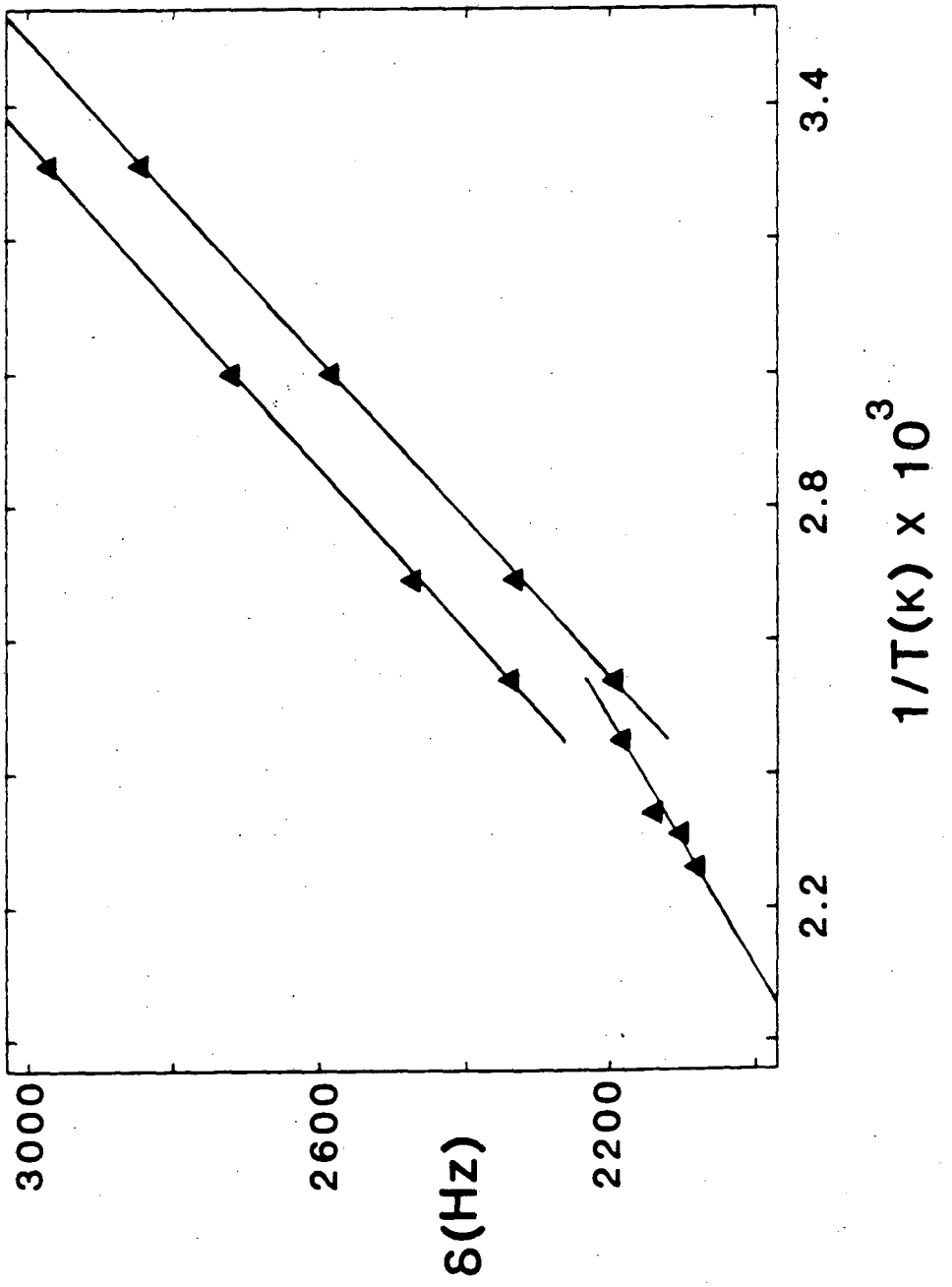

value for $\Delta G^{\ddagger}$ is not inconsistent with a bond breaking process occurring during the isomerization reaction.

It is interesting to note that the infrared spectrum of the complex gives no indication of the presence of more than one isomer in cyclohexane or toluene solution at room temperature (see Table III). Isomer XII has C_{2h} symmetry while isomer XIII has C_{2v} symmetry. It is predicted by group theory that the C_{2h} isomer (XII) should have three infrared active ν-CO bands, and that the C_{2v} isomer XII should have six infrared active ν-CO bands. A reasonable explanation for observing only three bands is that the CO vibrations do not couple well through the O-Yb-O bonds, and therefore the energy differences between the bands for the two isomers are small and are not resolved in the infrared spectrum. The net result is that only three bands are observed which are really a composite of the nine bands predicted for the two isomers.

In order to test whether or not the isomerization is an inter- or intra-molecular process, the following crossover reaction was performed. Equimolar quantities of $\{[(Me_5C_5)_2Yb(III)][(C_5H_5)Mo(CO)_3]\}_2$ and $\{[(Me_5C_5)_2Yb(III)][(Me_3SiC_5H_4)Mo(CO)_3]\}_2$ were reacted with one another at room temperature. The ^1H NMR spectrum of the reaction mixture (Figure 11) shows resonances due to both starting materials as well as another set of resonances which are due to the mixed Cp ring product i.e., $[(Me_5C_5)_2Yb(III)]_2[(C_5H_5)Mo(CO)_3][(Me_3SiC_5H_4)Mo(CO)_3]$. Unfortunately, the ratio of the mono-ring to mixed-ring products cannot be measured accurately because each compound exists as <u>cis</u> and <u>trans</u> isomers in solution giving a total of six compounds in solution. Examination of Figure 11 shows that these cannot possibly be integrated to give a believable product ratio.

Figure 11. 250MHz ^{1}H NMR Spectrum of a 1:1 Mixture of $\{(C_5Me_5)_2Yb(III)(\mu_2\text{-}OC)_2Mo(CO)(C_5H_5)\}_2$ and $\{(C_5Me_5)_2Yb(III)(\mu_2\text{-}OC)_2Mo(CO)(C_5H_4SiMe_3)\}_2$

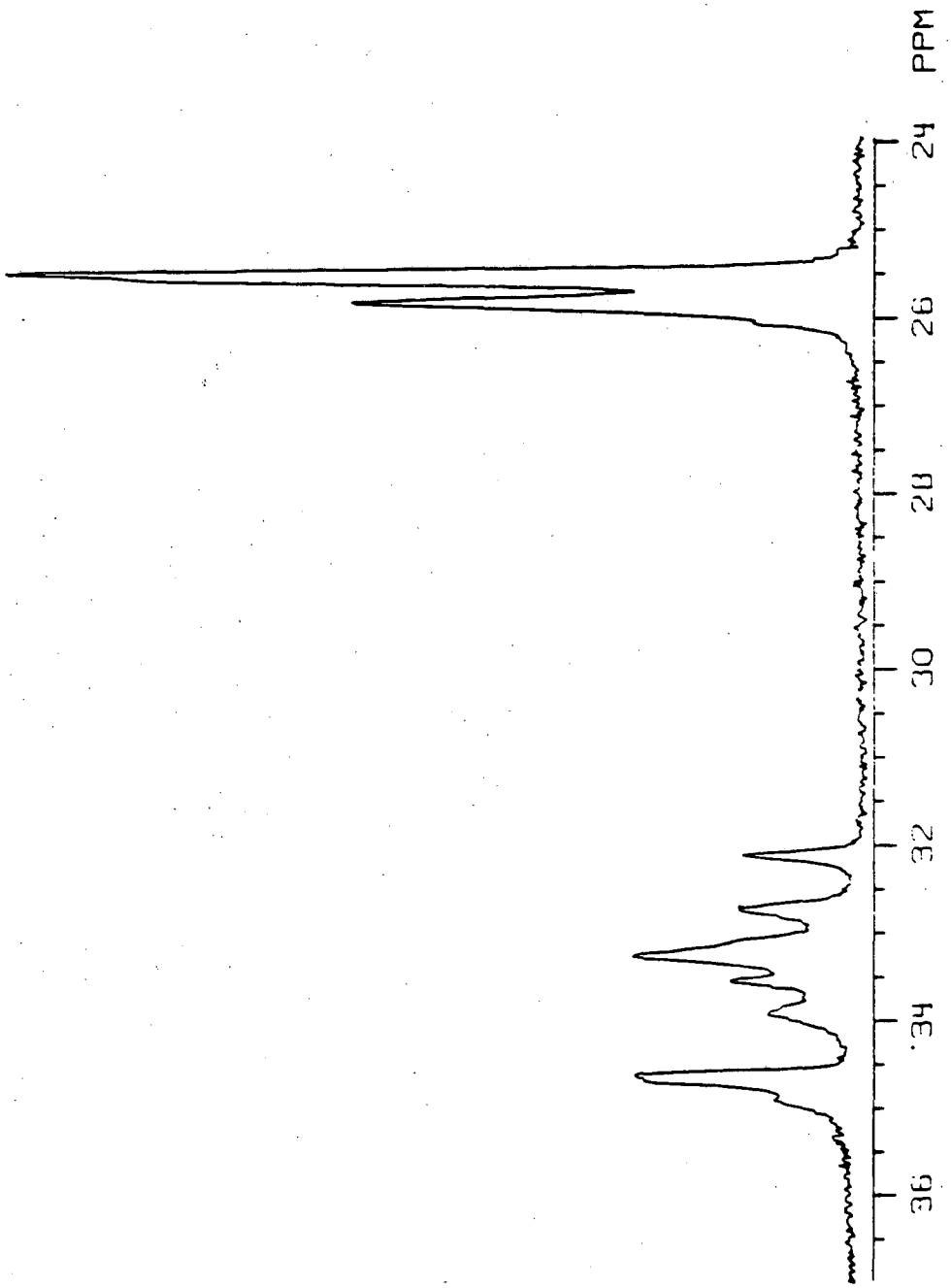

The fact that we observe a crossover reaction means that the dimeric molecules are dissociating in some fashion in solution. The most probable bond to break is a Yb-O bond which would allow the complex to open up and react with another molecule of itself causing cross-over, or by breaking apart into monomeric complexes, which will also lead to crossover. We cannot determine if the isomerization occurs by the same mechanism as the crossover reaction or not, since we cannot separate ^1H NMR resonances from one another.

In order to determine whether the non-rigidity of the Mo compound was a general phenomenon, and to see if we could quantitatively understand the crossover in absence of isomerization, a crossover experiment was performed with the $\{[(Me_5C_5)_2Yb(III))(RC_5H_4Fe(CO)_2)]\}_2$ compounds. These compounds offer the advantage that they cannot exist as isomers in solution, and only three compounds can be formed in a crossover reaction involving them. When the $Me_3SiC_5H_4Fe$ derivative and the MeC_5H_4Fe derivative are mixed at room temperature, the ^1H NMR of the mixture reveals a mixture of the two starting materials and the mixed ring product in a 1:1:2 statistical ratio as shown in Figure 12. When the mixture of products from the crossover reaction is heated to 164°C only one MeC_5H_4 and one $Me_3SiC_5H_4$ environment is observed. This means that the crossover equilibrium has become fast on the NMR time scale at 164°C. The $\Delta G^{\ddagger}$ for this process can be estimated using the two site exchange equation (a plot of δ vs. 1/T(K) is shown in Figures 13a-c). As can be seen in the plots shown in Figures 13a-c, the coalescence temperature and peak separations at coalescence differ from peak to peak. The average value of $\Delta G\ddagger$ calculated from all six plots is 19.4(±0.4)kcal mol^{-1}. The range of calculated values is 19.0 to

Figure 12. ^1H NMR Spectrum of a 1:1 Mixture of $\{(C_5Me_5)_2Yb(III)(\mu_2\text{-}OC)_2Fe(C_5H_4Me)\}_2$ and $\{(C_5Me_5)_2Yb(III)(\mu_2\text{-}OC)_2Fe(C_5H_4SiMe_3)\}_2$

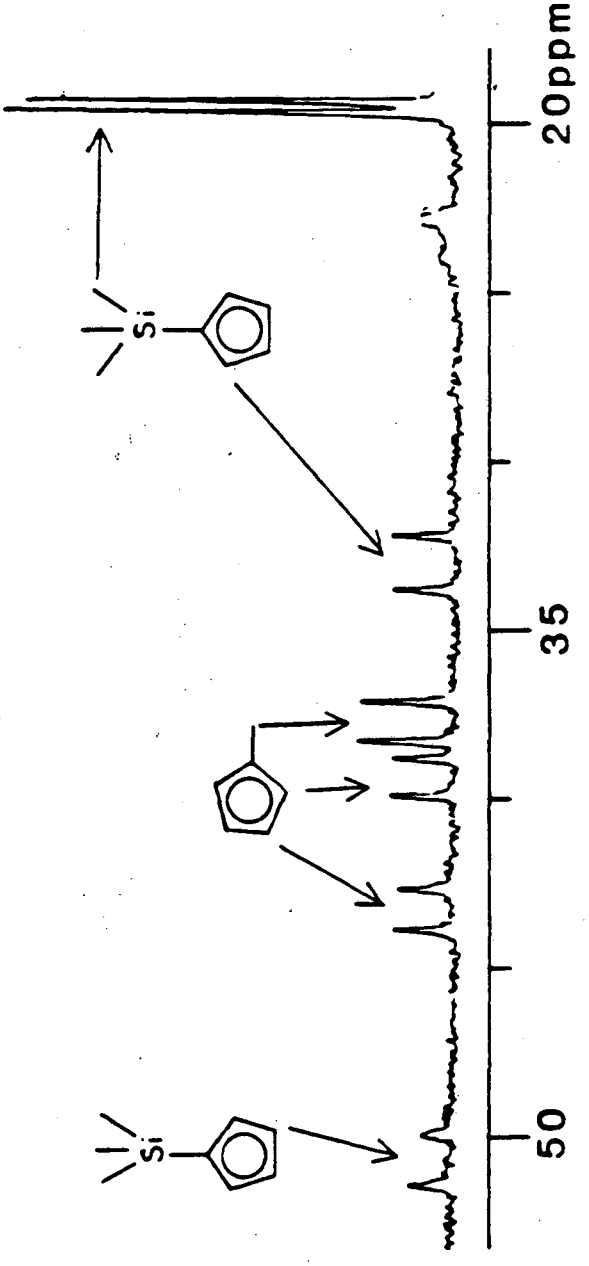

Figure 13a. Plot of δ vs. 1/T for the Me_3Si Protons of the Yb-Fe Crossover Reaction

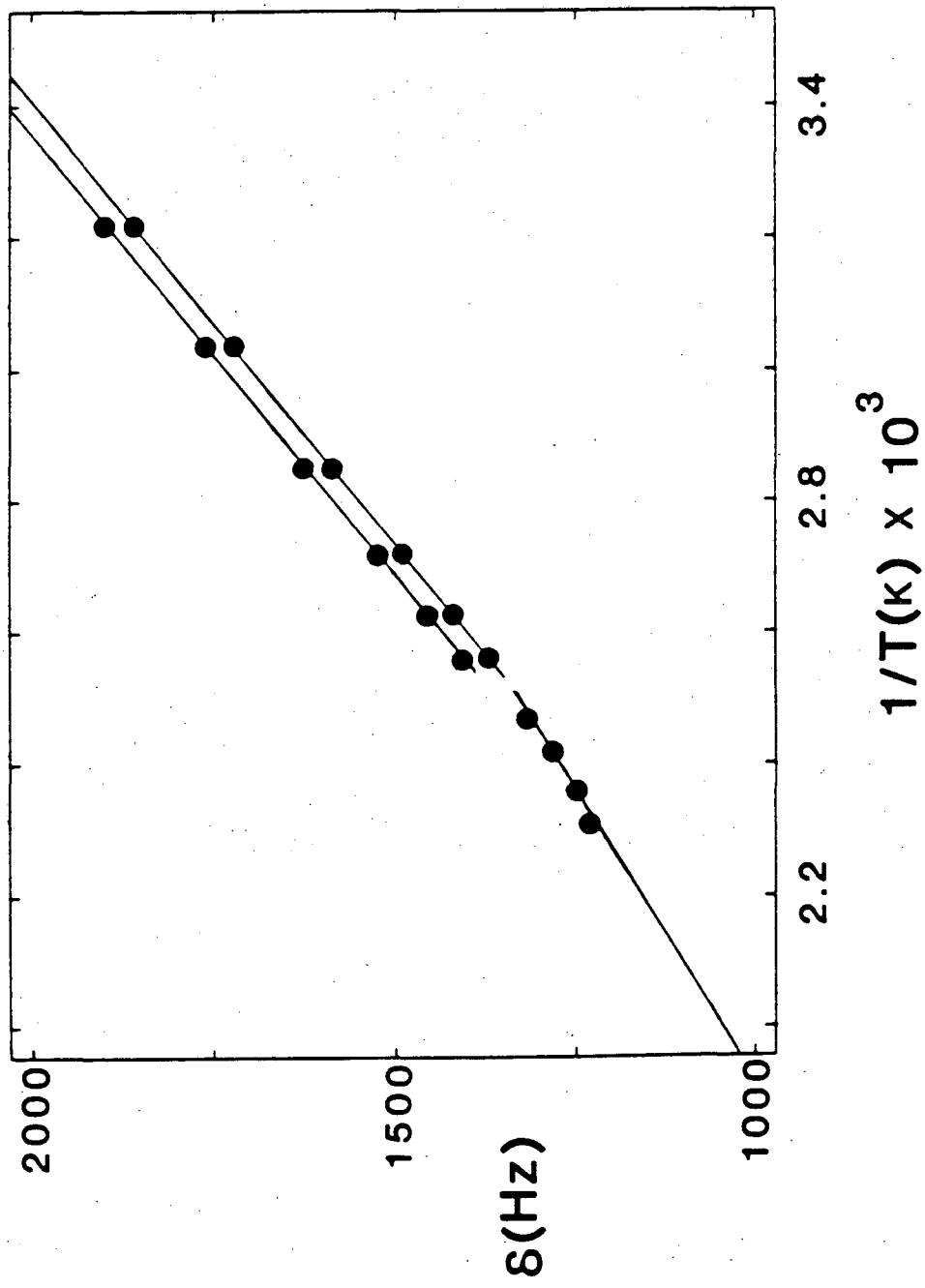

Figure 13b. Plot of δ vs. 1/T for the Fe-Yb Crossover Reaction ● = one set of Me_3SiCp Ring Protons; ▲ = One set of MeCp Ring Protons; ■ = the Other Set of Me_3SiCp Ring Protons

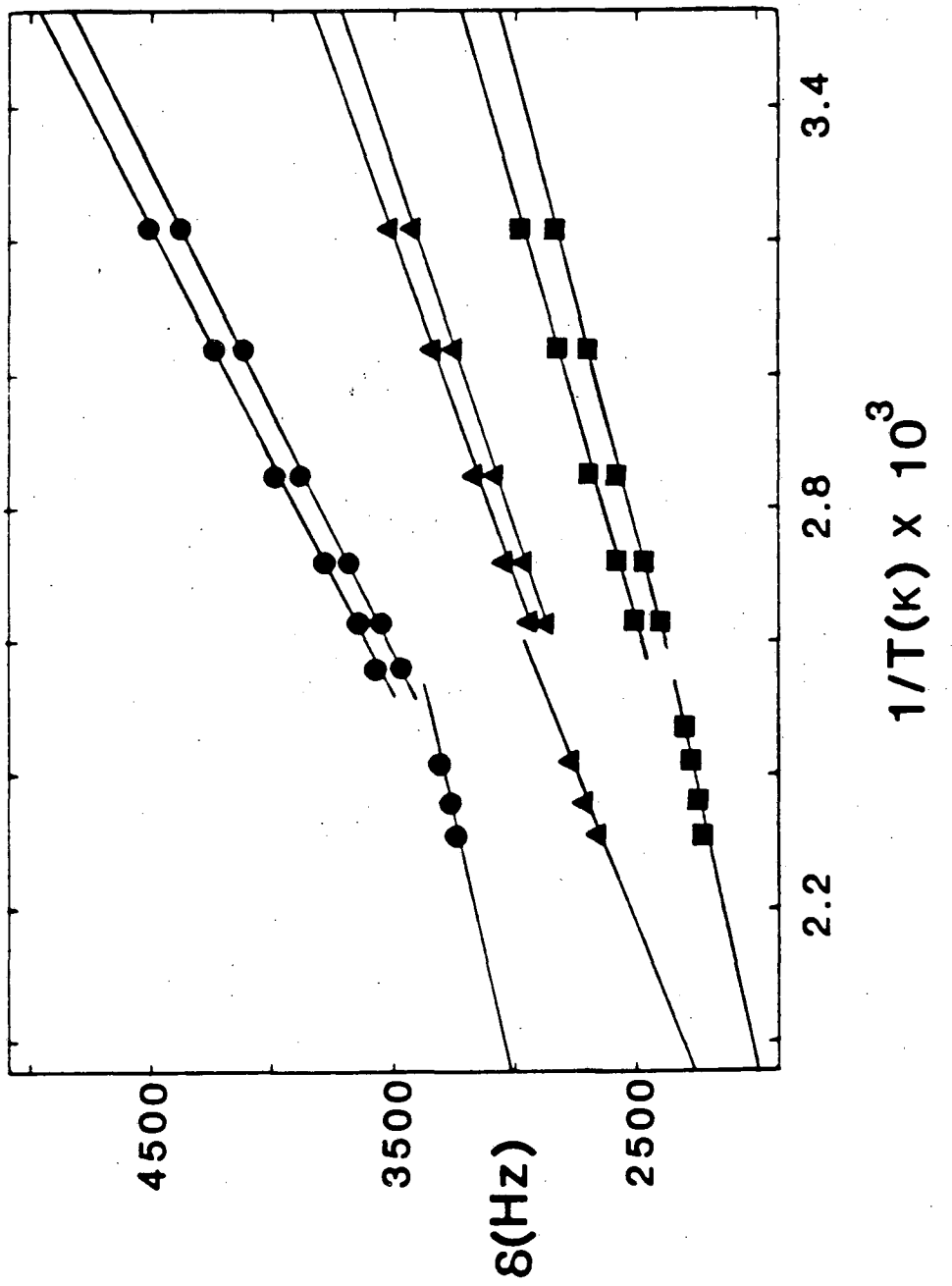

Figure 13c. Plot of δ vs. 1/T for the Fe-Yb Crossover Reaction. ▲ = one Set of MeCp Ring Protons; ■ = Me Protons

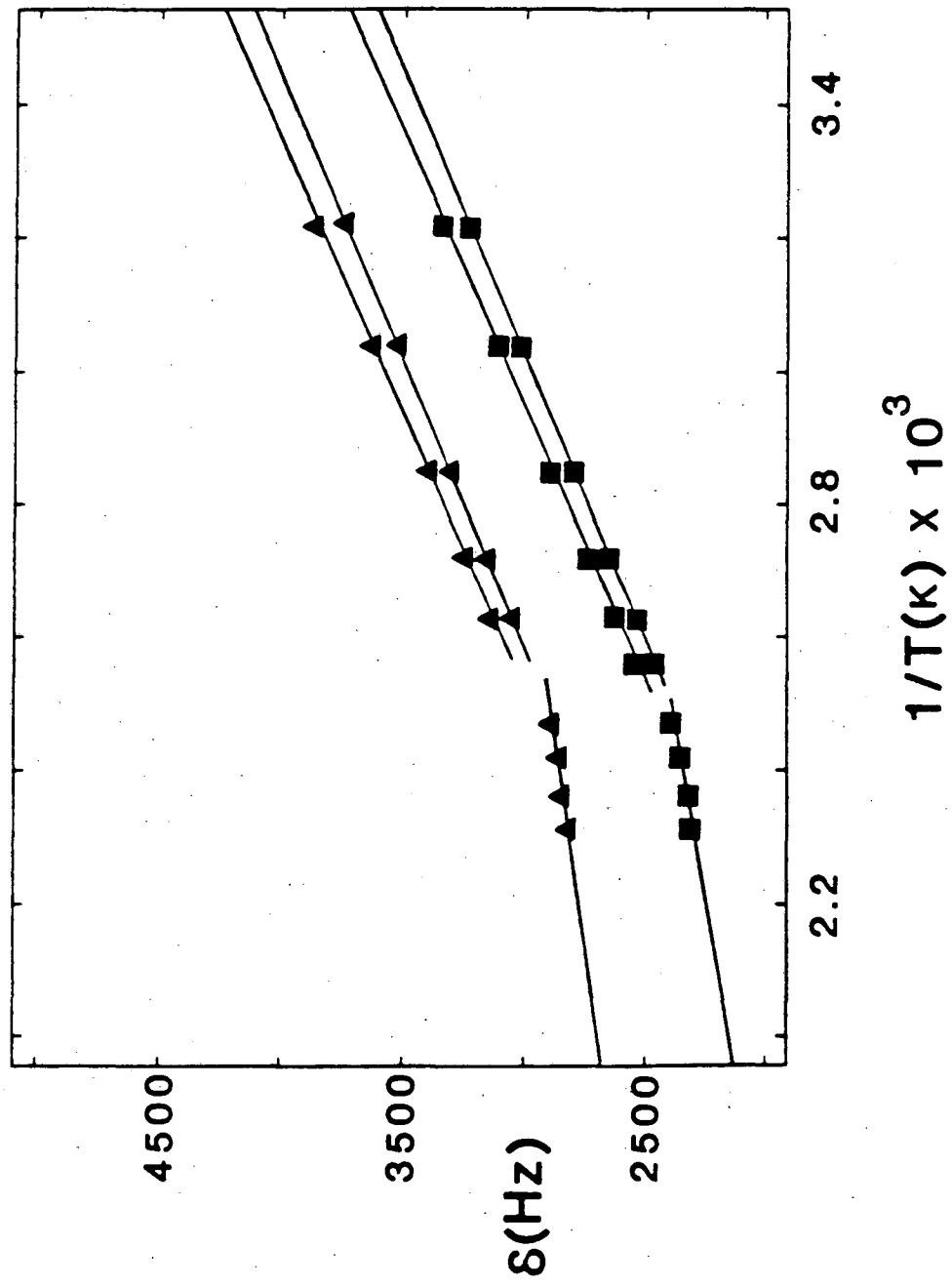

Scheme I

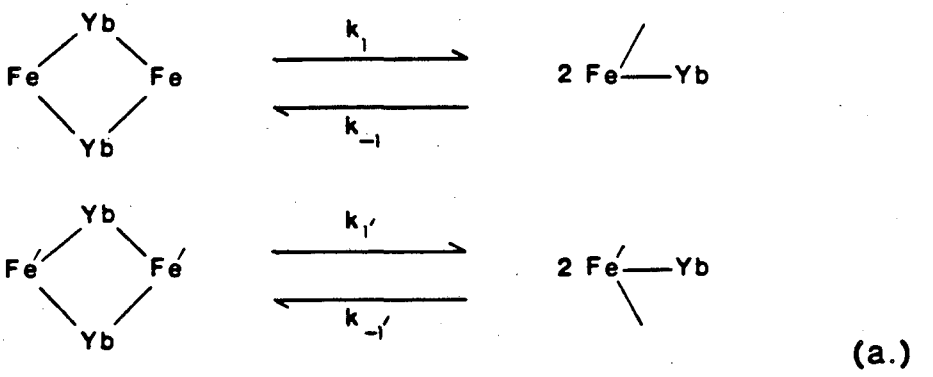
Yb
Fe
Fe
Yb
k_1
k_{-1}
2 Fe—Yb
Yb
Fe′
Fe′
Yb
$k_{1'}$
$k_{-1'}$
2 Fe′—Yb

(a.)

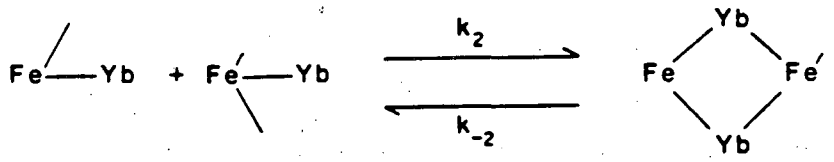
Fe—Yb + Fe′—Yb
k_2
k_{-2}
Yb
Fe
Fe′
Yb

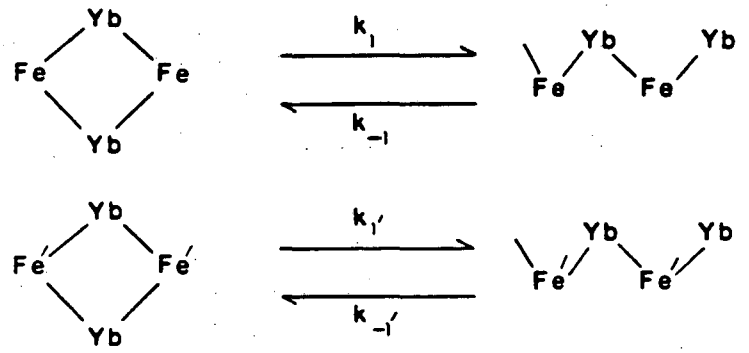
Yb
Fe
Fe
Yb
k_1
k_{-1}
Yb
Fe
Fe
Yb
Yb
Fe′
Fe′
Yb
$k_{1'}$
$k_{-1'}$
Yb
Fe′
Fe′
Yb

(b.)

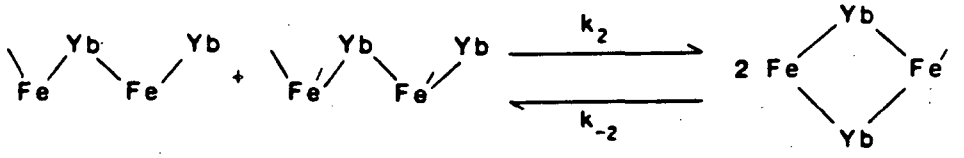
Yb
Fe
Fe
Yb
+
Yb
Fe′
Fe′
Yb
k_2
k_{-2}
2 Fe
Yb
Fe′
Yb

19.8kcal mol^{-1}. The Fe and Ru compounds undergo a similar crossover reaction which produces a statistical mixture of products as well.

The similarity of the activation energies of the Mo isomerization process and the Fe-crossover reaction suggests to us that they proceed through a common mechanism. Two of the most plausible mechanisms are shown in Scheme I. In pathway (a) in Scheme I the complexes dissociate completely to form monomeric intermediates (FeYb and Fe'Yb), and these then combine to give the mixed product. Using the method of initial rates, the reaction rate of path (a) is given in equation (2) below.

$$\text{rate} = \frac{k_1 k_1' k_2}{k_{-1}\ k_{-1}'} [Fe_2Yb_2]^{1/2} [Fe'_2Yb_2]^{1/2} \qquad (2)$$

Thus, initially the reaction is half order in starting material.

In pathway (b) in Scheme I, one Yb-O bond of the dimers breaks to give an intermediate which is an opened dimer ($FeYb_2Fe$, $Fe'Yb_2Fe'$). Two of these intermediates then react to give the crossover product. Under the initial conditions of the reaction the rate is given by eqn 3, and

$$\text{rate} = \frac{k_1 k_1' k_2}{k_{-1}\ k_{-1}'} [Fe_2Yb_2][Fe'_2Yb_2] \qquad (3)$$

the reaction will be first order in starting materials. Unfortunately, we have been unable to obtain meaningful kinetic data on this reaction

because of the low solubility of the complexes, and the broad lines in the ^1H NMR spectra.

Solution Studies with Added Ligands L

When the compounds studied here are dissolved in THF, or reacted with two equivalents of pyridine, the added base serves to cleave the dimeric species into monomers of formulae $[(Me_5C_5)_2Yb(III)L][(C_5H_4)M(CO)_x]$ (L= THF, pyridine). These complexes have only one low energy band in the ν-CO region of their ir spectra. This implies that there is only one Yb-O-C-M interaction, with the other coordination site on Yb being filled by L. Low temperature NMR studies indicate that addition of two equivalents of THF to $[(Me_5C_5)_2Yb(III)(\mu\text{-}OC)_2FeCp]_2$ does not produce any detectable amount of the monomeric THF adduct in solution at -70°C. However, addition of four to six equivalents of THF produces an equilibrium mixture of species which are observable as separate sets of MeC_5H_4 resonances in the ^1H NMR spectrum at -70°C. Not only are the three resonances due to the dimer observed at δ67.8, 64.4, and 56.7, but also six resonances at δ46.2, 40.7, 39.1, 36.8, 34.4, and 34.4 are observed. These may be due to the complexes labeled B and C in eqn (4). If this mixture is warmed to -40°C only one MeC_5H_4 environment is observed indicating that the equilibria are fast on the NMR time scale at this temperature. Addition of two equivalents of pyridine to the $Me_3SiC_5H_4Fe$ derivative results in complete cleavage of the dimeric complex with formation of the compound $[(Me_5C_5)_2Yb(III)py][(Me_3SiC_5H_4)Fe(CO)_2]$ the latter complex may be crystallized from diethyl ether. These experiments indicate that the

qualitative basicities of the lone pair of electrons on the coordinated hetero atom is THF<CO<<py.

The conclusion which can be drawn from the solution studies of these complexes is that they are not rigid dimeric species in solution. At first glance this behavior may seem a bit odd given the high oxygen affinity of electropositive metal atoms. However, it should not be forgotten that lanthanide ions are kinetically labile ions so that it should be expected that equilibria of the type given in eqn (4) will be facile. Further, the transition metal carbonyl anions are in a sense like an alkoxide which undergoes facile ligand exchange processes in solution.[21] The qualitative result that the carbonyl oxygen atoms

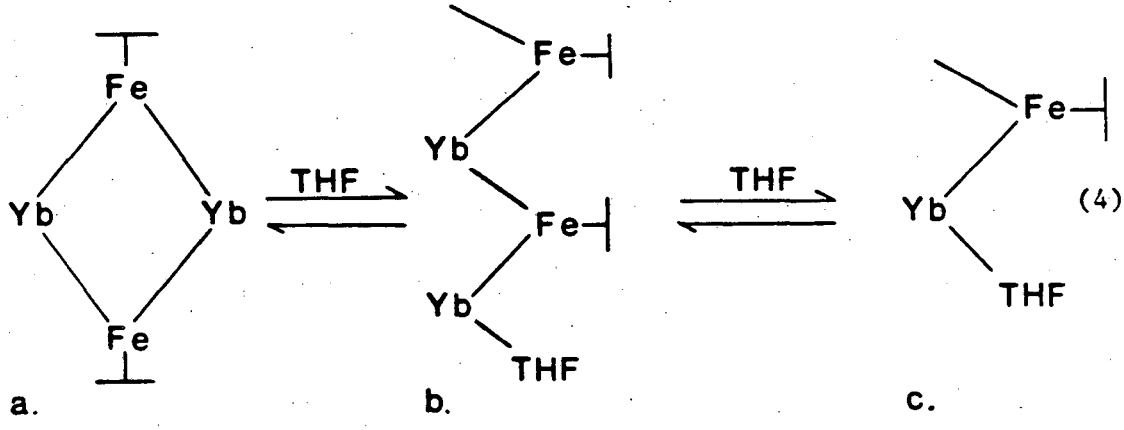

(4)

of transition metal carbonyl anions are more basic towards $(C_5Me_5)_2Yb(III)$ than THF suggests that in these anions a considerable amount of the negative charge in the complex is delocalized onto the carbonyl oxygen atoms, and is consistent with the low ν-CO's in the complexes.

When $(Me_5C_5)_2Yb{\cdot}OEt_2$ is reacted with one equivalent of $(C_5H_5)Fe(CO)_2I$, there is quantitative conversion to a complex having the

Table X. ν–CO of Products of the Reaction of Various Mononuclear Metal Carbonyl Complexes with $(C_5Me_5)_2Yb\cdot OEt_2$.

Transition Metal Compound	Medium	Obsd. Bands
$MeMn(CO)_5$ (under CO)	Nujol	2005s, 1967vs, 1945vs, 1590vs, 1485s cm^{-1}
Acetyl $Mn(CO)_5$	Nujol	2120m, 2070m, 2062m, 2042m, 2025m, 2005m, 1960BrVs, 1922s, 1585vs, 1545s, 1485m cm^{-1}
$(C_5H_5)Co(CO)PPh_3$	Nujol	1933s, 1845vs, 1800sh, 1665w, 1605vs cm^{-1}

stoichiometry $[(Me_5C_5)_2YbI]_2[(C_5H_5)_2Fe_2(\mu_3CO)_2(CO)_2]$. The ir spectrum of the complex is consistent with a structure in which both bridging carbonyl oxygen atoms are functioning as Lewis bases toward a pair of $(C_5Me_5)_2YbI$ molecules. This complex is similar to complexes formed by the reaction of $[(C_5H_5)Fe(CO)_2]_2$ with AlR_3 compounds.[22] Dissolution of the Yb compound in THF results in the formation of $[(C_5H_5)Fe(CO)_2]_2$ and $(Me_5C_5)_2YbI\cdot THF$ which were charaterized by their infrared and mass spectra. The net result of this reaction is transfer of the I^- ion from Fe to Yb with concurrent oxidation of Yb and reduction of Fe.

The metal carbonyl dimer $(C_5H_5)_2Ni_2(\mu_2CO)_2$ reacts with two equivalents of $(Me_5C_5)_2Yb\cdot OEt_2$ under N_2 to give a dark green-black complex which can be crystallized from diethyl ether. The infrared spectrum of this complex in the ν-CO region is quite complicated, with seven bands observed (see Table X), and at least two of these are due to Yb-O-C-Ni interactions. When the reaction is carried out under an atmosphere of carbon monoxide, a bright red complex was formed which is soluble in pentane, but which was only obtained as an impure powder.

Reaction of (acetyl)$Mn(CO)_5$ with one equivalent of $(Me_5C_5)_2Yb\cdot OEt_2$ produces a red-brown complex which has the stoichiometry $[(C_5Me_5)_2Yb][(acetyl)Mn(CO)_5]$ from elemental analysis. The infrared spectrum of this complex in the ν-CO region is listed in Table (X) and is very complex having twelve bands. The presence of bands at 1485 and 1395cm^{-1} suggests that in this molecule the ytterbium atom coordinates to the acetyl carbonyl oxygen atom. Since the complex crystallizes very well, an X-ray study is warranted.

Reaction of $(Me_5C_5)_2Yb\cdot OEt_2$ with one equivalent of $MeMn(CO)_5$ under an atmosphere of carbon monoxide produces a red-brown complex that was

shown to have the stoichiometry $[(Me_5C_5)_2Yb^{\cdot}OEt_2][(acetyl)Mn(CO)_5]$ by elemental analysis. The complex is paramagnetic as shown by the chemical shift and line width of the peaks in its ^1H NMR spectrum. The infrared spectrum has a number of bands in the ν-CO region (see Table X). The presence of the band at $1485cm^{-1}$ suggests that an acetyl group may have been formed which is coordinated to the ytterbium fragment. This reaction has precedence because addition of Lewis acids such as $AlBr_3$ to $MeMn(CO)_5$ induces methyl migration to form an acetyl group which ends up coordinated to the $AlBr_3$.[23] Clearly, the only way in which the above complex can ever be properly characterized is by single crystal X-ray diffraction methods.

Reactions with $(RC_5H_4)M(CO)_2$ (M=Co, R=H, Me, Me_3Si; M=Rh, R=H)

In order to determine whether or not $(C_5Me_5)_2Yb^{\cdot}OEt_2$ could be used to reduce 18 electron mononuclear transition metal complexes, a series of reactions were carried out between $(Me_5C_5)_2Yb^{\cdot}OEt_2$ and $(RC_5H_4)Co(CO)_2$ complexes. The reason for choosing the complexes of the cobalt series is that they can be reduced using sodium amalgam to give the dimeric radical anions $(C_5H_5)_2Co_2(CO)_2^-$ or, in the case of rhodium, the trinuclear complex $(C_5H_5)_2Rh_3(CO)_4^-$.[24,25] The ease with which the starting dicarbonyl complexes are reduced made them likely candidates for reaction with $(Me_5C_5)_2Yb^{\cdot}OEt_2$. It was also of interest to see if the products of such reactions would be similar to the products derived from alkali metal reductions, as was the case for the reactions between $(Me_5C_5)_2Yb^{\cdot}OEt_2$ and transition metal carbonyl dimers.

Bis(pentamethylcyclopentadienyl)ytterbium ether complex reacts with

the complexes $(RC_5H_4)M(CO)_2$ (M=Co, R=H, Me, Me_3Si; M=Rh, R=H) in either a 1:1 or 2:3 molar ratios to give good yields of dark blue-black complexes having the stoichiometry $[(Me_5C_5)_2Yb(III)]_2[(RC_5H_4)_2M_3(CO)_4]$. The complexes are paramagnetic as judged by the chemical shift and line widths of the peaks in their ^1H NMR spectra which are found in Table (XI). A plot of $1/\chi_M$ vs. T is given in Figure 14. The complex follows Curie-Weiss behavior from 5-30K with C_n=2.64(2); θ=-1.05(16)K and μ_{eff}=4.61(2) B.M. per Yb atom and from 100-300K with C_m-3.067(6), θ=-14.50(46)K and μ_{eff}=4.973(5) B.M. per Yb atom. The trinuclear transition metal fragment has 47 valence electrons making it a radical species. This accounts for the large value of μ_{eff}. The experimental value per Yb atom of 4.97 B.M. is just the sum of the value found for $(Me_5C_5)_2Yb(III)$ in transition metal carbonyl complexes ca. 4.30 B.M. and one-third the value of a free electron (i.e., 1.73/3 BM=.57 B.M.). This suggests that the ytterbium spins and the spins on cobalt are not interacting appreciably at room temperature. In agreement with this, the EPR spectrum of the complex is observable and shows one very broad signal at a g value of 2.083 at room temperature and at 77K. Unfortunately, no cobalt (I=7/2) hyperfine coupling could be resolved.

The infrared spectra of these complexes in the ν-CO region are very simple and have only one band at ca. 1590cm^{-1}. The ^1H NMR spectra have resonances which can be assigned to the C_5Me_5 rings bonded to ytterbium and cyclopentadienyl rings bonded to cobalt in a 2:1 ratio. The simple infrared spectrum and reasonable ratio of pentamethycyclopentadienyl to cyclopentadienyl rings in the complex suggested a simple stoichiometry such as in XIV below. Such a simple structure does not make good

Table XI. ^1H NMR Data for $[(C_5Me_5)_2Yb]_2[(\mu_3\text{-}OC)_4M_3(C_5H_4R)_2]$ Compounds

Compound	Color	^1H NMR Spectrum
$[(C_5Me_5)_2Yb]_2[(\mu_3\text{-}OC)_4Co_3(C_5H_5)_2]$	Blue	$\delta 5.39(\nu 1/2=47Hz, 30H)$; $\delta 32.51(\nu 1/2=34Hz, 5H)$
$[(C_5Me_5)_2Yb]_2[(\mu_3\text{-}OC)_4Co_3(MeC_5H_4)_2]$	Blue	$\delta 4.84(\nu 1/2=48Hz, 30H)$; $\delta 28.87(\nu 1/2=39Hz, 2H)$ $\delta 30.12(\nu 1/2=32Hz, 2H)$; $\delta 84.07(\nu 1/2=49Hz, 3H)$
$[(C_5Me_5)_2Yb]_2[(\mu_3\text{-}OC)_4Co_3(Me_3SiC_5H_4)_2]$	Blue	$\delta 4.09(\nu 1/2=12Hz, 9H)$; $\delta 5.34(\nu 1/2=49Hz, 30H)$; $\delta 17.25(\nu 1/2=40Hz, 2H)$; $\delta 75.45(\nu 1/2=39Hz, 2H)$
$[(C_5Me_5)_2Yb]_2[(\mu_3\text{-}OC)_4Rh_3(C_5H_5)_2]$	Blue	$\delta 6.30(\nu 1/2=48Hz, 30H)$; $\delta -13.26(\nu 1/2=56Hz, 5H)$

Figure 14. Plot of $1/\chi_M$ vs. T for $[(C_5Me_5)_2Yb(III)]_2$ $[(\mu_3\text{-}OC)_4Co_3(C_5H_4SiMe_3)_2]$

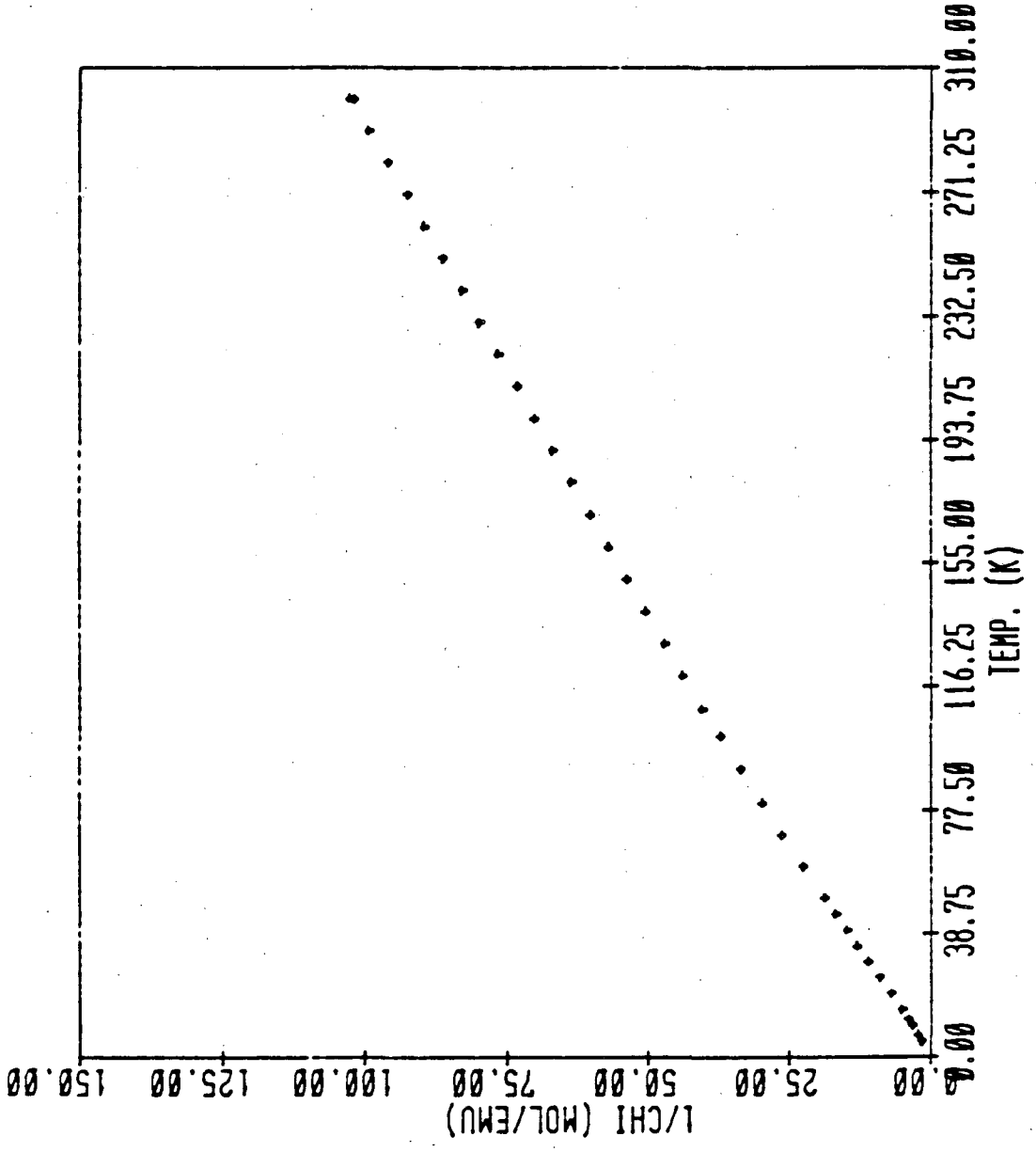

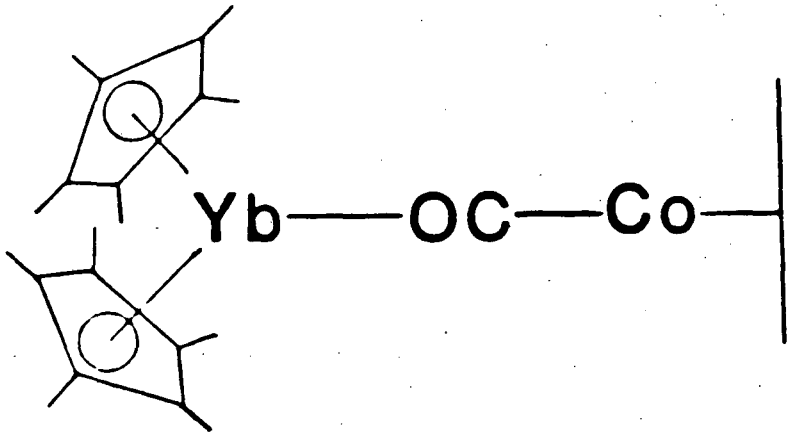

XIV

chemical sense since the cobalt atom has only 17 valence electrons and the ytterbium is formally seven coordinate. The actual stoichiometry and structure of the complex was only discovered by a single crystal X-ray diffraction study.

X-Ray Diffraction Studies

A single crystal X-ray diffraction study was used to characterize the product of the reaction between $(C_5Me_5)_2Yb{\cdot}OEt_2$ and $(Me_3SiC_5H_4)Co(CO)_2$. An ORTEP drawing is found in Figure 15. Tables of bond lengths and angles can be found in Tables (XII) and (XIII), respectively. The molecule crystallizes in the tetragonal space group $P4_12_12$, and consists of well separated molecules of stoichiometry $[(C_5Me_5)_2Yb(III)]_2[(\mu_3\text{-}OC)_4Co_3(Me_3SiC_5H_4)]$. The closest intermolecular contacts are between cyclopentadienyl ring carbon atoms, the shortest being between C_{15} and C_{24} at 3.58(1)Å.

Figure 15. ORTEP of $[(C_5Me_5)_2Yb(III)]_2[(\mu_3\text{-}OC)_4Co_3(C_5H_4SiMe)_3]$

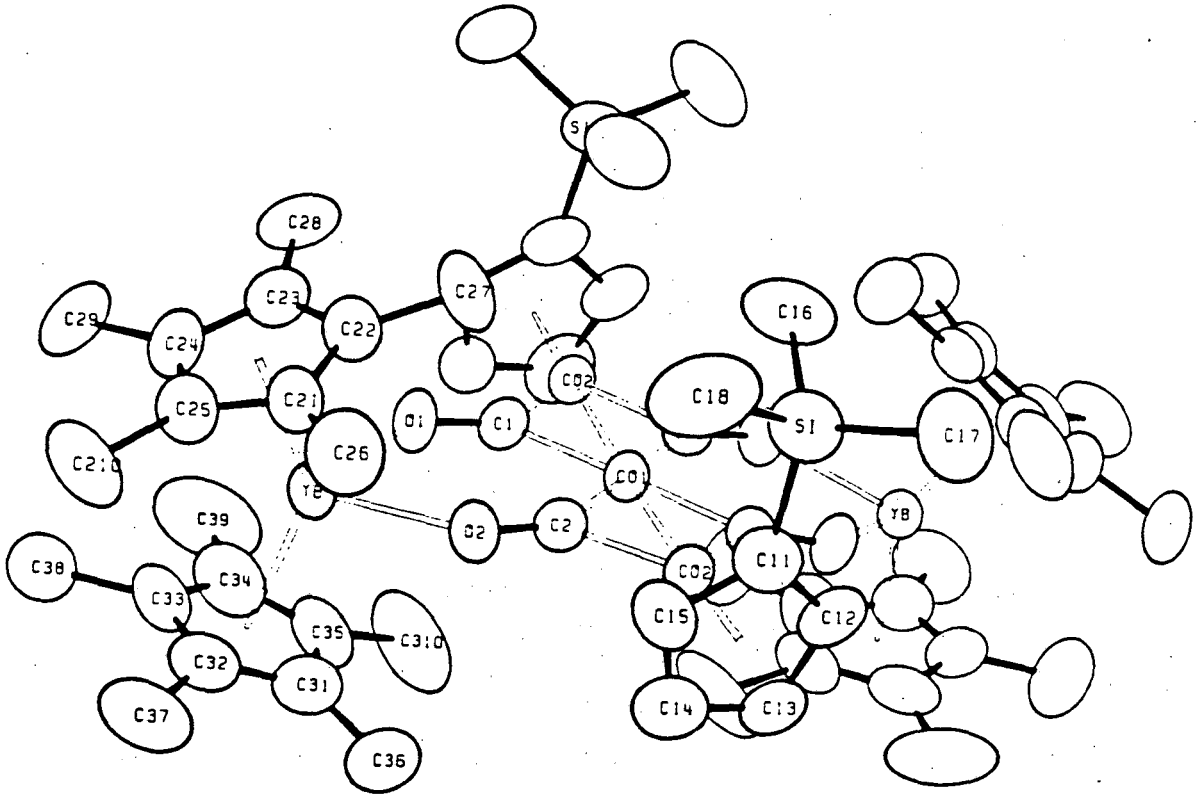

XBL 826-10527

Table XII. Selected Bond Lengths (Å) for $[(C_5Me_5)_2Yb(III)]_2[(\mu_3\text{-}OC)_4Co_3(C_5H_4SiMe_3)_2]$

Yb-O1	2.226(4)	C11-C12	1.431(9)
Yb-O2	2.233(4)	C12-C13	1.440(9)
Yb-C21	2.586(7)	C13-C14	1.467(10)
Yb-C22	2.567(6)	C14-C15	1.449(11)
Yb-C23	2.584(7)	C15-C11	1.451(9)
Yb-C24	2.630(7)	C11-Si	1.891(8)
Yb-C25	2.595(6)	Si-C16	1.929(9)
Yb-Cp2*	2.294	Si-C17	1.898(9)
Yb-C31	2.604(8)	Si-C18	1.916(8)
Yb-C32	2.608(7)	C21-C22	1.430(9)
Yb-C33	2.569(6)	C22-C23	1.425(10)
Yb-C34	2.542(7)	C23-C24	1.414(9)
Yb-C35	2.576(7)	C24-C25	1.431(10)
Yb-Cp3*	2.289	C25-C21	1.396(10)
Co1-Co2	2.363(1)	C21-C26	1.510(10)
Co1-C1	1.853(6)	C22-C27	1.515(9)
Co1-C2	1.874(6)	C23-C28	1.532(10)
Co2-C1	1.778(6)	C24-C29	1.511(10)
Co2-C2	1.792(6)	C25-C210	1.585(9)
Co2-C11	2.099(7)	C31-C32	1.421(11)
Co2-C12	2.109(6)	C32-C33	1.368(10)
Co2-C13	2.122(6)	C33-C34	1.359(11)
Co2-C14	2.118(6)	C34-C35	1.435(12)
Co2-C15	2.125(7)	C35-C31	1.418(13)
Co2-Cp1*	1.719	C31-C36	1.548(13)
C1-O1	1.244(6)	C32-C37	1.496(11)
C2-O2	1.227(6)	C33-C38	1.594(10)
		C34-C39	1.522(14)
		C35-C310	1.528(10)

*Cp1, Cp2, and Cp3 are the centroids of the rings of the cyclopentadienide ligands.

Table XIII. Selected Bond Angles (deg) for $[(C_5Me_5)_2Yb(III)]_2[(\mu_3\text{-}OC)_4Co_3(C_5H_4SiMe_3)_2]$

O1-Yb-O2	73.97(14)	C25-C21-C22	107.2(7)
O1-Yb-Cp2*	104.7	C21-C22-C23	107.8(6)
O1-Yb-Cp3	106.6	C22-C23-C24	108.7(7)
O2-Yb-Cp2	105.6	C23-C24-C25	106.4(7)
O2-Yb-Cp3	106.5	C24-C25-C21	109.9(7)
Cp2-Yb-Cp3	140.0	C26-C21-C22	125.4(7)
Co2-Co1-Co2	176.48(5)	C26-C21-C25	127.3(7)
Co2-Co1-C1	48.0(2)	C27-C22-C21	126.0(7)
Co2-Co1-C2	48.4(2)	C27-C22-C23	126.2(7)
C1-Co1-C2	83.7(3)	C28-C23-C22	126.6(7)
C1-Co1-C1	178.8(3)	C28-C23-C24	124.6(8)
C2-Co1-C2	179.4(3)	C29-C24-C23	126.2(9)
Co1-Co2-C1	50.8(2)	C29-C24-C25	126.9(8)
Co1-Co2-C2	51.4(2)	C210-C25-C21	125.0(8)
Co1-Co2-Cp1*	177.9	C210-C25-C24	123.7(8)
C1-Co2-Cp1	128.0	C35-C31-C32	108.0(9)
C2-Co2-Cp1	129.9	C31-C32-C33	107.5(9)
Co1-C1-Co2	81.2(2)	C32-C33-C34	110.4(8)
Co1-C1-O1	142.1(4)	C33-C34-C35	108.7(9)
Co2-C1-O1	136.7(4)	C34-C35-C31	105.4(7)
Co1-C2-Co2	80.2(2)	C36-C31-C32	122.9(11)
Co1-C2-O2	143.1(5)	C36-C31-C35	129.0(10)
Co2-C2-O2	136.6(5)	C37-C32-C31	126.2(10)
Yb-O1-C1	138.5(3)	C37-C32-C33	125.6(9)
Yb-O2-C2	137.4(3)	C38-C33-C32	123.9(9)
C15-C11-C12	109.7(7)	C38-C33-C34	124.9(9)
C11-C12-C13	108.0(6)	C39-C34-C33	125.0(10)
C12-C13-C14	107.4(6)	C39-C34-C35	126.2(9)
C13-C14-C15	108.5(7)	C310-C35-C31	125.8(11)
C14-C15-C11	106.4(7)	C310-C35-C34	128.6(11)
Si-C11-C12	126.3(5)		
Si-C11-C15	124.0(6)		
C11-Si-C16	111.2(3)		
C11-Si-C17	108.6(4)		
C11-Si-C18	108.8(4)		

*Cp1, Cp2, and Cp3 are the centroids of the rings of the cyclopentadienide ligands.

The molecule has crystallographically imposed C_2 symmetry. The crystallographic C_2 axis passes through Co(1) perpendicular to the plane defined by Co(1), C(1), C(1'), C(2), C(2'). In addition to the crystallographic C_2 axis, the molecule contains two approximate mirror planes which are parallel to this axis and contain Co(1), Co(2) and Co(2'), and Co(1), Yb(1), and Yb(1'), respectively. Thus, the molecule has C_{2v} symmetry in the conformation shown in the ORTEP diagram.

The averaged Yb-C(C_5Me_5) distance is 2.590±0.020Å, and is in the range observed for trivalent ytterbium bound to C_5Me_5 rings. The presence of trivalent ytterbium is consistent with the observed paramagnetism and magnetic properties. The tricobalt cluster is therefore a dianion containing 47 valence electrons. The tricobalt core is nearly linear with the Co(2), Co(1), Co(2') angle being 176.5(1)°. The three cobalt atoms are bridged by four CO groups, with each end of the cobalt array capped by a $Me_3SiC_5H_4$ ligand. The four carbonyl oxygen atoms pairwise chelate the two $(C_5Me_5)_2Yb$ groups. The Co(1)-Co(2) distance of 2.363Å is similar to the distances found in $(C_5H_5)_2Co_2(CO)_2^-$ and $(C_5H_5)_2CO_2(CO)_2$ for which Co-Co bond orders of 1.5 and 2 have been proposed.[24] The atoms C(1), C(2), C(1'), C(2') and Co(1) are planar to within 0.015Å. Thus the coordination geometry of Co(1) is six coordinate and planar. Co(2) and the centroid of the $Me_3SiC_5H_4$ ring lie 0.08 and 0.19° from one side of the plane defined by C(1), C(2), C(1'), C(2') and Co(1) and O(1), O(2) and Yb lie 0.14, 0.08 and 0.4Å from the other side. The ytterbium atoms are pushed downward, relative to Figure 15, and the C_5Me_5 rings are tilted to allow the Me_3Si groups to fit into the structure.

The Co(1)-C(2), C(2,1) distances of 1.835(6) and 1.874(6)Å are

significantly longer than the Co(2)-C(1,2) distances of 1.778(6) and 1.792(6)Å. The Co(1),C(1),O(1), and Co(1),C(2),O(2) angles are slightly larger than the Co(2),C(1),O(1) and Co(2),C(2),O(2) angles indicating a tendency to distort toward a semi-bridged situation to relieve the electronic inequivalence of the cobalt atoms. Further distortion is prevented by the fact that the carbonyl oxygen atoms must coordinate to the Yb atoms, and any further enlargement of the Co(1),C(2),O(2) and Co(1),C(1),O(1) angles would push the oxygen atoms away from Yb. It is probable that the unequal angles and distances observed within the tricobalt tetracarbonyl core are imposed by the strong bonds formed between the carbonyl oxygen atoms and the ytterbium atoms.

V.T. NMR Studies

Examination of the solid state structure reveals that because both trimethylsilyl groups lie on the same side of the plane defined by the metal atoms, all four C_5Me_5 rings should not be chemically equivalent in the ^1H NMR spectrum. Figure 16 is a line drawing with a view down the

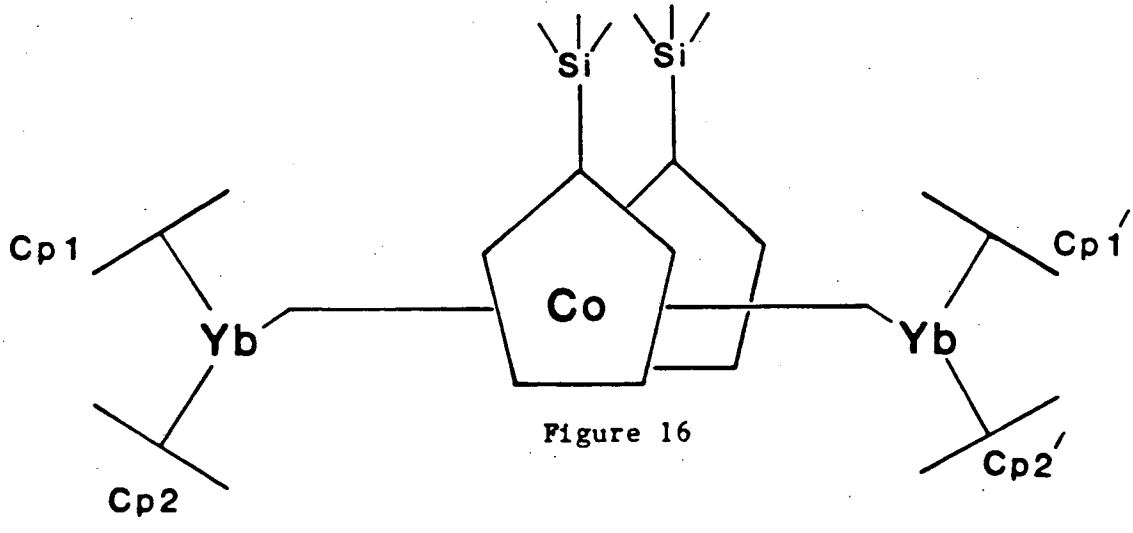

Figure 16

vector defined by the three cobalt atoms. This drawing clearly shows

that in this conformation there is no symmetry element which will interconvert Cp1 and Cp2. There is a C_2 axis which will interconvert Cp1 with Cp1'. If this conformation is observed in solution, then two resonances should be observed for the C_5Me_5 protons. At room temperature, only one resonance is observed in the ^1H NMR spectrum of the compound indicating that either the conformation in Figure 16 is not the conformation in solution, or that a fluxional process is occurring which causes the Cp1 and Cp2 environments to become averaged on the NMR time scale.

Cooling a solution of $[(C_5Me_5)_2Yb(III)\mu_3\text{-}(OC)_4Co_3(Me_3SiC_5H_4)_2]$ and observing its ^1H NMR spectrum reveals that the lines shift and broaden with lowered temperature as expected for a paramagnetic compound. In addition, at -56°C the resonance assigned to the C_5Me_5 protons splits into two peaks of equal area which shift further apart when the sample is cooled below -56°C. The chemical shifts of these two resonances are linear with respect to T^{-1} below their coalescence temperature. Plotting the chemical shift as a function of T^{-1} in the slow exchange portion of the spectrum, and extrapolating to the coalescence temperature allows determination of the peak separation at coalescence (see Figure 17 for a plot of $\delta\nu$ vs. 1/T). Using the $\Delta\nu$ measured in the above manner and using the two site exchange equation, we find that the $\Delta G^{\ddagger}$ for the exchange process is 9.8 kcal/mole.

The most plausible mechanism for the observed temperature dependence of the NMR spectrum of the compound is that at high temperature rotation of the trimethylsilylcyclopentadienyl rings is fast on the NMR time scale. Such rotation would cause Cp1 and Cp2 to have equivalent chemical environments. As the temperature is lowered, the rotation

Figure 17. Plot of δ vs. 1/T for the Coalescence of the C_5Me_5 Protons in $[(C_5Me_5)_2Yb(III)]_2[(\mu_3\text{-}OC)_4Co_3(C_5H_4SiMe_3)_2]$

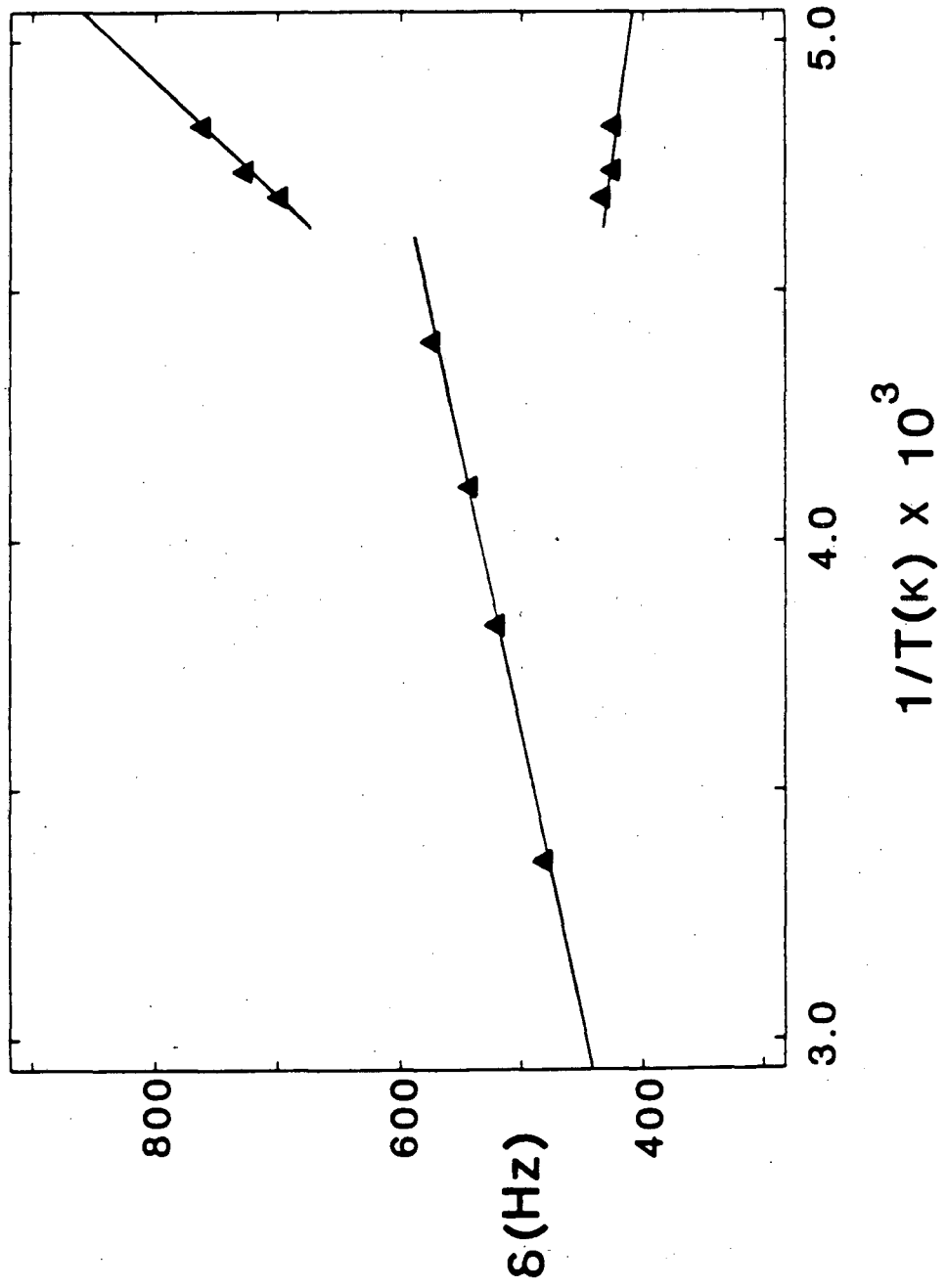

slows down, and the conformation in Figure 16 is the one which is observed in the ^1H NMR spectrum. The calculated activation energy for ring rotation is not unreasonably high given the severe steric restrictions that the Me_3Si groups place on the molecule. Variable temperature ^1H NMR studies on the related compound $[(C_5,Me_5)_2Yb(III)]_2[(\mu_3\text{-}OC)_4Co_3(Me_3SiC_5H_4)_2]$ reveal that only one resonance is observed for the C_5Me_5 protons down to the lowest temperature observed (-90°C). Evidently, replacing the large Me_3Si groups with less sterically demanding CH_3 groups lowers the activation energy for ring rotation enough so that the averaged conformation is the one observed in solution even at -90°C.

Chemical Reactivity and Solution Properties

One piece of data which appears inconsistent with the observed structure of the tricobalt molecule is the IR spectrum. There is only one ν-CO band in cyclohexane solution, or in a Nujol mull. Even though there are four carbonyl groups in the molecule, the spectra are not inconsistent with the structure. If free rotation of all the cyclopentadienyl rings in the compound is assumed, then the molecule has D_{2h} symmetry (and certainly the $Co_3(CO)_4$ core has D_{2h} symmetry). Group theory predicts that there should be two infrared active and two raman active C-O stretching frequencies. The two infrared active modes are the B_{1u} and the B_{3u} (if the Co-Co vector is defined as the z-axis and the CO vectors are parallel to the x-axis). The B_{3u} is x-polarized and is observed because the axis of polarization coincides with the CO vector. The B_{1u}, though allowed, is weak to the point of being

unobserved because it is polarized perpendicular to the C=O vector, and the dipole moment change in that direction when the CO stretches is so small that the absorption goes undetected.

The synthesis of these cobalt trimers is straightforward, with the exception of the $(C_5Me_5)Co$ derivative. Attempts to synthesize the $(C_5Me_5)Co$ compound in pure form were unsuccessful, yielding only a mixture of $[(C_5Me_5)_2Yb(III)]_2[(\mu_3\text{-}OC)_4Co_3(C_5Me_5)_2]$ and $(C_5Me_5)_2Co_2(\mu\text{-}CO)_2$. Small amounts of a third compound, which was identified as $[(Me_5C_5)_2Yb(III)][Co(CO)_4]$ from its infrared spectrum, could also be isolated. The isolation of the tetracarbonyl cobaltate complex suggested that perhaps a pathway existed between the $[Co(CO)_4]$ complex and the trinuclear complex.

When the complex $[(Me_5C_5)_2Yb(III)][Co(CO)_4]$ is refluxed with an excess of the diene, $Me_3SiC_5H_5$ in toluene, the only isolable product which is formed is $[(C_5Me_5)_2Yb(III)]_2[(\mu_3\text{-}OC)_4Co_3(Me_3SiC_5H_4)_2]$. It appears that the yield is virtually quantitative, with the excess ytterbium forming an insoluble black precipitate. When the same reaction was attempted with C_5Me_5H and $[(C_5Me_5)_2Yb(III)][Co(CO)_4]$, an intractable oily solid resulted. It appears that the C_5Me_5 group is just too bulky to form an isolable complex by either route.

The observation that $Co(CO)_4^-$ is formed in the reaction between $(C_5Me_5)Co(CO)_2$ and $(C_5Me_5)_2Yb{\cdot}OEt_2$ indicates that this reaction is indeed very similar to the reduction of $(C_5H_5)Co(CO)_2$ complexes with sodium amalgam. When $(C_5H_5)Co(CO)_2$ is reduced using sodium amalgam, $NaCo(CO)_4$ is produced along with the radical anion $[Na^+][(C_5H_5)_2Co_2(\mu_2\text{-}CO)_2]^{\cdot-}$.[24a] When the analogous reaction is performed with $C_5H_5Rh(CO)_2$, the products are $NaRh(CO)_4^-$ and the 46 electron mono-anion

$Na(C_5H_5)_2Rh_3(CO)_4$, which has exactly the same stoichiometry as the 47 electron dianions discussed here.[25] In all of these reductions, both a C_5H_5 ligand and CO ligands are lost from the transition metal center. This seemingly disparate behavior can be easily rationalized since the LUMO in $CpCo(CO)_2$ is both metal-CO and metal-cyclopentadienyl antibonding in nature.[26] Thus, reduction of $(C_5H_5)Co(CO)_2$ weakens both the metal ring bonds as well as the metal CO bonds. When sodium metal is used as the reductant, the products which are formed are dependent upon the chemistry of the resultant transition metal fragments, so that two different complexes are formed for Co or Rh. When $(C_5Me_5)_2Yb$ is used as the reductant, the coordination requirements of the ytterbium fragment determine the product of the reaction. It is the ability of ytterbium to form strong metal to oxygen bonds that drives this reaction to the observed products.

The presence of the odd coordination environment about the central cobalt atom and the unpaired electron in this compound suggests that this compound might be reactive toward small molecules such as H_2 and CO. This is true and these complexes do react with molecular hydrogen. The reaction between hydrogen and $[(C_5Me_5)_2Yb(III)]_2[(\mu_3\text{-}OC)_4Co(Me_3SiC_5H_4)]$ proceeds only slowly at 90°C, taking approximately two weeks to go to completion. Most of the product of the reaction is a black material which is insoluble in organic solvents. The other small fraction of product is the green cobalt dimer $(C_5Me_5)_2Co_2(\mu_2\text{-}CO)_2$. In order to determine if the complex was reacting with water in the hydrogen gas, the complex was reacted with water. The products of this reaction are $(Me_3SiC_5H_4)Co(CO)_2$ and the mixed ring dimer $(Me_3SiC_5H_4)(C_5Me_5)Co_2(\mu_2\text{-}CO)_2$. Due to the small yield of metal

containing product from these reactions, they were not studied in more detail. Preliminary studies show that the complex $[(C_5Me_5)_2Yb(III)]_2[(C_5H_5)_2Rh_3(CO)_4]$ reacts more rapidly with H_2 at room temperature, but the products of the reaction have not yet been characterized.

Coordination Complexes with Transition Metal Carbonyl Complexes

The products formed by the reactions of $(C_5Me_5)_2Yb^{\cdot}OEt_2$ and $RC_5H_4Co(CO)_2$ show that novel complexes can result from the reduction of 18 electron mononuclear organometallic complexes. A variety of mononuclear 18 electron molecules were reacted with $(C_5Me_5)_2Yb^{\cdot}OEt_2$ in order to establish the criteria for such electron transfer reactions to occur. The complexes discussed below are the best characterized examples of such reactions.

The complex $(C_5H_5)Co(CO)_2$ is easily reduced by $(C_5Me_5)_2Yb^{\cdot}OEt_2$. Substitution of one carbonyl group on cobalt with phosphine ligands should change both the reduction potential of the metal, and the basicity of the remaining CO ligand. It should be possible to change the reduction potential of $CpCo(CO)_2$ enough so that the complex cannot be reduced by $(C_5Me_5)_2Yb^{\cdot}OEt_2$.

Reaction of $(C_5H_5)Co(CO)PPh_3$ with $(C_5Me_5)_2Yb^{\cdot}OEt_2$ occurs at 90°C in toluene to give a dark red complex which crystallizes from diethyl ether, but will not redissolve in that solvent. The infrared spectrum of this material indicates that it has Yb-O-C-Co interactions (there are bands at 1665 and 1606 cm^{-1}, see Table X) as well as terminal CO groups. The high percentage of carbon in the molecule indicates the

presence of PPh_3, but this might only be an impurity. The ^1H NMR of the complex is complicated and uninformative except to indicate that the complex is paramagnetic as judged by the shifts and line widths of the peaks. The characterization of this complex was not pursued further.

Reaction of $(C_5Me_5)_2Yb{\cdot}OEt_2$ with two equivalents of $(C_5H_5)Co(CO)PMe_3$ does not result in electron transfer to the cobalt complex. The complex is diamagnetic and has the stoichiometry $[(C_5Me_5)_2Yb(II)][(\mu\text{-}OC)(C_5H_5)CoPMe_3]_2$. The infrared spectrum of this molecule as well as some other simple coordination complexes of divalent Yb are given in Table (XIV). The three band pattern observed for this molecule can be rationalized by realizing that the complex dissolves in Nujol. The spectrum is then consistent with the equilibrium shown in (5) below. This explains the observation of free $CpCo(CO)PMe_3$ as well as two other species containing lowered CO stretches. Once again only

$$[(C_5Me_5)_2Yb(II)][(\mu\text{-}OC)(C_5H_5)CoPMe_3]_2 \rightleftharpoons CpCo(CO)PMe_3 + (C_5Me_5)_2Yb \leftarrow OC\text{-}Co(Cp)PMe_3 \quad (5)$$

one band is observed for the 2:1 complex because CO vibrational modes do not strongly interact through the Yb-O bonds as was observed in the molybdenum complexes previously discussed.

Table XIV. Infrared Spectra in the ν-CO Region for Coordination Complexes of $(C_5Me_5)_2Yb(II)$.

Compound	Medium	ν-CO (cm^{-1})
$[(C_5Me_5)_2Yb(II)][(\mu_2\text{-}CO)CoPMe_3(C_5H_5)]_2$	Nujol	1923m, 1866vs, 1837vs
$[(C_5Me_5)_2Yb(II)][HCo(\mu_2\text{-}CO)(PMe_3)_3]_2$	Nujol	1913s, 1833m, 1795vs
$[(C_5Me_5)_2Yb(II)][MeCo(\mu_2\text{-}CO)(PMe_3)_3]$	Nujol	1900s, 1795s
$[(C_5Me_5)_2Yb(II)][(C_5H_5)Mn(CO)_3]$	Nujol	2010vs, 1941vs, 1925ssh, 1905vs, 1883vs, 1856vs
$[(C_5Me_5)Yb(II)][(MeC_5H_4)Mn(CO)_3]$	Nujol	1010s, 1954s, 1932vs, 1907m, 1870m, 1840sBr

In a similar fashion, $HCo(CO)(PMe_3)_3$ and $MeCo(CO)(PMe_3)_3$ form 2:1 and 1:1 complexes with $(C_5Me_5)_2Yb$ which are diamagnetic. Their infrared spectra in the ν-CO region are listed in Table (XIV). These molecules are soluble in Nujol and the observation of the free complex argues for equilibria such as that proposed for the $(C_5H_5)Co(CO)PMe_3$ complex. The ^{31}P NMR spectra of these molecules are broad even at -80°C. The broadness of the spectra are consistent with equilibria in solution such as those proposed in eqn (5) and postulating that the exchange is rapid even at -80°C.

As with the cobalt complexes discussed above, reaction of $(C_5Me_5)_2Yb{\cdot}OEt_2$ with one equivalent of $(RC_5H_4)Mn(CO)_3$ (R=H, Me) results in the formation of a diamagnetic coordination complex of the stoichiometry $[(C_5Me_5)_2Yb(II)][(RC_5H_4)Mn(CO)_3]$. These complexes are extremely air sensitive, and satisfactory elemental analyses and ^1H NMR spectra have not been obtained for them. The infrared spectra are given in Table (XIV) and each contain six bands in the ν-CO region. It appears that there are three bridging, and three terminal CO stretches. These patterns can be accounted for if the equilibrium shown in eqn (6) below exists. The dimeric complex 8 has essentially the same structure as $\{[(C_5Me_5)_2Yb(III)][(RC_5H_4)Mo(CO)_3]\}_2$ only with

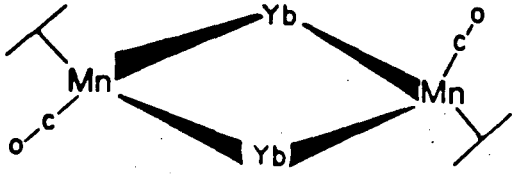

8.)

$$\rightleftharpoons 2\ Yb{\leftarrow}OC{-}Mn \qquad (6)$$

9.)

ytterbium(II), and Mn(I). This complex should have two bridging CO stretches and one terminal stretch. Complex 9 should have one bridging CO stretch, and two terminal stretches. An alternative explanation would be that the compounds in eqn (6) are also in equilibrium with free starting carbonyl complex giving a total of eight bands and four of them are pairwise accidentally degenerate.

The results described here indicate that if the transition metal center is too electron rich, or if its LUMO is too high in energy, then no electron transfer from ytterbium will occur. When trimethylphosphine is substituted onto a metal center in place of carbon monoxide the metal center becomes more electron rich, and because of metal CO back bonding, the oxygens of the remaining CO groups become more basic. The net result is that complexes of this type are not reduced by $(C_5Me_5)_2Yb{\cdot}OEt_2$, but rather form simple coordination complexes with $(C_5Me_5)_2Yb{\cdot}OEt_2$. The initial studies carried out here indicate that coordination to $(C_5Me_5)_2Yb$ does not drastically alter the chemistry of, for example, $MeCo(CO)(PMe_3)_3$. It was hoped that coordination to the ytterbium complex might induce methyl migration to the CO. This reaction mode is not observed in the free complex, and these results show that it does not occur when the complex is coordinated to ytterbium. Further reactivity studies are needed to find out if other reaction chemistry of such molecules is affected by coordination to $(C_5Me_5)_2Yb(II)$.

References

1. a.) Tilley, T. D. ; Andersen, R. A. J. Chem. Soc., Chem. Comm., 1981, 985. b.) Tilley, T. D.; Andersen, R. A. J. Am. Chem. Soc. 1982, 104, 1772.

2. a.) Carlin, R. L.; Van Duyneveldt, A. J., "Magnetic Properties of Transition Metal Compounds", Springer-Verlag: New York, 1977. b.) Figgis, B. N. "Introduction to Ligand Fields", Interscience: New York, 1966.

3. Darensbourg, M. Y., Darensbourg, D. J.; Burns, D.; Drew, D. A. J. Am. Chem. Soc. 1976, 98, 3127.

4. Ellis, J. E.; Flom, E. A. J. Organomet. Chem. 1975. 99. 263.

5. Ulmer, S. W.; Skurstad, P. M.; Burlitch, J. M.; Hughes, R. E. J. Am. Chem. Soc. 1973, 95, 4469.

6. Burlitch, J. M.; Leonowicz, M. E.; Petersen, R. B.; Hughes, R. E. Inorg. Chem. 1979, 18, 1097.

7. Wong, A.; Harris, M.; Atwood, J. D. J. Am. Chem. Soc. 1980, 102, 4529.

8. Pannell, K. H.; Jackson, D. J. Am. Chem. Soc. 1976, 98, 4443.

9. McVicker, G. B. Inorg. Chem. 1975, 14, 2087.

10. Darensbourg, M. Y.; Jimenez, P.; Sackett, J. R.; Hanckel, J. M.; Kamp, R. L. J. Am. Chem. Soc. 1982, 104, 1521.

11. Blackman, T.; Burlitch, J. M. J. Chem. Soc., Chem. Commun. 1973, 405.

12. a.) Krusic, P. J.; Fagan, P. J.; San Filippo, J., Jr. J. Am. Chem. Soc., 1977, 99, 250. b.) San Filippo, J., Jr.; Silbermann, T.; Fagan, P. J. J. Am. Chem. Soc. 1978, 100, 4834.

13. Tilley, T. D.; Andersen, R. A.; Zalkin, A.; Templeton, D. H. Inorg. Chem. 1982, 21, 2644.

14. Tilley, T. D.; Andersen, R. A.; Spencer, B.; Zalkin, A. Inorg. Chem. 1982, 21, 2647.

15. a.) Frenz, B. A.; Ibers, J. A.; Inorg. Chem., 1972, 11, 1109/ b.) Clegg, W.; Wheatley, P. J. J. Chem. Soc. A 1971, 3572; J. Chem. Soc. Dalton Trans. 1973, 90; 1974, 424, 511. c.) Katacher, M. L.; Simon, G. L. Inorg. Chem. 1972, 11, 1651. d.) Herberhold, M.; Wehrmann, F.; Neugebaur, D.; Huttner, G. J. Organomet. Chem. 1978, 152, 329.

16. a.) Martin, M.; Rees, B.; Mitschler, A. Acta. Crystalogr., Sect. B 1982, B38, b.) Churchill, M. R.; Amoh, K. N.; Wasserman, H. J.

Inorg. Chem. **1981**, 20, 1609.

17. Krotty, D. E.; Corey, E. R.; Anderson, T. J.; Glick, M. D.; Oliver, J. P. Inorg. Chem. **1977**, 16, 920.

18. Fischer R. D. in "NMR of Paramagnetic Molecules" LaMar, G. N.; DeW Horrocks, W.; Holm, R. H. eds. Academic Press, New York, 1973, pp. 521-549.

19. Gutowsky, H. S.; Holm, C. H. J. Chem. Phys. **1956**, 25, 1228.

20. Pignolet, L. H.; Lewis, R. A.; Holm, R. H. Inorg. Chem. **1972**, 11, 99.

21. Bradley, D. C.; Mehrotra, R. C.; Gaur, D. P. "Metal Alkoxides", Academic Press, San Francisco, 1978 pp. 122-134.

22. a.) Shriver, D. F. J. Organomet. Chem. **1975**, 94, 159; Acc. Chem. Res. **1970**, 3, 231. b.) Nelson, N. J.; Kime, N. E.; Shriver, D. F. J. Am. Chem. Soc. **1969**, 91, 5173.

23. Butts, S. B.; Holt, E. M.; Strauss, S. H.; Alcock, N. W.; Shriver, D. F. J. Am. Chem. Soc. **1979**, 101, 5864.

24. a.) Schore, N. E.; Ilenda, C. S.; Bergman, R. G. J. Am. Chem. Soc. **1977**, 99, 1781. b.) Cirjak, L. M.; Ginsburg, R. E.; Dahl, L. F. Inorg. Chem. **1979**, 17, 301. c.)

25. Jones, W. D.; White, M. A.; Bergman, R. G. J. Am. Chem. Soc. **1978**, 100, 6770.

26. Hofmann, P. Angew. Chem. Int. Ed. Engl. **1977**, 16, 536.

Chapter 2

Reaction of Bis(pentamethylcyclopentadienyl)ytterbium with Organic Molecules

Reactions with Heterocyclic Amines

The simple coordination chemistry of $(C_5Me_5)_2Yb{\cdot}OEt_2$ with various hetero-atom donors has been discussed in the Introduction. In Chapter 1 it was shown that transition-metal carbonyl complexes can be reduced by, as well as form coordination complexes with, $(C_5Me_5)_2Yb(II)$. The isolation of coordination complexes between $(C_5Me_5)_2Yb(II)$ and transition-metal carbonyl complexes indicates that the coordination chemistry of $(C_5Me_5)_2Yb(II)$ plays an important role in the electron transfer reactions. If the reduction potential of the coordinated ligand is less negative than that of $(C_5Me_5)_2Yb(II)$, then electron transfer into the ligand will occur. In this chapter, reactions between $(C_5Me_5)_2Yb{\cdot}OEt_2$ and various aromatic heterocyclic amines which result in the formation of $(C_5Me_5)_2Yb(III)L^{\cdot-}$ will be discussed, as will the interaction between $(C_5Me_5)_2M{\cdot}OEt_2$ (M=Eu, Yb) and the protic acid phenylacetylene.

Reaction of 2,2'-bipyridine with either $(C_5Me_5)_2Eu(THF)(OEt_2)$ or $(C_5Me_5)_2Yb{\cdot}OEt_2$ gives the complexes $(Me_5C_5)_2M(bipy)$. The europium complex is paramagnetic, and the magnetic susceptibility follows Curie behavior from 5-60K with μ_{eff}=7.73B.M..[1] This value is consistent with a divalent europium ion with an $^8S_{7/2}$ ground state. Divalent europium is therefore not sufficiently reducing to reduce bipyridine. This is

expected since the reduction potential of Eu(III) in aqueous solution is -0.35V.[2], while that of 2,2'-bipyridine is measured at -2.1V.[3] in non-aqueous solvents. Coordination of bipy to a metal does change the reduction potential of 2,2'-bipyridine to -0.83V in $[Ir(bipy)_3]^{3+}$.[4]

The brown complex formed by reaction of $(C_5Me_5)_2Yb{\cdot}OEt_2$ with bipy in toluene is paramagnetic as judged by the line widths and shifts of its ^1H NMR spectrum (Table I).[5] The magnetic moment in solution at 30°C is 2.4B.M., and the complex is also paramagnetic in the solid state (see below). Since divalent ytterbium complexes are diamagnetic, it appears that an electron has been transferred from ytterbium to bipyridine to give a complex which is best formulated as $[(C_5Me_5)_2Yb(III)][bipy^{\cdot}]$. It is reasonable to suggest that $(C_5Me_5)_2Yb{\cdot}L$ could transfer an electron into bipy since the oxidation petential of $(C_5Me_5)_2Yb{\cdot}L_2$ (L=MeCN) in MeCN has been estimated at +1.3V.[6]

In order to test the proposal that the ytterbium complex is a bipyridine radical ion, a series of $[(C_5Me_5)_2Ybbipy]^+[X]^-$ complexes were synthesized so that a detailed structural comparison could be made. The complex $[(C_5Me_5)_2Yb(III)][bipy^{\cdot}]$ reacts with silver iodide to give the brown complex $[(C_5Me_5)_2Ybbipy]^+[I]^-$. This complex may be converted back to $[(C_5Me_5)_2Yb(III)][bipy^{\cdot}]$ by reaction with sodium amalgam in THF. Addition of bipyridine to the trivalent complex $(C_5Me_5)_2YbCl{\cdot}THF$ results in the red-brown salt $[(C_5Me_5)_2Ybbipy]^+[(C_5Me_5)_2YbCl_2]^-$. This compound, which crystallizes very nicely from dichloromethane, has been characterized by single crystal X-ray diffraction methods(see below). When two equivalents of $[(C_5Me_5)_2Yb(III)][bipy^{\cdot}]$ react with $Co_2(CO)_8$, the compound $[(C_5Me_5)_2Ybbipy]^+[Co(CO)_4]^-$ results which unlike the compounds in Chapter 1, does not contain Yb-O-C-M interactions.

Table I. ^1H NMR Spectra of Some $(C_5Me_5)_2Yb(III)$ bipyridine and bipyrimidine Complexes.

Compound	Color	^1H NMR
$[(C_5Me_5)_2Yb(III)][bipy^{\bullet}]$	Brown	δ-13.11($\nu_{1/2}$ = 8Hz, 2H): δ4.11($\nu_{1/2}$ = 9Hz, 30H); δ25.32($\nu_{1/2}$ = 41Hz, 2H);
$[(C_5Me_5)_2Ybbipy]^+[(C_5Me_5)_2YbCl_2]^-$	Red	δ-1.91($\nu_{1/2}$ = 38Hz, 2H); δ1.43($\nu_{1/2}$ = 44Hz, 30H): δ3.23($\nu_{1/2}$ = 79Hz, 30H); δ15.82($\nu_{1/2}$ = 30Hz, 2H); δ58.00($\nu_{1/2}$ = 38Hz, 2H)
$[(C_5Me_5)_2Yb]_2bipm$		δ-4.10($\nu_{1/2}$ = 61Hz, 30H); δ4.23($\nu_{1/2}$ = 103Hz, 2H): δ68.52($\nu_{1/2}$ = 28Hz, 1H)

Since X-ray crystallography has been shown to be useful in determining the oxidation state of ytterbium, a comparison of the crystal structures of the complexes $(C_5Me_5)_2Yb(py)_2$,[7] $(C_5Me_5)_2Ybbipy$, and $[(C_5Me_5)_2Ybbipy)^+[(C_5Me_5)_2YbCl_2]^-$ is in order. If the $(C_5Me_5)_2Ybbipy$ complex contains Yb(III) and $bipy^{\cdot}$, then the bond length parameters for this complex should be significantly different from that of a divalent eight coordinate ytterbium complex and similar to that of a trivalent, eight-coordinate, ytterbium complex. The three complexes are perfect for such a comparison since they have equivalent coordination numbers, and essentially identical coordination environments. The only difference between them is the oxidation state of the ytterbium atom.

An ORTEP diagram of $(C_5Me_5)_2Ybbipy$ is shown in Figure 1. The molecule crystallizes in the orthorhombic crystal system in space group Pbca with two independent molecules in the asymmetric unit. Both molecules are chemically identical, and only a single ORTEP drawing is shown. Bond lengths for both molecules are found in Tables (II) and (III), respectively.

The averaged Yb-C distance in $(C_5Me_5)_2Ybbipy$ is 2.62°±0.01Å, the averaged Yb-ring centroid distance is 2.34Å and the averaged Yb-N distance is 2.32±0.01Å. The averaged ring centroid-Yb-ring centroid angle is 137°, while the averaged ring centroid-Yb-N angle is 107°. The averaged N-Yb-N angle is 69.9±0.2°.

An ORTEP drawing of $[(C_5Me_5)_2Ybbipy]^+[(C_5Me_5)_2YbCl_2]^-$ is shown in Figure 2, and a stereo view of the unit cell is shown in Figure 3. The bond lengths and angles are found Tables (IV) and (V), respectively. Data collection parameters, crystal data, and positional and thermal

Figure 1. ORTEP of $[(C_5Me_5)_2Yb(III)][bipy^{\cdot}]$

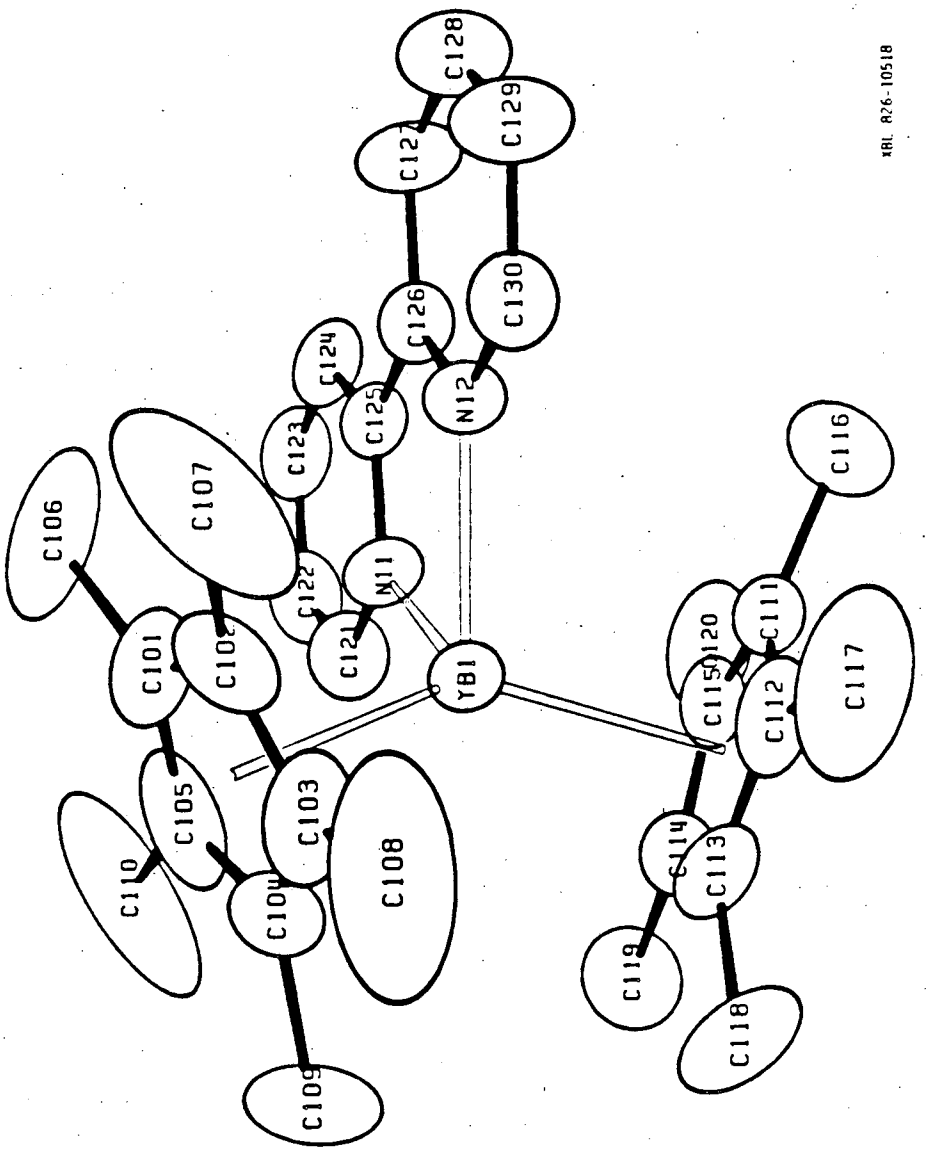

Table II. Bond Lengths (Å) for $[(C_5Me_5)_2Yb(III)][bipy^{\cdot-}]$, molecule 1

Yb1-C101	2.625(9)	N11-C121	1.361(9)
Yb1-C102	2.621(8)	N11-C125	1.371(8)
Yb1-C103	2.625(8)	C121-C122	1.403(10)
Yb1-C104	2.623(8)	C122-C123	1.397(11)
Yb1-C105	2.616(8)	C123-C124	1.365(10)
Yb1-Cp10*	2.343	C124-C125	1.421(9)
Yb1-C111	2.640(7)	C125-C126	1.436(9)
Yb1-C112	2.619(8)	C126-C127	1.418(10)
Yb1-C113	2.631(7)	C127-C128	1.394(11)
Yb1-C114	2.634(7)	C128-C129	1.414(12)
Yb1-C115	2.647(7)	C129-C130	1.407(11)
Yb1-Cp11*	2.346	N12-C126	1.385(9)
Yb1-N11	2.324(6)	N12-C130	1.360(9)
Yb1-N12	2.318(5)		

* Cp10 and Cp11 are the geometrical centroids of rings C101-C105 and C111-C115, respectively.

Table III. Bond Lengths (Å) for $[(C_5Me_5)_2Yb(III)][bipy^{\cdot-}]$, molecule 2

Yb2-C201	2.607(8)	N21-C221	1.359(9)
Yb2-C202	2.602(8)	N21-C225	1.383(9)
Yb2-C203	2.599(8)	C221-C222	1.373(11)
Yb2-C204	2.635(9)	C222-C223	1.442(12)
Yb2-C205	2.625(9)	C223-C224	1.387(11)
Yb2-Cp20*	2.339	C224-C225	1.431(10)
Yb2-C211	2.597(9)	C225-C226	1.433(9)
Yb2-C212	2.592(9)	C226-C227	1.406(10)
Yb2-C213	2.612(8)	C227-C228	1.403(11)
Yb2-C214	2.623(8)	C228-C229	1.429(12)
Yb2-C215	2.606(8)	C229-C230	1.409(11)
Yb2-Cp21*	2.332	N22-C226	1.394(9)
Yb2-N21	2.310(6)	N22-C230	1.351(9)
Yb2-N22	2.324(6)		

* Cp20 and Cp21 are the geometrical centroids of rings C201-C205 and C211-C215 respectively.

Figure 2. ORTEP of $[(C_5Me_5)_2Ybbipy]^+[(C_5Me_5)_2YbCl_2]^-$

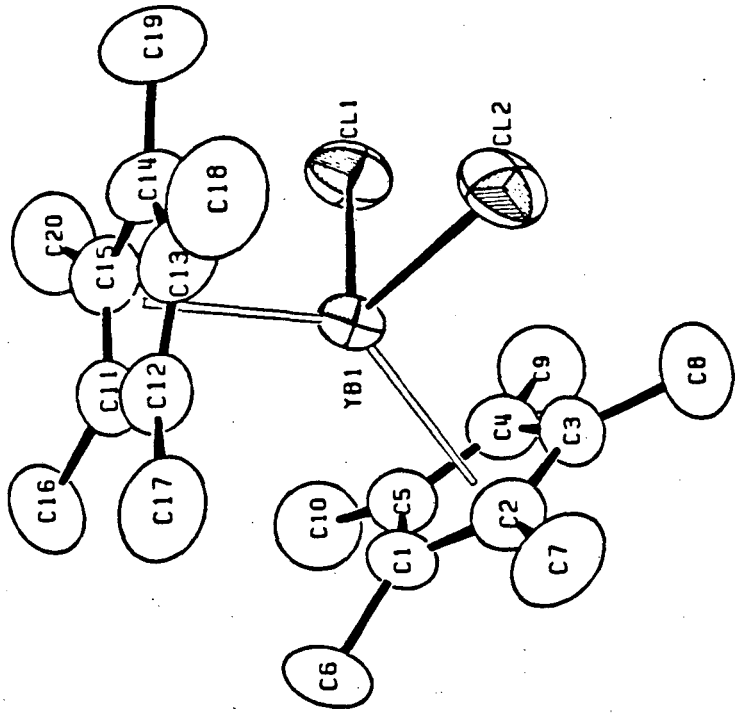

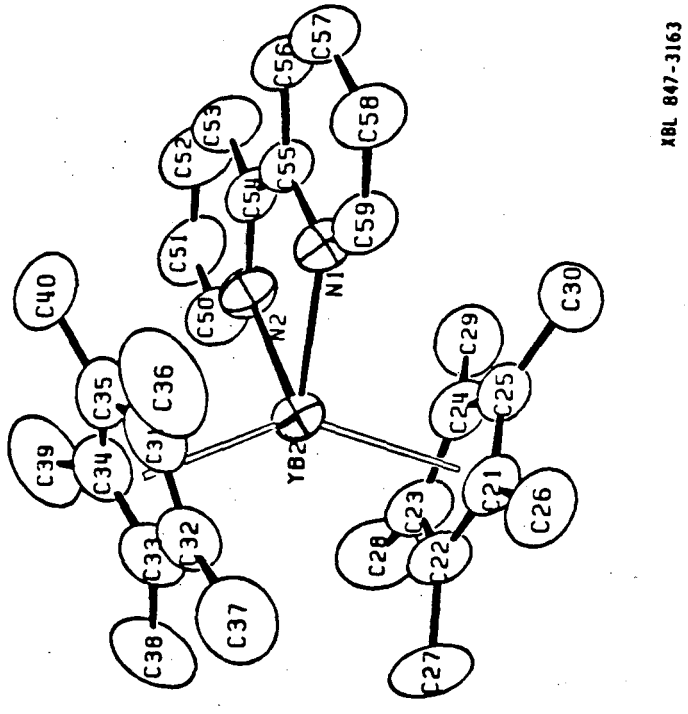

Figure 3. ORTEP Packing Diagram of $[(C_3Me_5)_2Ybbipy]^+[(C_5Me_5)_2YbCl_2]^-$.

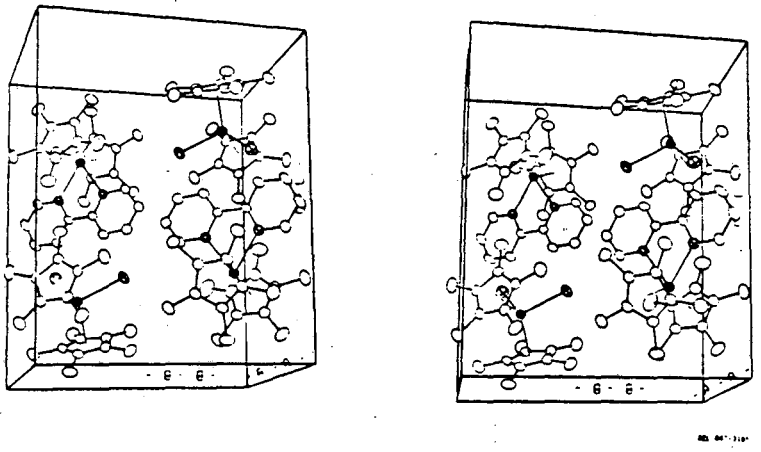

Table IV. Selected Bond Lengths (Å) for $[(C_5Me_5)_2Ybbipy]^+$ $[(C_5Me_5)_2YbCl_2]^-$

Yb1-Cl(1)	2.573(1)	Yb2-C31	2.592(4)
Yb1-Cl(2)	2.560(1)	Yb2-C32	2.591(3)
Yb1-C1	2.612(3)	Yb2-C33	2.588(4)
Yb1-C2	2.631(4)	Yb2-C34	2.592(4)
Yb1-C3	2.689(4)	Yb2-C35	2.587(4)
Yb1-C4	2.672(3)	Yb2-C113	2.302
Yb1-C5	2.612(3)	Yb2-C114	2.300
Yb1-C11	2.663(3)	N1-C55	1.347(4)
Yb1-C12	2.665(3)	N1-C59	1.342(4)
Yb1-C13	2.667(4)	N2-C50	1.336(4)
Yb1-C14	2.647(4)	N2-C54	1.340(4)
Yb1-C15	2.642(3)	C50-C51	1.369(5)
Yb1-C111	2.358	C51-C52	1.366(6)
Yb1-C112	2.371	C52-C53	1.378(5)
Yb2-N1	2.363(3)	C53-C54	1.389(5)
Yb2-N2	2.381(3)	C54-C55	1.492(4)
Yb2-C21	2.582(3)	C55-C56	1.381(5)
Yb2-C22	2.602(3)	C56-C57	1.383(5)
Yb2-C23	2.592(3)	C57-C58	1.374(5)
Yb2-C24	2.614(3)	C58-C59	1.371(5)
Yb2-C25	2.601(3)		

Table V. Selected Bond Angles (deg) for $[(C_5Me_5)_2Ybbipy]^+$ $[(C_5Me_5)_2YbCl_2]^-$

Cl(1)-Yb1-Cl(2)	97.25(3)	N2-C50-C51	123.5(4)
Cl(1)-Yb1-Cl11	104.61	C50-C51-C52	118.4(4)
Cl(1)-Yb1-Cl12	103.42	C51-C52-C53	119.6(4)
Cl(2)-Yb1-Cl11	103.78	C52-C53-C54	118.8(4)
Cl(2)-Yb1-Cl12	105.12	C53-C54-C55	121.8(3)
Cl11-Yb1-Cl12	135.93	C53-C54-N2	121.6(3)
N1-Yb2-N2	68.96(9)	C55-C54-N2	116.5(3)
N1-Yb2-Cl13	106.46	N1-C55-C54	116.0(3)
N1-Yb2-Cl14	105.54	N1-C55-C56	121.7(3)
N2-Yb2-Cl13	106.36	C54-C55-C56	122.3(3)
N2-Yb2-Cl14	104.74	C55-C56-C57	119.3(3)
Cl13-Yb2-Cl14	141.48	C56-C57-C58	119.1(3)
C55-N1-C59	117.9(3)	C57-C58-C59	118.5(3)
C50-N2-C54	118.1(3)	C58-C59-N1	123.3(3)

parameters can be found in the Experimental Section and Appendix (I), respectively. The molecule crystallizes in the triclinic crystal system in space group $P\bar{1}$. The cations and anions are well separated in the crystal lattice. The shortest contacts between the ions are between Cl(1) and C(53), Cl(2) and C(57), Cl(2) and C(58) (see Figure 3) at 3.526(4), 3.545(4) and 3.537(4)Å. Even though the contacts between anion and cation are not exceptionally short, the complex dissolves in acetonitrile as essentially a contact ion-pair since the equivalent conductance in that solvent is $11\Omega^{-1}cm^2mol^{-1}$. The equivalent conductance of a 1:1 electrolyte in CH_3CN lies between 120 and $160\Omega^{-1}$ cm^2mol^{-1}.[8] The observed value of Ω is therefore inconsistent with the complex being ionized in CH_3CN.

The averaged Yb-C distance in the cation is 2.594±0.006Å, the averaged Yb-ring centroid distance is 2.30Å, and the averaged Yb-N distance is 2.372±0.005Å. The ring centroid-Yb-ring centroid angle is 141.5° and the N-Yb-N angle is 68.96(9)°. The averaged Yb-C bond length in the anion is 2.650±0.023Å and the averaged Yb-ring centriod distance is 2.33Å. The averaged Yb-Cl distance is 2.567±0.004Å. The ring centroid-Yb-ring centroid angle is 135.9° and the Cl-Yb-Cl angle is 97.25(3)°. The Yb-C and Yb-Cl distances in the anion portion of the structure are identical to those found in $(C_5Me_5)_2YbCl(\eta_1\text{-dmpm})$[9] at 2.65±0.03 and 2.532(3)Å, respectively. The Yb-C distance in the anion portion of the structure is longer than that found in the cation by 0.06Å, but is probably not statistically significant.

Table (VI) contains a listing of bond lengths and magnetic susceptibility data for a number of di- and trivalent $(C_5Me_5)_2Yb$ complexes. The first two complexes are divalent and seven coordinate.

Table VI. Some Physical Properties of $(C_5Me_5)_2Yb(L)_x$ Complexes

Compound	Averaged Yb-(C_5Me_5) Distance, Å	Magnetic Suscept. per Yb Atom, μ_β(K)	References
$(C_5Me_5)_2Yb(OEt_2)$	2.69±0.02	diamagnetic	10
$(C_5Me_5)_2Yb(THF)$	2.66±0.02	diamagnetic	1
$(C_5Me_5)_2Yb(py)_2$	2.74±0.02	diamagnetic	7
$(C_5Me_5)_2Yb(S_2CNEt_2)$	2.63±0.02	3.39(5-55)	11
$(C_5Me_5)_2Yb(THF)[OCCo(Co)_3]$	2.596±0.002	4.1(303)	12
$[(C_5Me_5)_2Yb]_2Fe_3(CO)_{11}$	2.57±0.01	3.91(4-60)	13
$[(C_5Me_5)_2Yb]_2[Mn(CO)_5]_2$	2.57±0.01	3.57(5-20) 4.24(80-300)	14
$(C_5Me_5)_2Yb(bipy)$	2.62±0.01	2.4(303)	this work
$[(C_5Me_5)_2Yb(bipy)]^+$	2.594±0.006	3.81(5-25)	this work
$[(C_5Me_5)_2YbCl_2]^-$	2.65±0.03	4.99(90-300)	this work

The third complex $(C_5Me_5)_2Yb(py)_2$ is divalent and eight coordinate. The averaged Yb-C bond lengths are the same in all three of these complexes if the difference coordination numbers are taken into account.[15] The remaining complexes in Table (VI) contain trivalent ytterbium in eight coordination. The averaged Yb-C distances in these complexes range from 2.57 to 2.63Å. This value is shorter than that found in $(C_5Me_5)_2Yb(py)_2$ by 0.17 to 0.11Å. This difference is statistically significant, and is expected since Shannon suggests that Yb(II) is 0.16Å larger than Yb(III).[15]

The fact that the averaged Yb-C distance for $[(C_5Me_5)_2Yb(III)][bipy^{\cdot-}]$ is in the range found for Yb(III)-C ring distances is consistent with its assignment as a radical anion-Yb(III) complex. Furthermore, the average Yb-N distance in $[(C_5Me_5)_2Yb(III)][bipy^{\cdot-}]$ is also consistent with the assignment of this complex as a Yb(III)-bipy radical anion complex. Thus, the conclusion that Yb(III) is present in this complex is inescapable.

If the bipy ligand in $[(C_5Me_5)_2Yb(III)][bipy^{\cdot-}]$ is a radical anion, then there should be distortions in the bonding within the bipy ring relative to free bipy. The C-C and C-N bond lengths in free bipy, $[(C_5Me_5)_2Ybbipy]^+[(C_5Me_5)_2YbCl_2]^-$, and $[(C_5Me_5)_2Yb(III)][bipy^{\cdot-}]$ are found in Table (VII). Comparison of the C-C and C-N bond lengths in free bipy and $[(C_5Me_5)_2Ybbipy]^+[(C_5Me_5)_2YbCl_2]^-$ shows that bipy is not distorted when it coordinates to $(C_5Me_5)_2Yb$. When bipy coordinates to Cp_2Ti, the LUMO of bipy is the $B_1(\pi^*)$ molecular orbital which is shown in (I) below.[16] Since Cp_2Ti and $(C_5Me_5)_2Yb$ have the same symmetry,

Table VII. Carbon-Carbon and Carbon-Nitrogen Bond Lengths (Å) in Bipyridines[a]

Compound	2-2'	2-3 2'-3'	3-4 3'-4	4-5 4'-5'	5-6 5'-6'	2-N 2'-N	6-N 6'-N
bipy[b]	1.490(3)	1.394(2)	1.385(2)	1.384(3)	1.384(2)	1.346(2)	1.341(2)
$[(C_5Me_5)_2Yb(bipy]^+$ $[(C_5Me_5)_2YbCl_2]^-$	1.492(2)	1.389(5)	1.378(5)	1.366(6)	1.369(5)	1.343(4)	1.339(4)
$[(C_5Me_5)_2Yb(III)][bipy^{\cdot-}]$	1.434(2)	1.419(7)	1.387(11)	1.421(15)	1.398(13)	1.383(9)	1.358(4)

a.) The value in parentheses is the averaged deviation from the mean value, when more than one value is averaged, and is the esd for a single value.

b.) Reference 21.

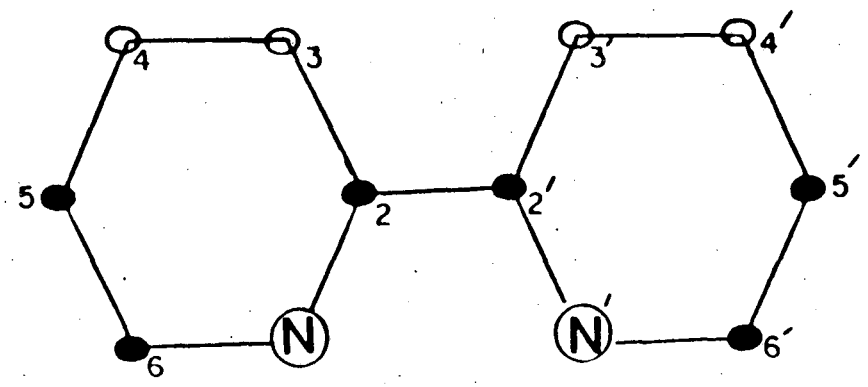

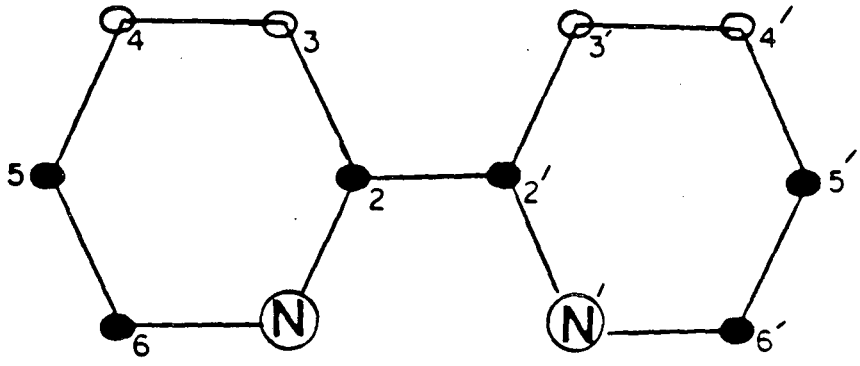

I

the LUMO of bipy in $[(C_5Me_5)_2Yb(III)][bipy^{\cdot}]$ should have the same symmetry.

When coordinated bipy is reduced, the extra electron will reside in the MO shown in (I). Relative to free bipy, the following bonds should lengthen: C(2,2')-C(3,3'), C(4,4')-C(5,5'), C(5,5')-C(6,6') and N,N'-C(2,2'), and the following bonds should contract: C(2)-C(2'), C(2,2')-C(3,3'), and N,N'-C(6,6'). Examination of Table (VII) reveals that this prediction does not quite hold. The bonds which are supposed to stretch do indeed stretch, but within the rings the bonds which should shrink remain essentially the same. The bond which should show the most change in length, the C(2)-C(2') bond, (which goes from a pure sp^2-sp^2 single bond to one which has much more double bond character) shows a dramatic contraction. This dramatic change in bond length shows unequivocally that $[(C_5Me_5)_2Yb(III)][bipy^{\cdot}]$ does indeed have a bipy radical anion.

It has been shown that the bipyridine radical anion has a diagnostic optical spectrum as would be expected for a species in which the odd electron is located in a π^* molecular orbital. Table (VIII) lists the absorption maxima (λmax) for a series of ytterbium(III) complexes with C_5Me_5 groups, and that of the sodium bipyridine radical anion[17] in the visible and near infrared region.

Table VIII. Optical Spectra of Some Bipyridine Compounds

Compound	λ_{max} in nm (ϵ in $1mol^{-1}$ cm^{-1})
$(C_5Me_5)_2YbCl(THF)$ in CH_2Cl_2	535(174), 885(10), 902(10), 913(12), 958(49), 987(33), 1006(44)
$[(C_5Me_5)_2Yb(bipy)][I]$ in CH_2Cl_2	882(7), 899(10), 905(12), 926(11), 945(14), 950(27), 955(41), 978(42), 1004(201), 1022(7), 1032(9)
$[(C_5Me_5)_2Yb(bipy)]$	876(12), 895(12), 900(12), 904(15), 912(10)
$[(C_5Me_5)_2YbCl_2]$ in CH_2Cl_2	927(14), 945(20), 950(36), 956(54), 962(55), 966(78), 977(54), 986(36), 1005(192), 1022(18), 1032(10)
$(C_5Me_5)_2Yb(bipy)$[a] in toluene	385(8.98), 475(4.79), 505(5.71), 800(2.37), 855(2.63), 890(2.96), 1020(0.88)
Nabipy[a] in THF	386(29.5), 532(6.2), 5.62(6.5), 752(1.1), 833(1.5), and 952(1.3)

a.) $\epsilon \times 10^{-3}$ in 1 mol^{-1} cm^{-1}.

b.) Reference 17.

In the region from 700 to 1100nm, the Yb(III) complexes have many sharp weak absorptions due to f-f transitions. The $Na^{+}Bipy^{\dot{-}}$ complex has three broad intense ($1500>\varepsilon>1100$) absorptions at 752, 833 and 952nm, respectively. The spectrum of $[(C_5Me_5)_2Yb(III)][bipy^{\dot{-}}]$ is similar to that of Nabipy in this region, as it shows strong bands at 800, 855 and 890nm ($2960>\varepsilon>2370$), respectively. The similarity of the rest of the spectra of these two complexes is more evidence for the presence of a bipy radical-anion in the ytterbium complex.

The infrared spectrum is also diagnostic of bipyridine radical anions since they have a strong absorption at 950-980cm^{-1} due to ring deformations.[18] The infrared spectrum of $[(C_5Me_5)_2Yb(III)][bipy^{\dot{-}}]$ contains a very strong band at 947cm^{-1} and this region has no absorptions in $[(C_5Me_5)_2Ybbipy]^{+}[(C_5Me_5)_2YbCl_2]^{-}$. Thus the infrared spectral data are also consistent with the presence of a bipy radical anion in $[(C_5Me_5)_2Yb(III)][bipy^{\dot{-}}]$.

The magnetic susceptibility and magnetic resonance (EPR, NMR) behavior of $[(C_5Me_5)_2Yb(III)][bipy^{\dot{-}}]$ is neither trivial nor quantitatively explainable. Figure 4 shows a plot of $1/\chi_M$ vs. T for the complex $[(C_5Me_5)_2Ybbipy]^{+}[(C_5Me_5)_2YbCl_2]^{-}$. This complex follows Curie-Weiss behavior from 5-25K [$K_m=C_M(T-\theta)^{-1}$] with C_M=1.817(21), and θ=-0.86(18)K and μ_{eff}=3.81(7)B.M. and from 90-300K with C_M=3.113(6); θ=-35.98(44) and μ_{eff}=4.990(5)B.M., and is typical of trivalent ytterbium. A plot of $1/\chi_M$ vs. T is given for $[(C_5Me_5)_2Yb(III)][bipy^{\dot{-}}]$ in Figure 5. The curve is not linear with temperature, and is suggestive of antiferromagnetic coupling at low temperature though the Néel temperature has not been reached. No attempt has been made at fitting the observed curve to a coupling model to extract the coupling

Figure 4. Plot of $1/\chi_M$ vs. T for $[(C_5Me_5)_2Ybbipy]^+[(C_5Me_5)_2YbCl_2]^-$

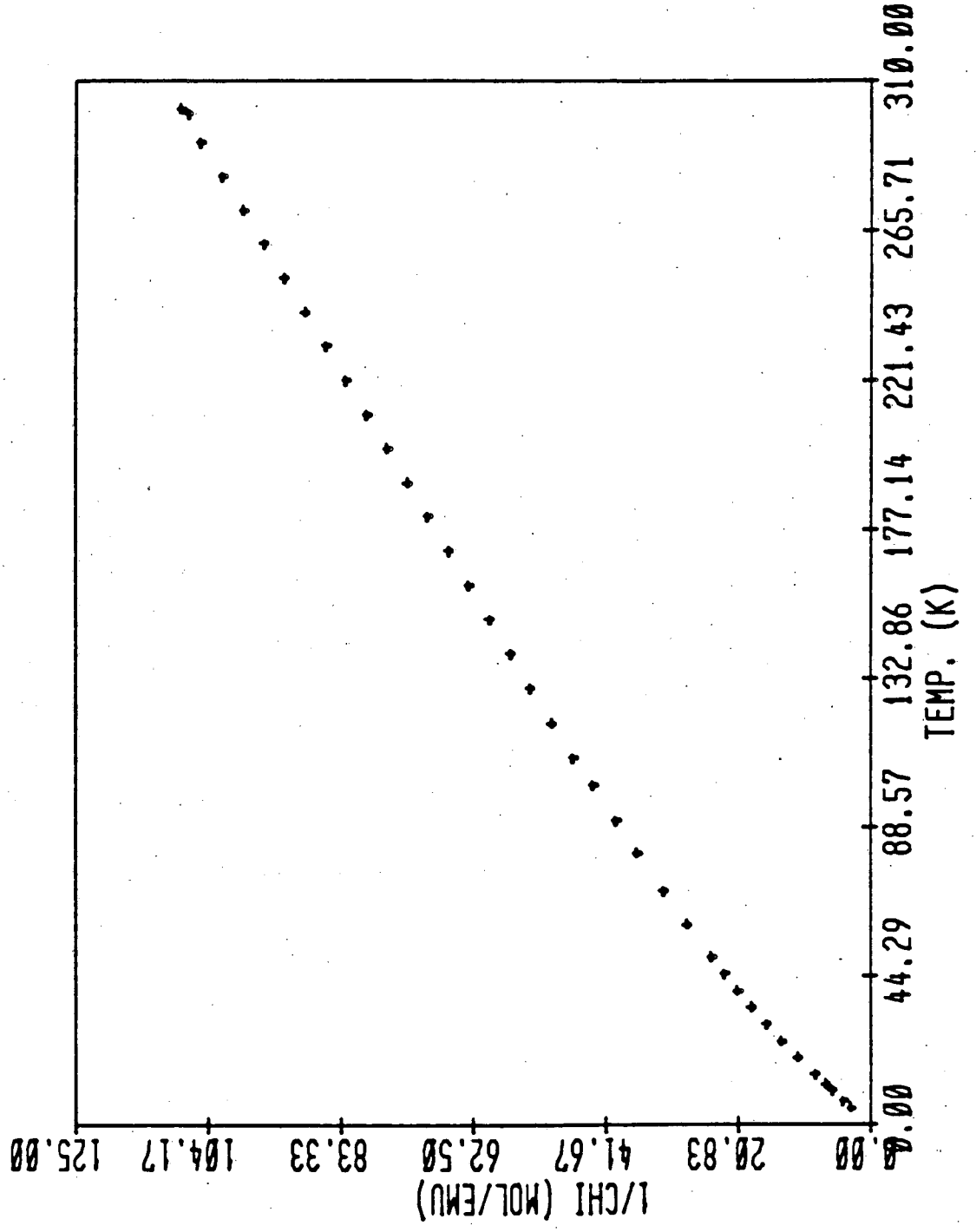

Figure 5. Plot of $1/\chi_M$ vs. T for $[(C_5Me_5)_2Yb(III)][bipy^{\dot{-}}]$

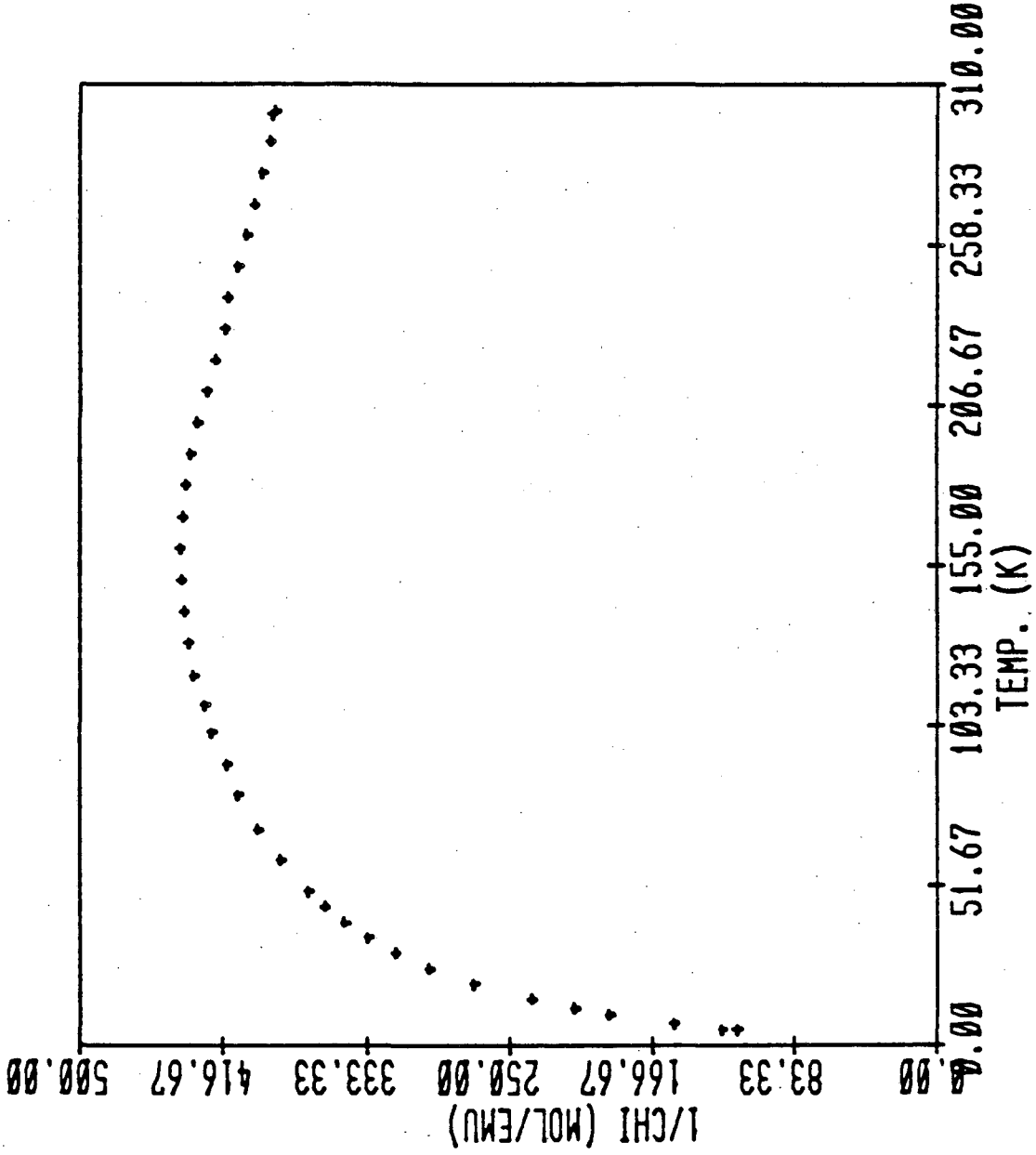

constant, J. Any reasonable model would require coupling a spin of $^1/_2$ (the electron on bipy$^{\dot{-}}$) with the electron on Yb which has $^2F_{7/2}$ ground state, and which interacts in an unknown fashion with a thermally accessable first crystal field excited state.[19] Thus, any reasonable model would present a major calculational problem. The fact that the ordering temperature is not reached until below 5K means that the energy of interaction is on the order of a few cm^{-1}.

The ^1H NMR and EPR data support the contention that the electrons on Yb(III) and on bipy$^{\dot{-}}$ are weakly coupled. Normally, the electrons in organic radicals relax slowly (slow T_{2e}) allowing room temperature observation of the EPR spectrum. The slow relaxation of electrons in organic radicals causes fast relaxation of magnetic nuclei (larger T_{2H}) which broadens the ^1H NMR spectra to the point of being unobservable. The opposite is true of unpaired electrons on lanthanide ions. The large spin-orbit coupling in lanthanides causes their T_{2e}'s to be fast making EPR unobservable at room temperature because of line broadening. This in turn causes slower ^1H relaxation which causes broadened, but observable ^1H NMR spectra.[20]

The observation of ^1H NMR proton resonances on bipy in $[(C_5Me_5)_2Yb(III)][bipy^{\dot{-}}]$ suggests that this radical is not a typical organic radical, it behaves more like an electron on Yb(III). The EPR spectrum of $[(C_5Me_5)_2Yb(III)][bipy^{\dot{-}}]$ is observable only at temperatures of less than 10K (with a g value of 2.0007), at low microwave powers. This sort of EPR behavior is atypical of an organic radical, and more nearly like that of a lanthanide ion. Qualitatively, these observations can be explained if the unpaired electron on Yb is coupling to the unpaired electron on bipy, causing the relaxation time of the bipy

electron to decrease dramatically. This allows the observation of the ^1H NMR spectrum and makes the EPR signal prone to saturation at high microwave powers.

It is unfortunate that the interesting electronic properties of the $[(C_5Me_5)_2Yb(III)][bipy^{\bullet-}]$ complex cannot be explained more quantitatively. The mechanism of interaction between the radical on bipy and the unpaired electron on ytterbium would seem to indicate that there is some covalent interaction between the two species. Whatever the nature of the interaction between the two electrons in $[(C_5Me_5)_2Yb(III)][bipy^{\bullet-}]$, it is not sufficient to have any type of radical species attached to Yb(III) to see such interactions. Recall that the complex $[(C_5Me_5)_2Yb(III)][(\mu_3\text{-}OC)_4Co_3(C_5R_5)_2]$ contains a 47 electron trinuclear cobalt radical. This complex shows magnetic behavior consistent with no interaction between the electrons on the ytterbium atoms and the radical on the trinuclear cobalt species. The relative energies of the ytterbium(III) electron and the unpaired electron on the ligand must be similar for coupling to be important.

The observation that $(C_5Me_5)_2Yb{\cdot}OEt_2$ reduces 2,2'-bipyridine to give a $Yb(III)(bipy^{\bullet-})$ complex suggests that other ligands such as bipyrimidine (see II below) might also undergo electron transfer in a similar fashion. Since 2,2'-bipyrimidine(bipm) can potentially coordinate to two Yb atoms, it is conceivable that two electrons (one from each divalent Yb) could be transferred into the ligand. Such

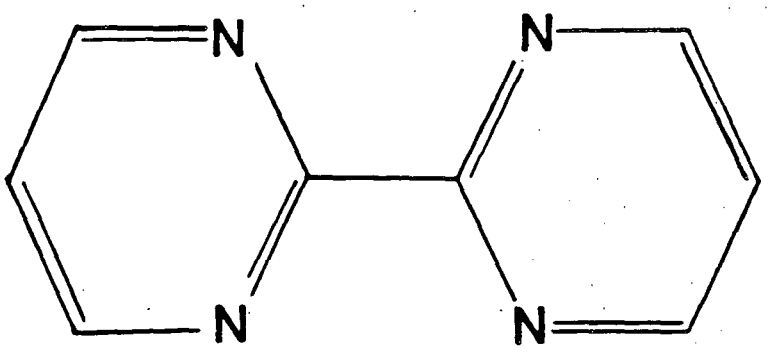

II

a material might have interesting electronic and magnetic properties.

The complex, $(C_5Me_5)_2Yb{\cdot}OEt_2$, reacts with either one or one-half an equivalent of bipm to give the dark purple complex $[(C_5Me_5)_2Yb]_2bipm$ in which the bipm group chelates a pair of $(C_5Me_5)_2Yb$ groups. The complex is paramagnetic as judged by its ^1H NMR spectrum (see Table I). The parent ion isotopic distribution in the mass spectrum of the complex can be simulated, and a comparison of the calculated vs. observed peak intensities is given in Table(IX). The fact that the complex is paramagnetic suggests that, as in the case of bipy, at least one electron has been transferred into the bipm ligand.

The magnetic susceptibility of the solid complex reveals some interesting behavior. A plot of χ_M vs. T for the complex $[(C_5Me_5)_2Yb]_2bipm$ is shown in Figure 6. There is a maximum in this curve at ca. 12K, and the uncorrected μ_{eff} of the complex approaches 5.97B.M. at 300°K. At temperatures below 12K the complex becomes diamagnetic. This behavior is consistent with antiferromagnetic coupling between the unpaired spins in the molecule. The value of μ_{eff} at high temperatures (5.97B.M.) is just the sum of the μ_{eff} for one Yb(III) ion (ca. 4.30B.M.) and a free electron (1.73B.M.). This

Table IX. Observed and Simulated Parent Ion Manifold in the Mass Spectrum of $[(C_5Me_5)_2Yb]_2[bipm]$

Mass (amu)	Obs. Rel. Peak Intensity(%)	Calc. Rel. Peak Intensity(%)
1039	3.90	3.56
1040	15.3	14.22
1041	33.7	33.2
1042	57.5	56.8
1043	83.6	84.1
1044	100	100
1045	92.6	93.0
1046	92.5	93.6
1047	54.9	54.3
1048	46.6	46.5
1049	20.1	14.5
1050	10.9	10.6
1051	4.00	3.95

Figure 6. Plot of χ_M vs. T for $[(C_5Me_5)_2Yb]_2bipm$.

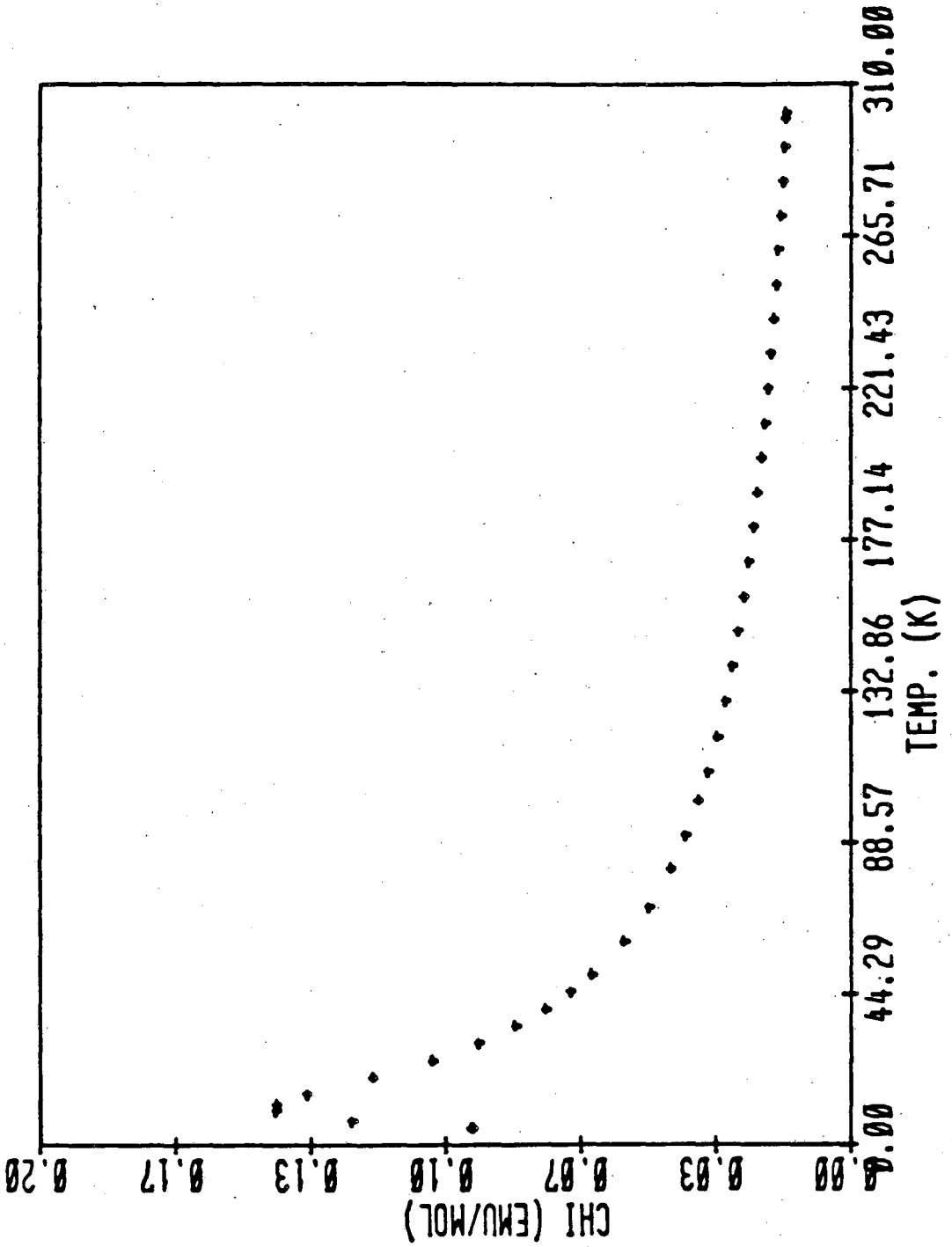

suggests that there has been only one electron transferred into bipm, and that the complex is best described as a mixed valence complex Yb(III)(bipm$^{\cdot}$)Yb(II). The observed antiferromagnetic coupling is consistent with magnetic interaction between the Yb(III) ion and the radical on bipm. The ^{1}H NMR spectrum at room temperature has only one type of C_5Me_5 environment which indicates that any electronic interaction that is occurring occurs fast on the NMR timescale at this temperature.

Simulation of the experimental χ_M vs. T curve for $[(C_5Me_5)_2Yb]_2bipm$ has not been attempted since once again it requires coupling of the bipm radical $S = {}^1/_2$ to the Yb(III) with a $^2F_{7/2}$ ground state.[19] In the simplest view of the interaction, the high temperature magnetic susceptibility is due to the situation drawn in III. There are two spins which do not interact, one on Yb and one on bipm. At low temperature, they interact and pair as in IV. Needless to say, this

III IV

is an extremely simple explanation, but quantitatively gives an idea of what is happening. The observation of a Neél point in the curve lends credibility to the assignment of the magnetic interaction as antiferromagnetic coupling. The fact that the Neél temperature is only

12K suggests that the interaction, though stronger than that in $(C_5Me_5)_2Yb(III)[bipy^{\cdot-}]$, is still rather weak, and is probably on the order of 10 to 20cm^{-1}.

Since structural studies had been helpful in characterizing $[(C_5Me_5)_2Yb(III)][bipy^{\cdot-}]$, a single crystal X-ray crystallographic study was carried out on $[(C_5Me_5)_2Yb]_2bipm$. The molecule crystallizes in the triclinic space group $P\bar{1}$ with two molecules in the unit cell along with two toluene molecules of crystallization. There are two independent half molecules in an asymmetric unit. All of the pentamethyl-cyclopentadienyl rings are two fold disordered, as is the toluene molecule. The two independent half molecules are chemically equivalent. Figure 7 is an ORTEP drawing of one of the molecules. Initially, the coordination about the Yb atom, and the bond lengths within the bipm rings will be discussed. This will be followed by a discussion of how the disorder was modeled, and how the disorder relates to the structure.

Tables (X) and (XI) contain a listing of bond lengths and angles for the complex. The data collection parameters can be found in the Experimental Section, and the thermal and positional parameters are in Appendix (I). An X-ray structure determination of free bipyrimidine was also performed. A high angle (2θ=55°) low temperature (-105°C) data set was used to solve the crystal structure of bipm in order to reduce the errors in the measured bond lengths and angles. An ORTEP drawing of bipm is given in Figure 8, and the bond lengths and angles are found in Table (XII). The data collection parameters are found in the Experimental Section, while the positional and thermal parameters are found in Appendix (I).

Figure 7. ORTEP of $[(C_5Me_5)_2Yb]_2bipm$

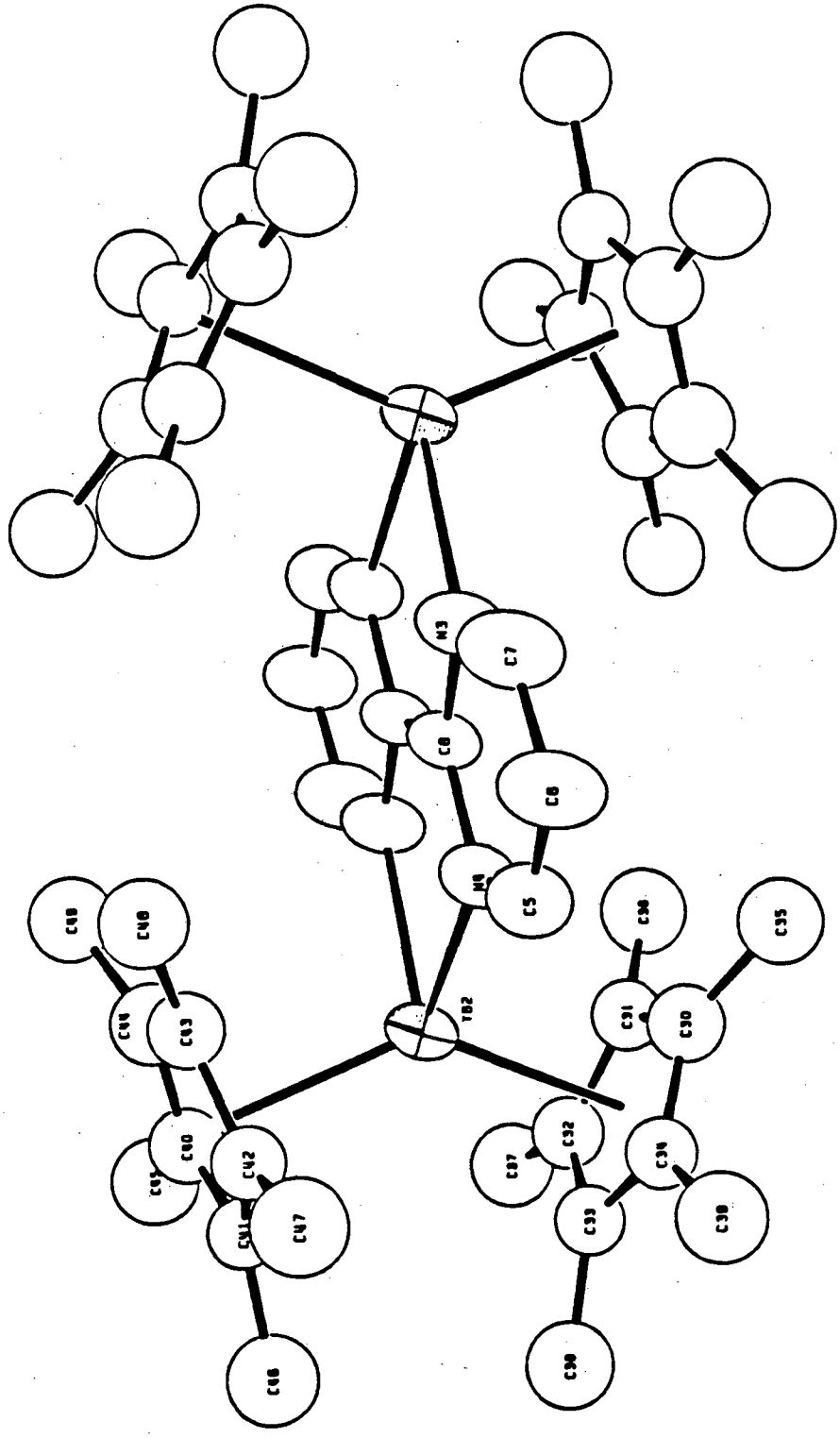

Table X. Selected Bond Lengths (Å) for $[(C_5Me_5)_2Yb]_2[bipm^{\cdot-}]$

Yb1-C10	2.614(4)	Yb2-C301	2.556(12)
Yb1-C11	2.576(4)	Yb2-C311	2.572(9)
Yb1-C12	2.601(5)	Yb2-C321	2.596(8)
Yb1-C13	2.598(5)	Yb2-C331	2.592(8)
Yb1-C14	2.620(4)	Yb2-C341	2.548(8)
Yb1-Cp1	2.314	Yb2-C31	2.271
Yb1-C20	2.632(7)	Yb2-C401	2.565(9)
Yb1-C21	2.601(7)	Yb2-C411	2.614(7)
Yb1-C22	2.581(8)	Yb2-C421	2.610(8)
Yb1-C23	2.615(7)	Yb2-C431	2.585(8)
Yb1-C24	2.611(8)	Yb2-C441	2.575(10)
Yb1-Cp2	2.312	Yb2-Cp41	2.291
Yb1-C201	2.626(8)	Yb1-N1	2.333(3)
Yb1-C211	2.663(9)	Yb1-N2	2.326(3)
Yb1-C221	2.661(9)	Yb2-N3	2.321(3)
Yb1-C231	2.631(7)	Yb2-N4	2.334(3)
Yb1-C241	2.658(7)	C1-N1	1.295(5)
Yb1-Cp21	2.357	C1-C2	1.420(6)
Yb2-C30	2.695(12)	C2-C3	1.413(6)
Yb2-C31	2.671(10)	C3-N2	1.315(5)
Yb2-C32	2.658(9)	C4-N1	1.426(5)
Yb2-C33	2.702(7)	C4-N2	1.431(5)
Yb2-C34	2.699(8)	C4-C4	1.360(7)
Yb2-Cp3	2.398	C5-N4	1.317(5)
Yb2-C40	2.689(9)	C5-C6	1.395(7)
Yb2-C41	2.704(8)	C6-C7	1.387(7)
Yb2-C42	2.663(8)	C7-N3	1.325(6)
Yb2-C43	2.692(9)	C8-N3	1.425(5)
Yb2-C44	2.695(11)	C8-N4	1.407(5)
Yb2-Cp4	2.402	C8-C8	1.358(8)

Table XI. Selected Bond Angles (deg) for $[(C_5Me_5)_2Yb]_2[bipm^{\cdot-}]$

N1-Yb1-N2	72.85(10)	Cp3-Yb2-Cp4	139.2
N1-Yb1-Cp1	107.3	Cp31-Yb2-Cp41	137.3
N1-Yb1-Cp2	106.0	C4-N1-C1	117.5(3)
N1-Yb1-Cp21	106.5	N1-C1-C2	124.7(4)
N2-Yb1-Cp1	106.6	C1-C2-C3	115.5(4)
N2-Yb1-Cp2	105.2	C2-C3-N2	123.8(4)
N2-Yb1-Cp21	107.3	C3-N2-C4	117.5(3)
Cp1-Yb1-Cp2	139.2	N2-C4-N1	121.0(3)
Cp1-Yb1-Cp21	137.5	N2-C4-C4	118.8(4)
N3-Yb2-N4	72.7(11)	N1-C4-C4	120.2(4)
N3-Yb2-Cp3	109.9	C8-N4-C5	117.8(3)
N3-Yb2-Cp4	105.9	N4-C5-C6	124.1(4)
N3-Yb2-Cp31	104.4	C5-C6-C7	116.0(4)
N3-Yb2-Cp41	106.1	C6-C7-N3	124.3(4)
N4-Yb2-Cp3	104.9	C7-N3-C8	117.1(4)
N4-Yb2-Cp4	103.9	N3-C8-N4	120.7(3)
N4-Yb2-Cp31	109.9	N3-C8-C8	119.0(5)
N4-Yb2-Cp41	107.3	N4-C8-C8	120.3(4)

Figure 8. ORTEP of 2,2'-bipyrimidine

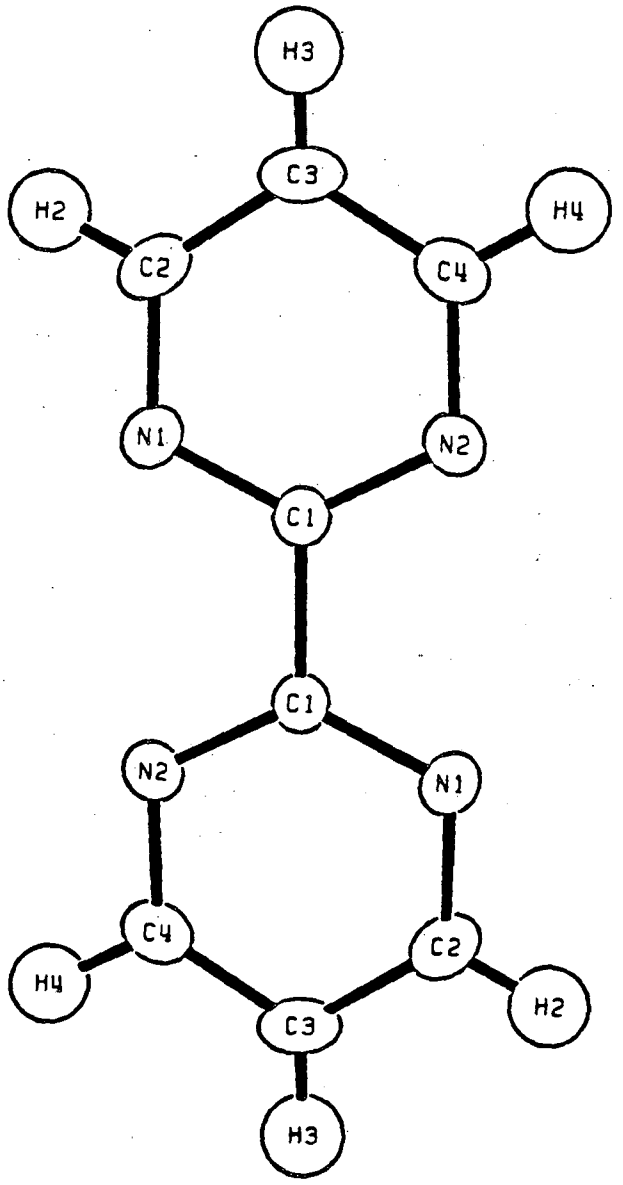

XBL 847-3164

Table XII. Bond Angles (deg) and Lengths (Å) for bipyrimidine.

N1-C1-N2	126.18(6)	N1-C1	1.336(1)
N1-C1-C1'	116.95(7)	N1-C2	1.336(1)
N2-C1-C1'	116.87(8)	N2-C1	1.335(1)
C1-N1-C2	115.89(6)	N2-C4	1.341(1)
C1-N2-C4	115.64(7)	C1-C1'	1.501(1)
N1-C2-C3	123.16(7)	C3-C2	1.373(1)
C2-C3-C4	115.94(7)	C3-C4	1.374(1)
N2-C4-C3	123.19(7)	C2-H2	0.950(10)
N1-C2-H2	115.8(6)	C3-H3	0.941(10)
C3-C2-H2	120.9(6)	C4-H4	1.008(9)
C2-C3-H3	120.6(6)		
C4-C3-H3	123.5(6)		
N2-C4-H4	117.1(5)		
C3-C4-H4	119.7(5)		

The bipyrimidine complex consists of two $(C_5Me_5)_2Yb$ groups which are bridged by a molecule of bipm. The coordination about Yb is pseudo-tetrahedral with the centroid of each C_5Me_5 ring occupying one vertex, and two N atoms of the bipm group occupying the other vertices. The Yb-N averaged distance is 2.328±0.006Å which is similar to that found in $[(C_5Me_5)_2Yb(III)][bipy^{\cdot}]$. Figure 9 shows a comparison of C-C and C-N bond lengths in free bipm and the Yb complex, as well as the amount a given bond has changed in going from the free ligand to the complex. It is obvious that there are large distortions in the C-C and C-N bond lengths within bipm when the free ligand is compared with the complex. These distortions range from just on the edge of statistical significance to a change of many σ for the C-C bridgehead bond.

The distortions of the C-C and C-N bonds, which are caused by transfer of an electron into the bipm ligand, indicate that the π* MO of bipm which accepts the electron has the topology shown in V (below). When an MO such as this one (the B_{1u} under D_{2h} symmetry)

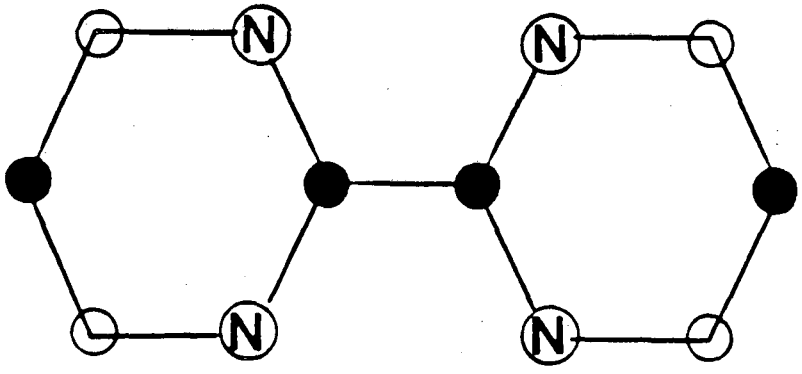

V

is populated, the N(1,2)-C(2,4) and C(1)-C(1') distances should get shorter and the C(1)-N(1,2) and C(3)-C(4,2) distances should lengthen. This is exactly the distortion of the bipm rings which is observed in

Figure 9. Comparison of Intra-ring C-C and C-N Bond Lengths in Free bipm and the Complex $[(C_5Me_5)_2Yb]_2bipm$

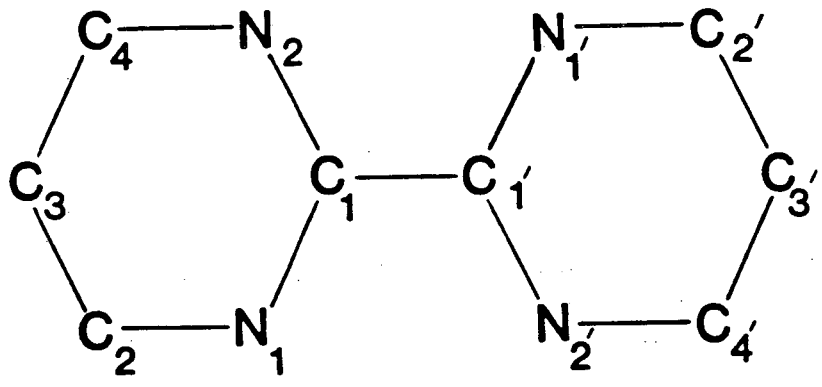

Bond	Yb(Complex)	Free Bipm	(Complex - Bipm)
N1-C1	1.416(10)	1.336(1)	0.080
N2-C1	1.428(3)	1.335(1)	0.093
N2-C4	1.306(11)	1.341(1)	-0.035
N1-C2	1.320(5)	1.336(1)	-0.016
C2-C3	1.407(12)	1.373(1)	0.034
C3-C4	1.400(13)	1.374(1)	0.022
C1-C1'	1.359(1)	1.501(1)	-0.142

$[(C_5Me_5)_2Yb]_2$bipm, and is consistent with the proposal that the bipm ligand has been reduced, and that the unpaired electron resides in the B_{1u} π^* orbital.

The disorder in the C_5Me_5 rings, which are bound to Yb in the complex, was discovered during refinement of the structure when difference Fourier syntheses revealed ten peaks of equal size associated with C_5Me_5 methyl groups rather than five. The ring carbon atoms could not be resolved from one another. The disorder was modeled by constrained isotropic refinement of the C_5Me_5 rings. The positions of both sets of ring carbon atoms for each disordered C_5Me_5 ring were calculated from the position of their associated methyl groups. The C-C and C-Me distances were fixed at 1.420 and 1.500Å, respectively. The C_{ring}-C_{ring}-C_{ring} and C_{ring}-C_{ring}-Me angles were fixed at 108 and 126°, respectively. These isotropic bodies were then refined. This strategy was used to model the disorder of both rings bound to Yb2 and one ring bound to Yb1. One ring on Yb1 could not be modeled in the above fashion because the methyl groups could not be resolved from one another. When this ring was removed from the structure, and a difference Fourier calculated, seven peaks were observed in the area of the missing ring having roughly equal heights. Only two of the five methyl groups could be resolved into their respective components in this manner. There was also a large spread (2.55-2.75Å) in the distances of the ring carbon atoms to the Yb atom. This suggests that the ring is probably disordered in a fashion such that the two components eclipse one another, with one component being closer to the metal than the other, as was found in the other C_5Me_5 rings.

The averaged Yb-C_{ring} bond lengths are given in Table (XIII). These

Table XIII. Ytterbium to Ring Carbon Atom Averaged Bond Lengths for $[C_5Me_5)_2Yb]_2[bipm^-]$. (Å)[a,b]

Yb1-C10-14(ave)	2.602(17)	Yb2-C30-34(ave)	2.685(19)
Yb1-C20-24(ave)	2.608(19)	Yb2-C301-304(ave)	2.573(21)
Yb1-C201-241(ave)	2.648(18)	Yb2-C40-44(ave)	2.689(15)
		Yb2-C401-441(ave)	2.590(21)

a.) The bracketed numbers represent the standard deviation of the average of the five lengths.

b.) C20-24 and C201-204 are the two half occupancy components of a single disordered C_5Me_5 ring, as are C30-34, C301-341 and C40-44, C401-441.

averaged bond lengths fall into two ranges, either from 2.57 to 2.60Å or 2.65 to 2.69Å. The atom numbering system of the rings is such that, for example, C(30)-C(34) and C(301)-C(341) are half occupancy rings on the same side of Yb2. Thus, it appears that half of the time the Yb sites in the crystal are occupied by Yb atoms which have rings which are 2.68Å from the Yb atom, and the other half of the time they are occupied by Yb atoms which have rings that are 2.59Å away. This suggests that there are Yb(II) and Yb(III) ions occupying any given Yb site in the crystal. The complex is therefore in a trapped valence electronic configuration as observed by X-ray diffraction in the solid state.

It has been demonstrated that the complex $(C_5Me_5)_2Yb{\cdot}OEt_2$ is a strong enough reductant to reduce the ligands bipy and bipm. Furthermore, these complexes have interesting magnetic and electronic properties. Unfortunately, the theory of the electronic structure of lanthanide ions cannot be used to rationalize this behavior in a simple fashion. The observation that $(C_5Me_5)_2Yb$ reduces bipy and $(C_5Me_5)_2Eu$ does not reduce bipy is consistent with the reduction potentials of Yb(III) and Eu(III) which were discussed in the Introduction.[2] There should be other reactions in which these two complexes will exhibit differing electron transfer behavior. One such reaction is the reaction with the protic acid H-C≡C-Ph.

Reactions with Phenyl Acetylene

When $(C_5Me_5)_2Yb{\cdot}OEt_2$ is mixed with one equivalent of H-C≡C-Ph, a red crystalline material is isolated which is paramagnetic as judged by the line widths and chemical shifts in the ^1H NMR spectrum. The integrated

intensity of the ^1H NMR peaks indicate that there is a 1:1 ratio of C_5Me_5 and phenyl rings in the complex. The complex cannot have the stoichiometry $(C_5Me_5)Yb(C\equiv C-Ph)$ and be paramagnetic since Yb(II) complexes are diamagnetic. The actual stoichiometry of the complex was determined from the single crystal X-ray diffraction study of the complex and found to be $(C_5Me_5)_4Yb_3(Ph-C\equiv C)_4$.

An ORTEP drawing of the complex is given in Figure 10. The bond lengths and angles are found in Tables (XIV) and (XV). The data collection parameters and crystal data are found in the Experimental Section, while positional and thermal parameters can be found in Appendix (I). Examination of Figure 10 shows the complex to be a linear array of three ytterbium atoms. The ytterbium atoms on each end are each bound to a pair of C_5Me_5 groups, and are bridged to the central ytterbium atom by four phenylacetylide groups. The overall structure is very compact, and shows no evidence for the presence of a hydride ligand. Thus, the stoichiometry of eight anionic ligands and three Yb atoms demands a mixed valence formulation for this compound.

Examination of the $Yb-C_{ring}$ and $Yb-C_{bridge}$ bond lengths allows assignment of the oxidation states of the three individual Yb atoms. The $Yb(1,2)-C_{ring}$ averaged bond length of 2.61(2)Å is in the range found for trivalent $(C_5Me_5)_2YbL_2$ complexes,[9,11-14] and significantly shorter than that (2.742(7)Å) found in the divalent complex $(C_5Me_5)_2Yb(py)_2$. The averaged Yb(1,2)-C(C≡CPh) bond length is 2.40(2)Å and the averaged Yb(3)-C(C≡CPh) bond length is 2.52(1)Å. The bond length data support the proposition that Yb(1,2) are trivalent, and Yb(3) is divalent, since Shannon suggests that the radius of Yb(III) is 0.16Å smaller than Yb(II).[15] Thus, $(C_5Me_5)_4Yb_3(C\equiv CPh)_4$ is an Yb(III,II,III) mixed valence

Figure 10. ORTEP of $(C_5Me_5)_4Yb_3(\mu_2\text{-}C{\equiv}CPh)_4$

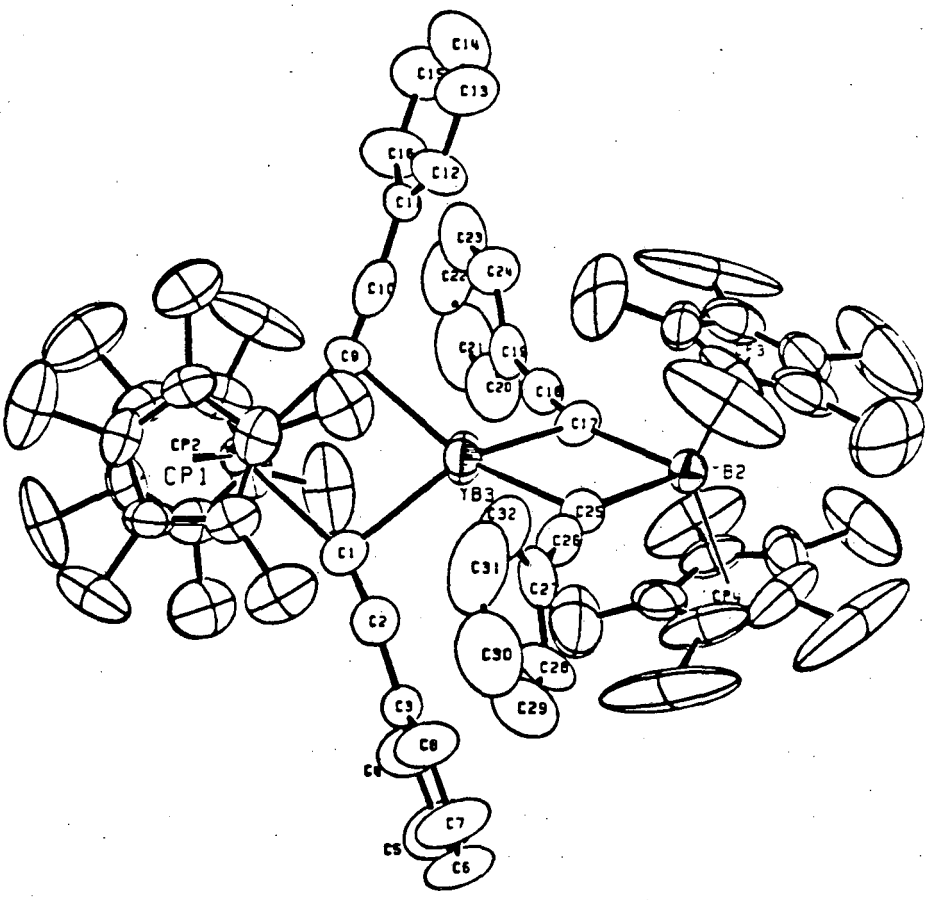

Table XIV. Selected Bond Lengths for $(C_5Me_5)_4Yb_3(\mu_2\text{-}C{\equiv}CPh)_4$

Yb1-C40	2.606(6)	C1-C2	1.236(8)
Yb1-C41	2.650(6)	C9-C10	1.205(8)
Yb1-C42	2.620(6)	C17-C18	1.220(8)
Yb1-C43	2.631(6)	C25-C26	1.214(8)
Yb1-C44	2.592(6)	C10-C11	1.493(10)
Yb1-Cp1*	2.315	C2-C3	1.477(8)
Yb1-C50	2.607(6)	C18-C19	1.453(8)
Yb1-C51	2.591(7)	C26-C27	1.468(9)
Yb1-C52	2.605(6)	C11-C12	1.390(9)
Yb1-C53	2.593(7)	C11-C16	1.359(9)
Yb1-C54	2.603(7)	C12-C13	1.388(10)
Yb1-Cp2*	2.321	C13-C14	1.336(13)
Yb2-C60	2.601(8)	C14-C15	1.341(13)
Yb2-C61	2.652(8)	C15-C16	1.420(12)
Yb2-C62	2.647(8)	C3-C4	1.387(9)
Yb2-C63	2.630(7)	C4-C5	1.407(11)
Yb2-C64	2.628(7)	C5-C6	1.347(12)
Yb2-Cp3*	2.345	C6-C7	1.324(10)
Yb2-C70	2.631(7)	C7-C8	1.334(9)
Yb2-C71	2.595(7)	C8-C3	1.366(8)
Yb2-C72	2.582(7)	C19-C20	1.330(10)
Yb2-C73	2.599(9)	C20-C21	1.391(12)
Yb2-C74	2.605(8)	C21-C22	1.332(17)
Yb2-Cp4*	2.326	C22-C23	1.333(16)
Yb1-C1	2.358(6)	C23-C24	1.346(11)
Yb1-C9	2.409(6)	C24-C19	1.432(9)
Yb2-C17	2.413(6)	C27-C28	1.398(9)
Yb2-C25	2.426(6)	C28-C29	1.397(9)
Yb3-C1	2.509(6)	C29-C30	1.379(13)
Yb3-C9	2.534(6)	C30-C31	1.304(13)
Yb3-C17	2.516(6)	C31-C32	1.380(11)
Yb3-C25	2.537(6)	C32-C27	1.362(9)

* Cp=centroid of preceding 5 carbon atoms.

Table XV. Selected Bond Angles for $(C_5Me_5)_4Yb_3(\mu_2\text{-}C{\equiv}CPh)_4$ (deg)

Cp1-Yb1-Cp2	138.7	C17-Yb3-C25	81.4(2)
Cp1-Yb1-C1	104.0	Yb1-C1-Yb3	97.6(2)
Cp1-Yb1-C9	104.4	Yb1-C9-Yb3	95.6(2)
Cp2-Yb1-C1	104.9	Yb2-C17-Yb3	96.8(2)
Cp2-Yb1-C9	106.4	Yb2-C25-Yb3	45.9(2)
C1-Yb1-C9	86.0(2)	Yb1-C1-C2	156.3(6)
Cp3-Yb2-Cp4	137.2	Yb1-C9-C10	153.7(5)
Cp3-Yb2-C17	105.9	Yb2-C17-C18	161.0(5)
Cp3-Yb2-C25	104.8	Yb2-C25-C26	151.7(5)
Cp4-Yb2-C17	104.0	Yb3-C1-C2	104.5(5)
Cp4-Yb2-C25	107.1	Yb3-C9-C10	109.4(5)
C17-Yb2-C25	85.9(2)	Yb3-C17-C18	101.8(5)
C1-Yb3-C9	80.3(2)	Yb3-C25-C26	112.2(4)
C1-Yb3-C17	134.2(2)	C1-C2-C3	172.9(7)
C1-Yb3-C25	113.9(2)	C9-C10-C11	176.1(6)
C9-Yb3-C17	113.6(2)	C17-C18-C19	175.2(7)
C9-Yb3-C25	143.4(2)	C25-C26-C27	175.9(6)

Cp1-4 are the centroids of the C_5Me_5 rings.

complex with idealized D_{2d} symmetry.

The coordination geometry about Yb(1) and Yb(2) is pseudo-tetrahedral in nature with ring centroid-Yb-ring centroid angles of 139 and 137°, respectively. The C(1)-Yb(1)-C(9) angle is 86.0(2)° and the C(17)-Yb(2)-C(25) angle is 85.9(2)°. Thus, the coordination geometry about Yb(1) and Yb(2) is similar to a large number of $(C_5Me_5)_2Yb(III)L_2$ compounds.

The Yb-C-Yb angles range from 95-97° and are similar to those found in a number of complexes which contain acetylide ligands which bridge electro-positive metal atoms. These complexes include $(MeC_5H_4)_4Sm_2(\mu\text{-}C{\equiv}CPh)_2$,[22] $Cp_4Er_2(\mu\text{-}C{\equiv}CCMe_3)_2$,[23] $Me_4Al_2(\mu\text{-}C{\equiv}C\text{-}Me)_2$,[24] and $Ph_4Al_2(\mu\text{-}C{\equiv}CPh)_2$[25].

The coordination environment about Yb(3) can be described as that of a slightly flattened tetrahedron. The dihedral angle between the planes defined by C(1), Yb(3), C(9) and C(17), Yb(3), C(25) is 65.2°, whereas the same dihedral angle in a perfect tetrahedron would be 90°. In addition to the four terminal carbon atoms, the β carbon atoms of the phenylacetylide ligands are also in close contact with Yb(3). The Yb(3)-C(2,10,18,26) distances fall in the range 3.013(6)Å-3.200(6)Å. Clearly Yb(3) is trying to increase its coordination number to something greater than four by pulling the β carbon atoms of the phenylacetylide groups toward it. The Yb(1,2)-C_α-C_β average angle is 155.7° while the Yb(3)-C_α-C_β angle is 106.9°. Closer interaction between the β carbon atoms on the phenylacetylide ligands and Yb(3) is prevented by close contacts between the phenyl rings and the C_5Me_5 rings (for example, the C(12)-C(69) distance is 3.26Å).

Further evidence in support of the assignment of $(C_5Me_5)_4Yb_3(C{\equiv}CPh)_4$

as a mixed valence complex comes from solid state magnetic susceptibility studies. A plot of $1/\chi_M$ vs. T for $(C_5Me_5)_4Yb_3(C{\equiv}CPh)_4$ is shown in Figure 11. If Yb(1) and Yb(2) are assumed to be Yb(III) ions then the complex follows Curie-Weiss behavior from 5 to 30K with C_M=1.59(3), θ=-1.98(41) and μ_{eff} per Yb(III)=3.58(4)B.M., and from 80 to 300K with C_M=2.540(4), θ=-24.94(36) and μ_{eff} per Yb(III)=4.526(4)B.M. These values show that the complex is a Class I or trapped valence complex, i.e., there is no electron exchange between the Yb(III) centers.

Reaction of one equivalent of phenyl acetylene with $(C_5Me_5)_2Eu{\cdot}OEt_2$ in toluene results in the precipitation of an orange solid which may be crystallized from THF. The ^1H NMR spectrum of the complex is unobservable, and the infrared spectrum has a band in the ν-C≡C region of the spectrum. If the compound is hydrolyzed with D_2O, a ^1H NMR spectrum of a C_6D_6 extract of the hydrosylate contains resonances assignable to C_5Me_5D, THF and PhC≡C-D in a 1:2:1 ratio. In order to fully characterize the compound, a single crystal X-ray diffraction study was performed.

Figure 12 contains an ORTEP drawing of the europium complex. The bond lengths and angles are found in Tables (XVI) and (XVII), while the data collection parameters are found in the Experimental Section, and positional and thermal parameters are deposited in Appendix (I). Figure 11 reveals that the complex consists of two $(C_5Me_5)Eu(II)$ groups which are bridged by two phenyl acetylide groups. The coordination sphere of each europium atom is completed by two molecules of THF. The averaged $Eu-C_{ring}$ distance is 2.815(18)Å which is similar to that found in the complex $(C_5Me_5)_2Eu(OEt_2)$ which is 2.80(1). The Eu(1) to C_{bridge}

Figure 11. Plot of $1/\chi_M$ vs. T for $(C_5Me_5)_4Yb_3(\mu_2\text{-}C{\equiv}CPh)_4$

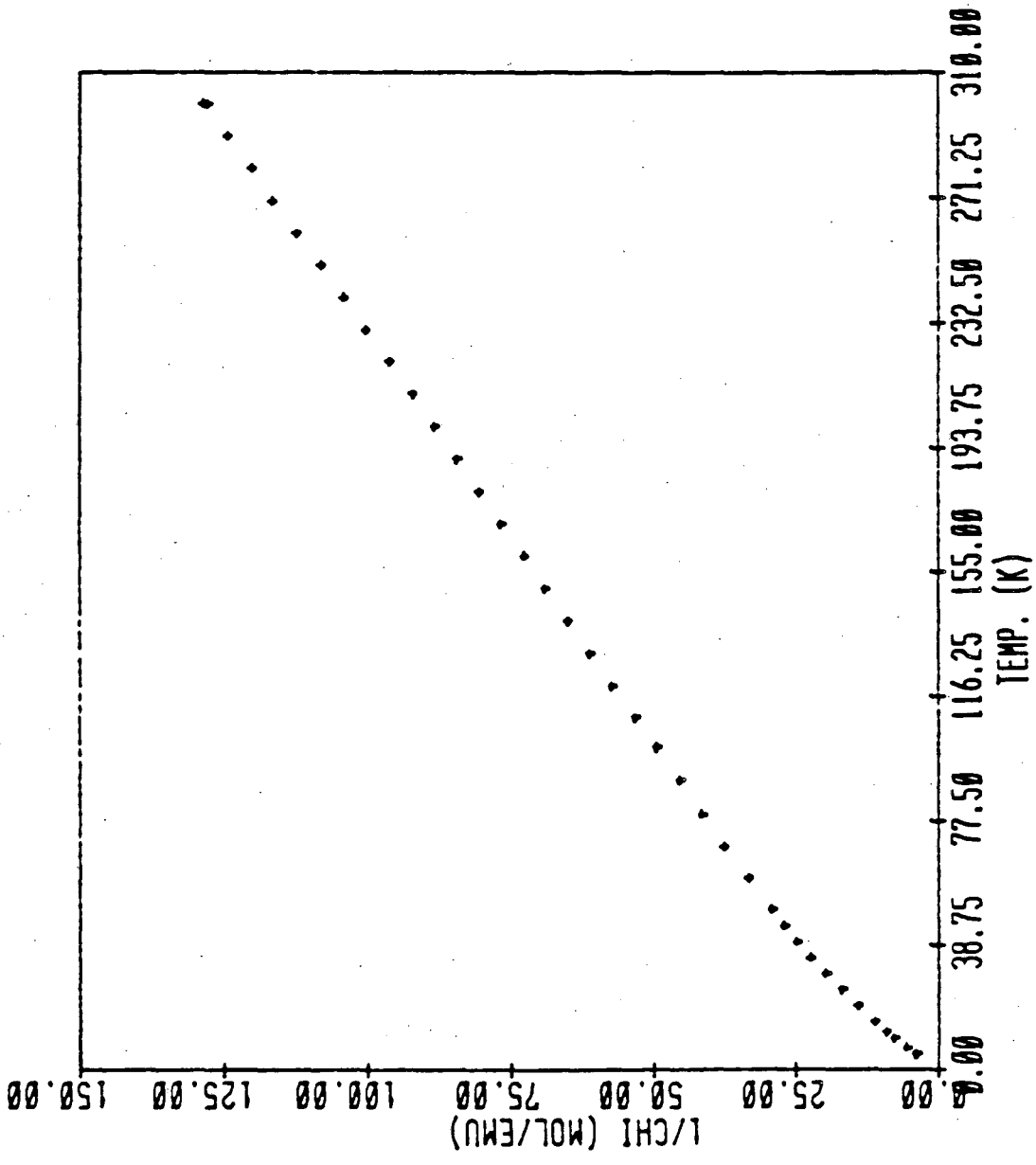

Figure 12. ORTEP of $(C_5Me_5)_2Eu_2(\mu_2\text{-}C{\equiv}CPh)_2(THF)_4$

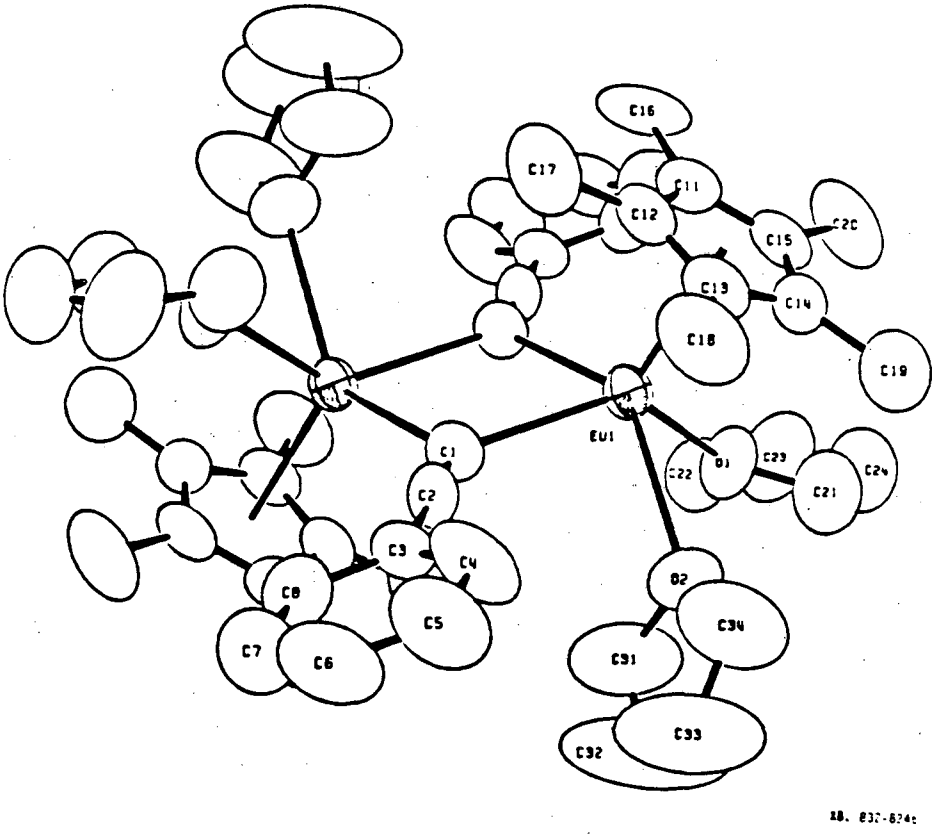

Table XVI. Bond Lengths (Å) for $(C_5Me_5)_2Eu_2(\mu_2\text{-}C{\equiv}CPh)_2(THF)_4$

Eu1-O1	2.602(5)	C6-C7	1.343(13)
Eu1-O2	2.642(5)	C7-C8	1.386(10)
Eu1-C1	2.702(7)	C11-C12	1.390(10)
Eu1-C1	2.709(7)	C11-C15	1.411(11)
Eu1-C11	2.838(8)	C11-C16	1.541(10)
Eu1-C12	2.792(8)	C12-C13	1.415(11)
Eu1-C13	2.807(7)	C12-C17	1.494(12)
Eu1-C14	2.809(8)	C13-C14	1.407(10)
Eu1-C15	2.830(7)	C13-C18	1.507(9)
Eu1-C100*	2.550(1)	C14-C19	1.488(11)
O1-C21	1.422(10)	C15-C20	1.511(10)
O1-C22	1.438(9)	C15-C14	1.386(9)
O2-C31	1.450(12)	C21-C24	1.533(12)
O2-C34	1.406(12)	C22-C23	1.441(12)
C1-C2	1.188(8)	C23-C24	1.474(15)
C2-C3	1.440(9)	C31-C32	1.395(16)
C3-C4	1.348(10)	C32-C33	1.315(19)
C3-C8	1.379(9)	C33-C34	1.459(17)
C4-C5	1.435(11)	C15-C14	1.386(9)
C5-C6	1.334(14)	C15-C20	1.511(10)

* C100 is the centroid of the C_5Me_5 ring.

Table XVII. Bond Angles (deg) for $(C_5Me_5)_2Eu_2(\mu_2\text{-}C{\equiv}CPh)_2(THF)_4$

O1-Eu1-C2	73.89(18)	C11-C12-C13	108.4(8)
O1-Eu1-C1	86.59(19)	C15-C11-C16	125.9(8)
O1-Eu1-C1	135.52(19)	C11-C12-C17	124.0(10)
O1-Eu1-C100*	111.39(13)	C12-C13-C14	107.6(7)
O2-Eu1-C1	132.23(20)	C12-C13-C18	125.2(8)
O2-Eu1-C1	80.39(19)	C14-C13-C18	127.2(8)
O2-Eu1-C100	113.37(15)	C13-C14-C15	107.6(7)
C1-Eu1-C1	84.59(21)	C13-C14-C19	126.8(8)
C1-Eu1-C100	114.32(14)	C15-C14-C19	125.5(8)
C1-Eu1-C100	111.96(14)	C14-C15-C20	127.7(9)
Eu1-C1-Eu1	95.41(21)	C11-C15-C20	123.0(9)
Eu1-C1-C2	129.1(6)	C14-C15-C11	109.3(7)
Eu1-C1-C2	135.5(6)	C13-C12-C17	127.4(8)
C1-C2-C3	178.9(7)	O1-C21-C24	105.7(8)
C2-C3-C4	122.6(7)	C21-C24-C23	104.5(9)
C2-C3-C8	119.8(7)	C24-C23-C22	106.6(8)
C3-C4-C5	120.6(8)	C23-C22-O1	107.7(8)
C4-C5-C6	118.6(9)	C22-O1-C21	105.2(6)
C5-C6-C7	122.6(9)	O2-C31-C32	107.7(12)
C6-C7-C8	118.1(9)	C31-C32-C33	107.2(14)
C7-C8-C3	122.4(8)	C32-C33-C34	110.9(12)
C12-C11-C15	107.1(7)	C33-C34-O2	104.1(11)
C12-C11-C16	126.9(10)	C34-O2-C31	106.7(8)

*C100 is the centroid of the C_5Me_5 ring.

distances are the same within experimental error at 2.702(7) and 2.709(7)Å. The averaged Eu-$O_{1,2}$ distance is 2.62±0.01Å which is similar to the distance of 2.594(4) found in $(C_5Me_5)_2Eu(OEt_2)$. The europium atom is formally seven coordinate (if the C_5Me_5 ring takes up three coordination sites). The geometry about the europium atom is that of a square pyramid with the centroid of the C_5Me_5 ring occupying the axial site and the two bridging acetylide groups and two THF molecules occupying the basal sites. The Eu1-C1-Eu1' angle is 95.4(2)° and is similar to that found in $(C_5Me_5)_4Yb_3(C{\equiv}CPh)_4$ as well as the trivalent samarium complex $(MeC_5H_4)_4Sm_2(\mu\text{-}C{\equiv}CPh)_2$[22]. The C1-Eu1-C1' angle is 84.6(2)°, and the bridging phenylacetylide is slightly asymmetric with the Eu1-C1-C2 and Eu1'-C1-C2 angles being 129.1(6) and 135.5(6)°, respectively.

The major difference in the two reactions between $(C_5Me_5)_2M(OEt_2)$ and phenylacetylene is that the ytterbium(II) species gets oxidized, and the europium complex does not. In both reactions, the phenylacetylene functions as a protic acid and protonates a C_5Me_5 ring to produce pentamethylcyclopentadiene. This is understandable since the pKa of phenylacetylene is 20.5[26] while the pKa of pentamethylcyclopentadiene is 27.5.[27] The reduction product of the ytterbium reaction has not been identified, but the most likely candidate is H_2. The ytterbium reaction was followed using ^1H NMR spectroscopy, and no H_2 could be positively identified in the products. Following the reaction by ^1H NMR did reveal that the reaction proceeds slowly at room temperature, many intermediates are observable, and the only product of the reaction is the one which is isolated. Evidently, the stronger reducing power of $(C_5Me_5)_2Yb{\cdot}OEt_2$ allows it to reduce H^+ to H_2, while in the case of

$(C_5Me_5)_2Eu(OEt_2)$, the phenylacetylene can only act as a protic acid to remove the pentamethyl-cyclopentadienyl rings.

References

1.) Tilley, T. D.; Andersen, R. A.; Spencer, B.; Ruben, H.; Zalkin, A.; Templeton, D. H. Inorg. Chem. **1980**, 19, 2999.

2.) Morss, L. R.; Hans, H. O. J. Chem. Thermodyn. **1973**, 5, 513.

3.) Tokel-Takvoryan, N. E.; Hemingway, R. E.; Bard, A. J. J. Am. Chem. Soc. **1973**, 95, 6582.

4.) Kahl, J. L.; Hanck, K. W.; De Armond, K. J. Phys. Chem **1978**, 82, 540.

5.) Tilley, T. D. Ph.D. Thesis University of California, Berkeley, Berkeley, California, U.S.A. 1982.

6.) Finke, R. G.; Kennan, S.; Schiraldi, D. A.; Watson, P. L. 'Sixteenth Rare Earth Research Conference', Florida State University, April 18-21, 1983.

7.) Tilley, T. D.; Andersen, R. A.; Spencer, B.; Zalkin, A. Inorg. Chem. **1982**, 21, 2647.

8.) Geary, W. J. Coord. Chem. Rev. **1971**, 7, 81.

9.) Tilley, T. D.; Andersen, R. A.; Zalkin, A. Inorg. Chem. **1983**, 22, 856.

10.) Watson, P. L.; Harlow, R. L.; Whitney, J. F. personal communication.

11.) Tilley, T. D.; Andersen, R. A.; Zalkin, A.; Templeton, D. H. Inorg. Chem. **1982**, 21, 2644.

12.) Tilley, T. D.; Andersen, R. A. J. Chem. Soc., Chem. Comm. **1981**, 985.

13.) Tilley, T. D.; Andersen, R. A. J. Am. Chem. Soc. **1982**, 104, 1772.

14.) Boncella, J. M.; Andersen, R. A. Inorg. Chem. **1984**, 23, 432.

15.) Shannon, R. D. Acta. Cryst. **1976**, 32A, 751.

16.) McPherson, A. M.; Fieselmann, B. F.; Lichtenberger, D. L.; McPherson, G. L.; Stucky, G. D. J. Am. Chem. Soc. **1979**, 101, 3425.

17.) Konig, E.; Kremer, S. Chem. Phys. Lett. **1970**, 5, 87.

18.) Saito, Y.; Takimoto, J.; Hutchinson, B.; Nakamoto, K. Inorg. Chem. **1972**, 11, 2003.

19.) Carlin, R. L.; van Duyneveldt, A. J. "Magnetic Properties of Transition Metal Compounds", Springer-Verlag, New York, **1977**, pp. 15-20.

20.) Swift, T. J. in "NMR of Paramagentic Molecules". LaMar, G. N.; Horrocks, W., DeW, Jr.; Holm, R. H., Academic Press, **1973**, New York, pp. 53-83.

21.) Chisholm, M. H.; Huffman, J. C.; Rothwell, I. P.; Bradley, P. G.; Kress, N.; Woodruff, W. H. J. Am. Chem. Soc. **1981**, 103, 4945.

22.) Evans, W. J.; Bloom, I.; Hunter, W. E.; Atwood, J. L. Organometallics **1983**, 2, 709.

23.) Atwood, J. L.; Hunter, W. E.; Wayda, A. L.; Evans, W. J. Inorg. Chem. **1981**, 20, 4115.

24.) Stucky G. D.; McPherson, A. M.; Rhine, W. E.; Eisch, J. J.; Considine, J. L. J. Am. Chem. Soc. **1974**, 96, 1941.

25.) Almenningen, A.; Fernhold, L.; Haaland, A. J. Organomet. Chem. **1978**, 155, 245.

26.) Streitwieser, A., Jr.; Heathcock, C. H. "Introduction to Organic Chemistry", MacMillan, New York, **1976**, p. 1191.

27.) Bordwell, F. G.; Baisch, M. J. J. Am. Chem. Soc. **1983**, 105, 6188.

Chapter 3

Chemistry of Bis(hexamethyldisilylamido)ytterbium

Preparation

In the preceding chapters the chemistry of the divalent complex $(C_5Me_5)_2Yb{\cdot}OEt_2$ was discussed. This complex undergoes a wide variety of redox reactions which result in the formation of trivalent ytterbium complexes. Another complex of divalent ytterbium which posesses good solubility properties and has a low coordination number is $[(Me_3Si)_2]_2Yb(OEt_2)_2$. The chemistry of this complex and some of its derivatives will be discussed in this chapter and, as will be shown, the chemistry of this molecule is quite different from that of $(C_5Me_5)_2Yb{\cdot}OEt_2$.

The complex $[(Me_3Si)_2N]_2Yb(OEt_2)_2$ is synthesized from YbI_2 and $NaN(SiMe_3)_2$ as shown in eqn. (1). It would appear from eqn (1)

$$YbI_2 + 2NaN(SiMe_3)_2 \xrightarrow{OEt_2} [(Me_3Si)_2N]_2Yb(OEt_2)_2 + 2NaI \qquad (1)$$

that the synthesis of $[(Me_3Si)_2]_2Yb(OEt_2)_2$ is straightforward. This is not the case. If reaction, conditions and stoichiometries are not absolutely correct, the reaction gives the diethyl ether complex in yields as low as two percent. When the reactants are mixed at 0°C, the solution slowly turns blue-green in color with a yellow-green

precipitate. This precipitate is probably colored by unreacted YbI_2. After one hour at 0°C, the reaction mixture is allowed to warm to room temperature. The solution turns light orange in color after stirring at room temperature for two to three hours. The complex may then be crystallized from the reaction solution after filtration by concentrating the solution and cooling it to -70°C overnight. When the reaction is carried out as described above, the overall yield is 65-70%.

It appears that low yields of $[(Me_3Si)_2]_2Yb(OEt_2)_2$ result for one of two reasons. Either the solution is allowed to warm to room temperature too fast, or there is a slight excess of $NaN(SiMe_3)_2$ present. In either case, the reaction mixture turns dark red after warming to room temperature. The highest yield of product isolated from such red solutions was 40%. The fate of the remainder of the material in the reaction is unknown at this time. It does, however, have at least two complexes in it, both of which are soluble in diethyl ether. One of them is insoluble in pentane, and contains iodide as shown by a silver nitrate test.

The observation that a very small excess of $NaN(SiMe_3)_2$ in the reaction mixture results in, on average, at least a two-fold reduction in yield shows that there is a $NaN(SiMe_3)_2$ catalyzed pathway to products other than $[(Me_3Si)_2]_2Yb(OEt_2)_2$. The $NaN(SiMe_3)_2$ catalysis was discovered when the same batches of YbI_2, $NaN(SiMe_3)_2$ and diethyl ether were used in two separate preparations of $[(Me_3Si)_2]_2Yb(OEt_2)_2$. One reaction gave a 30% yield of the desired product, while the other gave 70%. The only difference in the two reactions was that the reaction which gave 30% yield had $NaN(SiMe_3)_2$ in ca. 0.05mmol excess while the reaction which gave 70% yield had YbI_2 in ca. 0.1mmol excess. The total

scale of these reactions were ca. 12mmol. The reaction was then run a third time with a 3% excess of YbI_2 and gave a 65% yield showing that small amounts of excess $NaN(SiMe_3)_2$ lead to a drastically different product distribution.

Since only small amounts of excess $NaN(SiMe_3)_2$ are needed to produce unacceptable yields of $[(Me_3Si)_2]_2Yb(OEt_2)_2$, the purity of the YbI_2 used is extremely important. If the YbI_2 is impure, then weighing out what appears to be equimolar quantities of reactants will always leave an excess of $NaN(SiMe_3)_2$. To avoid this problem it is suggested that a slight excess (1-3%) of YbI_2 be used to insure a proper stoichiometry. A detailed recipe is given in the Experimental Section.

The coordinated ether molecules in $[(Me_3Si)_2N]_2Yb(OEt_2)_2$ are labile, and they are easily displaced by more basic ethers such as THF or 1,2-dimethoxyethane.[1] Bidentate phosphines will also displace diethyl ether to form the complexes $[(Me_3Si)_2N]_2Yb{\cdot}L_2$ (L_2=dmpe, dmpm, diphos).[2,12] When the complex $[(Me_3Si)_2N]_2Yb(OEt_2)_2$ is dissolved in hydrocarbon solvents, red solutions result indicating that perhaps even hydrocarbons can displace the coordinated diethyl ether. The diethyl ether can be removed from $[(Me_3Si)_2N]_2Yb(OEt_2)_2$ by evaporating a toluene solution of the complex under reduced pressure at 80°C. The resultant red residue may be recrystallized from pentane to give red needles of a complex with the stoichiometry $[(Me_3Si)_2N]_2Yb$.

The complex $[(Me_3Si)_2N]_2Yb$ is found to be dimeric by mass spectrometry, since it gives a parent ion at M/e=986amu. At room temperature, both the ^1H and ^{13}C NMR spectra have only one peak at δ0.32 and 6.47, respectively. At -92°C there are two peaks in the ^{13}C NMR spectrum at δ6.05 and 5.88, and two equal area peaks in the ^1H NMR

spectrum at δ0.48 and 0.36, respectively. The two peaks in each spectrum are assigned to the bridging and terminal silyamido groups of a dimeric complex which has the structure shown in I below. The proposed structure is the same as that found for the Mn complex

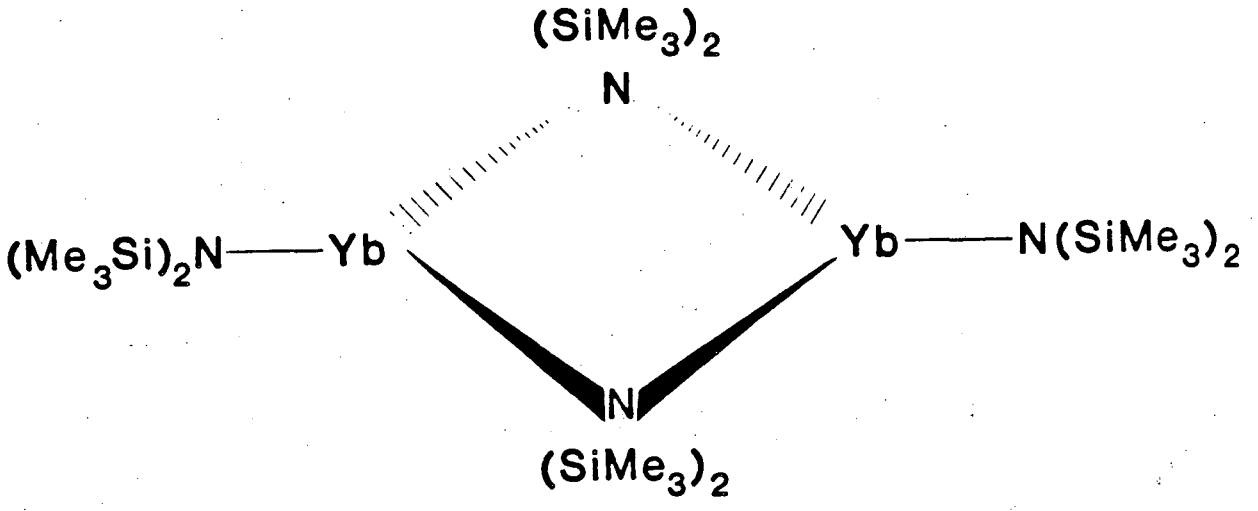

I.

$\{[(Me_3Si)_2N]_2Mn\}_2$.[3,4] At -56°C the two separate resonances in the ^1H NMR spectrum of $\{[(Me_3Si)_2N]_2Yb\}_2$ coalesce. Use of the simple two site exchange approximation,[26] T_c=217K, and a peak separation of 8Hz at coalescence gives $\Delta G^{\ddagger}_{T_c}$=11.3kcal mol^{-1} for the bridge-terminal exchange of the amido groups.

In order to confirm the proposed structure, a single crystal X-ray diffraction study of $\{[(Me_3Si)_2N]_2Yb\}_2$ at -95°C was undertaken. An ORTEP diagram of the molecule is shown in Figure 1, and the bonds lengths and angles in the molecule are found in Tables (I) and (II), respectively. A list of positional and thermal parameters can be found in Appendix (I). The complex crystallizes in the triclinic space group $P\bar{1}$ with one dimer in the asymmetric unit. The individual molecules are well separated from one another with the closest intermolecular contact

Figure 1. ORTEP of $\{[(Me_3Si)_2N]_2Yb\}_2$

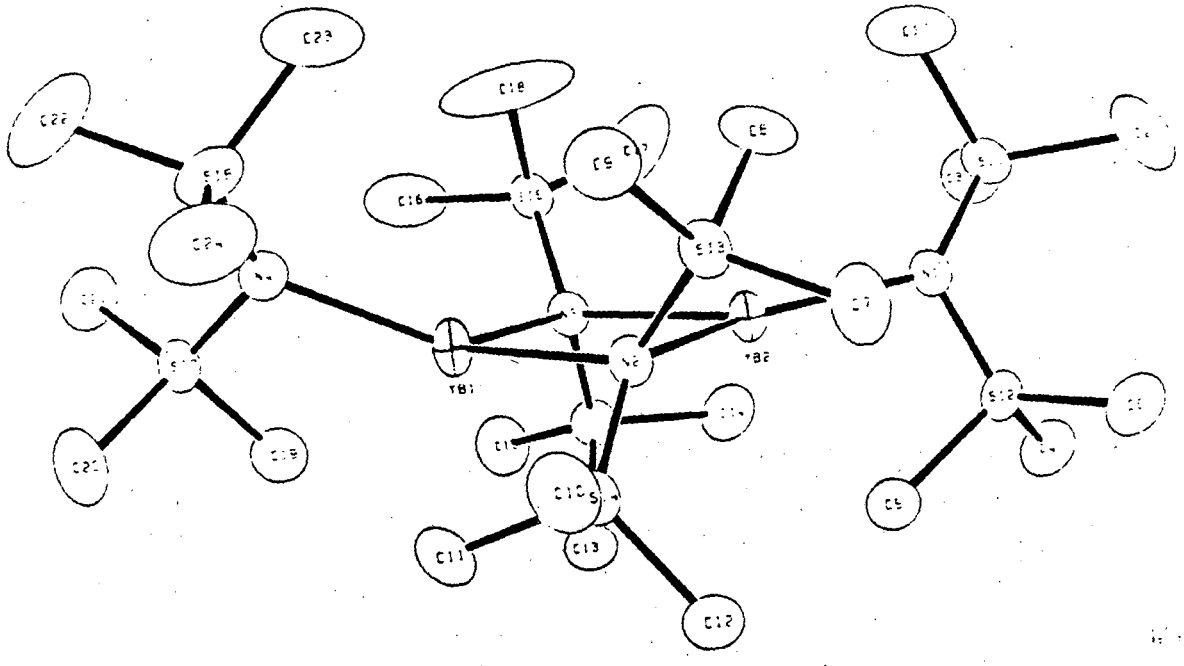

Table I. Bond Lengths (Å) of $\{[(Me_3Si)_2N]_2Yb\}_2$

Yb1-N2	2.492(3)	Si4-C12	1.866(4)
Yb1-N3	2.445(3)	Si5-N3	1.726(3)
Yb1-N4	2.300(3)	Si5-C13	1.871(4)
Yb2-N1	2.310(3)	Si5-C14	1.876(4)
Yb2-N2	2.573(3)	Si5-C15	1.860(4)
Yb2-N3	2.497(3)	Si6-N3	1.721(3)
Si1-N1	1.710(3)	Si6-C16	1.829(6)
Si1-C1	1.870(5)	Si6-C17	1.837(5)
Si1-C2	1.868(5)	Si6-C18	1.831(5)
Si1-C3	1.870(4)	Si7-N4	1.691(3)
Si2-N1	1.691(3)	Si7-C19	1.881(4)
Si2-C4	1.862(4)	Si7-C20	1.845(4)
Si2-C5	1.898(4)	Si7-C21	1.876(4)
Si2-C6	1.875(4)	Si8-N4	1.699(3)
Si3-N2	1.728(3)	Si8-C22	1.873(5)
Si3-C7	1.873(5)	Si8-C23	1.887(5)
Si3-C8	1.881(4)	Si8-C24	1.869(5)
Si3-C9	1.872(4)	Yb1-C11	2.823(4)
Si4-N2	1.726(3)	Yb1-C19	2.888(4)
Si4-C10	1.872(4)	Yb2-C5	2.785(4)
Si4-C11	1.891(4)	Yb2-C8	2.820(4)

Table II. Bond Angles (deg) of $\{[(Me_3Si)_2N]_2Yb\}_2$

N2-Yb1-N3	93.54(9)	N2-Si3-C9	115.82(18)
N2-Yb1-N4	129.37(10)	C7-Si3-C8	103.61(22)
N3-Yb1-N4	126.87(10)	C7-Si3-C9	108.55(21)
N1-Yb2-N2	138.81(10)	C8-Si3-C9	106.05(20)
N1-Yb2-N3	130.40(10)	N2-Si4-C10	115.56(17)
N2-Yb2-N3	90.37(9)	N2-Si4-C11	109.80(16)
Yb1-N2-Yb2	86.64(9)	N2-Si4-C12	115.47(16)
Yb1-N3-Yb2	89.38(9)	C10-Si4-C11	103.55(19)
Yb2-N1-Si1	133.45(16)	C10-Si4-C12	105.49(20)
Yb2-N1-Si2	103.27(13)	C11-Si4-C12	105.91(19)
Si1-N1-Si2	122.59(17)	Yb1-N3-Si5	115.96(13)
N1-Si2-C4	116.44(18)	Yb1-N3-Si6	110.24(13)
N1-Si2-C5	106.26(16)	Yb2-N3-Si5	98.81(12)
N1-Si2-C6	115.51(17)	Yb2-N3-Si6	117.93(13)
C4-Si2-C5	106.04(19)	Si5-N3-Si6	120.16(16)
C4-Si2-C6	106.89(20)	N3-Si5-C13	107.30(15)
C5-Si2-C6	104.66(20)	N3-Si5-C14	111.03(16)
N1-Si1-C1	111.08(18)	N3-Si5-C15	117.88(17)
N1-Si1-C2	114.19(19)	C13-Si5-C14	108.01(18)
N1-Si1-C3	112.17(17)	C13-Si5-C15	106.59(19)
C1-Si1-C2	105.66(25)	C14-Si5-C15	105.62(18)
C1-Si1-C3	106.34(23)	N3-Si6-C16	115.35(19)
C2-Si1-C3	106.87(20)	N3-Si6-C17	113.13(20)
Yb1-N4-Si7	104.02(14)	N3-Si6-C18	108.88(22)
Yb1-N4-Si8	128.31(16)	C16-Si6-C17	107.4(4)
Si7-N4-Si8	125.28(19)	C16-Si6-C18	102.7(3)
N4-Si7-C19	108.13(17)	C17-Si6-C18	108.7(4)
N4-Si7-C20	114.66(20)	N2-Yb1-C11	67.36(10)
N4-Si7-C21	115.94(18)	N2-Yb1-C19	149.17(10)
C19-Si7-C20	105.21(22)	N3-Yb1-C11	127.20(11)
C19-Si7-C21	104.51(20)	N3-Yb1-C19	93.04(11)
C20-Si7-C21	107.40(21)	N4-Yb1-C11	100.48(11)
N4-Si8-C22	114.44(22)	N4-Yb1-C19	66.70(11)
N4-Si8-C23	110.74(20)	C11-Yb1-C19	84.82(12)
N4-Si8-C24	110.87(19)	N1-Yb2-C5	67.92(11)
C22-Si8-C23	105.6(3)	N1-Yb2-C8	89.98(12)
C22-Si8-C24	107.0(3)	N2-Yb2-C5	97.27(11)
C23-Si8-C24	107.8(3)	N2-Yb2-C8	65.84(11)
Yb1-N2-Si3	129.69(14)	N3-Yb2-C5	122.54(10)
Yb1-N2-Si4	98.57(12)	N3-Yb2-C8	111.43(12)
Yb2-N2-Si3	94.06(12)	C5-Yb2-C8	123.63(13)
Yb2-N2-Si4	132.60(14)	Yb2-C5-Si2	82.54(13)
Si3-N2-Si4	116.24(16)	Yb2-C8-Si3	83.21(13)
N2-Si3-C7	112.95(17)	Yb1-C11-Si4	84.22(13)
N2-Si3-C8	108.94(16)	Yb1-C19-Si7	80.20(14)

being 3.785(6)Å between the methyl groups C(5) and C(21).

The molecule consists of a dimer of the empirical formula $Yb[N(SiMe_3)_2]_2$. This molecule has no crystallographically imposed symmetry, and there is not even any approximate symmetry in the molecule. Both Yb atoms are bound to one terminal $N(SiMe_3)_2$ group and two $N(SiMe_3)_2$ groups which bridge the Yb atoms. The two Yb-N terminal distances are 2.300(3)Å and 2.310(3)Å for Yb(1)-N(4) and Yb(2)-N(1), respectively. The remaining silylamide groups bridge the two Yb atoms asymmetrically with Yb(1)-N(2,3) distances of 2.492(3)Å and 2.445(3)Å and Yb(2)-N(2,3) distances of 2.573(3)Å and 2.497(3)Å, respectively. In addition to the bonding interactions with the nitrogen atoms, there are close contacts between the Yb atoms and four of the methyl groups of the silylamide ligands. The contact distances between Yb(1) and C(19) and C(11) are 2.888(4) and 2.823(4)Å, while the distances between Yb(2) and C(8) and C(5) are 2.820(4) and 2.785(4)Å. The contacts between the Yb atoms and the methyl groups are extremely short, and can be compared to the Yb(II)-C_{ring} average distance for $(C_5Me_5)_2Yb(py)_2$ which is 2.74Å.[5]

The close contacts between the methyl groups and Yb atoms cause some rather marked distortions of the molecule. The $Yb_2(\mu\text{-}N)_2$ core is planar to within 0.02Å. The close methyl contacts on Yb(2), [C(8),C(5)] occur from methyl groups disposed above and below the $Yb_2(\mu\text{-}N)_2$ plane. The methyl groups which approach Yb(1),[C(19),C(11)] do so from the same side of the $Yb_2(\mu\text{-}N)_2$ plane. The approach of C(19) and C(11) from the same direction causes N(4) to be displaced from the $Yb_2(\mu\text{-}N)_2$ plane by 1.07Å. Two of the interacting methyl groups C(8) and C(11) are on the same bridging $N(SiMe_3)_2$ ligand. Their interaction with Yb(2) and Yb(1) causes the dihedral angle between the planes defined by Yb(1), Yb(2),

N(2), N(3) and N(2), Si(4), Si(3) to be 62°. The corresponding dihedral angle between the planes defined by Yb(1), Yb(2), N(2), N(3) and N(3), Si(5), Si(6) is 79°. Thus, the methyl interactions cause a 17° twist of the bridging $(Me_3Si)_2N$ group containing N(2) toward the Yb atoms. The remaining two Yb-C-methyl interactions occur between methyl carbons on the terminal $(Me_3Si)_2N$ ligands (C(5), C(19)) and the Yb atoms. The Yb-C interaction with methyl groups on terminal $(Me_3Si)_2N$ ligands causes a distortion of these ligands and is shown in Figure 2. Examination of

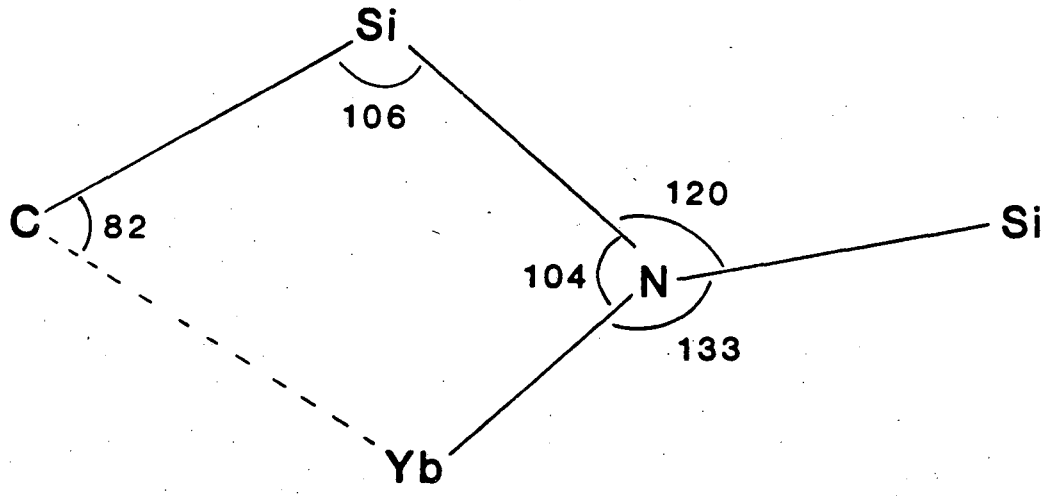

Figure 2

Figure 2 reveals that the Yb-C interaction has caused the Yb-N-Si bridged angle to decrease from 120° to 104°, and the Yb-N-Si unbridged angle to open to 133°. The $Yb\text{-}C_{bridge}\text{-}Si$ angles for all four Yb-C interactions vary between 80° and 84°. This angle is similar to those found in molecules in which methyl groups bridge two electropositive metal atoms such as $[(C_5H_5)_2M]_2(\mu_2\text{-}Me)_2$ (M=Yb, Y)[6] or $Al_2Me_4(\mu_2\text{-}Me)_2$[7].

The hydrogen atoms were located in the crystal structure of

$\{[(Me_3Si)_2N]_2Yb\}_2$, but were not refined, and were placed in calculated positions. The shortest Yb-H contact was between Yb(2) and H(82) (on C(8)) at 2.23Å, and the remaining Yb-H distances range from 2.52-2.96Å. Since the Yb(2)-H(82) distance was the only one which indicated the possibility of a Yb-H bonding interaction, difference Fourier maps in the region of C(8) were calculated with H(81)-(83) missing to see if perhaps placing H(81)-(83) in calculated positions was unwarranted. These difference syntheses indicate that the H atoms are in the correct positions.

The observation that there is a short Yb-H contact on only one of the four methyl groups which are close to the Yb atom suggests that these interactions are occurring primarily between the metal atoms and the carbon atoms. The $Yb-C_{bridge}-Si$ angles also support such a conclusion. These same types of Ln-Me interactions have also been observed in the solid state for the compounds $[(Me_3Si)_2N]_2Ybdmpe$[2] and $NaM[N(SiMe_3)_2]_3$ (M=Eu,Yb)[1]. The Yb-C distances and Yb-C-X angles for compounds which contain bridging Me group are found in Table (III). Since there is no evidence of these M-C interactions by either infrared or low temperature NMR spectroscopy, the energy of the interactions must be small. All of these molecules are highly coordinatively unsaturated, and the ligands which are present are too bulky to allow further oligomerization. The only way in which the metal atom can become electronically and coordinatively saturated is to interact with the hydrocarbon ligands.

The complexes $\{[(Me_3Si)_2N]_2M\}_2$ (M=Mn,Co)[3,4] are essentially isostructural with the Yb complex, except that they have no short M-Me interactions. The size of the metal atom must be important in

Table III. Some Yb-Me Bridging Lengths and Angles

Compound	X	X-Me-Yb (deg)	Yb-Me Å	References
$[(Me_3Si)_2N]_2Ybdmpe$	Si	80	3.04	2
$NaYb[N(SiMe_3)_2]_3$	Si	78.6(3.0)	2.88(3)	1
$NaEu[N(SiMe_3)_2]_3$	Si	83.4(1.0)	3.07(7)	8
$Me_2Al(\mu\text{-}Me)_2YbCp_2$	Al	78.9(6)	2.59(3)	9
$Me_2Al(\mu\text{-}Me)_2YCp_2$	Al	80.8	2.58(1)	this work
$\{[(Me_3Si)_2N]_2Yb\}_2$	Si	82(1)	2.83(4)	this work
$[(Me_3Si)_2N]_2Yb(AlMe_3)_2$	Al	73.8(1) 65.9(7)	2.767(6) 3.12(8)	this work this work
	Si	83.5(3)	3.053(14)	

determining if such interactions are to occur. Both high spin Mn(II) and Co(II) are smaller than Yb(II) by 0.19 and 0.37Å, respectively. Replacing a smaller metal atom in a bridged structure, as is observed for $\{[(Me_3Si)_2N]_2M\}_2$, with a larger one will lengthen all the M-N bonds thereby exposing more of the metal, and increasing the possibility for interaction with the hydrocarbon portion of the ligands.

The preparation of the complex $[(Me_3Si)(t\text{-}Bu)N]_2Yb$ was attempted to see what effect replacing a Me_3Si group with a bulkier t-Bu group would have on the observed Yb-C interactions. Unfortunately, the complex $[(Me_3Si)(t\text{-}Bu)N]_2Yb(OEt_2)_x$ was isolated in poor (10%) yield. However, a reinvestigation of this complex is warranted since the importance of the stoichiometry of the reaction between YbI_2 and $NaN(SiMe_3)_2$ was not known when these experiments were carried out. The synthesis of the amine and $NaN(SiMe_3)(t\text{-}Bu)$ are found in the Experimental Section.

The complex $\{[(Me_3Si)_2N]_2Yb\}_2$ undergoes a variety of reactions with Lewis bases to form adducts. It does not react with internal acetylenes, or simple olefins. It does react with carbon monoxide to give a red hydrocarbon insoluble material which contains a band at $2090cm^{-1}$ in its infrared spectrum. The insolubility of this material prevented further characterization. The band at $2090cm^{-1}$ in the infrared spectrum is consistent with the presence of a CN^- or Me_3SiNC ligand. Such a reaction has precedence since $NaN(SiMe_3)_2$ reacts with CO to give NaCN and $(Me_3Si)_2O$.[11]

Reactions with Protic Acids

The observation that H-C≡C-Ph reacts with $[(Me_3Si)_2N]_2Yb(OEt_2)_2$[12] to

give the known divalent complex $[Yb(C\equiv CPh)_2]_x$[13] suggests that a wide variety of protic acids might give novel complexes of divalent Yb. In addition, unlike the complex $(C_5Me_5)_2Yb\cdot OEt_2$, electron transfer reactions do not usually occur during the protonolysis reactions of $[(Me_3Si)_2N]_2Yb$ complexes.

The easiest way in which the reaction between $\{[(Me_3Si)_2N]_2Yb\}_2$ and protic acids can be viewed is that the reaction occurs between the strong base $(Me_3Si)_2N^-$ and a proton source. Thus, a reaction is predicted to be thermodynamically feasible if the pKa of the proton source is less than the pKa of $HN(SiMe_3)_2$. The pKa of $HN(SiMe_3)_2$ has not been measured, but it must be less than that of NH_3 (pKa=35)[14] since $HN(SiMe_3)_2$ reacts with $NaNH_2$ to give $NaN(SiMe_3)_2$ and NH_3. The fact that $\{[(Me_3Si)_2N]_2Yb\}_2$ reacts with HC_5Me_5 suggests that the pKa of $HN(SiMe_3)_2$ is greater than 27.5 since the pKa of C_5Me_5H is 27.5.[15] The Yb complex does not react with $HCPh_3$ which has a pKa of 31.5[16], but the steric bulk of $HCPh_3$ may prevent the reaction for kinetic reasons rather than thermodynamic ones.

When $\{[(Me_3Si)_2N]_2Yb\}_2$ is mixed with two molar equivalents of $(C_5H_5)W(CO)_3H$ per monomer, an instantaneous reaction occurs which gives a yellow solid that is insoluble in hydrocarbons. The yellow solid may be crystallized from THF or a mixture of THF and hexane. The infrared spectrum of the complex has three bands in the ν-CO region of the spectrum at 1895, 1755, and 1675 cm^{-1}. The presence of the 1675 cm^{-1} band is strong evidence for a Yb-O-C-W interaction. The infrared spectrum of the complex is virtually identical to that of the complex $[Mg(THF)_4][(\mu_2\text{-}OC)Mo(CO)_2(C_5H_5)]_2$ which is known by X-ray crystallography.[17] The structures must be similar, if not identical,

and are shown in II. In this reaction, the transition metal hydride

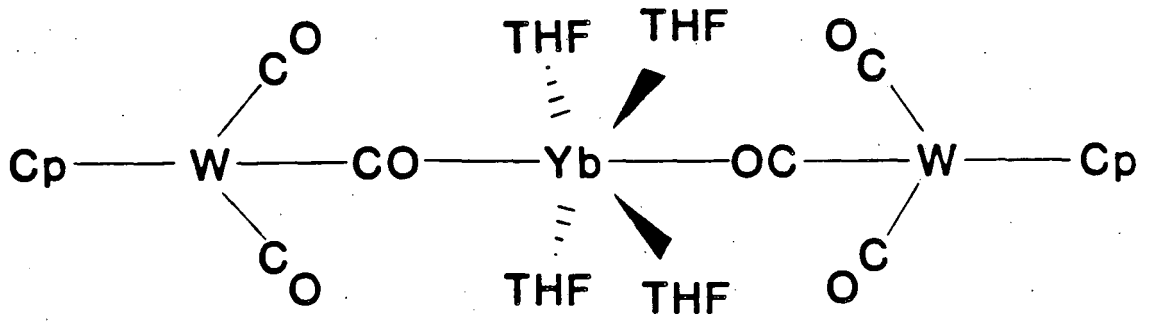

II

hydride behaves as a weak acid and removes the $(Me_3Si)_2N$ groups from the Yb atom as $HN(SiMe_3)_2$.

As has been briefly mentioned, the complex $\{[(Me_3Si)_2N]_2Yb\}_2$ reacts with pentamethylcyclopentadiene. When $\{[(Me_3Si)_2N]_2Yb\}_2$ is mixed with one molar equivalent of Me_5C_5H or $EtMe_4C_5H$ per monomer, the reaction mixture immediately turns dark red. Both reactions yield red complexes which may be crystallized as large octahedral prisms. Both complexes have a stoichiometry of one ring and one silylamide group, but the solubilities of the two complexes are strikingly different. The C_5Me_4Et complex is soluble in pentane while the C_5Me_5 complex is insoluble in pentane and only sparingly soluble in warm toluene. The complex $\{(C_5Me_5)Yb[N(SiMe_3)_2]\}_2$ has a dimeric structure in the solid state which has been confirmed by a single crystal X-ray diffraction study. The complex $\{(EtC_5Me_4)Yb[N(SiMe_3)_2]\}_2$ also has a dimeric structure as indicated by the observation of $[M-C_5Me_4Et]^+$ and $[M-N(SiMe_3)_2]^+$ ions in

the mass spectrum at M/e 917 and 906amu, respectively.

The complex $[(C_5Me_5)YbN(SiMe_3)_2]_2$ crystallizes in the orthorhombic space group Pbca with four dimers in the unit cell. Tables (IV) and (V) contain lists of bond lengths and bond angles, while an ORTEP drawing of the molecule is found in Figure 3. The data collection parameters for the low temperature (-95°C) structure can be found in the Experimental Section, and tables of positional and thermal parameters are found in Appendix (I).

The dimeric molecules pack as well separated units with the closest intermolecular contacts being C(12) to C(30) and C(12) to C(34), both at 3.61Å. Each Yb atom is coordinated to two $N(SiMe_3)_2$ groups which bridge the Yb atoms and one C_5Me_5 ring. The molecule has crystallographically imposed inversion symmetry, but the Yb-N(bridge) distances are quite unsymmetrical at 2.630(3) and 2.445(3)Å, respectively. The averaged Yb-C_{ring} distance is 2.743(24)Å. The large standard deviation in this number is due to a large spread in the Yb-C distances rather than large uncertainties in the individual numbers. The centroid of the C_5Me_5 ring sits only 0.001Å out of the plane defined by Yb(1), N(1), Yb(1'), N(1'). The dihedral angle between this plane and the one defined by N(1), Si(1) and Si(2) is 91°.

The averaged Yb-C_{ring} distance, at 2.74Å, is exactly the same as that found in the divalent complex $(C_5Me_5)_2Yb(py)_2$.[5] There is a large difference between these two molecules since the pyridine complex is formally eight coordinate while the complex $\{(C_5Me_5)Yb[N(SiMe_3)]_2\}_2$ is formally only five coordinate. Since the ionic radius of a metal atom in a given oxidation state decreases as the coordination number falls, it is expected that the Yb-C_{ave} bond length in the five coordinate

Figure 3. ORTEP of $\{(C_5Me_5)Yb[N(SiMe_3)_2]\}_2$

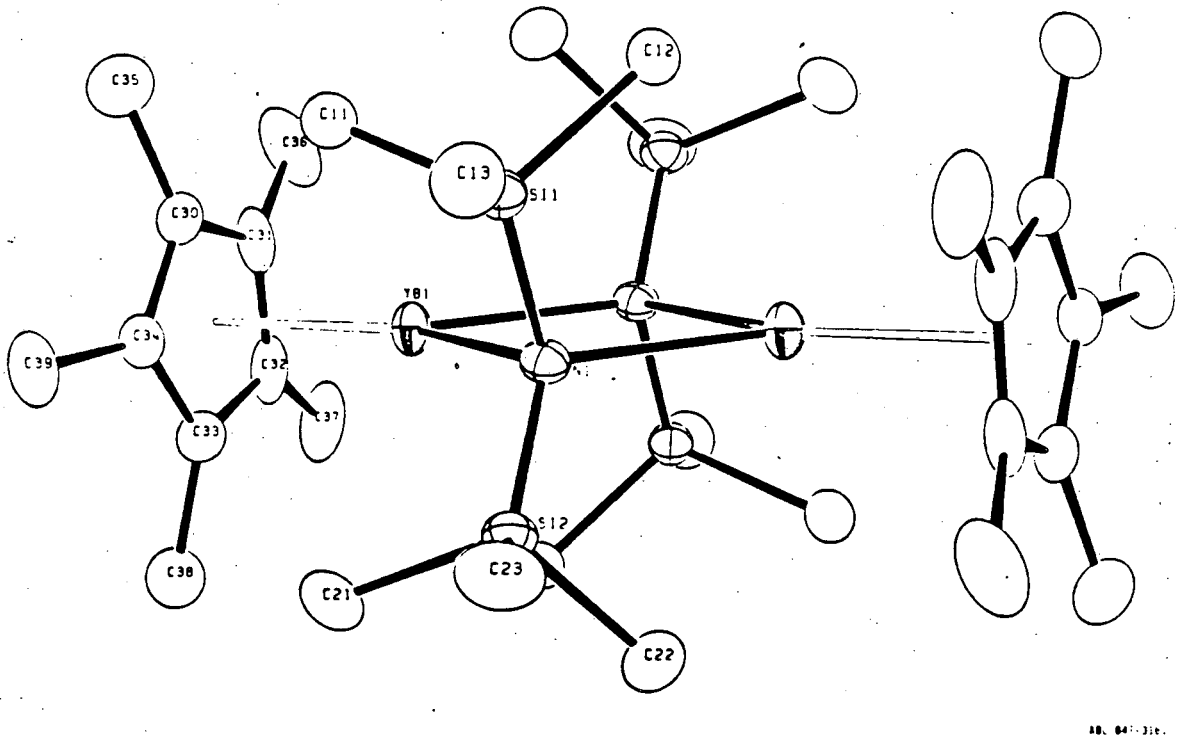

Table IV. Bond Lengths (Å) of $\{(C_5Me_5)Yb[N(SiMe_3)_2]\}_2$

Yb1-N1	2.630(3)	Si2-C21	1.868(5)
Yb1-N1'	2.445(3)	Si2-C22	1.860(5)
Yb1-C30	2.749(4)	Si2-C23	1.872(4)
Yb1-C31	2.767(4)	C30-C31	1.391(6)
Yb1-C32	2.754(4)	C31-C32	1.409(6)
Yb1-C33	2.719(4)	C32-C33	1.425(5)
Yb1-C34	2.724(4)	C33-C34	1.437(6)
Yb1-C100	2.465(1)	C34-C30	1.403(6)
Si1-N1	1.715(3)	C30-C35	1.520(7)
Si1-C11	1.876(5)	C31-C36	1.508(6)
Si1-C12	1.895(5)	C32-C37	1.490(6)
Si1-C13	1.862(5)	C33-C38	1.492(7)
Si2-N1	1.706(3)	C34-C39	1.506(6)

C100 is the centroid of the C_5Me_5, ring N1' is the inversion related N atom.

Table V. Bond Angles (deg) of $\{(C_5Me_5)Yb[N(SiMe_3)_2]\}_2$

N1-Yb1-N1'	83.28(11)	Yb1-N1-Si1	105.87(14)
N1-Yb1-C100	149.51(7)	Yb1-N1-Si2	114.08(16)
N1'-Yb1-C100	127.22(7)	Si1-N1-Si2	127.39(20)
N1-Si1-C11	111.10(18)	C30-C31-C32	109.2(4)
N1-Si1-C12	108.99(18)	C31-C32-C33	107.4(4)
N1-Si1-C13	118.34(20)	C32-C33-C34	107.1(4)
C11-Si1-C12	105.53(20)	C33-C34-C30	107.7(4)
C11-Si1-C13	104.88(21)	C34-C30-C31	108.5(4)
C12-Si1-C13	107.18(22)	C30-C31-C36	126.0(5)
N1-Si2-C21	111.04(18)	C32-C31-C36	123.5(4)
N1-Si2-C22	110.25(20)	C31-C32-C37	125.5(4)
N1-Si2-C23	116.74(19)	C33-C32-C37	126.5(5)
C21-Si2-C22	106.12(21)	C32-C33-C38	126.4(4)
C21-Si2-C23	105.99(22)	C34-C33-C38	125.9(4)
C22-Si2-C23	106.05(23)	C33-C34-C39	125.5(4)
Yb1-N1-Yb1'	96.72(11)	C30-C34-C39	126.2(4)
Yb1-N1-Si1	99.21(14)	C34-C30-C35	124.8(4)
Yb1-N1-Si2	108.25(14)	C31-C30-C35	125.6(4)

C100 is the centroid of the C_5Me_5 ring.
The primed atoms are the inversion related atoms.

complex will be shorter than that in the eight coordinate complex. The discrepancy in the observed and expected bond lengths can be explained when the intramolecular contacts between the C_5Me_5 and $(Me_3Si)_2N$ ligands are examined.

There are three rather short intramolecular contacts between the methyl groups on the silyl amido ligand and the methyl groups on the C_5Me_5 ring; C(11)-C(35)(3.41Å), C(22')-C(36) (3.55Å) and C(12')-C(37) (3.56Å). The observed close contacts cause a tilting of the C_5Me_5 ring away from the Yb atom. This is illustrated by the Yb-C(30, 31, 32) averaged length of 2.757(9)Å as compared to the Yb-C(33, 34) average of 2.724(4)Å. Thus, the C_5Me_5 ring carbons which are bound to the methyl groups which are in contact with the silylamido methyl groups, are pushed away from the metal atom. The net result of all the intraligand interactions is that the averaged Yb-C ring bond length in this molecule is prevented from being as short as it would be in absence of ligand-ligand repulsions. Since this is the case, the distortion is easily rationalized.

Even though the complex $\{(C_5Me_5)Yb[N(SiMe_3)_2]\}_2$ is rather insoluble in hydrocarbons, it undergoes instantaneous reaction with dmpe to give the purple monomeric complex $(C_5Me_5)Yb[N(SiMe_3)_2]$dmpe. This complex is soluble in toluene, and slightly soluble in pentane. The low temperature $^{31}P\{^1H\}$ NMR spectrum of the complex has one broad peak at δ -39. This indicates that the dmpe is probably undergoing monodentate to bidentate interconversions which are fast on the NMR timescale. The complex undergoes reaction with AgI, but the products have not yet been characterized.

When the complex $\{[(Me_3Si)_2N]_2Yb\}_2$ is reacted with two equivalents

of C_5Me_5H per monomer in pentane, the red complex $\{(C_5Me_5)_2Yb[N(SiMe_3)_2]\}_2$ precipitates out of solution within 10-15 minutes. Stirring of the solution for an additional 24hr results in disappearance of the precipitate and formation of a dark orange-brown solution. The green complex $(C_5Me_5)_2Yb[HN(SiMe_3)_2]$ can be crystallized from this solution (see Table (VI) for spectral data). If the same reaction is carried out with C_5Me_4EtH, an oily black solid may be isolated from the pentane reaction liquors at -70°C. This black solid gives a red solution in benzene, and contains a 2:1 ratio of bound C_5Me_4Et to $HN(SiMe_3)_2$ by ^1H NMR spectroscopy. This solid may be dissolved in diethyl ether to give a green solution from which $(C_5Me_4Et)_2Yb{\cdot}OEt_2$ may be crystallized. In an attempt to remove the excess $HN(SiMe_3)_2$, the mother liquors which produced the black solid were heated to 145°C at 10^{-2}torr for 12hr. The only product which could be isolated from the pyrolysis was the trivalent complex $(C_5Me_4Et)_2Yb$-$N(SiMe_3)_2$. Figure (4) contains the calculated and observed parent ion envelope of the mass spectrum of this complex.

If the reaction between $\{[(Me_3Si)_2N]_2Yb\}_2$ and two equivalents of C_5Me_5H is carried out in toluene a different product can be obtained. After 24hr of reaction, an orange-brown solution results which is similar in color to the one observed if the reaction is done in pentane. Removal of the toluene at room temperature results in a green solid which may be redissolved in pentane. A dark green material can be crystallized from the pentane solution which, unlike $(C_5Me_5)_2Yb[HN(SiMe_3)_2]$, loses solvent when dried under vacuum to give a greenish-brown microcrystalline powder. This material is the base-free complex $(C_5Me_5)_2Yb$. The complex $(C_5Me_5)_2Yb$ dissolves in non-polar

Figure 4. Observed and Calculated Mass Spectra of $(C_5Me_4Et)_2Yb[N(SiMe_3)_2]$

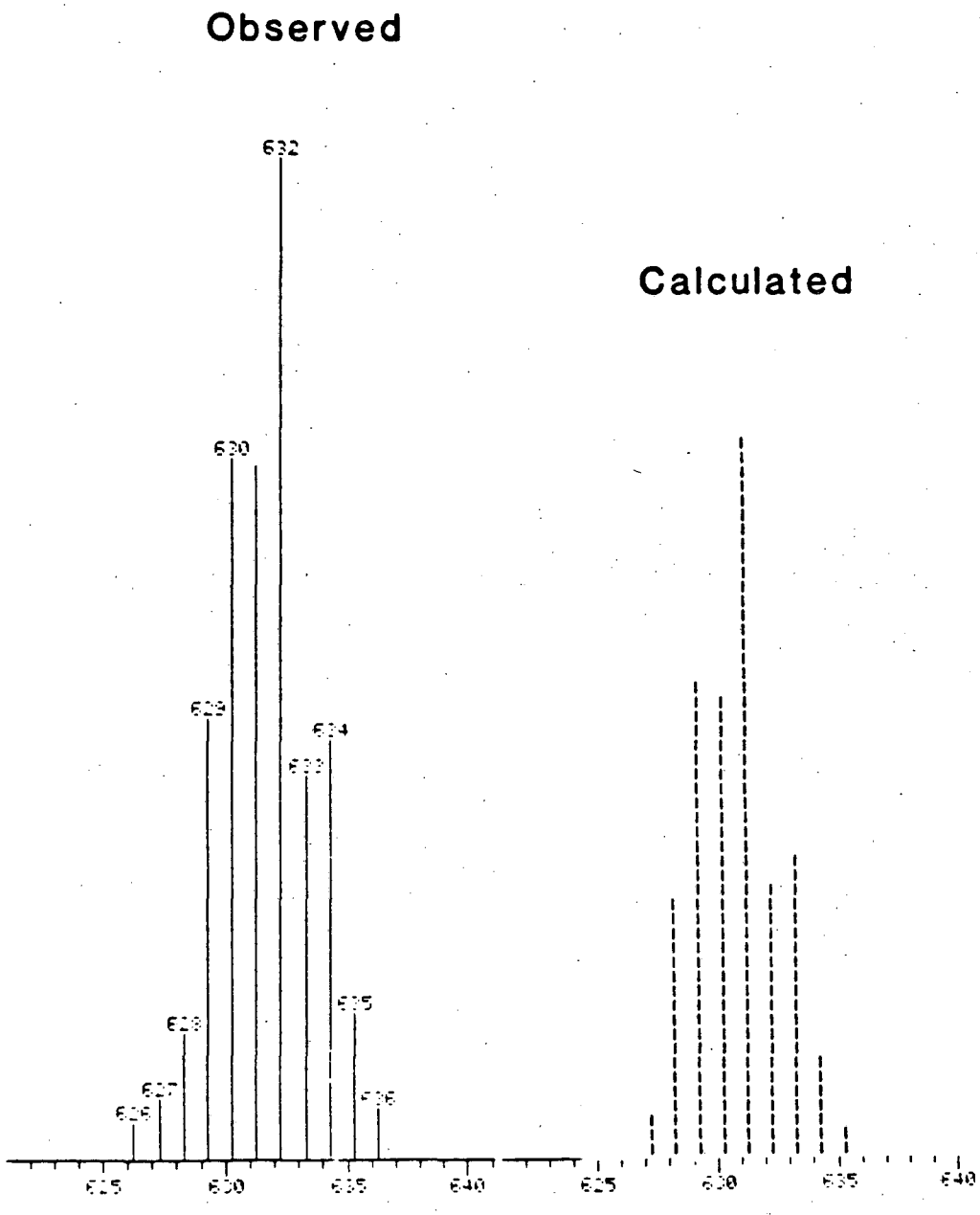

Table VI. ^1H NMR Data for Some $(C_5Me_5)_2YbL$ Complexes

Compound	Color	^1H NMR (C_6D_6, 31°C)
$(C_5Me_5)_2Yb[HN(SiMe_3)_2]$	Dark green	δ0.087(s, 18H); δ1.93(s, 30H)
$(C_5Me_5)_2Yb$	Green-brown	δ1.92(s)
$(C_5Me_4Et)_2Yb \cdot OEt_2$	Green	δ0.914(t, $^3J_{H-H}$=6.9Hz, 3H); δ1.19(t, $^3J_{H-H}$=7.4Hz, 3H); δ2.10(s, 6H); δ2.15(s, 6H); δ2.55(q, $^3J_{H-H}$=7.4Hz, 2H) 2.99(q, $^3J_{H-H}$=6.9Hz, 2H)

solvents to give red solutions, but crystallizes from them as green crystals. The complex is rather stable thermally since it melts reversibly at 190°C to give a red liquid which solidifies and turns green when cooled. In a similar manner, if the reaction between C_5Me_4EtH and $\{[(Me_3Si)_2N]_2Yb\}_2$ is carried out in toluene, and the toluene removed under reduced pressure and the residue redissolved in pentane, a red powder may be isolated from the pentane solution at -70°. This red powder has not yet been characterized. The reactions described above are shown in Scheme I.

The observation that removal of toluene from a toluene solution of $(C_5Me_5)_2Yb[HN(SiMe_3)_2]$ results in displacement of $H\text{-}N(SiMe_3)_2$ indicates that toluene in large excess displaces $HN(SiMe_3)_2$ from $(C_5Me_5)_2Yb$. Thus, toluene functions as a Lewis base towards $(C_5Me_5)_2Yb$. If the pentane from a pentane solution of $(C_5Me_5)_2Yb[HN(SiMe_3)_2]$ is removed under reduced pressure, and the resultant green solid crystallized from pentane, the complex $(C_5Me_5)_2Yb[HN(SiMe_3)_2]$ is isolated. These experiments indicate that pentane does not displace, though toluene does displace, $HN(SiMe_3)_2$ from $(C_5Me_5)_2Yb[HN(SiMe_3)_2]$.

The complex $(C_5Me_5)_2Sm$ has been prepared very recently, by sublimation of $(C_5Me_5)_2Sm(THF)_2$ at 135°C.[18] All attempts to prepare the analogous ytterbium process by high temperature sublimation techniques have failed. When $(C_5Me_5)_2Yb(L)$ (L=THF, OEt_2) is heated in vacuum the only material that sublimates is an orange waxy solid which is paramagnetic, as judged by ^1H NMR, indicating the formation of a Yb(III) product.[12] The amide $(C_5Me_4Et)_2Yb(N(SiMe_3)_2$ can be synthesized by heating the residue of the reaction between C_5Me_4EtH and $\{[(Me_3Si)_2N]_2Yb\}_2$ to 145°C (10^{-2}torr) after the solvent has been

Scheme I

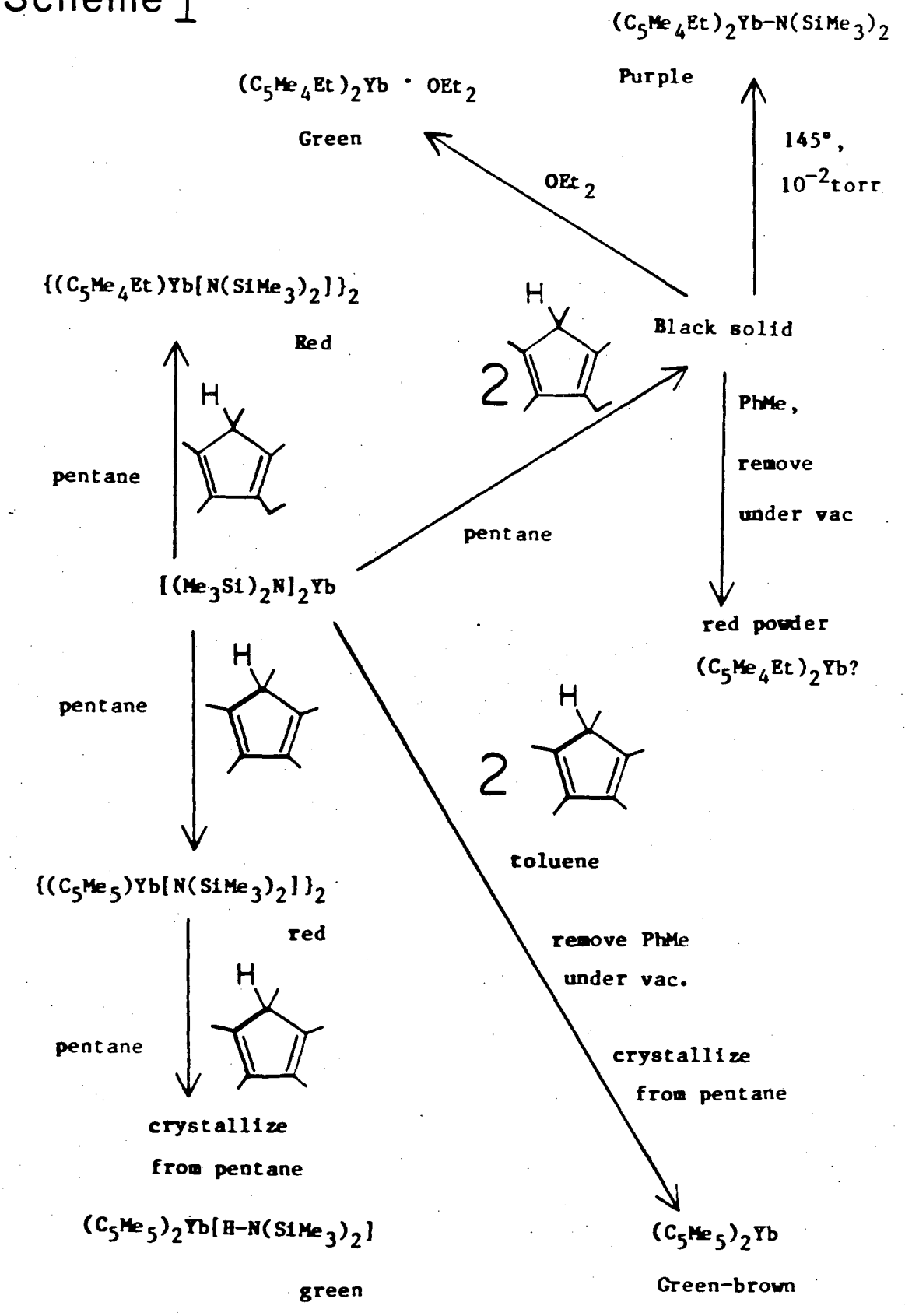
$(C_5Me_4Et)_2Yb-N(SiMe_3)_2$
Purple
$(C_5Me_4Et)_2Yb \cdot OEt_2$
Green
OEt_2
145°,
10^{-2}torr
$\{(C_5Me_4Et)Yb[N(SiMe_3)_2]\}_2$
Red
Black solid
2
H
PhMe,
remove
under vac
pentane
pentane
$[(Me_3Si)_2N]_2Yb$
red powder
$(C_5Me_4Et)_2Yb$?
pentane
2
toluene
$\{(C_5Me_5)Yb[N(SiMe_3)_2]\}_2$
red
remove PhMe
under vac.
pentane
crystallize
from pentane
crystallize
from pentane
$(C_5Me_5)_2Yb[H-N(SiMe_3)_2]$
green
$(C_5Me_5)_2Yb$
Green-brown

removed. It appears that at high temperatures $(C_5Me_5)_2YbL$ is quite reactive toward hetero-atom donors so that the only way in which $(C_5Me_5)_2Yb$ can be synthesized is by displacement of L with an excess of a very weak ligand at room temperature. The very weak ligand may then be removed at room temperature under vacuum. Further experimental study of this system is warranted.

Reaction with Lewis Acids

The observation that $\{[(Me_3Si)_2N]_2Yb\}_2$ is a dimer in the solid state with $(Me_3Si)_2N$ groups that bridge the two Yb atoms indicates that the nitrogen atoms of the coordinated amido groups can act as Lewis bases. Since the $[(Me_3Si)_2N]_2Yb$ fragment is very coordinatively unsaturated, compounds containing both Lewis acid and base sites can coordinate to both the nitrogen atoms of the $(Me_3Si)_2N$ groups and the ytterbium atom. This behavior is observed in the compound $NaYb[N(SiMe_3)]_3$ in which the two metal atoms are bridged by $(Me_3Si)_2N$ groups.

The reaction of electropositive metal alkyls and hydrides with $\{[(Me_3Si)_2N]_2Yb\}_2$ should produce complexes in which the $(Me_3Si)_2N$ groups bridge the two metals.[1] Since the $[(Me_3Si)_2N]_2Yb$ fragment is coordinatively unsaturated, the alkyl or hydride ligands might also be expected to bridge the two metal atoms. Trialkylaluminum complexes are likely candidates to form alkyl bridges because complexes which contain alkyl groups that bridge between the Al atom and an early d or f block metal have been isolated.[19] Such materials are of interest relative to the mechanism of the Ziegler-Natter polymerization process[20a-d] as well as their structure and bonding.[20e-h]

The reaction of $\{[(Me_3Si)_2N]_2Yb\}_2$ with two equivalents of Al_2R_6

(R=Me, Et) is instantaneous at room temperature. The products of these reactions have the stoichiometry $[(Me_3Si)_2N]_2Yb(AlR_3)_2$ as determined by their ^1H NMR spectra, and the observation of a parent ion in the mass spectrum of the $AlMe_3$ complex. The complex $[(Me_3Si)_2N]_2Yb(AlMe_3)_2$ may be crystallized from pentane, in high yield, as bright yellow plates. The complex $[(Me_3Si)_2N]_2Yb(AlEt_3)_2$ is a low melting solid which does not crystallize from pentane in a reproducible fashion. Since the stoichiometry of these complexes rule out structures that contain more than one Yb atom (assuming that the Al atom is bound to the $N(SiMe_3)_2$ group), there was a good possibility that the complexes contain alkyl groups which bridge the Al and Yb atoms. A single crystal X-ray diffraction study at low temperature was performed on the complex $[(Me_3Si)_2N]_2Yb(AlMe_3)_2$ to investigate this possibility.

An ORTEP drawing of the molecule is given in Figure 5. The bond lengths and angles in this molecule are found in Tables (VII) and (VIII). A listing of positional and thermal parameters can be found in Appendix (I), while the details of the data collection are found in the Experimental Section. The structure determination was carried out at -95°C in order to minimize the effects of thermal motion on the structure determination.

The complex consists of a monomeric $Yb[N(SiMe_3)_2]_2$ fragment in which each lone pair of electrons on the nitrogen atoms is coordinated to aluminium so that the coordination number of the nitrogen and aluminium atoms is four. The averaged Al-N distance of 1.963(5)Å and the averaged Yb-N-Al angle of 80.1(7)° are similar to those found in $Me_4Al_2(\mu\text{-}Me)(\mu\text{-}NPh_2)$[21] at 2.003(3)Å and 85.6(1)°, and $Me_4Al_2(\mu\text{-}NMe_2)_2$[22] at 1.96(1)Å and 91.6(2)°, respectively. The YbN(1,2) bond lengths of 2.510(2) and

Figure 5. ORTEP of $[(Me_3Si)_2N]_2Yb(AlMe_3)_2$

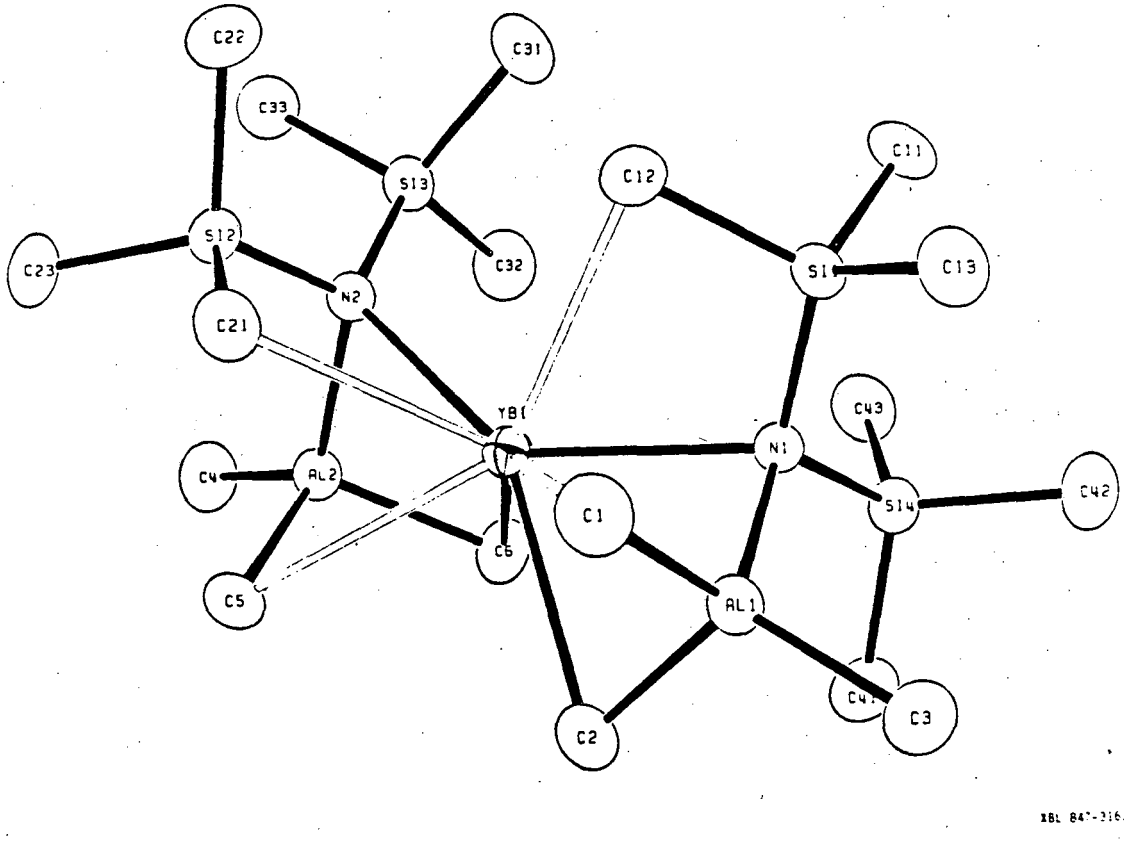

XBL 84?-316.

Table VII. Bond Lengths (Å) of $[(Me_3Si)_2N]_2Yb(AlMe_3)_2$

Yb1-N1	2.510(2)	Si2-C21	1.883(2)
Yb1-N2	2.573(2)	Si2-C22	1.868(2)
Yb1-C1	3.202(3)	Si2-C23	1.864(2)
Yb1-C2	2.788(2)	Si3-N2	1.761(2)
Yb1-C5	3.042(2)	Si3-C31	1.866(3)
Yb1-C6	2.756(2)	Si3-C32	1.861(3)
Yb1-C12	3.067(2)	Si3-C33	1.860(2)
Yb1-C21	3.039(2)	Si4-N1	1.758(2)
Si1-N1	1.755(2)	Si4-C41	1.862(2)
Si1-C11	1.865(2)	Si4-C42	1.870(2)
Si1-C12	1.879(2)	Si4-C43	1.866(2)
Si1-C13	1.862(2)	N1-Al1	1.973(2)
Si2-N2	1.753(2)	N2-Al2	1.953(2)

Table VIII. Bond Angles (deg) of $[(Me_3Si)_2N]_2Yb(AlMe_3)_2$

N1-Yb1-N2	131.56(5)	N1-Si1-C13	113.45(10)
N1-Yb1-C2	73.52(6)	C11-Si1-C12	104.26(11)
N1-Yb1-C5	152.56(6)	C11-Si1-C13	106.37(11)
N1-Yb1-C6	100.68(6)	C12-Si1-C13	108.95(11)
N1-Yb1-C12	63.01(6)	N2-Si2-C21	110.18(9)
N1-Yb1-C21	135.16(6)	N2-Si2-C22	114.70(10)
N2-Yb1-C2	148.35(6)	N2-Si2-C23	112.82(10)
N2-Yb1-C5	68.77(6)	C21-Si2-C22	102.97(11)
N2-Yb1-C6	71.94(6)	C21-Si2-C23	108.23(11)
N2-Yb1-C12	90.06(6)	C22-Si2-C23	107.32(12)
N2-Yb1-C21	63.59(6)	N2-Si3-C31	112.69(10)
C2-Yb1-C5	81.72(7)	N2-Si3-C32	112.79(10)
C2-Yb1-C6	85.76(7)	N2-Si3-C33	111.55(10)
C2-Yb1-C12	121.20(7)	C31-Si3-C32	104.60(12)
C2-Yb1-C21	115.39(7)	C31-Si3-C33	109.25(11)
C5-Yb1-C6	65.24(7)	C32-Si3-C33	105.49(11)
C5-Yb1-C12	143.19(6)	Yb1-N1-Si1	104.47(8)
C5-Yb1-C21	66.73(6)	Yb1-N1-Si4	122.97(8)
C6-Yb1-C12	137.74(7)	Yb1-N1-Al1	81.83(6)
C6-Yb1-C21	123.13(6)	Si1-N1-Si4	115.79(10)
C12-Yb1-C21	77.00(6)	Si1-N1-Al1	114.28(9)
Yb1-C1-Al1	64.68(7)	Si4-N1-Al1	113.08(9)
Yb1-C2-Al1	74.03(7)	Yb1-N2-Si2	101.95(7)
Yb1-C5-Al2	67.21(7)	Yb1-N2-Si3	126.93(8)
Yb1-C6-Al2	73.65(7)	YB1-N2-AL2	79.24(6)
Yb1-C12-Si1	83.22(8)	Si2-N2-Si3	116.37(10)
Yb1-C21-Si2	83.90(8)	Si2-N2-Al2	114.34(9)
N1-Si1-C11	114.66(10)	Si3-N2-Al2	112.77(9)
N1-Si1-C12	108.66(9)		

2.573(2)Å are longer than the equivalent bond length of 2.46(2)Å in $NaYb[N(SiMe_3)_2]_3$,[1] and within the range of the four Yb-N bridge bond lengths in $\{[(Me_3Si)_2N]_2Yb\}_2$ (from 2.445 to 2.573Å). The N(1)-Yb-N(2) angle of 131.56(5)° is similar to that found in $[(Me_3Si)_2N]_2Ybdmpe$[2] which is 123.6(6)°.

The nonlinearity of the N(1)-Yb-N(2) angle is caused by coordination of the $AlMe_3$ methyl groups C(2,6) and C(1,5) to the Yb atom. The Yb-μ-C bond lengths fall into three ranges; two short distances, Yb-C(2,6) of 2.788(2) and 2.756(2)Å, respectively having Yb-C(2,6)-Al(1,2) angles of 74.03(7)Å and73.65(7), respectively, one intermediate distance, Yb-C(5) of 3.042(2) and the Yb-C(5)-Al angle of 67.2(7)°, and one long distance, Yb-C(1) of 3.202(3)Å. The two shortest Al-C distances are close to those found in $(C_5H_5)_2Yb(\mu\text{-}Me)_2AlMe_2$[8] and $[(C_5H_5)_4Y]_2(\mu\text{-}Me)_2$[6] of 2.59(2) and 2.54(1)Å, respectively. The bridging angles Yb-C-Al are also similar to the equivalent angles found in $Cp_2Yb(\mu\text{-}Me)_2AlMe_2$[8] and $Cp_2Y(\mu\text{-}Me)_2AlMe_2$[9] of 78.9(6)° and 80.8(4)°, respectively. Since the radius of Yb(II) is ca. 0.1Å larger than that of Yb(III) or Y(III), the two longer Yb-C distances are still shorter than the sum (3.3Å) of the van der Waals radius of a carbon atom and the metallic radius of divalent ytterbium (1.7Å).

The Al-Me bond lengths show significant variation depending upon whether or not the methyl group bridges between Yb and Al. The averaged Al-Me(terminal) bond length (A(1,2)-C(3,4)) is 1.959(2)Å. The Al-Me(bridge) bond lengths fall into two categories. The averaged Al(1,2)-C(3,6) bond length is 2.029(2)Å, and the averaged Al(1,2)-C(1,5) bond length is 2.009(3)Å. Thus, the methyl groups which have the shortest contact with Yb have the longest bonds to Al. The averaged N-Al-

C(bridge) angle is 106.1(1.6°), and the averaged N-Al-C(term) angle is 116.6(4)°. These angles are similar to the equivalent angles in $Me_4Al_2(\mu\text{-}Me)(\mu\text{-}NPh_2)$ of 108.9(10)° and 113.1(1.1)°, respectively.

A comparison of the $M\text{-}C_{term}$ and $M\text{-}C_{bridge}$ bond lengths for $[(Me_3Si)_2N]_2Yb(AlMe_3)_2$ and related complexes is found in Table (IX). Inspection of Table (IX) reveals that the bridging Al-C distances in $[(Me_3Si)_2N]_2Yb(AlMe_3)_2$ are ca. 0.1Å shorter than these distances in related compounds. This is shown quantitatively by defining Δ as the averaged terminal Al-C distance minus the averaged bridging Al-C distance for the related compounds in Table (IX). The Δ-values show that the bridge bonds in $[(Me_3Si)_2N]_2Yb(AlMe_3)_2$ are approximately midway between bridging and terminal Al-C bonds in length and presumably in strength. As a consequence of the shorter bridging Al-C lengths in $[(Me_3Si)_2N]_2Yb(AlMe_3)_2$, the bridging Yb-C bonds are proportionally longer and weaker.

The relative weakness of the Yb-Me-Al interaction in $[(Me_3Si)_2N]_2Yb(AlMe_3)_2$ in the solid state is apparently true in solution since only one type of Me environment is observed for both the $AlMe_3$ and $N(SiMe_3)_2$ protons in the ^1H NMR spectrum at -80°C. If there were a chemical shift difference between the bridging and terminal Me protons on the $AlMe_3$ groups of 1.0Hz at -80°C, then the upper limit of $\Delta G^{\ddagger}_{Tc}$ is ca. 10kcal mol^{-1}. This may be compared with $\Delta G^{\ddagger}_{Tc}$ for bridge-terminal exchange in $Me_4Al_2(\mu\text{-}Me)_2$ and in $Cp_2Y(\mu\text{-}Me)_2AlMe_2$ of ca. 11 and 16kcal mol^{-1}, respectively. In the case of the complex $[(Me_3Si)_2N]_2Yb(AlEt_3)_2$, the ^1H NMR resonances for both the $(Me_3Si)_2N$ and $AlEt_2$ resonances broaden severely as the temperature is lowered from 25° to -80°C. Unfortunately, even at -80°C still only one Et and one $(Me_3Si)_2N$

Table IX. Comparison of Al-C Briding and Terminal Distances in Some Al Complexes Which Contain Bridging Alkyl Groups

Compound	Al-C_b a (Å)	Al-C_t b (Å)	Δ^c (Å)	$M^{Me}Al$ (deg)	$X^{Al}Me_b$ (x, deg)	References
$Me_4Al_2(\mu\text{-}Me)_2$	2.125(2)	1.935(2)	0.17	75.7(1)	Me, 104.3(1)	7
$Me_4Al_2(\mu\text{-}Me)(\mu\text{-}NPh_2)$	2.142(2)	1.948(5)	0.19	78.9(2)	N, 94.7(2)	21
$Me_4Al_2(\mu\text{-}Me)_4Mg$	2.13(2)	1.96(1)	0.17	77.7(3)	Me, 105.7(1)	23
$Me_2Al(\mu_2Me)_2YCp_2$	2.10(1)	1.94(1)	0.16	80.8(4)	Me, 112(1)	9
$Me_2Al(\mu_2\text{-}Me)_2YbCp_2$	2.13(2)	2.00(1)	0.13	78.9(6)	Me, 113.3(8)	8
$[(Me_3Si)_2N]_2Yb(AlMe_3)_2$	2.009(2) 2.029(1)	1.959(2)	0.05 0.07	65.9(7) 73.8(1)	107.7(4) 104.5(6)	this work

a.) b = bridging carbon atom

b.) t = terminal carbon atom

c.) Δ is $[Al\text{-}C_b]\text{-}[Al\text{-}C_t]$

environment are observed. Presumably, the bridge-terminal exchange could be stopped on the NMR timescale by using AlR_3 compounds with bulkier R groups.

Because of the Yb-C(2,6)-Al bridge bonding, there is a possibility of substantial interactions between the Yb atom and the H atoms on C(2,6). The H atoms on C(2,6) were located in the structure determination and it was found that H(2,3,4,6,) are 2.63, 2.72, 3.13, and 2.53Å from Yb. Since two H atoms on each methyl group are relatively close to Yb while the third points away the structure found is that of III rather than IV (below). This suggests that the Yb-Me

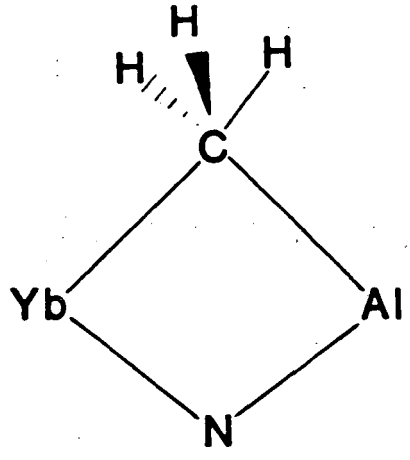

III

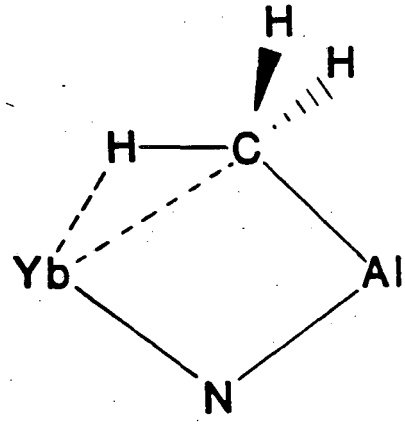

IV

interaction occurs by way of carbon rather than through hydrogen.

In addition to the short Yb-C-Al distances, two of the methyl groups on the silicon atom have short Yb-C contacts. The Yb-C(12,21) distances are 3.067(2) and 3.039(2)Å, respectively. Similar interactions are observed in $\{[(Me_3Si)_2N]_2Yb\}_2$, $NaYb[N(SiMe_3)_2]_3$.[1] and $[(Me_3Si)_2N]_2Ybdmpe$.[2] The longer Yb-C(12,21) contacts suggest that the

Yb-C-Si interactions are weaker than the analogous Yb-C-Al interaction. The averaged $Si-C_{terminal}$ distance is 1.864(3)Å, while the Si-C(12,21) averaged distance is 1.881(2)Å. Due to the small esd's in the structure, the difference is statistically significant, and the absolute bond lengthening of 0.017Å is consistent with the hypothesis that the Yb-C-Si bridging interaction is very weak indeed.

Although the Yb-C-Al bridging interaction is weak, the chemistry of $[(Me_3Si)_2N]_2Yb(AlMe_3)_2$ is substantially different from trimethylaluminium or its coordination complexes. In particular, $[(Me_3Si)_2N]_2Yb(AlMe_3)_2$ polymerizes ethylene at 20°C and 12atm whereas trimethylaluminium does not polymerize ethylene under such mild conditions.[24] The complex $[(Me_3Si)_2N]_2Yb(AlMe_3)_2$ does not react with PhC≡CPh, though it does react with PMe_3 to give an orange crystalline material which has not yet been characterized. When $[(Me_3Si)_2N]_2Yb(AlMe_3)_2$ is reacted with propylene a very slow reaction occurs which results in small amounts of polypropylene, but because of the small yields, small amounts of impurity may be catalyzing the reaction, and not $[(Me_3Si)_2N]_2Yb(AlMe_3)_2$.

The complex $\{[(Me_3Si)_2N]_2Yb\}_2$ also reacts with two equivalents of a variety of other Lewis acids such as $Mg(CH_2CMe_3)_2$, $LiCH(SiMe_3)_2$, and $HAl(i\text{-}Bu)_2$ to give complexes. Unfortunately, these materials are oils which are difficult to purify and characterize. The complex between $HAl(i\text{-}Bu)_2$ and $[(Me_3Si)_2N]_2Yb$ is of interest because of the possibility that it has Yb-H-Al interactions. Clearly, the reaction between $HAlMe_2$ and $\{[(Me_3Si)_2N]_2Yb\}_2$ should be investigated since the product should be more tractable.

Finally, when $\{[(Me_3Si)_2N]_2Yb\}_2$ is mixed with two equivalents of KH

in pentane for three days, a reaction occurs which gives a light red solution. and a light red precipitate. The complex formed is only sparingly soluble in hexane, but is quite soluble in toluene. A white solid may also be crystallized from the reaction mixture which has been shown to be $KN(SiMe_3)_2$ by its melting point.[27] The ^1H NMR spectrum at 25°C contains one resonance at δ0.26 due to Me_3Si protons and two broad resonances at 1.43 and 3.55δ, respectively. The integrated intensity of these peaks indicates that they occur in an 18:1:1 ratio. The peaks at δ1.43, and δ3.55 are in the region found for Lu and Y hydrides.[25] The ^1H NMR spectrum is temperature dependent with the Me_3Si resonance splitting into three peaks with a 1:3:1 ratio at -40°C. The hydride resonances also split, but the peaks are very broad and weak making accurate integration difficult. The complex appears to be diamagnetic by ^1H NMR, and the stoichiometry appears to be $\{K[H_2YbN(SiMe_3)_2]\}_x$. The temperature dependence of the ^1H NMR suggests that the complex might have a complicated structure in solution. Unfortunately, attempts to grow X-ray quality crystals of the complex have not yet been successful.

References

1.) Tilley, T. D.; Andersen, R. A.; Zalkin, A. Inorg. Chem. **1984**, 23, 2271.

2.) Tilley, T. D.; Andersen, R. A.; Zalkin, A. J. Am. Chem. Soc. **1982**, 104, 3725.

3.) Bradley, D. C.; Hursthouse, M. B.; Malik, K. M. A.; Moseler, R. Trans. Met. Chem. **1978**, 3, 253.

4.) Power, P. P. personal communication.

5.) Tilley, T. D.; Andersen, R. A.; Spencer, B.; Zalkin, A. Inorg. Chem. **1982**, 21, 2647.

6.) Holton, J.; Lappert, M. F.; Ballard, D. G. H.; Pearce, R.; Atwood, J. L.; Hunter, W. E. J. Chem. Soc., Dalton Trans. **1979**, 51.

7.) Huffman, J. C.; Streib, W. E. J. Chem. Soc., Chem. Comm. **1971**, 911.

8.) Holton, J.; Lappert, M. F.; Ballard, D. G. H.; Pearce, R.; Atwood, J. L.; Hunter, W. E. J. Chem. Soc., Dalton Trans. **1979**, 45.

9.) Scollary, G. R. Austral. J. Chem. **1978**, 31, 411.

10.) Shannon, R. D. Acta. Cryst. **1976**, 32A, 751.

11.) Wannagat, U.; Seyffert, H. Angen. Chem. Int. Ed. **1965**, 4, 438.

12.) Tilley, T. D. Ph.D. Thesis University of California, Berkeley, Berkeley, California. **1982.**

13.) Deacon, G. B.; Koplick, A. J. J. Organomet. Chem. **1978**, 146, C43.

14.) Hendrickson, J. H.; Cram, D. J.; Hammond, G. S. "Organic Chemistry" 3rd ed. McGraw-Hill, San Francisco, **1970**, p. 304.

15.) Bordwell, F. G.; Baisch, M. J. J. Am. Chem. Soc. **1983**, 105, 6188.

16.) Streitweiser, A., Jr.; Heathcock, C. H. "Introduction to Organic Chemistry", MacMillan, New York, **1976**, p. 1192.

17.) Ulmer, S. W.; Skurstad, P. M.; Burlitch, J. M.; Hughes, R. E. J. Am. Chem. Soc. **1979**, 18, 1097.

18.) Evans, W. J.; Hughes, L. A.; Hanusa, T. P. J. Am. Chem. Soc. **1984**, 106, 4270.

19.) a.) Ballard, D. G. H.; Pearce, R. J. Chem. Soc., Chem. Comm. **1975**, 621. b.) Watson, P. L. J. Am. Chem. Soc. **1982**, 104, 337. c.) Watson, P. L. J. Am. Chem. Soc. **1983**, 105, 6491. d.) Watson, P. L.; Roe, D. C. J. Am. Chem. Soc. **1982**, 104, 6471.

20.) a.) Davidson, P. J.; Lappert, M. F.; Pearce, R. Chem. Rev. **1976**, 76, 219. b.) Schrock, R. R.; Parshall, G. W. Chem. Rev. **1976**, 76, 243. c.) Kruger, C.; Schutowski, J. C.; Berke, H.; Hoffmann, R. Z. Naturforsch. **1978**, 336, 36B, 1110. d.) Jonas, K. Adv. Organomet. Chem. **1981**, 19, 97. e.) "Comprehensive Organometallic Chemistry"; Wilkinson, G.; Stone, F. G. A.; Able, E. W., Eds.; Permagon Press, Oxford, **1982**, Vol. 3, p. 475. f.) Sinn, H.; Kaminsky, W. Adv. Organomet. Chem. **1980**, 18, 99. g.) Watson, P. L.; Herskovitz, T. "A. C. S. Symposium Series", **1983**, 212, 459. h.) "Organometallics of the f-Elements", Marks, T. J.; Fischer, R. D. Eds.; Reidel, Holland, **1978**, p. 379.

21.) Magnuson, V. R.; Stucky, G. D. J. Am. Chem. Soc. **1969**, 91, 2544.

22.) Hess, H.; Hinderen, A.; Steinhauser, S. Z. Anorg. Allgem. Chem. **1970**, 377, 1.

23.) Atwood, J. L.; Stucky, G. D. J. Am. Chem. Soc. **1969**, 91, 2538.

24.) Coates, G. E.; Wade, K. "Organometallic Compounds", Vol. 1, Methuen, London, **1969**, p. 320.

25.) Evans, W. J.; Meadows, J. H.; Hanusa, T. P. J. Am. Chem. Soc. **1984**, 106, 4454. b.) Evans, W. J.; Meadows, S. H.; Wagda, A. L.; Hunter, W. E.; Atwood, J. L. J. Am. Chem. Soc. **1982**, 104, 2008. c.) Evans, W. J.; Meadows, J. H.; Wayda, A. L.; Hunter, W. E.; Atwood, J. L. J. Am. Chem. Soc. **1982**, 104, 2015.

26.) Gutowsky, H. S.; Holm, G. H. J. Chem Phys. **1956**, 25, 1228.

27.) Burger, H.; Seyffert, H. Angew. Chem. Int. Edn. **1964**, 104, 2015.

Experimental Section

General

Infrared spectra were recorded on a Perkin-Elmer 557 grating spectrophotometer as Nujol mulls between CsI or KBr windows. Mass spectra were taken with an AEI 12 mass spectrometer. The ^{1}H (90MHz), $^{13}C\{^{1}H\}$ (22.5MHz) nuclear magnetic resonance spectra were recorded on a JEol Fx-90Q spectrometer and referenced to Me_4Si(δ=0, ^{1}H and ^{13}C spectra). The ^{31}P NMR spectra were measured at either 72.9 MHz or 81MHz on the departmental machines at the University of California, Berkeley and referenced to 85% H_3PO_4(δ=0). Elemental analyses were performed by the analytical laboratories at the University of California, Berkeley. Melting points were measured in sealed capillaries and are uncorrected. The optical spectra were measured on a Cary 17 UV-visible spectrophotometer.

All of the compounds studied here are air and moisture sensitive, consequently all operations were conducted under a nitrogen atmosphere using standard schlenk techniques or a vacuum atomosphere inert atmosphere glove box. Reactions which were carried out at elevated pressures were performed in Fischer-Porter glass pressure bottles.

All solvents used for reactions were distilled from benzophenone ketyl under nitrogen prior to use. Pyridine was distilled from sodium, and phosphines were dried over KOH prior to use. Deuterated solvents for NMR studies were distilled from molten potassium and stored under nitrogen over sodium prior to use. All other chemicals were of reagent grade quality unless otherwise specified.

Pentamethylcyclopentadienide and tetramethylethylcyclopentadiene

were prepared according to literature procedures.[1] Sodium pentamethylcyclopentadiene was prepared by reaction of the diene with $NaNH_2$ in THF. The sodium salt is soluble in THF, and isolation of the sodium salt is accomplished by filtration of the THF solution followed by evaporation of the THF. The resultant gray-green powder is then washed with diethyl ether (3×200ml) to give NaC_5Me_5 as an off-white powder. Sodium bis(trimethylsilyl)amide[2] and the lanthanide dihalides (EuI_2, YbI_2)[3] were prepared according to literature procedures. The $[C_5H_4RM(CO)_x]_2$ molecules were prepared according to literature procedures[4], but were purified via recrystallization rather than sublimation. The compounds $(C_5H_4R)Co(CO)_2$ (R=Me_3Si, Me, H) were prepared by reaction of the diene with $Co_2(CO)_8$[4], but were purified by filtering the crude reaction mixture through a frit filled with ca. 60cm of alumina. Removal of excess CH_2Cl_2 left the pure products as dark red oils.

Magnetic susceptibility Studies

Magnetic susceptibility measurements were made on a S.H.E. Corp. model 905 SQUID magnetometer. Sample containers used in these studies were made from an alloy of aluminum containing 3% silicon which was purchased from Varian. The sample containers were held together with a 2cm piece of 0.0127mm copper wire. and were sealed with silicon stopcock grease. The variation in the susceptibility of the empty sample container due to differing amounts of grease was less than 3%. Design of the sample containers is available from Dr. N. Edelstein at Lawrence Berkeley Laboratories.

Approximately 30-40mg of the compound was finely ground with a mortar and pestle in an argon filled dry box. This sample was then loaded into the sample holder which was closed and sealed with silicon grease. The sample container was then removed from the dry box. Any excess grease was removed. The container was then wired closed, and a piece of cotton thread was tied to the wire. The sample was then suspended in the sample chamber of the magnetometer. The sample chamber was then evacuated to a pressure of 100 microns, and refilled with dry helium three times.

Sample measurements were taken automatically at the following temperatures and fields. At 5KG: 5-15K every 2.5K, from 15-50K every 5K, from 50-300K every 10K, and at 40KG: 300-100K every 20K, from 100-30K every 10K, from 30-5K every 5K. All sample runs were corrected for container magnetism and compound diamagnetism using published Pascal constants.

Temperature Independent Paramagnetism was taken to be zero for Yb(III). Magnetic susceptibility was calculated as

$$\chi_M = \frac{(\text{total signal-container signal}) \cdot \text{M.W.}}{H \cdot \text{Weight}} - \chi_{dia} - \text{T.I.P.}$$

Samples which followed Curie-Weiss behavior were fitted to the equation

$$\frac{1}{\chi_M} = -\frac{\theta}{C} + \frac{T}{C}$$

using a linear least-squares program written by Dr. E. Gamp. The effective magnetic moments of the complexes were calculated using the equation

$$\mu_{eff} = 2.8279 \sqrt{\chi_M \cdot (T - \theta)}$$

Chapter 1

$[(C_5Me_5)_2Yb(III)][Mn(CO)_5]\cdot{}^1/_4\,C_7H_5$

Bis(Pentamethylcyclopentadienyl)ytterbium(II) diethyletherate (1.0g, 0.0019mol) in toluene (20ml) was added to a solution of $Mn_2(CO)_{10}$ (0.38g, 0.0097mol) in toluene (20ml). The reaction mixture turned dark blue upon mixing. After ca. 12hr. of stirring the dark blue solution was filtered, concentrated to saturation at room temperature (ca. 40ml), and cooled to -10°C. The dark blue needles were collected and dried under reduced pressure. The mother liquors were then concentrated to ca. 10ml, and cooled to -10°C; combined yield 1.1 g, 82%. Mp. darkens at 270°C, decomposes at 318-320°C. Anal. Calcd. for $C_{25}H_{30}O_5MnYb\cdot{}^1/_4\,C_7H_8$: C, 48.6; H, 4.88. Found: C, 48.6; H, 4.70. ^1H NMR (+25°C): δ8.75($\nu_{1/2}$= 47Hz, 30H), 2.11(0.75H) (the aromatic protons on the toluene of crystallization were obscurred by residual C_6D_5H in the C_6D_6 solvent). Ir (Nujol): 2735w, 1965vbrvs, 1937sh, 1928sh, 1882m, 1840s, 1775vbrvs, 1062w, 1024m, 800w, 735m, 728m, 695sh, 682vs, 650m, 645m, 592w, 555s, 500m, 463m, 425m, 395m, 325s, 285w cm^{-1} (Cyclohexane) 1984m, 1962s, 1955s, 1945m, 1778m, 1762s, 1750m, 1723m cm^{-1}.

$[(C_5Me_5)_2Yb(III)][Re(CO)_5]\cdot{}^1/_4\,C_7H_8$

Bis(Pentamethylcyclopentadienyl)ytterbium(II) diethyletherate (0.21g, .00040 moles) in toluene (25ml) was added to a solution of $Re_2(CO)_{10}$ (.13g, .00020 moles). The reaction mixture turned dark red over the course of two days. After ca. 48hr. of stirring, the dark red solution was filtered, and concentrated to ca. 5ml. and cooled to -10°C. The

dark red microcrystals were collected and dried under reduced pressure, 0.17g (53%) yield: Mp. 315°-320°C (dec). Anal. Calcd. for $C_{25}H_{30}O_5ReYb \cdot 1/4\, C_7H_8$: C, 40.5: H, 4.07. Found: C, 40.4; H 4.18. ^1H NMR (C_6D_6, 25°C): δ9.56($\nu_{1/2}$= 110Hz, 30H) δ2.10(0.8H). (The residual C_6D_5H in the solvent obscured the aromatic protons on the toluene of crystallization). Ir (Nujol): 2720w, 1982sh, 1972vs, 1950s, 1945sh, 1750brvs, 1015w, 950m, 795w, 715m, 625w, 585s cm^{-1}.

Reaction of $[(C_5Me_5)_2Yb(III)][Mn(CO)_5] \cdot 1/4\, C_7H_8$ with CH_3I.

1.7 Ml of a 0.10M solution of CH_3I(.0017 moles) in toluene was added to a toluene solution (20ml) containing 0.09g(0.0014mol) of $[(C_5Me_5)_2Yb(III)][Mn(CO)_5] \cdot 1/4\, C_7H_8$ at room temperature. The mixture slowly turned from blue to red-brown. After 12hr. of stirring the toluene was removed under reduced pressure. The residue was extracted with pentane (ca. 3ml), and the ir spectrum of this extract was measured, (2108m, 2040vw , 2010vs, 1990s cm^{-1}), which is identical to the published spectrum of $MeMn(CO)_5$.[5]

Reaction of $[(C_5Me_5)_2Yb(III)]Re(CO)_5] \cdot 1/4\, C_7H_8$ with CH_3I

Methyl Iodide (0.26 ml. of a 0.50 M solution 0.00013mol) was added to a solution of $[(C_5Me_5)_2Yb(III)][Re(CO)_5] \cdot 1/4\, C_7H_8$ (0.10g, 0.00013mol) in toluene (10ml) at room temperature. After stirring for ca. 24hr., the toluene was removed under reduced pressure. The residue was extracted with pentane (10ml), and the ir spectrum of the pentane extract was measured, 2140w, 2095sh, 2065s, 2035vs, 2020vs, 1995vs, 1978vs, 1960wsh 1943m cm^{-1}, due to a mixture of $MeRe(CO)_5$ and $Re_2(CO)_{10}$.[6,7]

Hydrolysis of the Mn-Yb and Re-Yb Compounds.

Ca. 30mg of the Mn or Re compounds were hydrolyzed with D_2O in C_6D_6. The only resonances observed in the ^1H NMR spectrum of the C_6D_6 solutions were those of C_5Me_5D and C_7H_8 in an 8:1 ratio.

$\{[(C_5Me_5)_2Yb(III)][(C_5H_5)Fe(CO)_2]\}_2$

Bis(pentamethylcyclopentadienyl)ytterbium(II) diethyletherate (0.57g, 0.0011mol) in toluene (30ml) was added to a solution of $[(C_5H_5)Fe(CO)_2]_2$ (0.20gm 0.00056mol) in toluene (30ml). The reaction mixture turned dark red immediately and tiny black crystals precipitated from solution. After stirring for 12hr., the reaction mixture was allowed to settle. The toluene solution was then filtered and cooled to -10°C. The crystalline residue was extracted with toluene (3 x 60ml). The toluene extracts were combined and concentrated to ca. 30ml, and cooled to -10°C. The combined yield of the black microcrystals was 0.55g (80%) Mp. 350°C (dec). Anal. Calcd. for $C_{27}H_{35}FeO_2Yb$: C, 52.3; H, 5.68. Found: C, 51.6; H, 5.70. ^1H NMR (C_6D_6, 30°C) δ8.09($\nu_{1/2}$=36Hz, 30H), δ35.23($\nu_{1/2}$=13Hz, 5H). Ir (Nujol): 3100w, 2730w, 2005w, 1965m, 1960m, 1800vbrvs, 1665ssh. 1165w, 1110w, 1060w, 1015m, 892w, 840m, 810m, 800m, 725w, 695w, 655m, 605sh, 583s, 512s, 395sh, 378m, 355w, 320s, 279sh cm^{-1}.

$\{[(C_5Me_5)_2Yb(III)][(C_5H_5)Fe(CO)_2]\}_2$

Bis(pentamethylcyclopentadienyl)ytterbium(II) diethyletherate (1.25g. 0.0024mol) in toluene (50ml) was added to a solution of $[(CH_3C_5H_4)Fe(CO)_2]_2$ (0.46g, 0.0012mol) in toluene (40ml). The reaction mixture turned dark red upon mixing. After stirring for 12hr. the

solution was filtered, and concentrated to ca. 40ml under reduced pressure and cooled to -10°C. The small black prisms were collected and dried under reduced pressure. The mother liquors were then concentrated to ca. 10ml and cooled to -10°C. More black prisms were collected. The combined yield was 1.2g (78%), Mp. 340°C (dec). Anal. Calcd. for $C_{28}H_{37}FeO_2Yb$: C, 53.0; H, 5.88. Found: C, 52.7: H, 5.76. ^1H NMR (C_6D_6, 25°C) δ7.91($\nu_{1/2}$=45Hz, 30H), 38.52($\nu_{1/2}$=7.8Hz, 3H), 40.31 ($\nu_{1/2}$=8.6Hz, 2H). 44.19($\nu_{1/2}$=11Hz 2H). Ir (Nujol): 3095w, 2730w, 2015w, 1972m, 1958sh, 1785brvs, 1725brvs, 1665s, 1165w, 1062w, 1020Brm, 930w, 885w, 855w, 823w, 801m, 725m, 695w, 660m, 630w, 585s, 514s, 390m, 360m, 322s, 285sh cm^{-1}, (Cyclohexane) 1787vs, 1723vs, cm^{-1}. Crystals suitable for single crystal x-ray diffraction were grown by cooling a saturated methylcyclohexane solution from 60° to room temperature over a period of 24hr.

$\{[(C_5Me_5)_2Yb(III)][(Me_3SiC_5H_4)Fe(CO)_2]\}_2$

The complex $(C_5Me_5)_2Yb{\cdot}OEt_2$ 0.50g (0.00097 moles) in toluene (20ml) was added to 0.24g (0.00048 moles) of $[Me_3SiC_5H_4Fe(CO)_2]_2$ in toluene (20ml). The mixture was allowed to react for ca. 20hr. The reaction mixture was then filtered and concentrated to ca. 15ml, and cooled to -10°C. The black prisms of product were collected, and dried under reduced pressure. A second crop of crystals was obtained by concentrating the mother liquors to ca. 2ml and cooling to -10°C. The combined yield was 0.57g (86%). Anal. Calcd. for $C_{30}H_{43}O_2FeSiYb$: C, 52.0; H, 6.26. Found C, 51.4; H, 6.13. Ir (Nujol): 3100w, 3170w, 2720w, 1795brs, 1730brs, 1365m, 1243m, 1158m, 1059w, 1040m, 1017w, 902m, 865m, 832s, 798m, 750m, 690m, 630m, 620w, 585m, 579sh, 508m, 430w, 380m,

340w, 315s, 280m cm^{-1}. ^1H NMR (C_6D_6 29°C): δ50.21($\nu_{1/2}$=3Hz 2H); δ32.33($\nu_{1/2}$=12Hz, 2H); δ19.45($\nu_{1/2}$=10Hz, 9H); δ8.01($\nu_{1/2}$=37Hz, 30H). When heated in a sealed capillary the compound lightened in color at 100-120°C, and melted with decomposition at 40-245°C.

$[(C_5Me_5)_2YbI]_2[(C_5H_5)_2Fe_2(CO)_4]$

Bis(pentamethylcyclopentadienyl)ytterbium(II) diethyletherate (0.44g, 0.00085mol) in toluene (40ml) was added to a solution of $(C_5H_5)Fe(CO)_2I$ (0.25g, 0.00082mol) in toluene (20ml). Upon mixing, copious amounts of red-purple precipitate formed. After stirring for ca. 24 hr. the precipitate was allowed to settle. The supernatent was discarded. The red-purple powder was dried under reduced pressure. The complex melted with decomposition 220°-240°C. Anal. Calcd. for $C_{54}H_{70}Fe_2I_2O_4Yb_2$: C, 43.40; H, 4.72; I, 17.0. Found: C, 42.4; H, 4.73; I, 17.5. Ir (Nujol): 3960w, 3310w, 3110w, 3070w, 2720w, 2015vs, 1985sh. 1945 msh, 1825m, 1740m, 1640BrVs, 1425m, 1165m, 1051w, 1010m, 995m, 869wsh, 860w, 840s, 830sh. 817w, 660vs, 608m, 595s, 587m, 570w, 523s, 509 w, 490w, 470w, 445w, 370brm, 355m, 298s, 275sh cm^{-1}.

Dissolution of the complex in THF (20ml) gave a violet colored solution. The violet solution was filtered and concentrated to ca. 3ml, and cooled to -10°C. The purple prisms were collected and dried under reduced pressure, and were shown to be $(C_5Me_5)_2YbI\cdot THF$ by comparison of the IR to that of an authentic sample, and by mass spectrscopy (M^+-THF=571). The solvent from the supernatent was removed under reduced pressure. The residue contained $[(C_5H_5)Fe(CO)_2]_2$ by comparison of its ir with the literature value.

$[(C_5Me_5)_2Yb(III)(py)][(Me_3SiC_5H_4)Fe(CO)_2]$

Bis(pentamethylcyclopentadienyl)ytterbium diethyletherate 0.4g(0.002mol) in toluene (60ml) was reacted with 0.50g (0.0010mol) of $[Me_3SiC_5H_4Fe(CO)_2]_2$ for 12hrs. at room temperature. Pyridine (0.16ml, 0.0020mol) was added and the reaction mixture was stirred for 8hr. The toluene was removed under reduced pressure, and the resultant residue was dissolved in diethylether (ca. 30ml). The ether solution was filtered, concentrated to ca. 10ml and cooled to -10°C for 1 week. Dark red-black prisms were isolated, and dried under reduced pressure to give a yield of 1.3g (82%). Anal. Calcd. for $C_{35}H_{48}FeNO_2SiYb$; C, 54.47; H, 6.27; N, 1.81: Found· C, 52.14; H, 6.23; N, 1.61. Ir (Nujol): 3710w. 3250w, 3085w, 3065w, 2720w, 1870VsBr, 1678vsbr, 1601s, 1570w, 1488m, 1440m, 1360m, 1300w, 1244s, 1218m. 1215m, 1180w, 1166m, 1157s, 1067w, 1041s, 1032w, 1021m, 1008m, 900m, 880w, 865m, 833s, 802m, 790w, 758s, 706s 692m, 643m, 630m, 594m. 550s, 507s 448w, 435w, 385m, 375m, 315s, 290msh, 245w cm^{-1}. ^1H NMR (C_7D_8, 29°C): δ4.46, (30H); δ6.30, (9H); δ9.92, (2H): δ10.24. (2H).

$\{[(C_5Me_5)_2Yb(III)][(Me_3SiC_5H_4)Ru(CO)_2]\}_2$

Bis(pentamethylcyclopentadienyl)ytterbium(II) diethyletherate (0.72g, 0.0014mol) in toluene (40ml) was added to a solution of $[(Me_3SiC_5H_4)Ru(CO)_2]_2$ (0.41g, 0.00070mol) in toluene (30ml). The reaction mixture slowly turned dark red as it was stirred for ca. 24hr. The mixture was filtered, concentrated to ca. 25ml and cooled to -10°C. The resultant purple prisms were collected, and dried under reduced pressure. Two more crops of crystals were obtained from the

mother liquors, and the combined yield was 85% When heated in a sealed capillary the compound melted with decomposition at 250-255°C. Anal. Calcd. for $C_{30}H_{43}O_2$ RuSiYb: C, 48.8; H, 5.87. Found: C, 48.3; H, 5.67. ^{1}H NMR (C_6D_6, 31°C): δ8.27($\nu_{1/2}$=41Hz, 30H), δ19.55($\nu_{1/2}$=7.4Hz, 9H), δ31.87($\nu_{1/2}$=10Hz, 2H), δ43.80($\nu_{1/2}$=9.4Hz, 2H). Ir (Nujol): 2730w, 1815vs, 1730vs, 1242s, 1156s, 1037m, 1015w, 898m 865m, 833s, 816s, 782m, 751m, 740w, 690m, 625m, 523s, 520w, 487m, 415m cm^{-1}.

Reaction of CH_3I with $\{[(C_5Me_5)_2Yb(III)][(C_5H_5)Fe(CO)_2]\}_2$

Methyl Iodide (0.00019mol) in toluene solution (1.5ml, .13M) was added to a solution of $\{[(C_5Me_5)_2Yb(III)][(C_5H_5)Fe(CO)_2]\}_2$ (0.10g, 0.00016mol) in toluene (30ml) at room temperature. After stirring for 24hr., the toluene was removed under reduced pressure. The residue was extracted with pentane (15ml), and the ir spectrum of the pentane extract contained the following bands in the ν-CO region; 2045vw, 2017s, 1984w, 1965vs, 1945wsh, 1798s, due to $(C_5H_5)_2Fe_2(CO)_2$.[8] The mass spectrum of the residue had peaks consistent with the following ions: $(C_5Me_5)_2YbI^+$(571), $(C_5Me_5)_2Yb^+$(444), $(C_5Me_5)YbI^+$(435), and $(C_5Me_5)Yb^+$(309).

Reaction of CH_3I with $\{[(C_5Me_5)_2Yb(III)][(C_5H_4CH_3)Fe(CO)_2]\}_2$

Methyl Iodide (0.00016 moles) in toluene solution (0.33ml, 0.50M) was added to a solution of $\{[Yb(C_5Me_5)_2][(C_5H_5)Fe(CO)_2]\}_2$ (0.10g, 0.00016mol) in toluene (20ml) at room temperature. After stirring for 24hr., the toluene was removed under reduced pressure. The residue was extracted with pentane (10ml), and the ir spectrum of the pentane extract contained the following bands in the ν-CO region; 2005s, 1955vs.

1885s, due to $(MeC_5H_4)_2Fe_2(CO)_4$. The mass spectrum of the residue had peaks consistent with the following ions: $(C_5Me_5)_2YbI^+$(571), $(C_5Me_5)_2Yb^+$(444), $(C_5Me_5)YbI^+$(435), and $(C_5Me_5)Yb^+$(309).

$\{[C_5Me_5)_2Yb(III)][(C_5H_5)Mo(CO)_3]\}_2$

Bis(pentamethylcyclopentadienyl)ytterbium(II) diethyletherate (0.53g, 0.0010mol) in toluene (30ml) was added to a solution of $[(C_5H_5)Mo(CO)_3]_2$ (0.25g, 0.00051mol) in toluene (10ml). The reaction mixture turned dark purple upon mixing. After stirring for ca. 12hr the solution was filtered, concentrated to ca. 5ml, then ca. 5ml pentane was added. The resultant solution was then cooled to -70°C. The dark purple prisms (0.36g, 51%) were collected and dried under reduced pressure. Mp. 335°C (dec). Anal. Calcd. for $C_{28}H_{35}MoO_3Yb$: C, 48.8; H, 5.12. Found: C, 49.0; H, 5.14. ^1H NMR (25°C) δ8.16($\nu_{1/2}$=62Hz, 30H) δ32.85($\nu_{1/2}$=10Hz, 5H). Ir (Nujol): 3110brw, 2730w, 2030w, 1942vs, 1931vs, 1730brs, 1680brs, 1609s, 1165w, 1110w, 1057w,1022w, 1005m, 783s, 725w, 640w, 615m, 584m, 503s, 482m, 470sh, 390m, 321s, 268sh cm^{-1}. (Cyclohexane) 1940vs, 1730vs, 1680vs, 1680vs cm^{-1}.

$\{[(C_5Me_5)_2Yb(III)][Me_3SiC_5H_4Mo(CO)_3]\}_2$

The ether complex of Bis(pentamethylcyclopentadienyl)ytterbium(II) (0.79g,0.0015mol) in toluene (60ml) was added to Trimethylsilylcyclopentadienyl molybdenum tricarbonyl dimer (0.48g, 0.00076mol) in toluene (15ml). The reaction mixture was stirred for ca. 12hr. The purple solution was filtered, and the filtrate was concentrated under reduced pressure to ca. 20ml. Cooling to -10°C afforded purple prisms of product. The product was collected, and dried

under reduced pressure. The mother liquors were concentrated further to ca. 2ml, and cooled to -10°C producing another crop of crystals in a combined yield of 0.87g (76%). Mp. 300-310° (dec). Anal. Calcd. for $C_{62}H_{86}O_6Si_2Yb_2Mo_2$: C, 48.9: H, 5.70. Found: C, 48.3: H, 5.79. ^1H NMR (250MHz, 25°C); δ34.8, (1.76H); 34.63, (2.0H); 33.50, (1.76H); 32.05, (2.0H); 25.58, (7.92H); 25.30, (9H); 8.98, (13.2H); 8.27, (30H); 7.55, (13.2H). Ir (Cyclohexane): ν-CO-1944s, 1730s, 1682s cm^{-1}.

Reaction of $\{[(C_5Me_5)_2Yb(III)][(C_5H_5)Mo(CO)_3]\}_2$ with Methyl Iodide

Methyl iodide (0.00017mol) was added via syringe to a solution of $\{[(C_5Me_5)_2Yb^+][C_5H_4Mo(CO)_3^-]\}_2$ (0.10g,0.000072mol) in toluene (30ml). The solution was stirred for ca. 12hr, and the solvent was then removed under reduced pressure. The residue was then extracted into pentane and the ir spectrum of the pentane extract showed bands attributable to $C_5H_5Mo(CO)_3Me$[9] as well as a small amount of $C_5H_5Mo(CO)_3I$.[10]

Reaction of $\{[(C_5Me_5)_2Yb(III)][C_5H_5Mo(CO)_3]\}_2$ with $[(C_5Me_5)_2Yb(III)][Mo(CO)_3C_5H_4SiMe_3]$

The complex $\{[(C_5Me_5)_2Yb(III)][C_5H_5Mo(CO)_3]\}_2$ (0.11g,0.000016mol) in toluene (30ml). The resultant solution was then stirred at room temperature for ca. 24hr. The solvent was then removed under reduced pressure. ^1H NMR studies were then carried out on the residue.

$[(C_5Me_5)_2Yb(III)]_2[(C_5H_5)_2Co_3(CO)_4]$

Bis(pentamethylcyclopentadienyl)ytterbium(II) diethylether (1.0g, 0.0019mol) in toluene (30ml) was added to cyclopentadienycobalt

dicarbonyl (0.50g, 0.0028mol) in toluene (5ml). The solution slowly turned dark blue as it was stirred for 48hr. It was then filtered, and cooled to -10°C. The dark blue microcrystals were collected and dried under reduced pressure. A second crop of microcrystals was isolated from the mother liquor, and the combined yield was 0.74g (59%). When heated in a sealed capillary the compound melted at 130°C with decomposition as a green gas evolved which crystallized on the sides of the capillary. Anal. Calcd. for $C_{54}H_{70}Co_3O_4Yb_2$: C, 49.7; H, 5.40. Found: C, 49.6; H, 5.38. ^1H NMR (25°C): δ5.39($\nu_{1/2}$=47Hz, 30H); 32.51 ($\nu_{1/2}$=34Hz: 5H). Ir (Nujol): 3240w, 3100w, 2730w, 1590vs, 1075brw, 1010w, 900w, 843w, 835w, 812m, 725w, 660s, 572w, 543m, 530shw cm^{-1}.

$[(C_5Me_5)_2Yb(III)]_2[(MeC_5H_4)_2Co_3(CO)_4] \cdot C_7H_8$

Bis(pentamethylcyclopentadienyl)ytterbium(II) diethylether(1.1g, 0.0022mol) in toluene (50ml) was mixed with methylcyclopentadienylcobaltdicarbonyl (.66g, .0032mol) in toluene (5ml). The solution was heated to 90°C for 12hr, then cooled to room temperature, filtered, and concentrated to ca. 25ml. Cooling to -10°C yielded small dark purple prisms which were collected and dried under reduced pressure. Two more crops of crystals were isolated from the mother liquor, and the combined yield was 0.93g (65%). When heated in a sealed capillary the compound decomposed at 195°C with melting, and evolved copious quantities of a green gas. Anal. Calcd. for $C_{56}H_{74}Co_3O_4Yb_3 \cdot C_7H_8$: C, 53.1; H, 5.79. Found: C, 53.2; H, 5.75. ^1H NMR (30°C): δ4.84($\nu_{1/2}$=48Hz, 30H); 28.87($\nu_{1/2}$=39Hz; 2H); 30.12 ($\nu_{1/2}$=32Hz; 2H); 84.07($\nu_{1/2}$=49Hz, 3H); δ2.09 (3H); the aromatic hydrogens of the toluene of solvation were obscured by the residual C_6D_5H in the C_6D_6 solvent. Ir (Nujol): 3217w,

3070w, 2715w, 1575vs, 1051w, 1035w, 1013m, 962brw, 923w, 885w, 858w, 845w, 819w, 800m, 790sh, 760w, 712m, 650s, 610wsh, 580w, 564m, 531m, 432w, 390sh, 365m, 308s, 295msh, 260w, 225w, 205w cm^{-1}.

$[(C_5Me_5)_2Yb(III)]_2[(Me_3SiC_5H_4)_2Co_3(CO)_4]$

Bis(pentamethylcyclopentadienyl)ytterbium diethylether (0.96g, 0.0019mol) in toluene (30ml) was mixed with trimethylsilylcyclopentadienylcobaltdicarbonyl in toluene (5ml). The solution slowly turned deep blue upon heating to 70°C for 12hr. The solution was cooled to room temperature, filtered, and then concentrated to ca. 15ml. Cooling the concentrate to -10°C produced dark blue prisms which were collected and dried under reduced pressure. Two more crops of crystals were isolated from the mother liquor, and the combined yield was 0.89g (65%). Anal. Calcd. for $C_{60}H_{68}Co_3O_4Si_2Yb_2$: C, 49.7; H, 5.98. Found: C, 47.83; H, 6.01. ^1H NMR (25°C): δ4.09($\nu_{1/2}$=12Hz, 9H); 5.34($\nu_{1/2}$=49Hz, 30H); 17.25($\nu_{1/2}$=40Hz, 2H); 75.45($\nu_{1/2}$=39Hz, 2H). Ir (Nujol): 3120w, 3080w, 2715w, 1658w, 1575vs, 1350w, 1240m, 1157m, 1034m, 1015w, 895m, 870w, 826s, 800m, 745m, 715w, 682w, 645s, 623m, 608wsh, 562w, 530m, 509w, 433w, 410w, 390w, 380w, 360m, 307s, 295msh, 280m, 260w, 225w cm^{-1} EPR: g=2.0827 in methylcyclohexane at room temperature, and at 77K.

$[(C_5Me_5Yb(III)]_2[(C_5H_5)_2Rh_3(CO)_4]$

Bis(pentamethylcyclopentadienyl)ytterbium(II) diethylether(.25g, 0.00043mol) in toluene (20ml) was mixed with cyclopentadienylrhodiumdicarbonyl (0.17g, 0.00074mol) in toluene (5ml). The solution turned blue-green immediately and was stirred for 12hr, filtered, and the

filtrate concentrated to ca. 5ml. Cooling the concentrate to -10°C produced dark blue microcrystals which were collected, and dried under reduced pressure in a yield of 0.12g (38%). Anal. Calcd. for $C_{54}H_{70}O_4Rh_3Yb_2$: C, 45.10; H, 4.90. Found: C, 44.2; H, 4.81. Ir (Nujol): 3130w, 3080w, 2715w, 1583vs, 1335m, 1050w, 1020w, 1000m, 887w, 828m, 804wsh, 787s, 720w, 610m, 560m, 506w, 385w, 340w, 315s, 300msh, 278w, 228w, 210w cm^{-1}. ^1H NMR (C_6D_6, 27°C): δ6.30($\nu_{1/2}$=48Hz, 30H); -13.26($\nu_{1/2}$=56Hz, 5H).

Reaction of $Me_3SiC_5H_5$ with $[(C_5Me_5)_2Yb(III)THF][Co(CO)_4]$

Bis(pentamethylcyclopentadienyl)ytterbium(III) tetrahydrofuran-tetracarbonylcobaltate (0.30g, 0.00044mol) in toluene (50ml) was mixed with 1ml (0.006mol, an excess) of $Me_3SiC_5H_5$ in toluene (5ml) and the reaction mixture was refluxed for 48hr. During the reflux period a black precipitate formed, and the solution darkened. The toluene was then removed under reduced pressure, and the resultant residue was extracted with pentane (2 x 30ml). The combined extracts were concentrated to ca. 10ml. Cooling of the extract to -70°C produced a dark blue microcrystalline solid which was identified as $[(C_5Me_5)_2Yb]_2[(Me_3SiC_5H_4)_2Co_3(CO)_4]$ by its ir in Nujol. The infrared spectrum of the residue which did not extract into pentane exhibited bands due to $[(C_5Me_5)_2Yb]_2[(Me_3SiC_5H_4)_2Co_3(CO)_4]$.

Reaction of $[(C_5Me_5)_2Yb^+]_2[(Me_3SiC_5H_4)_2Co_3(CO)_4{}^{2-}]$ with H_2O in the Presence of H_2

$[(C_5Me_5)_2Yb(III)]_2[(Me_3SiC_5H_4)_2Co_3(CO)_4]$ (0.30g, 0.00021mol) in toluene (30ml) was reacted with 1ml of H_2O under an atmosphere of H_2. The

reaction mixture was stirred for 12hr. During the course of the reaction the toluene layer turned bright green, and the H_2O layer was milky white with precipitate. Anhydrous $MgSO_4$ was added ot the mixture in air. The toluene layer was then decanted, and the toluene was removed under reduced pressure. The residue was then dissolved in pentane (10ml). The pentane solution was then concentrated to ca. 5ml, and cooling to -70°C produced green prisms. Ir (Nujol): 1775s, 1760s, 1352m, 1300w, 1243m, 164m, 1035m, 1020wsh, 898m, 835s, 755w, 720w, 695w, 638w, 627w, 590w, 540w, 520w cm^{-1}. ^1H NMR: δ-0.08(9H); 1.24(15H); 4.74 (apparent triplet J=2Hz, 2H); 5.04 (apparent triplet J=2Hz). $^{13}C\{^1H\}$NMR: δ0.33($\underline{Me}_3Si$); 8.64($\underline{Me}_5C_5$); 84.79; 86.04; 94.72; 96.32. The above spectra are consistent with the compound being $(Me_3SiC_5H_4)(C_5Me_5)Co_2(\mu_2\text{-}CO)_2$.

The second crop of crystals contained the above compound as well as a compound with the following ir absorptions: 2025w,1966m,1795s,1775w, 1760cm^{-1}, and the peaks due to $(Me_3SiC_5H_4)(C_5Me_5)Co_2(\mu\text{-}CO)_2$. The ^1H NMR spectrum contained absorptions at δ 0.04(9H); 4.46 (apparent triplet J=2Hz, 2H); 4.87 (apparent triplet J=2Hz, 2H). The data are consistent with the presence of $(Me_3SiC_5H_4)_2Co_2(CO)_2$.[11] The two peaks at 2025 cm^{-1} and 1966 cm^{-1} are due to a small amount of $Me_3SiCo(CO)_2$. Finally, a solution ir study (pentane) of the residue from the mother liquor from the second crop of crystals showed bands at 2025s, 1968s, 1799m, 1776m, 1760w cm^{-1}. The ^1H NMR spectrum shows weak peaks due to the compounds described above as well as peaks due to $Me_3SiC_5H_4Co(CO)_2$ at δ.103(9H); 4.45 (apparent triplet J=2Hz, 2H); 4.70 (apparent triplet J=2Hz).

Reaction of $[(C_5Me_5)_2Yb(III)]_2[(Me_3SiC_5H_4)_2Co_3(CO)_4]$ with H_2

The compound $(C_5Me_5)_2Yb(III)]_2[(Me_3SiC_5H_4)_2Co_3(CO)_4]$ (0.30g, .00021mol) in toluene (30ml) was placed into a thick walled glass pressure bottle, and pressurized with H_2 (18atm) at 100°C for two weeks. During this time the solution turned green, and copious quantities of a black precipitate formed. The toluene solution was filtered, and the filtrate was evaporated to dryness. The residue was dissolved in pentane (10ml), and the solution was concentrated to ca. 1ml. Cooling to -70°C yielded green prisms. Ir (Nujol): 1750s, 1360m, 1150m, 1070w, 1022m, 720w, 633w, 590w, 545w, 525w, 420w, 405m cm^{-1}. ^1H NMR: δ1.41 (singlet). $^{13}C\{^1H\}$NMR: δ8.83($\underline{Me}_5C_5$); 94.57($Me_5\underline{C}_5$). Ms m/e 444$[(C_5Me_5)Co(CO)^+]$amu; m/e 194$[(C_5Me_5)Co^+]$amu. As a control experiment, $[(C_5Me_5)_2Yb(III)]_2[Me_3Si(C_5H_4)Co_5(CO)_4]$ (0.30g, .00021mol) in toluene (20ml) was placed into a glass pressure bottle and pressurized with argon to 18atm, and heated to 100°C for 2 weeks. The toluene was then removed under reduced pressure and the ir spectrum of the residue revealed that it was unreacted starting material.

Reaction of $(C_5Me_5)_2Yb{\cdot}OEt_2$ with Acetylmanganesepentacarbonyl

Bis(pentamethylcyclopentadienyl)ytterbium(II) diethyletherate (0.42g, 0.00081mol) in toluene (40ml) was reacted with acetylmanganese-pentacarbonyl (0.21g, 0.00084mol) in toluene (20ml). The reaction mixture turned deep red upon mixing. The solution was stirred for 12hr, filtered, and the filtrate was concentrated to ca. 30ml. Cooling the solution to -10°C overnight produced red-brown prisms which were isolated and dried under reduced pressure. Mp 140-145°C (dec). Anal.

Calcd. for $C_{26}H_{33}O_6MnYb$: C, 46.6; H, 4.96. Found: C, 45.7; H, 4.32. Ir (Nujol): 2725w, 2120m, 2076m, 2062m, 2042m, 2010m, 2000m, 1970vsbr, 2045vs, 1922s, 1768w, 1585vs, 1545s, 1485m, 1395s, 1332m, 1100m, 1075m, 1015w, 965w, 930m, 722m, 650ssh, 633vs, 617ssh, 579m, 550w, 502w, 470m, 443m, 400m, 380w, 340w, 307s, 298sh cm^{-1}.

Reaction of $(C_5Me_5)_2Yb{\cdot}OEt_2$ with $MeMn(CO)_5$ Under CO

Bis(pentamethylcyclopentadienyl)ytterbium(II) diethylether (0.49g, 0.00095mol) was dissolved in 40ml of toluene and a stream of carbon monoxide was passed throught the solution for ca. 1 min. In a separate flask, (0.20g, 0.00095mol) of methylmanganesepentacarbonyl was dissolved in 20ml of toluene and a stream of carbon monoxide gas was passed through the solution for ca. 1 min. The solution containing the ytterbium complex was then added to the $MeMn(CO)_5$ under a blsnket of CO. The reaction mixture turned dark red immediately. The solution was stirred overnight, and then filtered, and the filtrate was concentrated to ca. 30ml and then cooled to -10°C. The dark brown-red prisms were collected and dried under recuded pressure. Mp 185°C (dec). Anal. Calcd. for $C_{31}H_{43}O_7MnYb$: C, 49.3; H, 5.69. Found: C, 49.4; H, 5.27. Ir (Nujol): 3185w, 2725w, 2005s, 1970brvs, 1945brs, 1590vs, 1485s, 1332m, 1125m, 1020m, 734m, 795w, 722m, 688w, 640ssh, 632s, 616s, 577s, 550msh, 501w, 465m, 430m, 413w, 380m, 340w, 306s cm^{-1}. ^1H NMR (C_6D_6): δ1.36 ($\nu_{1/2}$=64Hz, 3H), 7.97 ($\nu_{1/2}$=110Hz, 30H). When a sample of the compound was hydrolyzed with D_2O, and extracted with C_6D_6 and ^1H NMR specrtum of the extract revealed C_5Me_5D and $C_4H_{10}O$ in a 2:0.2 ratio.

Reaction of $(C_5Me_5)_2Yb{\cdot}OEt_2$ with $(C_5H_5)_2Ni_2(\mu\text{-}CO)_2$

Bis(pentamethylcyclopentadienyl)ytterbium(II) diethylether (0.69g, 0.0013mol) in toluene (30ml) was added to cyclopentadienylnickelcarbonyl dimer (0.20g, 0.00066mol) in toluene (20ml). The reaction mixture was stirred for ca. 10hr. The toluene was removed under reduced pressure and the black residue was then dissolved in ca. 30ml of diethylether. The ether solution was filtered, and the filtrate was concentrated to ca. 15ml and cooled to -10°C overnight. The green-black plates were isolated and dried under reduced pressure. Anal. found: C, 48.4; H, 5.71. Ir (Nujol): 3390w, 2725w, 2000s, 1875m, 1855m, 1832s, 1815m, 1735w, 1645sbr, 1258w, 1160w, 1017m, 783s, 725w, 630brm cm^{-1}. When this reaction was caried out under an atmosphere of carbon monoxide, the reaction mixture turned dark red, and the only product that was isolated was a red powder from pentane. The infrared spectrum of this compound had extremely broad peaks and was totally uninformative.

$[(C_5Me_5)_2Yb][(C_5H_5)Co(\mu\text{-}CO)PMe_3]_2$

Cyclopentadienylcobaltcarbonyltrimethylphosphine (0.52g, 0.0023mol) was dissolved in toluene (ca. 20ml) and the resultant solution added to a toluene solution (ca. 30ml) (1.2g, 0.0023mol) of bis(pentamethylcyclopentadienyl)ytterbium diethyletherate. The reaction mixture was heated to 80°C for 8hr. The solution was allowed to cool to room temperature, filtered, and the filtrate was concentrated to ca. 10ml and cooled to -10°C. The dark green crystals were collected and dried under reduced pressure to give 0.87g of product (84% yield based upon $(C_5H_5)Co(CO)PMe_3$). Anal. Calcd. for $C_{38}H_{58}Co_2O_2P_2Yb$: C, 50.7; H, 6.50. Found: C, 50.7; H, 6.45. ^1H NMR (C_6D_6, 30°C): δ1.05 (d, J_{P-H}=9.3Hz, 18H); δ2.23 (s, 30H); δ4.72 (s, 10H). Ir (Nujol): 3100w,

2720w, 1923m, 1866vs, 1837vs, 1406w, 1345w, 1300w, 1282m, 1278m, 1105m, 1007m, 979m, 948s, 935ssh, 890w, 847m, 830w, 791s, 730ssh, 722s, 688m, 673sm 569s, 480m, 455w, 398m, 362m, 323m, 260s, 215w cm^{-1}. A sample of the complex was dissolved in C_6D_6 and hydrolyzed. The ^1H NMR spectrum of the C_6D_6 solution revealed the presence of $(C_5H_5)Co(CO)PMe_3$ δ4.63(s,5H); δ0.96 (d, J_{P-H}=9.1Hz, 18H) and C_5Me_5H in a 1:1 ratio.

$[(C_5Me_5)_2Yb][HCo(\mu\text{-}CO)(PMe_3)_3]_2$

Bis(pentamethylcyclopentadienyl)ytterbium diethyletherate (0.19g, 0.00038mol) in toluene (10ml) was reacted with hydridocobalt tris(trimethylphosphine)carbonyl (0.12g, 0.00038mol) in toluene (20ml). The reaction solution turned brown-orange upon mixing. The solution was stirred for ca. 10hr, and then filtered. The filtrate was concentrated to ca. 5ml and cooled to -10°C overnight. Green prisms were collected and dried under reduced pressure. A second crop of crystals was obtained by concentrating the mother liquors to ca. 1ml and cooling to -10°C. The combined yield was 85% based upon $HCo(CO)(PMe_3)_3$. Anal. Calcd. for $C_{40}H_{86}P_6O_2Co_2Yb$: C, 44.7; H, 8.06. Found: C, 44.2; H, 7.49. ^1H NMR, (C_7D_8, -78°C): δ2.64 (broad singlet, 30H), δ0.99 (broad singlet, 54H). ^{31}P NMR C_7D_8 -70°C: δ5.23 (broad singlet). Ir (Nujol): 2720w, 1913s, 1833m, 1795vs, 1420m, 1301wsh, 1294s, 1278s, 1150brw, 1015w, 957s, 930vs, 840m, 712s, 670msh, 661s, 583w, 480w, 365s, 260m cm^{-1}.

$[(C_5Me_5)_2Yb][MeCo(\mu_2\text{-}CO)(PMe_3)_3]$

Bis(pentamethylcyclopentadienyl)ytterbium diethyletherate (0.37g, 0.00073mol) in toluene (10ml) was added to methylcobaltcarbonyl

tris(trimethylphosphine) (0.24g, 0.00073mol) in toluene (10ml). The reaction mixture immediately turned orange-green. The solution was stirred for ca. 12hr. The reaction mixture was filtered, and the filtrate was concentrated to ca. 5ml and cooled to -10°C. Green prisms were isolated and dried under reduced pressure to give 0.4g of product(71%). Anal. Calcd. for $C_{31}H_{60}OP_3CoYb$: C, 48.1; H, 7.82. Found: C, 47.8; H, 7.83. Ir (Nujol): 2720w, 1900s, 1795s, 1417s, 1305m, 1293s, 1276s, 1145brs, 1017w, 930s, 845m, 713s, 702s, 665msh, 657s, 565m, 360s, 275m cm^{-1}. ^1H NMR (C_7D_8) 25°C: δ-0.45 (q, $^3J_{P-H}$=14.3Hz, 3H); δ1.08 (m, 27H); δ2.30 (s, 30H). Some samples may contain excess PMe_3. ^{31}P NMR (C_7D_8) -83°C: δ1.25 (broad singlet).

Reactions of $[(Me_3Si)_2N]_2Yb(OEt_2)_2$ with Transition Metal Carbonyl Complexes

Reaction of Bis(hexamethyldisilylamido)ytterbium diethyletherate with the transition metal carbonyl complexes $Mo(CO)_6$, $Co_2(CO)_8$, $Mn_2(CO)_{10}$, and $Fe_3(CO)_{12}$ produced $Yb[N(SiMe_3)_2]_3$ as the only isolable product. The residues from the reactions contained products having Yb-O-C-M interactions, but attempts to crystallize these materials were unsuccessful. Reaction of $[(Me_3Si)_2N]_2Yb\cdot(OEt_2)_2$ with $C_5H_4Fe(CO)_2I$ resulted in the formation of a red precipitate and a red solution in toluene. The red solid had an ir spectrum similar to $[C_5H_5Fe(CO)_2]_2 \cdot 2Yb(C_5Me_5)_2I$, and the red solution contained $[C_5H_5Fe(CO)_2]_2$. Recrystallization of the red ppt from THF gave yellow crystals of $YbI_3\cdot(THF)_x$.

$[(C_5Me_5)_2Yb][(C_5H_5)Mn(CO)_3]$

Bis(pentamethylcyclopentadienyl)ytterbium diethyl ether (0.44g, 0.00085mol) in toluene (30ml) was added to cyclopentadienylmanganese tricarbonyl (0.17g, 0.00083mol) in toluene (20ml). Upon mixing a green precipitate formed while the solution remained dark green. The mixture was stirred overnight and the green solution was filtered from the green precipitate. The green solid was dissolved in ca. 40ml of toluene. The toluene solution was filtered and combined with the green reaction liquors. The combined extracts were then concentrated to ca. 40ml and cooled to -10°C. The green hair-like needles were collected and dried under reduced pressure. A second crop of crystals was grown by concentrating the mother liquors to ca. 10ml and cooling to -10°C. The combined yield was ca. 0.25g, 80%. Anal. Calcd. for $C_{28}H_{35}O_3MnYb$: C, 51.9; H, 5.40. Found: C, 48.7; H, 5.55. Ir (Nujol): 3070m, 2725w, 2010vs, 1941vs, 1925ssh, 1905vs, 1883vs, 1856vs, 1160brw, 1060w, 1010m, 845s, 728w, 695w, 668vs, 637vs, 558m, 537s, 518m, 505m, 375m, 310msh, 270s cm^{-1}.

$[(C_5Me_5)_2Yb][(MeC_5H_5)Mn(CO)_3]$

Bis(pentamethylcyclopentadienyl)ytterbium diethylether (0.65g, 0.0013mol) in toluene (ca. 30ml) was reacted with methylcyclopentadienyl manganese tricarbonyl (0.28g, 0.0013mol) in toluene (10ml). The reaction mixture was perceptibly darker in color than the original solution of $(C_5Me_5)_2Yb{\cdot}OEt_2$. The solution was stirred overnight, and then concentrated to ca. 20ml and the concentrate was cooled to -10°C. The combined yield was 0.36g, 65% (based upon the manganese compound). Anal. Calcd. for $C_{29}H_{37}O_3MnYb$: C, 52.6; H, 5.59. Found: C, 49.06; H, 5.26. Ir (Nujol): 3050w, 2710w, 2010s, 1954s, 1932vs, 1907m, 1870m,

1840sbr, 1140vw, 1020w, 835wbr, 715w, 661m, 630m, 528w, 500w, 379w, 305m, 295m, 260w cm^{-1} ^1H NMR δ1.50(s); 2.29(s); 4.01(m); 4.05(m). Due to observation of large amounts of decomposition products, the integration of the above spectrum is meaningless.

Reaction of $(C_5Me_5)_2Yb^{\cdot}OEt_2$ with $(C_5H_5)Co(CO)PPh_3$

Bis(pentamethylcyclopentadienyl)ytterbium diethylether (0.82g, 0.0016mol) in toluene (40ml) was added to cyclopentadienyl cobalt carbonyl triphenyl phosphine in toluene (20ml). There was no visible reaction in 12hr. Heating the solution to 90° for 12hr caused the solution to turn dark brown. The solution was cooled to room temperature, and filtered. Attempts to grow crystals from toluene were unsuccessful. The toluene was then removed under reduced pressure, and the red-brown residue was extracted into ca. 30ml of diethylether. The ether solution was concentrated to ca. 15ml and cooled to -10°C. Small red prisms were collected and dried under reduced pressure. Anal. found: C, 67.3; H, 5.19. Ir (Nujol): 3070W, 3050w, 2720w, 1933s, 1844vs, 1800msh, 1665w, 1606vs, 1434s, 1305w, 1181w, 1155w, 1110w, 1088s, 1010w, 995w, 790m, 740m, 723w, 691s, 674s, 565w, 529s, 507s, 448w, 420w, 330w, 260w cm^{-1}.

Chapter 2

$[(C_5Me_5)_2Ybbipy]^+[I]^-$

Bis(pentamethylcyclopentadienyl)ytterbium bipyridine, (0.76g, 0.0013mol) in toluene (15ml), was reacted with AgI (0.30g, 0.0013mol) for 24hr. The resultant brown microcrystalline precipitate was isolated by filtration, and washed with pentane (2 x 10ml). The precipitate was then dissolved in CH_2Cl_2 (ca. 10ml), and the CH_2Cl_2 solution was filtered from silver metal formed in the reaction. Pentane (ca. 40ml) was carefully layered onto the CH_2Cl_2 solution, and diffusive mixing of the pentane and CH_2Cl_2 at room temperature resulted in a quantitative yield of brown plates. Mp 125°-130°C (dec). Anal. Calcd. for $C_{30}H_{38}IN_2Yb$; C, 49.6; h, 5.27; I, 17.5; N, 3.85; Found: C, 47.9; H, 5.23; I, 16.7; N, 3.63. Ir (Nujol): 3040w, 2620w, 1595s, 1560w, 1432vs, 1308s, 1275w, 1167w, 1150m, 1092w, 1058w, 1016s, 770s, 734m, 718w, 644w, 627w, 585w, 420w, 380w, 312s cm^{-1}.

Reduction of $[(C_5Me_5)_2Ybbipy]^+[I]^-$

Bis(pentamethylcyclopentadienyl)ytterbium(III) bipyridineiodide (0.17g, 0.00023mol) in THF (50ml) was reacted with excess sodium amalgam. The reaction turned dark brown and the reaction mixture was stirred for 12hr. The THF was then removed under reduced pressure, and the brown residue was then extracted with hexane (30ml), then filtered. The hexane was then removed from the filtrate under reduced pressure to yield a brown microcrystalline solid which was identified as Bis(Pentamethylcyclopentadienyl)ytterbium bipyridine by its ir spectrum and its melting point.[12]

$[(Me_5C_5)_2Ybbipy]^+[(Me_5C_5)_2YbCl_2]^-$

The THF adduct of Bis(Pentamethylcyclopentadienyl)ytterbium chloride (0.23g, 0.00042mol) was dissolved in ca. 20ml of toluene and was added to 2,2'-bipyridine (0.03g, 0.00019mol) in 10ml of toluene. A reaction occurred immediately forming a brown microcrystalline precipitate. After stirring the reaction for 20min, the precipitate was allowed to settle, and the supernatent liquid was discarded. The residue was washed with toluene (2 x 10ml), and dissolved in dichloromethane ca. 5ml. Pentane (ca. 50ml) was carefully layered onto the CH_2Cl_2 solution. Diffusive mixing over the course of 3 days resulted in an essentially quantitative yield. Mp 264-266°C(dec). Anal. Calcd. for $C_{50}H_{68}Cl_2N_2Yb_2$: C, 53.9; H, 6.15; Cl, 6.36; N, 2.51; Found: C, 53.85; H, 6.07; Cl, 5.55; N, 2.50. The compound has a conductivity [Λ) of 11.2 $\Omega^{-1}cm^2\ mol^{-1}$ in CH_3CN solution. Ir (Nujol): 3060w, 2620w, 1598s, 1570w, 1489m, 1435vs, 1312s, 1230w, 1175vw, 1159w, 1126w, 1100w, 1058w, 1033w, 1018s, 799w, 766vs, 733m, 717W, 647w, 631w, 613vw, 586w, 415w, 380w, 370w, 291s, 275m, 232s cm^{-1}. ^1H NMR ($CDCl_3$ 28°C): δ8.00 (2H); 15.82 (2H): 3.23 (30H); 1.43 (30H); -1.91 (2H). The remaining proton in the bipyridine ring was not located.

$[(C_5Me_5)_2Ybbipy]^+[Co(CO)_4]^-$

Bis(Pentamethylcyclopentadienyl)ytterbiumbipyridine, (0.49g, 0.00082mol) in toluene ca. 30ml was added to $Co_2(CO)_8$ (0.14g, 0.00041mol)in toluene (20ml) at room temperature. Upon mixing, a rust red microcrystalline precipitate slowly formed. After stirring overnight the solid was isolated, washed with pentane (3 x 20ml), and dried under reduced

pressure to give a quantitative yield of red-brown microcrystals. Anal. Calcd. for $C_{34}H_{38}N_2O_4CoYb$; C, 53.0; H, 4.97; N, 3.63; Found: C, 50.8; H, 4.83; N, 3.62. Mp 183-186°C(dec). Ir (Nujol): 3070w, 2625w, 1885vvs, 1596s, 1570w, 1490m; 1435vs, 1322s, 1175m, 1160m, 1120w, 1105w, 1060w, 1043w, 1021m, 1013m, 969w, 898w, 762vs, 735m, 720w, 650w, 632w, 595w, 560vs, 430w, 390w, 320s cm^{-1}.

$[(C_5Me_5)_2Yb]_2$4,4'-Bipyridine

A solution of 4,4' bipyridine (0.07g, 0.00047mol) in THF (20ml) was added to bis(pentamethylcyclopentadienyl)ytterbium diethyletherate (0.49g, 0.00094mol) in THF (20ml). Upon addition of the 4,4' bipyridine, the reaction mixture turned from red to dark blue-green. After ca. one minute of reaction, a purple powder began to precipitate from solution, and the mixture was stirred for 12hr. The THF solution was filtered away from the purple precipitate. Concentration of the THF filtrate to ca. 30ml and cooling it to -10°C produced a purple powder. The purple powder was collected and dried under reduced pressure. It is insoluble in aromatic and aliphatic hydrocarbons and diethyl ether, though it reacts with CH_2Cl_2, and acetone. It was characterized only by its ir spectrum (Nujol): 2720w, 2540w, 1595vs, 1550vs, 1495s, 1346s, 1287w, 1260w, 1217vs, 1195vs, 1162w, 1093w, 1065w, 1048w, 1014vs, 971vs, 960vs, 922msh, 798m, 777m, 750w, 723w, 705w, 695w, 685w, 665w, 611s, 590w, 505w cm^{-1}.

$[(Me_3Si)_2N]_2Yb$ (bipyridine)

Bipyridine (0.12g, 0.00077mole) in toluene (10ml) was added to a solution of $[(Me_3Si)_2N]_2Yb(OEt_2)_2$ (0.50g, 0.00077mol) in toluene

(30ml). The reaction mixture immediately turned a very dark brown-yellow color. The solution was stirred for 20hr, and the toluene was removed under reduced pressure leaving a dark green-black residue. The residue was dissolved in 75ml of pentane, the pentane solution was filtered, and the filtrate concentrated to ca. 20ml and cooled to -20°C. The dark purple needles were collected and dried under reduced pressure to give 0.40g of product, 80% yield. Anal. Calcd. for $C_{22}H_{44}N_4Si_4Yb$: C, 40.7; H, 6.82; N, 8.62. Found: C, 40.8; H, 6.65; N, 8.49. Ir (Nujol): 1596w, 1495m, 1435m, 1365w, 1292w, 1245s, 1148m, 1079msh, 1065s, 985s, 945s, 876msh, 866s, 840sh, 822s, 770w, 753s, 722m, 688w, 662m, 604w, 442w, 382w, cm^{-1}. ^1H NMR (30°C, C_6D_6): δ0.837 ($\nu_{1/2}$=12Hz, 2H): δ1.16($\nu_{1/2}$=10Hz, 2H): δ10.26($\nu_{1/2}$=59Hz, 36H). the remaining protons in the bipyridine rings were not located.

$[(C_5Me_5)_2Yb]_2$(bipyrimidine)·(toluene)

Bis(pentamethylcyclopentadienyl) ytterbium diethyletherate (1.2g, 0.0022mol) in 60ml toluene was added to 2,2'bipyrimidine (0.18g, 0.0011mol) in toluene (50ml). The reaction mixture immediately turned dark-red brown. After stirring for 12hr, a red-brown crystalline precipitate had separated from the reaction mixture. The solution was filtered and the filtrate was concentrated to ca. 50ml. Cooling to -10°C afforded black-brown needles which were collected and dried under reduced pressure. The mother liquors were concentrated to ca. 20ml and cooled to -10°C producing a second crop of crystals. A third crop may also be obtained, and the red-brown precipitate from the original reaction mixture may also be crystallized from toluene to give product. The total yield was 1.1g, 90%. Mp 305-308°C. Anal. Calcd.

for $C_{55}H_{73}N_4Yb_2$: C, 58.1; H, 6.48; N, 4.93. Found: C, 58.0; H, 6.81; N, 5.01. Ir (Nujol): 2725w, 2670w, 2480w, 1735w, 1672w, 1635w, 1605msh, 1589vs, 1555w, 1365vs, 1270vs, 1160w, 1091s, 1040vs, 946m, 725m, 693m, 675s, 618s, 587w, 460w, 385m, 303s, 242w cm^{-1}. Ms(E.I., 70 E.V.) 1044 M^+, 910$(M-C_5Me_5)^+$, 775$(M-2C_5Me_5)^+$, 641$(M-3Me_5C_5)^+$, 507$(M-4Me_5C_5)^+$, 467$(C_5Me_5Ybbpm)^+$, 443$(C_5Me_5)_2Yb)^+$.

$(C_5Me_5)_4Yb_3(C\equiv C-Ph)_4$

Phenylacetylene (0.23g, 0.0022mol) in toluene (10ml) was added to a solution of $(C_5Me_5)_2Yb\cdot OEt_2$ (0.86g, 0.0017mol)in toluene (20ml) at room temperature. The mixture slowly turned red over a period of 24hr. The reaction mixture was then filtered, and the filtrate concentrated to ca. 5ml under reduced pressure. cooling to -10°C afforded red needles of product in 52% yield. More product may be obtained by adding ca. 10ml of pentane to the mother liquors and cooling them to -70°C. Mp 275-278°C. Anal. Calcd. for $C_{72}H_{80}Yb_3$: C, 59.1; H, 5.50. Found: C 59.3; H, 5.51. ^1H NMR (26°C, C_6D_6): δ3.49($\nu_{1/2}$=25Hz, 30H); δ10.55($\nu_{1/2}$=20Hz, 1H); δ12.69($\nu_{1/2}$=20Hz, 2H) δ25.47($\nu_{1/2}$=21Hz, 2H). Ir (Nujol): 3076w, 3047w, 2718w, 2040m, 1593w, 1571w, 1483m, 1441w, 1193m, 1070w, 1023m, 917w, 756s, 729m, 690s, 542m, 502m, 388m, 310s cm^{-1}.

$[(C_5Me_5)Eu(C\equiv CPh)(THF)_2]_2$

Bis(pentamethylcyclopentadienyl)europium diethyletherate (0.76g, 0.0015mol) was dissolved in toluene (30ml). To this solution was added phenylacetylene (0.26ml, 0.0015mol). The reaction mixture was stirred for ca. 20hr. During this time a yellow-orange solid precipitated from the reaction mixture. The supernatent solution was then removed by

filtration and discarded. and the solid was washed with pentane (3x10ml), and the washings were discarded. The solid was dissolved in THF (40ml) and filtered. Concentration of the filtrate to ca. 20ml and cooling to -10°C produced orange prisms in 47% yield. Anal. Calcd. for $C_{26}H_{36}O_2Eu$; C, 58.64; H, 6.81. Found: C, 43.36; H, 5.73. Ir (Nujol): 3070wsh, 3050w, 2715w, 2025w, 1593s, 1568m, 1482s, 1290w, 1189s, 1171m, 1066m, 1035vs, 995w, 905msh, 890s, 758vs, 752ssh, 720w, 693vs, 665w, 660w, 619w, 532m, 480m, 355w, 285s, 275msh, 252vs, 240msh, 230w cm^{-1}. The proton NMR spectrum of a hydrolyzed sample of the compound revealed the presence of C_5Me_5H, THF and phenylacetylene in a 1:2:1 ratio.

Chapter 3

$[(Me_3Si)_2N]_2Yb(OEt_2)_2$

Sodium hexamethyldisilylamide (2.56g, 0.0140mol) in diethyl ether (150ml) was cooled to 0°C and added to a slurry of YbI_2 (3.18g, 0.00745mol) in diethyl ether (50ml) at 0°C. The reaction mixture was stirred at 0°C for 1hr. The reaction mixture consisted of a blue-green solution above a yellow-green precipitate. The reaction was then allowed to warm to room temperature which caused it to turn light orange. The reaction was stirred at room temperature for 3hrs. The light orange ether solution was filtered and the filtrate concentrated to ca. 30ml. Cooling of the concentrate to -70°C overnight afforded large prisms of product which are yellow at -70°C and orange at room temperature.[13] A second crop of crystals may be grown from the mother liquors at -70°C to give a combined yield of 3.2g (71%). This reaction must be run with a small exess of YbI_2. If it is not, then even small amounts of excess $NaN(SiMe_3)_2$ will catalize another reaction which results in as yet uncharacterized products. If this occurs, then yields of the desired $[(Me_3Si)_2N]_2Yb(OEt_2)_2$ may be as low as 2%.

$\{[(Me_3Si)_2N]_2Yb\}_2$

Bis(Hexamethyldisilylamido)ytterbium bisdiethyletherate (1.02g; 0.00159mol) was dissolved in 20ml of toluene. The red solution was heated to 80° for 2hr, and then the toluene was then removed under reduced pressure while maintaining the solution at 80°C. The bright red-orange residue was then extracted with pentane (40ml), and the pentane solution was filtered and concentrated to ca. 10ml and cooled to

-20°C. Bright red-orange needles were collected and dried under reduced pressure. The mother liquors were concentrated to ca. 1ml and cooled to -20°C to produce a second crop of crystals in a combined yield 0.60g, 76%. If the residue obtained from the removal of the toluene is a solid, and not an oil, then a quantitative yield of product may be obtained as an orange microcrystalline powder by total removal of pentane from the pentane extract of this solid. M.P. 150-153°C. Ir (Nujol); 1250s, 1175w, 1020s, 930s, 875s, 820s, 755s, 660s, 605msh, 595s, 410s, 390msh, 375s, 362ssh, 285w, 245w cm^{-1}. Anal. Calcd. for $C_{12}H_{36}N_2Si_4Yb$: C, 29.2; H, 7.35; N, 5.67. Found: C, 27.4; H, 7.19; N, 4.85. ^1H NMR (31°C, C_6H_6), δ0.341(s). ^{13}C NMR, δ6.47. Ms 988[M^+], 828[$M-N(SiMe_3)_2]^+$, 494[$M-2N(SiMe_3)_2]^+$, 479[$Yb[N(SiMe_3)_2]_2^-Me]^+$, 334[$YbN(SiMe_3)_2]+$.

$[Yb(THF)_3][(\mu_2-CO)_2W(CO)(C_5H_5)]_2$

Bis(hexamethyldisilylamido)ytterbium bis(diethylether) (0.34g, 0.00053mol) in toluene (10ml) was added to cyclopentadienyltungsten tricarbonylhydride (0.35g, 0.0010mol) in toluene (30ml). A yellow precipitate formed immediately. The reaction mixture was stirred for 1 hr, and then the toluene was removed under reduced pressure. The yellow solid was dissolved in ca. 20ml of THF, and the THF solution was concentrated to ca 2ml. Cooling of the THF concentrate to -20°C afforded bright yellow prisms. The yellow prisms were collected, and dried under reduced pressure which caused them to become opaque and crumble into powder. Addition of hexane(5ml) to the mother liquors resulted in precipitation more microcrystalline product. The combined yield was 0.41g, 73%. Anal. Calcd. for $C_{28}H_{34}O_9W_2Yb$: C, 31.87; H,

3.25. Found: C, 31.63; H, 3.25. Ir (Nujol): 3775w, 3630w, 3080w, 1895s, 1755vs, 1675vs, 1420w, 1350w, 1295w, 1175w, 1103w, 1080s, 1007m, 955w, 913m, 873s, 837w, 818w, 794s, 720w, 616s, 601s, 557m, 516s, 509msh, 494s, 330m cm^{-1}.

$\{(Me_5C_5)Yb[N(SiMe_3)_2]\}_2$

Pentamethylcyclopentadiene (0.20ml, 0.0013mol) in toluene (20ml) was added to bis(hexamethyldisilylamido)ytterbium (0.63g, 0.0013mol) in toluene (40ml). The reaction mixture turned dark red over a period of 1hr. The solution was stirred for 12hr, was filtered, and the filtrate was then concentrated to ca. 40ml and cooled to -10°C. The large red octahedra were isolated and dried under reduced pressure to give 0.28g of product (46% yield). Mp 315-320°C(dec). Anal. Calcd. for $C_{16}H_{33}NSi_2Yb$: C, 41.0; H, 7.10; N, 2.99. Found: C, 36.73; H, 6.81; N, 2.30. Ir (Nujol): 2725w, 1250s, 1050w, 1003vs, 854s, 826vs, 809s, 759m, 732s, 690w, 663m, 614w, 585w, 567m, 394s, 360m, 260s, 240s, 218m cm^{-1}. ^1H NMR (C_6D_6, 31°C, 200MHz) δ0.090 (s, H); δ0.228(s, H); δ2.07 (s, H); δ2.11 (s, H). When a sample of the compound was hydrolized, a C_6D_6extract of the hydrosylate had the following NMR spectrum at room temperature: δ0.081 (s, 18H); δ0.970 (t, $^3J_{H-D}$=1.1Hz,3H) δ1.73 (s, 6H); δ1.78(s, 6H) which is the spectrum of a 1:1 mixture of C_5Me_5D and $DN(SiMe_3)_2$.

$(C_5Me_5)[(Me_3Si)_2N]Yb$ dmpe (dmpe=1,2-Bis(dimethylphosphino)ethane)

1,2 Bis(dimethylphosphino)ethane (0.10ml, 0.09g, 0.00060mol) was added a solution of Pentamethylcyclopentadienyl ytterbium hexamethyldisilylamide (0.28g, 0.0060mol) in toluene (30ml). The solution immediately turned

dark purple. The reaction mixture was stirred for 1hr, filtered, and the filtrate concentrated to ca. 5ml and cooled to -10°C for 2 days. The large purple prisms were isolated and dried under reduced pressure. The mother liquors were concentrated to ca. 1ml and cooled to -20°C to produce a second crop of crystals. The total yield was 0.35g, 95%. Mp 226-229°C. Anal. Calcd. fo $C_{22}H_{49}NP_2Si_2Yb$: C, 42.7; H, 7.98; N, 2.26; P, 10.01. Found: C,41.5; H,8.00; N,2.08; P,8.23. ^1H NMR (C_6D_6, 31°C) δ0.30 (s, 18H); δ0.733 (s, 12H); δ0.966 (apparent t, separation = 6.3Hz, 4H); δ2.26 (s, 15H). $^{13}P\{^1H\}$ NMR, (C_6D_6, 30°C) δ-36.0 (broad singlet). Ir (Nujol): 2720w, 1417m, 1298w, 1283w, 1243s, 1230s, 1051s, 936m, 922m, 870s, 825sh, 812s, 758m, 742m, 719m, 690w, 657m, 600w, 585w cm^{-1}.

$(C_5Me_5)_2Yb[HN(SiMe_3)_2]$

Pentamethylcyclopentadiene (0.59ml, 0.68g, 0.0038mol) in pentane (10ml) was added to bis(hexamethyldisilylamido)ytterbium (0.93g, 0.0019mol) in pentane (30ml). The reaction mixture slowly darkened, and a red-orange microcrystalline precipitate formed in 15min. The reaction mixture was stirred for an additional 15hr. The red-orange precipitate had redissolved, and the reaction solution was orange-brown. The solution was filtered and the filtrate concentrated to ca. 7ml and cooled to -20°C. The green feathery needles were isolated and dried under reduced pressure. Another crop of crystals may be obtained from the mother liquors. Total combined yield was 0.56g, 49%. Mp Anal. Calcd. for $C_{26}H_{49}NSi_2Yb$: C, 51.6; H, 8.16; N, 2.31. Found: C, 50.6; H, 7.84; N, 2.16. Ir (Nujol): 3205s, 2725m, 1305w, 1265s, 1260s, 1250s, 1163s, 1156s, 1015m, 977m, 930m, 850vsbr, 797msh, 790wsh, 763s, 719w, 698s,

679wsh, 653s, 620m, 586m, 551s, 365sbr, 260s cm^{-1}. ^1H NMR (31°C, C_6D_6): δ0.087 (s, 18H); δ1.93 (s, 30H). $^{13}C\{^1H\}$ NMR (C_6D_6, 31°C): δ2.62($\underline{Me}_3Si$); δ10.72($\underline{Me}_5C_5$); δ113.82($\underline{C}_5Me_5$).

$(C_5Me_5)_2Yb$

Pentamethylcyclopentadiene (0.42ml, 0.36g, 0.0026mol) in toluene (20ml) was added to a solution of $\{[(Me_3Si)_2N]_2Yb\}_2$ (0.66g, 0.0013mol Yb) in toluene (20ml). The reaction mixture slowly turned dark red. After stirring for 24hr, the toluene was removed under reduced pressure leaving a solid green residue. The residue was dissolved in pentane (30ml) and the pentane solution was filtered. The filtrate was concentrated to ca. 10ml and cooling to -25°C afforded large green needles which crumbled and turned brown-green upon removal of solvent under reduced pressure. A second crop of crystals may be obtained from the mother liquors to give a combined yield of 0.45g, 78%. When heated in a sealed capillary, the compound gradually turns orange as the temperature is raised above 130° until it melts from 189-191°C to give a red liquid which turns green when it resolidifies at room temperature. Anal. Calcd. for $C_{20}H_{30}Yb$: C, 54.2; H, 6.82. Found: C, 53.8; H, 6.96. Ir (Nujol): 2725w, 1155w, 1015m, 792w, 718m, 665w, 584w, 352m, 274s cm^{-1}. ^1H NMR (C_6D_6, 30°C): δ1.92(s). ^{13}C NMR (C_6D_6, 30°C): δ10.61($\underline{Me}_5C_5$); δ113.43($\underline{C}_5Me_5$).

$\{(EtMe_4C_5)Yb[N(SiMe_3)_2]\}_2$

Tetramethylethylcyclopentadiene (0.22g, 0.0015mol) in pentane (10ml) was added to bis(hexamethyldisilylamido)ytterbium (0.72g, 0.0015mol) in pentane (30ml). The reaction mixture slowly turned dark red after the

addition of the diene. After stirring for 15hr the pentane solution was filtered and concentrated to ca. 10ml. The concentrated solution was cooled to -20°C overnight. The large red prisms were collected and dried under reduced pressure. The mother liquors were concentrated to ca. 2ml and cooled to -20°C to give a second crop of crystals. The total yield was 0.50g, 69%. Mp 252-255°C Anal. Calcd. for $C_{17}H_{35}NSi_2Yb$: C, 42.3; H, 7.31; N, 2.90. Found: C, 34.3; H, 7.50; N, 1.89. ^1H NMR (C_7D_8, 30°C, 200MHz) δ0.232 (s, 18H); δ1.02 (t, $^3J_{H-H}$=7.3Hz, 3H); δ2.05 (s, 6H); δ2.12 (s, 6H); δ2.55 (q, $^3J_{H-H}$=7.3Hz, 2H). Ir (Nujol): 2730m, 1375m, 1314w, 1260sh, 1243vs, 1125brw, 1062w, 1048w, 1013m, 948vsbr, 855vs, 825vsbr, 760s, 745s, 664s, 613m,584s, 402s, 353m, 305s, 268m, 240w cm^{-1}. Ms 816[$M-N(SiMe_3)_2^+$]; 804 [$M-C_5Me_4Et^+$]; 667{$Yb_2[N(SiMe_3)_2]_2^+$}; 655 [$(Yb_2(C_5Me_4Et)N(SiMe_3)_2)^+$].

Reaction of $EtMe_4C_5H$ with $\{[(Me_3Si)_2N]_2Yb\}_2$

a.) $(EtMe_4C_5)_2Yb\cdot OEt_2$

Tetramethylethylcyclopentadiene (0.89g, 0.0059mol) in pentane (20ml) was mixed with $[(Me_3Si)_2N]_2Yb]_2$ (1.46g, 0.0029mol) in pentane (20ml). The reaction solution slowly turned deep red. After stirring for 20hr, the solution was filtered and the filtrate concentrated to ca. 10ml. Cooling of the concentrate to -70° precipitated a green-black solid from solution. The solid was isolated, but melted into a black oil at room temperature. The oil was dissolved in diethyl ether (30ml) to give a bright green solution. The green ether solution was filtered and the filtrate concentrated to ca. 5ml. Cooling of the concentrate afforded green prisms, 0.50g, 37%. Mp. 161-165°C. Anal. Calcd. for $C_{26}H_{44}OYb$:

C, 57.2; H, 8.13. Found: C, 56.1; H, 7.92. Ir (Nujol): 2720w, 1305w, 1144m, 1070s, 1037m, 1012w, 920w, 832w, 715w, 420w, 350w, 300m, 267w, 240w cm^{-1}. ^1H NMR (C_6D_6, 30°C, 200MHz): δ0.914 (t, $^3J_{H-H}$ = 6.9Hz, 3H); δ1.189 (t, $^3J_{H-H}$ = 7.4Hz, 3H); δ2.105(2, 6H); δ2.150(s, 6H); δ2.550(q, $^3J_{H-H}$ = 7.4Hz, 2H); δ2.991(q, $^3J_{H-H}$ = 6.9Hz, 2H). ^{13}C NMR (C_6D_6, 30°C): δ11.046($C_5\underline{Me}_4Et$); δ11.277($C_5\underline{Me}_4Et$); δ12.881($Me_4C_5CH_2\underline{CH}_3$); δ16.547($O(CH_2\underline{CH}_3)_2$); δ19.754($C_5Me_4\underline{CH}_2Me$); δ66.257($O(\underline{CH}_2Me)_2$); 111.99 ($Me_4\underline{C}_4CEt$); 112.81($Me_4\underline{C}_4CEt$); 119.64($C_4C_4\underline{C}Et$).

b.) $(EtMe_4C_5)_2YbN(SiMe_3)_2$

The mother liquors from part a.) were evaporated to a dark red oil The dark red oil was heated to 145°C under vacuum (10^{-2}torr) for 12hr. During this time, a small amount of red material had sublimed up the walls of the flask. The sublimate and remaining resiude were dissolved in pentane (20ml). The pentane solution was concentrated to ca. 3ml and the concentrate was cooled to -70°C. The small purple prisms of product were isolated and dried under reduced pressure to give 0.44g, 24% yield. Mp. The compound darkens at 190°C, and melts from 235-245°C. Anal. Calcd. for $C_{28}H_{52}NSi_2Yb$: C, 53.2; H, 8.29; N, 2.21. Found: C, 50.94; H, 8.66; N, 1.84. Ir (Nujol) 2730w, 1604w, 1308w, 1250s, 1240s, 1150w, 1095w, 1045m, 1018w, 984vs, 866vs, 834s, 815s, 772s, 743m, 660s, 603s, 588w, 437m, 365s cm^{-1}. Ms. 632 (Me^+); 617($M-Me^+$); 483($M-C_5Me_4Et^+$); 471($M-N(SiMe_3)_2^+$). Parent ion simulation M/e, Calc. (found): 636, 5.01(5.13); 635, 15.47(14.78); 634, 42.98(42.04); 633, 39.15(38.39); 632, 100(100); 631, 65.30(69.23); 630, 67.03(70.18); 629, 36.88(44.20); 628, 7.36(12.70); 627, 0.10(6.11). There is some proton loss on fragmentation which causes the slightly high values of the

relative peak areas for the lower mass portion of the envelope.

Bis(Hexamethyldisilylamodoytterbium bis(trimethylaluminium)

Trimethyl Aluminium (1.38ml of a 1.6M solution, 0.0022mol) in pentane was added to Bis(hexamethyldisilylamido)ytterbium (0.55g, 0.0011mol) in pentane (20ml) at room temperature. The reaction mixture turned bright yellow instantaneously. The reaction mixture was stirred for one hour, and was filtered. The filtrate was concentrated ca. 5ml, and cooling of the concentrate to -20°C overnight afforded bright yellow plates which were collected and dried under a stream of N_2. The mother liquors were concentrated to ca. 1ml and cooled to -20°C to give a second crop of plates. The combined yield was 0.68g, 96%. Found: C, 31.9; H, 8.57; N, 3.41. Ir (Nujol): 2720w, 2640wBr, 1260s, 1250s, 1213m, 1187m, 880BrS, 832s, 774m, 755m, 728wsh, 675sBr, 615w, 530m, 505m, 442s, 360w cm^{-1}. ^1H NMR (30°C, C_7D_8) δ-0.250(s, 18H); δ0.278(s,36H). ^{13}C NMR (-75°C, C_7D_8) δ0.851(s), δ5.36(s). Ms(C.I.) 637(M^+-H), 550(M-H-$AlMe_4^+$), 492{$[(Me_3Si)_2N]_2Yb-H^+$].

Bis(hexamethyldisilylamido)ytterbium bis(triethylaluminium)

Triethylaluminium (1.30ml of a 0.99M solution, 0.0013mol) in pentane was added to Bis(hexamethyldisilylamido)ytterbium (0.37g, 0.00065mol) in pentane (20ml). The reaction mixture turned bright yellow upon mixing of the reagents. The reaction solution was stirred for one hour and was then concentrated to ca. 1ml and cooled to -20°C. This did not result in crystal formation. Further cooling to -70°C did not induce crystallization. The remaining pentane was removed under reduced pressure to give a yellow oil. Sometimes prolonged standing at room

temperature will induce this oil to crystallize. Attempts to wash the crystals so formed with cold (-70°) pentane have not yet proven successful. ^{1}H NMR (30°C, C_7D_8, 200MHz): δ0.337(q, J=7.8Hz, 12H), δ0.271(s, 36H), δ1.375(triplet J=7.8Hz, 18H).

Reaction of $\{[(Me_3Si)_2N]_2Yb\}_2$ with KH

Bis(hexamethyldisilylamido)ytterbium (0.80g, 0.0016mol) in pentane (30ml) was added to solid KH (0.14g, 0.0035mol). The reaction mixture was vigorously stirred for three days. Over this time period, the solid KH took on a pink color, and the pentane solution turned pink. The pentane was then removed under reduced pressure. The red residue which remained was extracted with hexane (2x50ml), and the combined extracts were concentrated to ca. 75ml. Cooling of the concentrate afforded red platelets which were isolated and dried under reduced pressure. Another crop of crystals may be obtained from the mother liquors, but sometimes this and subsequent crops of crystals contain white crystals of $KN(SiMe_3)_2$[14] as a contaminant. The compound $KN(SiMe_3)_2$ may also be extracted out of the hexane insoluble residue with toluene, and crystallized from toluene or large volumes of hexane. The total yield of red product is 0.3-0.4g. M.p. 100-103°C. Ir (Nujol) 1240s, 1080sh, 1058vs, 1000vs, 862s, 815vsBr, 755s, 741s, 653s, 602m, 580s, 380s, 356m cm^{-1}. ^{1}H NMR (C_7D_8, 30°C): δ0.26(2, 18H); δ1.43(broad s, 1H): δ3.55(broad s, 1H). ^{13}C NMR (C_7D_8, 30°C): δ6.22. Anal. Found: C, 25.81; H, 8.05; N, 4.09.

$NaN(t\text{-}Bu)(SiMe_3)$

(t-Butyl)(trimethylsilyl)amine was made according to the procedure of

Abel et. al.[15] The preparation which follows is adapted from the preparation of lithium amides by Reetz and Schuster.[16] Trimethylsilyl (t-butyl)amine (9.29g, 0.0639mol) and small chunks of sodium metal (1.47g, 0.0639mol) were added to a 300ml three necked flask containing 100ml of dry diethyl ether. A 100ml dropping funnel was charged with styrene (3.33g, 0.0320mol) and 30ml of dry diethylether. The styrene solution was added to the amine/sodium mixture over the course of 1.5hr. The solution slowly turned slightly yellow and cloudy. The sodium metal became shiny and a red crust was evident in the cracks and crevices in the sodium chunks. The reaction mixture was stirred for 15hr. At this time virtually all the sodium metal had reacted. The ether solution was concentrated to ca. 100ml and cooled to produce crystals of product which crumble upon drying under reduced pressure. Two more crops of crystals may be grown from the mother liquors to give a combined yield of 7.3g, 69%. ^{1}H NMR (C_6D_6, 31°C): δ0.174 (s, 9H), δ1.21 (s, 9H) $^{13C}\{^{1}H\}$NMR (C_6D_6, 30°C): δ7.34($\underline{Me}_3Si$), δ39.15($\underline{Me}_3C$) δ51.85($\underline{C}Me_3$).

$\{[(t\text{-}Bu)(Me_3Si)]N\}_2Yb(OEt_2)_2$

Sodium t-butyl trimethylsilylamide (1.23g, 0.00735mol) in ether (15ml) was cooled to -10°C, and added to a suspension of YbI_2 (1.57g, 0.00368mol) in diethylether (30ml) at 0°C. The reaction mixture slowly turned orange-red. The reaction mixture was stirred at 0°C for 1hr and then allowed to warm to room temperature. After stirring for 24hr the ether solution was filtered and concentrated to ca. 3ml and cooled to -70°C. After six days a red-orange microcrystalline powder was isolated in ca. 10% yield. ^{1}H NMR (C_6D_6, 31°C), δ0.336 (s, 18H); δ1.43 (s, 18H);

$^{13}C\{^{1}H\}$NMR (31°C, C_6D_6) δ6.08($\underline{Me}_3Si$); δ6.78($\underline{Me}_3Si$); δ14.93($OCH_2\underline{Me}$); δ37.59($\underline{Me}_3C$) δ53.15($\underline{C}Me_3$); δ66.33($O\underline{C}H_2Me$).

X-Ray Experimental

$[(C_5Me_5)_2Yb(III)(\mu_2\text{-}OC)_2Mo(CO)(C_5H_4SiMe_3)]_2$

Purple crystals of the compound were obtained by slow cooling of a toluene solution to -10°C. They were mounted in thin walled quartz capillaries in an argon filled dry box, and then were flame sealed. Preliminary precession photographs indicated monoclinic (2/m) Laue symmetry and yielded preliminary cell dimensions. Examination of the 0k0, and h01 zones showed systematic absences 0k0 h≠2n+1; h01, 1+h≠2n+1 consistent only with space group $P2_{1/n}$ (non-standard setting of $P2_{1/c}$).

The data crystal was then mounted on an Enraf-Nonius CAD4 automated diffractometer[23] and centered in the beam. Automatic peak search and indexing yielded the same unit cell as did the precession photographs, and confirmed the Laue symmetry. Accurate cell dimensions and orientation matrix were determined by a least-squares fit to the setting angles of the unresolved MoKα components of 24 symmetry related reflections with 2θ between 24 and 30°. The results are given in Table (I) along with the parameters used for data collection.

The 4709 raw intensity data were converted to structure factor amplitudes and their esp's by correction for scan speed, background and Lorentz-polarization effects[(17-19)]. Analysis of the azimuthal scan data[26] showed a small variation in the average relative intensity (I_{min}/I_{max} = .927) curve. An empirical absorption correction[18] using the average relative intensity curve of the azimuthal scan data was performed because of the irregular shape of the crystal.

Rejection of systematically absent and redundant data yielded a

unique set of 4293 data which were used to solve and refine the structure. Analysis of a three-dimensional Patterson map revealed the positions of the ytterbium and molybdenum atoms. The remaining atoms in the structure were found using the standard Fourier techniques, and the structure was refined using standard least-squares techniques. Hydrogen atoms were placed in idealized positions having fixed thermal paramters, and were included in structure factor calculations, but were not refined.

The final residuals for 335 vaiables refined against the 3327 data for which $F^2 > 3\sigma(F^2)$ were R = 2.07%, wR = 2.59% and GOF = 1.739. The R value for all 4293 data was 4.35%.

The quantity minimized by the least-squares program was $\sum w(|F_o| - |F_c|)^2$, where w is the weight of a given observation. The p-factor [20], used to reduce the weight of intense reflections, was set to 0.015 in the final stages of refinement. The analytical forms for the scattering factor tables for the neutral atoms were used [21] and all non-hydrogen scattering factors were corrected for both the real and imaginary components of anomalous dispersion[22].

Inspection of the residuals ordered in ranges of $\sin\theta/\lambda$, $|F_o|$, and parity and value of the individual indexes showed no unusual features or trends. There was evidence of secondary extinction in the low-angle, high-intensity data, and a correction for secondary extinction was applied.[25]. The largest peak in the final difference Fourier map had an electron density of .384 $e^-/Å^3$ near the Mo atom.

Table I. Crystal Data (25°C) for $[(C_5Me_5)_2Yb(III)(\mu_2\text{-}OC)_2Mo(CO)(C_5H_4SiMe_3)]_2$

Space Group	$P2_{1/m}$
a, Å	13.771(1)
b, Å	15.294(2)
c, Å	15.607(1)
β, deg	93.434(8)
V, $Å^3$	3294
z	2
fw	1520.70
d(calcd), g cm^{-3}	1.535
μ(calcd), cm^{-1}	32.5
size, mm	0.24×0.32×0.20
reflcns, collected	4709
reflcns, unique	4293
reflcns, $F_o^2>3\sigma(F_o^2)$	3327
R, %	2.07
R_w, %	2.59
GOF	1.739
monochromator	highly oriented graphite
radiation	MoKα (λ=0.71073Å)
scan range, type	$3°<2\theta<45°$
scan speed, deg min^{-1}	0.69-6.7
scan width, deg	$\Delta\theta = 0.55 + 0.347 \tan\theta$

$(C_5Me_5)_4Yb_3-(C\equiv C-Ph)_4$

A crystal of approximate dimensions 0.3×0.25×0.15mm was sealed inside a thin walled quartz capillary under argon. Preliminary precession photographs indicated monoclinic (2/m) Laue symmetry, and yielded preliminary cell dimensions. Inspection of the h01 and 0k0 zones showed systematic absences 0k0 k≠2n+1; h01, 1≠2n+1 consistent only with the space group $P2_{1/c}$.

The crystal for data collection was then transferred to an Enraf-Nonius CAD4 automated diffractometer [23] and centered in the beam. Automatic peak search and indexing yielded the same unit cell as found in the photographs, and confirmed the Laue symmetry. Accurate cell dimensions and the orientation matrix were determined from a least-squares fit to the setting angles of the unresolved MoKα components of 24 symmetry related reflections with 2θ between 24 and 25°. The results are given in Table (II) along with parameters for data collection.

The 9551 raw intensity data were converted to structure factor amplitudes and their esd's by correction for scan speed, background, Lorentz and polarization effects [17-19]. Analysis of the azimuthal scan data[26] showed a significant variation I_{min}/I_{max} = 0.75 in the average relative intensity curve. After solution and refinement of the structure confirmed the stoichiometry an analytical absorption correction was applied to the data using the sizes of the indexed faces of the crystal, and an 8×12×8 Gaussian grid of internal points.[18] The maximum and minimum transmission factors were 0.467 and 0.339, respectively.

Rejection of the systematically absent and redundant data yielded a unique set of 8763 data which were used to solve and refine the structure. Solution of the structure was hindered by the strong pseudo body centered nature of the crystal as observed in the precession photographs, and by the fact that more than 50% of the data having the condition hkl; h+k+l=odd are weak to the point of being unobserved. The positions of the Yb atoms were found using MULTAN. The remaining carbon atoms were found and refined using standard Fourier and least-squares techniques. All carbon atoms including those in the benzene molecule of solvation were refined anisotropically.

Hydrogen atoms were not refined and were included in structure factor calculations having fixed thermal paramters for all carbon atoms except those in Cp3, Cp4, and the benzene molecule. The large thermal parameters associated with Cp3, Cp4 and the benzene did not justify the inclusion of H atoms on these carbon atoms. Evidence of secondary extinction was observed in the low-angle, high-intensity data and a secondary extinction correction was applied to the data.[25]

The final residuals for 731 variables refined against the 5715 data for which $F^2>3\sigma(F^2)$ were R = 3.27%, wR = 4.57% and GOF = 3.05. The R value for all 8763 data was 8.89%.

The quantity minimized by the least-squares program was $\sum w(|F_o|-|F_c|)^2$, where w is the weight of a given observation. The p-factor,[20] used to reduce the weight of intense reflections, was set to 0.3 throughout the refinement. The analytical forms for the scattering factor tables for the neutral atoms were used[21] and all non-hydrogen scattering factors were corrected for both the real and imaginary components of anomalous dispersion.[22]

The largest peak in the final difference Fourier map had an electron density of .655 $e^-/Å^3$ and is found near C_{65}, a methyl carbon atom on Cp3.

Table II. Crystal Data (25°C) for $(C_5Me_5)_4Yb_3(C{\equiv}CPh)_4{\cdot}Bz$

Space Group	$P2_{1/c}$
a, Å	18.388(3)
b, Å	13.598(1)
c, Å	26.852(3)
β, deg	90.916(10)
V, Å	6713
z	4
fw	1542.68
d(calcd), g cm^{-1}	41.732
size, mm	6.30×0.25×0.15
reflcns, collected	9551
reflcns, unique	8763
reflcns, $F_o^2>3\sigma(F_o^2)$	5715
R, %	3.27
R_w, %	4.57
GOF	3.05
monochromater	highly oriented graphite
radiation	MoKα (λ = 0.71073Å)
scan range, type	$3°<2\theta<45°$, θ-2θ
scan speed, deg min^{-1}	0.63-6.7
scan width, deg	$\Delta\theta = 0.45+0.347\tan\theta$

X-Ray Write-up for $[(C_5Me_5)Eu\ C{\equiv}C\text{-}Ph^{\bullet}(THF)_2]_2$

In an argon filled dry box, an orange prism of approximate dimensions 0.38×0.27×0.10mm was lodged in a thin-walled quartz capillary which was subsequently flame sealed. Examination of the crystal using precession photography revealed orthorhombic (mmm) Laue symmetry, and yielded preliminary cell dimensions.

The crystal was then transferred to an Enraf-Nonius CAD4 automated diffractometer[23] and centered in the beam. Automatic peak search and indexing yielded the same unit cell as the precession photographs, and confirmed the Laue symmetry. Examination of the h01, 0kl, and hk0 zones showed the following systematic absences; 0kl: k≠2n+1, h01: l≠2n+1, hk0: h≠2n+1 consistent only with the space group Pbca. Accurate cell parameters and the orientation matrix were determined by a least-squares fit to the setting angles of the unresolved MoKα components of 24 symmetry related reflections with 2θ between 24 and 28°. The results are given in Table (III) along with the data collection parameters.

The 3660 data were converted to structure factor amplitudes and their esd's by correction for scan speed, background and Lorentz-polarization effects[(17-19)]. Examination of the azimuthal scan data[26] showed a significant variation I_{min}/I_{max} = 0.79 for the average relative intensity curve. An analytical absorption correction using the measured size and indexed faces of the crystal and a 14×10×4 gaussian grid of internal points was performed after the solution of the structure had confirmed the stoichiometry of the molecule.[18] The maximum and minimum transmission coefficients were 0.698 and 0.534, respectively.

Rejection of systematically absent data as well as redundant data

gave a set of 3251 unique data which were used to solve and refine the structure. The Europium atom positions were found using a three-dimensional Patterson synthesis. The remaining atom positions were found by standard Fourier and least-squares techniques. Hydrogen atoms were found and included in structure factor calculations for all carbon atoms except C_{31}-C_{34}. They were placed in idealized positions with fixed thermal parameters, and were not refined.

The final residuals for 262 variables refined against the 1744 data for which $F^2>3\sigma(F^2)$ were R = 2.64%, wR = 4.14% and GOF = 1.925. The R value for all 3251 data was 8.61%.

The quantity minimized by the least-squares program was $\sum w(|F_o|-|F_c|)^2$, where w is the weight of a given observation. The p-factor,[20] used to reduce the weight of intense reflections, was set to 0.03 throughout the refinement. The analytical forms for the scattering factor tables for the neutral atoms[21] were used and all non-hydrogen scattering factors were corrected for both the real and imaginary components of anomalous dispersion.[22]

Inspection of the residuals ordered in ranges of $\sin\theta/\lambda$, $|F_o|$, and parity and value of the individual indexes showed no unusual features or trends. There was no evidence of secondary extinction in the low-angle, high-intensity data.

The largest peak in the final difference Fourier map had an electron density of $.371e^-/Å^3$ near O_2.

Table III. Crystal Data (25°C) for $(C_5Me_5)_2Eu_2(C{\equiv}CPh)_2(THF)_4$

Space group	Pbca
a, Å	17.251(3)
b, Å	15.445(2)
c, Å	18.732(2)
V, Å	4999
z	4
fw	1065.07
d(calcd), g cm^{-3}	1.417
μ(calcd), cm^{-1}	25.33
size, mm	0.38×0.27×0.10
reflcns, collected	3660
reflcns, unique	3250
reflcns, $F_o^2 > 3\sigma(F_o^2)$	1744
R, %	2.64
R_w, %	4.14
GOF	1.925
monochromater	highly oriented graphite
radiation	MoKα (λ = 0.71073Å)
scan range, type	$3° < 2\theta < 45°$, θ-2θ
scan speed, deg min^{-1}	0.95-6.7
scan width, deg	$\Delta\theta = 0.80+0.347 \tan\theta$

$[(C_5Me_5)_2Ybbipy]^+[(C_5Me_5)YbCl_2]^-$

Red needles of the compound were grown by layering a CH_2Cl_2 solution of the compound with pentane. Crystals were cleared in the air, and lodged in thin-walled quartz capillaries. The capillaries were flushed with dry N_2 and then flame sealed. Examination of the crystals using precession photography indicated triclinic Laue symmetry. A crystal having approximate dimensions .43mm×.17mm×.15mm was mounted on an Enraf-Nonius CAD4 diffractometer[23] and centered in the beam. Automatic peak search and indexing confirmed the Laue symmetry and yielded cell parameters. There were no systematic absences, and the space group $P\bar{1}$ was confirmed by solution and refinement of the structure.

Accurate cell parameters and the orientation matrix were determined by a least-squares fit to the setting angles of the unresolved MoKα components of 24 symmetry related reflections having 2θ between 25 and 28°. The cell parameters are given in Table (IV) along with the data collection procedures and parameters.

The 6620 raw intensity data were converted to structure factor amplitudes and their esd's by correction for scan speed, background, and Lorentz-polarization effects[(17-19)]. Analysis of the azimuthal scan data[26] showed a significant variation I_{min}/I_{max} = .83 for the average relative intensity curve. An absorption correction using the measured size of the crystal, its indexed faces and a 12×12×6 gaussian grid of internal points was performed after solution of the structure had confirmed the stoichiometry.[18] The maximum and minimum transmission factors were 0.622 and 0.509, respectively.

Rejection of redundant data gave a unique set of 6220 data which

were used to solve and refine the structure. The structure was solved by analysis of a three-dimensional Patterson map to give the positions of the Yb and Cl atoms. The rest of the atoms were located using standard Fourier techniques and were refined using full matrix least-squares techniques. Hydrogen atoms were located, and placed in idealized positions having fixed thermal parameters, were not refined, but were included in structure factor calculations.

The final residuals for 506 variables refined against the 5140 data for which $F^2>3\sigma(F^2)$ were R = 2.03%, wR = 2.64% and GOF = 1.719. The R value for all 6223 data was 3.18%.

The quantity minimized by the least-squares program was $\sum w(|F_o|-|F_c|)^2$, where w is the weight of a given observation. The p-factor,[20] used to reduce the weight of intense reflections, was set to 0.02 throughout the refinement. The analytical forms for the scattering factor tables for the neutral atoms[21] were used and all non-hydrogen scattering factors were corrected for both the real and imaginary components of anomalous dispersion.[22]

Inspection of the residuals ordered in ranges of $\sin\theta/\lambda$, $|F_o|$, and parity and value of the individual indexes showed no unusual features or trends. There was evidence of secondary extinction in the low-angle, high-intensity data, and a secondary extinction correction[25] was applied.

There were 4 peaks between 0.6 and 0.8 e^-/A^3 near the two Yb atoms.

Table IV. Crystal Data (25°C) for $[(C_5Me_5)_2Yb(bipy)]^+[(C_5Me_5)YbCl_2]^-$

Space group	$P\bar{1}$
a, Å	10.8462(9)
b, Å	13.432(2)
c, Å	16.462(2)
α, deg	90.61(1)
β, deg	93.988(8)
γ, deg	95.60(1)
V, $Å^3$	2381
z	2
fw	1114.10
d(calcd), g cm^{-3}	1.554
μ(calcd), cm^{-1}	40.40
size, mm	0.43×0.17×0.15
reflcns, collected	6623
reflcns, unique	6220
reflcns, $F_o^2>3\sigma(F_o^2)$	5140
R, %	2.03
R_w, %	2.64
GOF	1.719
monochromater	highly oriented graphite
radiation	MoKα(λ = 0.71073Å)
scan range, type	$3°<2\theta<45°$
scan speed, deg min^{-1}	0.62-6.7
scan width, deg	$\Delta\theta = 0.50+0.347 \tan\theta$
decay	

2,2'-Bipyrimidine

Crystals were obtained by vacuum sublimation at 90°C and 10^{-2}torr. The compound is extremely hygroscopic, and the crystals were loaded into thin walled quartz capillaries in an argon filled dry box, and flame sealed. The data crystal was a prism having approximate dimensions 0.21mm×0.23mm×0.40mm.

Preliminary precession photographs indicated monoclinic (2/m) Laue symmetry and yielded preliminary cell dimensions. Examination of the 0k0, and h0l zones showed systematic absences 0k0; k≠2n+1; h0l; l+h≠2n+1 consistent only with space group $P2_{1/n}$.

The data crystal was mounted on an Enraf-Nonius CAD4 automated diffractometer,[23] cooled to -110°C and centered in the beam. Automatic peak search and indexing yielded the same cell as did the precession photographs, and confirmed the Laue symmetry. Accurate cell dimensions and the orientation matrix were determined by a least-squares fit to the setting angles of the unresolved MoKα components of 24 symmetry related reflections with 2θ between 22 and 32°. The results are given in Table (V) along with the data collection parameters.

The 1997 raw data were converted to structure factor amplitudes and their esd's by correction for scan speed, background, and Lorentz-polarization effects.[17-19] After removal of systematically absent data averaging of the redundant data gave 932 unique reflections. Analysis of the azimuthal scan data[26] showed no variation in intensity so that an absorption correction was unwarranted.

The unique set of 932 data were used to solve and refine the structure. The positions of the carbon and nitrogen atoms were

determined using MULTAN. The structure was refined using full matrix least-squares techniques, and the hydrogen atoms were located by Fourier methods. The carbon and nitrogen atoms were refined anisotropically, and the hydrogen atoms isotropically.

The final residuals for 68 variables refined against the 746 data for which $F^2>3\sigma(F^2)$ were R = 3.09%, wR = 4.66% and GOF = 2.141. The R value for all 932 data was 4.02%.

The quantity minimized by the least-squares program was $\sum w(|F_o|-|F_c|)^2$, where w is the weight of a given observation. The p-factor,[20] used to reduce the weight of intense reflections, was set to 0.03 throughout the refinement. The analytical forms for the scattering factor tables for the neutral atoms[21] were used and all non-hydrogen scattering factors were corrected for both the real and imaginary components of anomalous dispersion.[22]

Inspection of the residuals ordered in ranges of $\sin\theta/\lambda$, $|F_o|$, and parity and value of the individual indexes showed no unusual features or trends. There was strong evidence of secondary extinction in the low-angle, high-intensity data, and a correction was applied.[25]

The largest peak in the final difference Fourier map had an electron density of 0.36 $e^-/Å^3$.

Table V. Crystal Data (-110°C) for 2,2'-Bypyrimidine

Space group	$P2_1/n$
a, Å	3.8567(4)
b, Å	10.796(2)
c, Å	8.844(1)
β, deg	101.028(10)
V, $Å^3$	361.4
z	2
fw	158.17
d(calcd) g cm^{-3}	1.453
μ(calcd), cm^{-1}	0.9
size, mm	0.21×0.23×0.40
reflcns, collected	1997
reflcns, unique	932
reflcns, $F_o^2 > 3\sigma(F_o^2)$	746
R, %	3.09
R_w, %	4.66
GOF	2.141
monochromater	highly oriented graphite
radiation	MoKα (λ = 0.71073Å)
scan range, type	$3° \neq 2\theta \neq 55°$, θ-2θ
scan speed, deg min^{-1}	0.69-6.7
scan width, deg	$\Delta\theta = 0.50+0.347 \tan\theta$
decay	none observed

$[(C5Me_5)_2Yb]_2bipm \cdot PhMe$

Shiny black needles of the complex were cleaved and lodged into thin walled quartz capillaries in an argon filled dry box. The capillaries were then flame sealed. Preliminary precession photographs indicated triclinic Laue symmetry, and yielded preliminary cell parameters. The data crystal was then mounted on an Enraf-Nonius CAD4 automated diffractometer[23] and centered in the beam. Automatic peak search and indexing yielded the same unit cell as found in the precession photographs. The space group $P\bar{1}$ was confirmed by solution and refinement of the structure. Accurate cell dimensions and the orientation matrix were determined by a least-squares fit to the setting angles of the unresolved MoKα components of 24 symmetry related reflections with 2θ between 27 and 31°. The results are given in Table (VI) along with the data collection parameters.

The 6654 raw intensity data were converted to structure factor amplitues and their esd's by correcting for scan speed, background, and Lorentz-polarization effects.[17-19] Analysis of the azimuthal scan data[26] showed a variation of I_{min}/I_{max} of 0.885 in the average relative intensity curve. An analytical absorption correction was applied to the data using the sizes of the indexed faces of the crystal and a 14×8×6 Gaussian grid of internal points.[18] The maximum and minimum transmission factors were 0.522 and 0.445, respectively.

The unique set of 6654 data were used to solve and refine the structure. The Yb atoms were located through the use of a three-dimensional Patterson map. The remaining atoms were located through the use of standard Fourier techniques. During the course of refinement,

two types of disorder were observed. One occurred in the toluene molecule of solvation, while the other was observed in three out of the four (C_5Me_5) rings.

The disorder of the toluene molecules was modeled using two half occupancy molecules which were refined as constrained isotropic bodies. The C-C-C angles were constrained at 120°, the C_{ring}-C_{ring} bond lengths at 1.40Å, and the C-Me length at 1.500Å. Unfortunately, the methyl group on one of the half occupancy rings refused to refine well. Evidently this ring is also rotationally disordered over 2 or more positions, and the methyl group would not refine so it was removed from the structure.

The disorder of the C_5Me_5 rings was observed during refinement when ten half occupancy methyl groups were found for each disordered ring. The disorder rotation of one C_5Me_5 ring component with respect to the other as well as a difference in the distance of the components to the Yb atom. The disordered ring carbon atoms could not be resolved from one another. The model which was used consisted of two half occupancy C_5Me_5 rings each of which were refined as rigid isotropic bodies. The C-C(ring) distances were constrained to 1.420Å and the C-Me bonds were constrained to be 1.500Å. The C-C-C(ring) angles were constrained to be 108°, while the C-C-Me angles were constrained to be 126°. The positions of each of the ring carbon atoms was calculated form the observed positions of the attached methyl groups. Each C_5Me_5 ring was allowed to refine independently, and this resulted in the observed variation in Yb-C_{ring} bond lengths (see Chapter 2). The remaining C_5Me_5 ring showed evidence of disorder when the ring was removed and a difference Fourier was calculated, but the observation of only four half

occupancy methyl groups did not allow calculation of the positions of the remaining atoms of the half occupancy rings. A large spread in Yb-C_{ring} distance suggested that the disorder of the remaining C_5Me_5 ring did not involve much of a rotational component, but rather the two rings are merely different distances from the metal atom.

The final residuals for 510 variables refined against the 5707 data for which $F^2 > 3\sigma(F^2)$ were R = 2.95%, wR = 14.87% and GOF = 2.51. The R value for all 6654 data was 3.91%.

The quantity minimized by the least-squares program was $\sum w(|F_o| - |F_c|)^2$, where w is the weight of a given observation. The p-factor,[20] used to reduce the weight of intense reflections, was set to 0.03 throughout the refinement. The analytical forms for the scattering factor tables for the neutral atoms[21] were used and all non-hydrogen scattering factors were corrected for both the real and imaginary components of anomalous dispersion.[22]

Inspection of the residuals ordered in ranges of $\sin\theta/\lambda$, $|F_o|$, and parity and value of the individual indexes showed no unusual features or trends. There was evidence of secondary extinction in the low-angle, high-intensity data, and given the large extinction coefficient calculated (2.57×10^{-7}) it was included even though the H atoms were not included in the structure factor calculations.[25]

The largest peak in the final difference Fourier map had an electron density of 0.73 $e^{-1}/Å^3$.

Table VI. Crystal Data (25°C) for $[(C_5Me_5)_2Yb]_2bpm \cdot PhMe$

Space group	$P\bar{1}$
a, Å	10.5037(9)
b, Å	11.233(1)
c, Å	22.203(2)
α	93.248(9)
β, deg	90.529(7)
γ	102.519(8)
V, Å	2553
z	2
fw	1137.31
d(calcd), g cm^{-3}	1.480
μ(calcd), cm^{-1}	36.67
size, mm	0.34×0.24×0.20
reflcns, collected	6654
reflcns, unique	6654
reflcns, $F_o^2 > 3\sigma(F_o^2)$	5707
R, %	2.95
R_w, %	4.87
GOF	2.51
monochromater	highly oriented graphite
radiation	MoKα (λ = 0.71073Å)
scan range, type	$3° \leq 2\theta \leq 45°$, θ-2θ
scan speed, deg min^{-1}	0.625-6.7
scan width, deg	$\Delta\theta = 0.50+0.357 \tan\theta$
decay	none

$\{[(Me_3Si)_2N]_2Yb\}_2$

Red-orange platelets of the compound were grown by slowly cooling a saturated pentane solution to -25°C. A plate of approximate dimensions 0.45mm×0.32mm×0.10mm was lodged into a thin walled quartz capillary in an argon filled dry box. The capillary was then flame sealed. Examination of the crystals with preliminary precession photography indicated triclinic Laue symmetry. The crystal was then mounted on an Enraf-Nonius CAD4 automated diffractometer,[23] cooled to -95°C and centered in the beam. Automatic peak search and indexing confirmed the Laue symmetry and yielded cell parameters. The space group $P\bar{1}$ was confirmed by successful solution and refinement of the structure.

Accurate cell parameters were determined by a least-squares fit to the setting angles of the unresolved MoKα components of 24 symmetry related reflections having 2θ between 25 and 30°. The cell parameters are given in Table (VII) along with the data collection parameters.

The 6005 raw intensity data were converted to structure factor amplitudes and their esd's by correction for scan speed, background, and Lorentz-polarization effects.[17-19] Analysis of the azimuthal scan data[26] showed a significant variation I_{min}/I_{max} = 0.478 for the average relative intensity curve. An analytical absorption correction using the measured size of the crystal, its indexed faces and a 6≠10≠14 gaussian grid of internal points was performed.[18] The maximum and minimum transmission factors were 0.492 and 0.232, respectively.

Rejection of redundant data gave a unique set of 5821 data which were used to solve and refine the structure. The Yb atom positions were determined by analysis of a three-dimensional Patterson map. The

remaining atoms were found by conventional Fourier and difference Fourier techniques. The non-hydrogen atoms were refined anisotropically, while the hydrogen atoms were placed in calculated positions with fixed thermal parameters, and were included in structure factor calculations, but were not refined. The large thermal motion on C(16,17,18) is due to a rotational disorder which could not be resolved.

The final residuals for 344 variables refined against the 4844 data for which $F^2>3\sigma(F^2)$ were R = 2.19%, wR = 2.72% and GOF = 1.669. The R value for all 5821 data was 3.44%.

The quantity minimized by the least-squares program was $\sum w(|F_o|-|F_c|)^2$, where w is the weight of a given observation. The p-factor,[20] used to reduce the weight of intense reflections, was set to 0.02 throughout the refinement. The analytical forms for the scattering factor tables for the neutral atoms[21] were used and all non-hydrogen scattering factors were corrected for both the real and imaginary components of anomalous dispersion.[21]

Inspection of the residuals ordered in ranges of $\sin\theta/\lambda$, $|F_o|$, and parity and value of the individual indexes showed no unusual features or trends. There was evidence of secondary extinction in the low-angle, high-intensity data, and a secondary extinction correction was applied.[25]

The largest peak in the final difference Fourier map had an electron density of 0.97 $e^{-1}/Å^3$ and was associated with Yb(1).

Table VII. Crystal Data (-95°C) for $\{[(Me_3Si)_2N]_2Yb\}_2$

Space group	$P\bar{1}$
a, Å	8.868(1)
b, Å	12.561(2)
c, Å	21.560(3)
α, deg	73.84(1)
β, deg	86.70(1)
γ, deg	71.26(1)
V, $Å^3$	2225
z	2
fw	987.64
d(calcd), g cm^{-3}	1.474
μ(calcd), cm^{-1}	43.97
size, mm	0.45×0.32×0.10
reflcns, collected	6005
reflcns, unique	5821
reflcns, $F_o^2 > 3\sigma(F_o^2)$	4844
R, %	2.19
R_w, %	2.72
GOF	1.669
monochromater	highly oriented graphite
radiation	MoKα (λ = 7.1073Å)
scan range, type	$3° < 2\theta < 45°$
scan speed, deg min^{-1}	0.69-6.7
scan width, deg	$\Delta\theta = 0.55+0.347 \tan\theta$
decay	4.7%, corrected

$[(C_5Me_5)YbN(SiMe_3)_2]_2$

A dark red octahedron of approximate dimension 0.23×0.22×0.32mm was lodged into a thin walled quartz capillary in an argon filled dry box. The capillary was subsequently flame sealed. Preliminary precession photographs indicated orthorhombic (mmm) Laue symmetry, and yielded preliminary cell dimensions.

The crystal was transferred to an Enraf-Nonius CAD4 automated diffractometer,[23] cooled to -95° and centered in the beam. Automatic peak search and indexing yielded the same unit cell as the precession photographs and confirmed the Laue symmetry. Examination of the h01, 0k1, and kk0 zones showed the following systematic absences: 0k1; k≠2n+1, h01; l≠2n+1, hk0; h≠2n+1 consistent only with the space group Pbca. Accurate cell parameters and the orientation matrix were determined by a least-squares fit to the setting angles of the unresolved MoKα components of 24 symmetry related reflections with 2θ between 25 and 28°. The results as well as data collection parameters are found in Table (VIII).

The 2849 data were converted to structure factor amplitudes and their esd's by correction for scan speed, background, and Lorentz-polarization effects.[17-19] Examination of the azimuthal scan data[26] showed a significant variation I_{min}/I_{max} = 0.812 for the average relative intensity curve. An analytical absorption correction using the measured size and indexed faces of the crystal and a 8×10×8 gaussian grid of internal points was performed.[18] The maximum and minimum transmission factors were .482 and .374, respectively.

Rejection of systematically absent data gave a set of 2506 unique

data which were used to solve and refine the structure. The positions of the Yb and Si atoms were found using a three-dimensional Patterson map. The remaining atom positions were found using standard Fourier and difference Fourier techniques. The heavy atoms were refined anisotropically using full matrix least-squares techniques. The hydrogen atoms were located, and placed in idealized positions with fixed thermal parameters, and were included in structure factor calculations, but not refined.

The final residuals for 182 variables refined against the 1878 data for which $F^2 > 3\sigma(F^2)$ were R = 2.76%, wR = 13.60% and GOF = 1.925. The R value for all 2506 data was 4.61%.

The quantity minimized by the least-squares program was $\sum w(|F_o| - |F_c|)^2$, where w is the weight of a given observation. The p-factor, used to reduce the weight of intense reflections, was set to .025 in the final stages of the refinement. The analytical forms for the scattering factor tables for the neutral atoms[21] were used and all non-hydrogen scattering factors were corrected for both the real and imaginary components of anomalous dispersion.[22]

Inspection of the residuals ordered in ranges of $\sin\theta/\lambda$, $|F_o|$, and parity and value of the individual indexes showed no unusual features or trends. There was evidence of a secondary extinction in the low-angle, high-intensity data, and a secondary extinction correction was applied.[25]

The largest peak in the final difference Fourier map had an electron density of 1.05 $e^-/Å^3$ associated with the Yb atom.

Table VIII. Crystal Data (-95°C) for $\{[(C_5Me_5)Yb[N(SiMe_3)_2]]\}_2$

Space group	Pbca
a, Å	17.031(1)
b, Å	16.002(2)
c, Å	14.099(2)
V, $Å^3$	3843
z	4
fw	937.35
d(calcd), g cm^{-3}	1.62
μ(calcd), cm^{-1}	49.69
size, mm	0.23×0.22×0.32
reflcns, collected	2849
reflcns, unique	2506
reflcns, $F_o^2 > 3\sigma(F_o^2)$	1878
R, %	2.76
R_w, %	3.60
GOF	1.925
monochromater	highly oriented graphite
radiation	MoKα (λ = 0.71073Å)
scan range, type	$3° \leq 2\theta \leq 45°$, θ-2θ
scan speed, deg min^{-1}	0.69-6.7
scan width, deg	$\lambda\theta = 0.50+0.347 \tan \theta$
decay	less than 0.5%

$[(Me_3Si)_2N]_2Yb(AlMe_3)_2$

Bright yellow plates of the compound were obtained by slowly cooling a solution of the compound in pentane to -20°C. A fragment of one of these crystals was lodged into a thin-walled quartz capillary in an argon filled dry box. The capillary was then flame sealed.

Preliminary precession photographs indicated triclinic Laue symmetry, and the space group $P\bar{1}$ was confirmed by subsequent solution and refinement of the structure. The data crystal was then transferred to an Enraf-Nonius CAD4 automated diffractometer[23] and cooled to -95°C and centered in the beam. Automatic peak indexing procedures yielded the same triclinic cell found from the precession photos. The space group $P\bar{1}$ was confirmed by solution and refinement of the structure.

Accurate cell dimensions and the orientation matrix were determined by a least-squares fit to the setting angles of the unresolved MoKα components of the 24 symmetry related reflections having 2θ between 23 and 31°. The results are given in Table (IX) along with the data collection parameters.

The 4012 raw intensity data were converted to structure factor amplitudes and their esd's by correction for scan speed, background and Lorentz-polarization effects.[17-19] Analysis of the azimuthal scan data[26] showed a significant variation in the averaged relative intensity (I_{min}/I_{max} = 0.758). An empirical absorption correction using the average relative intensity of the azimuthal scan data was performed.[18]

The unique set of 4012 data were used to solve and refine the structure. Analysis of a three-dimensional Patterson synthesis revealed the positions of the Yb, Al and Si atoms. The remaining atoms in the

structure were found using standard Fourier techniques. The structure was refined using full matrix least-squares refinement. Hydrogen atoms except for H(1-6) were placed in idealized positions having fixed thermal parameters, and were included in structure factor calculations, but were not refined. Hydrogen atoms H(1-6) were placed where found in the difference Fourier maps, were included in structure factor calculations, but were not refined.

The final residuals for 245 variables refined against the 3814 data for which $F^2>3\sigma(F^2)$ were R = 1.69%, wR = 2.58% and GOF = 1.857.[5] The R value for all 4012 data was 1.90%.

The quantity minimized by the least-squares program was $\sum w(|F_o|-|_c|)^2$, where w is the weight of a given observation. The p-factor,[20] used to reduce the weight of intense reflections, was set to 0.01 throughout the refinement. The analytical forms for the scattering factor tables for the neutral atoms were used[21] and all non-hydrogen scattering factors were corrected for both the real and imaginary components of anomalous dispersion.[22]

Inspection of the residuals ordered in ranges of $\sin\theta/\lambda$, $|F_o|$, and parity and value of the individual indexes showed no unusual features or trends. There was evidence of secondary extinction in the low-angle, high-intensity data, and a secondary extinction correction was applied to the data.[25] The hydrogen atoms were located in the final difference Fourier maps, and were placed in calculated positions and included in structure factor calculations, but were not refined.

The largest peak in the final difference Fourier map had an electron density of 0.552 e^{-1}/A^3 and was associated with the ytterbium atom.

Table IX. Crystal Data (-95°C) for $[(Me_3Si)_2246]_2Yb(AlMe_3)_2$

Space group	$P\bar{1}$
a, Å	9.871(1)
b, Å	12.935(2)
c, Å	13.108(2)
α, deg	68.12(1)
β, deg	83.19(1)
γ, deg	84.39(1)
V, $Å^3$	1539
z	2
fw	637.99
d(calcd), g cm^{-3}	1.736
μ(calcd), cm^{-1}	32.45
size, mm	0.33×0.36×0.22
reflcns, collected	4012
reflcns, unique	4012
reflcns, $F_o^2 > 3\sigma(F_o^2)$	3814
R, %	1.69
R_w, %	2.58
GOF	1.857
monochromater	highly oriented graphite
radiation	MoKα (λ = 0.71073Å)
scan range, type	$3° < 2\theta < 45°$, θ-2θ
scan speed, deg min^{-1}	0.69-6.7
scan width, deg	0.50+0.347 tanθ
decay	2.75%, corrected

References

1.) Threlkel, R. S.; Bercaw, J. E. J. Organomet. Chem. 1977, 136, 1.

2.) Niederprum, H. and Wannagat, U. Chem. Ber. 1961, 94, 1540.

3.) Howell, J. K.; Pytlewski, L. L. J. Less-Common Met. 1969, 18, 437.

4.) Eisch, J. J.; King, R. B. "Organometallic Syntheses", Vol. 1, Academic Press, New York, 1965, pp. 105-119.

5.) Pitcher, E.; Stone, F. G. A. Spectrochim. Acta. 1962, 18, 585.

6.) Locke, J.; McCleverty, J. A. J. Chem. Soc., Chem. Comm. 1965, 102.

7.) Flitcroft, N.; Huggins, D. K.; Kaesz, H. D. Inorg. Chem., 1964, 3, 1123.

8.) Cotton, F. A.; Liehr, A. D.; Wilkinson, G. J. Inorg. Nucl. Chem. 1955, 1, 175.

9.) Piper, T. S.; Wilkinson, G. J. Inorg. Nucl. Chem. 1956, 3, 104.

10.) Sloan, T. E.; Wojcicki, A. Inorg. Chem., 1968, 7, 1268.

11.) Schore, N. E. J. Organomet. Chem. 1979, 173, 301.

12.) Tilley, T. D. PhD Thesis University of California, Berkeley, Berkeley, California, U.S.A., 1982.

13.) Tilley, T. D.; Andersen, R. A.; Zalkin, A. Inorg. Chem. 1984, 23, 2271.

14.) Burger, H.; Seyffert, H. Angew. Chem. Int. Ed. 1964, 3, 646.

15.) Able, E. W.; Willey, J. Chem. Soc. 1964, 1528.

16.) Reetz, M. T.; Urz, R.; Schuster, T. Synthesis 1983, 540.

17.) All calculations were performed on a PDP 11/60 equipped with 128 kilowords of memory, twin RK07 28 MByte disk drives, Versatec printer/plotter and TU10 tape drive using locally-modified Nonius-SDP[3] software operating under RSX-11M.

18.) Structure Determination Package User's Guide, 1982, B. A. Frenz and Associates, College Station, TX 77840.

19.) The data reduction formulae are:

$$F_o^2 = \frac{\omega}{Lp}(C-2B) \qquad \sigma_o(F_o^2) = \frac{\omega}{Lp}(C + 4B)^{1/2}$$

$$F_o = \sqrt{F_o^2} \qquad \sigma_o(F) = \frac{\sigma_o(F_o^2)}{2F_o}$$

where C is the total count in the scan, B the sum of the two background counts, 1 the scan speed used in deg/min, and

$$\frac{1}{Lp} = \frac{\sin 2\theta \, (1 + \cos^2 2\theta_m)}{1 + \cos^2 2\theta_m - \sin^2 2\theta}$$

is the correction for Lorentz and polarization effects for a reflection with scattering angle 2r and radiation monochromatized with a 50% perfect single crystal monochrometer with scattering angle $2r_m$.

20.)

$$R = \frac{\Sigma||F_o| - |F_c||}{\Sigma|F_o|} \qquad wR = \left\{ \frac{\Sigma w(|F_o| - |F_c|)^2}{\Sigma w F_o^2} \right\}^{1/2}$$

$$GOF = \left\{ \frac{\Sigma w(|F_o| - |F_c|)^2}{(n_o - n_v)} \right\}^{1/2}$$

where n_o is the number of observations, n_v the number of variable parameters, and the weights w were given by

$$w = \frac{4F_o^2}{\sigma^2(F_o^2)}, \quad \sigma^2(F_o^2) = \left\{ \sigma_o^2(F_o^2) + (pF^2)^2 \right\}$$

where p is the factor used to lower the weight of intense reflections.

21.) D. T. Cromer, J. T. Waber, "International Tables for X-ray Crystallography," Vol. IV, The Kynoch Press, Birmingham, England, 1974, Table 2.2B.

22.) D. T. Cromer, ibid., Table 2.3.1.

23.) Instrumentation at the University of California Chemistry Department X-ray Crystallographic Facility (CHEXRAY) consists of two Enraf-Nonius CAD-4 diffractometers, one controlled by a DEC PDP 8/a with an RK05 disk and the other by a DEC PDP 8/e with an RL01 disk. Both use Enraf-Nonius software as described in the CAD-4 Operation Manual, Enraf-Nonius, Delft, Nov. 1977, updated Jan. 1980.

24.) C. K. Johnson, Report ORNL-3794, Oak Ridge National Laboratory, Oak Ridge, Tenn., 1965.

25.) Zachariesen, W. H., Acta Crystallogr., 16, 1139 (1963).

26.) Reflections used for azimuthal scans were located near x = 90° and the intensities were measured at 10° increments of rotation of the crystal about the diffraction vector.

APPENDIX I: TABLES OF THERMAL AND POSITIONAL PARAMETERS

Table I. $\{[(C_5Me_5)_2Yb][(Me_3SiC_5H_4)Mo(CO)_3]\}_2$

Table of Positional Parameters and Their Estimated Standard Deviations

Atom	x	y	z	B(Å^2)
YB1	0.12175(1)	0.00093(1)	0.30177(1)	2.735(4)
MO1	0.25049(3)	0.01518(3)	0.62661(3)	3.830(9)
SI1	0.3476(1)	0.0168(1)	0.8538(1)	5.21(4)
O1	-0.0363(2)	-0.0033(2)	0.3294(2)	4.50(8)
O2	0.1578(3)	0.0031(2)	0.4434(2)	4.45(7)
O3	0.2652(3)	-0.1868(3)	0.6312(3)	8.4(1)
C1	0.2997(4)	0.1370(4)	0.7120(3)	5.8(1)
C2	0.3524(3)	0.0640(4)	0.7449(3)	4.9(1)
C3	0.4143(4)	0.0386(5)	0.6794(4)	8.0(2)
C4	0.3978(5)	0.0922(6)	0.6090(4)	10.6(2)
C5	0.3288(5)	0.1544(4)	0.6273(4)	9.1(2)
C6	0.3962(7)	-0.0940(5)	0.8559(5)	14.4(3)
C7	0.2216(6)	0.0160(6)	0.8854(5)	11.5(3)
C8	0.4192(5)	0.0854(5)	0.9298(4)	8.3(2)
C10	0.2195(3)	-0.1423(3)	0.3227(3)	4.0(1)
C11	0.2351(3)	-0.1164(3)	0.2410(3)	4.2(1)
C12	0.1465(4)	-0.1227(3)	0.1915(3)	4.2(1)
C13	0.0761(4)	-0.1531(3)	0.2454(3)	4.3(1)
C14	0.1220(3)	-0.1647(3)	0.3275(3)	4.0(1)
C15	0.3000(5)	-0.1516(4)	0.3925(4)	8.0(2)
C16	0.3333(4)	-0.1004(4)	0.2069(5)	8.0(2)
C17	0.1305(6)	-0.1129(4)	0.0968(4)	8.9(2)
C18	-0.0267(4)	-0.1796(4)	0.2208(5)	8.2(2)
C19	0.0751(5)	-0.1970(4)	0.4064(4)	7.7(2)
C20	0.2287(3)	0.1374(3)	0.2921(3)	4.3(1)
C21	0.1475(4)	0.1652(3)	0.3325(3)	4.6(1)
C22	0.0682(4)	0.1615(3)	0.2748(3)	4.8(1)
C23	0.0991(4)	0.1306(3)	0.1964(3)	5.1(1)
C24	0.2010(4)	0.1180(3)	0.2078(3)	4.9(1)
C25	0.3308(5)	0.1363(4)	0.3297(5)	10.2(2)
C26	0.1436(7)	0.2013(4)	0.4218(4)	9.8(2)
C27	-0.0338(5)	0.1934(4)	0.2873(5)	10.2(2)
C28	0.0387(6)	0.1244(5)	0.1133(4)	11.7(2)
C29	0.2664(6)	0.1028(4)	0.1381(5)	11.1(2)
C30	-0.1194(3)	-0.0069(3)	0.3449(3)	3.4(1)
C31	0.1958(3)	0.0065(3)	0.5141(3)	3.5(1)
C32	0.2595(4)	-0.1106(4)	0.6294(4)	5.5(1)

* -- Atoms refined with isotropic thermal parameters.
Anisotropically refined atoms are given in the form of the isotropic equivalent thermal parameter defined as:

$$(4/3) * [a^2*B(1,1) + b^2*B(2,2) + c^2*B(3,3) + ab(\cos\gamma)*B(1,2) + ac(\cos\beta)*B(1,3) + bc(\cos\alpha)*B(2,3)]$$

Table I. (cont.)

Table of Positional Parameters and Their Estimated Standard Deviations (cont.)

Atom	x	y	z	B(Å^2)
H11	0.2478	0.1692	0.7422	7.5**
H31	0.4572	-0.0106	0.6809	10.0**
H41	0.4235	0.0941	0.5569	10.0**
H51	0.2984	0.2048	0.5964	10.0**
H61	0.3971	-0.1216	0.9082	15.0**
H62	0.3612	-0.1314	0.8129	15.0**
H63	0.4642	-0.0943	0.8366	15.0**
H71	0.2173	-0.0058	0.9404	12.0**
H72	0.1975	0.0768	0.8847	12.0**
H73	0.1813	-0.0154	0.8452	12.0**
H81	0.4199	0.0633	0.9881	8.0**
H82	0.4873	0.0894	0.9164	8.0**
H83	0.3956	0.1448	0.9319	8.0**
H151	0.3299	-0.2079	0.3939	8.5**
H152	0.3508	-0.1085	0.3880	8.5**
H153	0.2752	-0.1426	0.4496	8.5**
H161	0.3615	-0.1535	0.1884	8.5**
H162	0.3282	-0.0607	0.1594	8.5**
H163	0.3772	-0.0748	0.2501	8.5**
H171	0.1424	-0.1667	0.0668	8.5**
H172	0.0633	-0.0965	0.0799	8.5**
H173	0.1711	-0.0688	0.0741	8.5**
H181	-0.0288	-0.2391	0.2014	8.5**
H182	-0.0658	-0.1750	0.2690	8.5**
H183	-0.0539	-0.1433	0.1761	8.5**
H191	0.0779	-0.2584	0.4104	8.5**
H192	0.1060	-0.1716	0.4567	8.5**
H193	0.0072	-0.1794	0.4042	8.5**
H251	0.3627	0.1898	0.3218	10.0**
H252	0.3324	0.1234	0.3901	10.0**
H253	0.3680	0.0903	0.3037	10.0**
H261	0.1560	0.2630	0.4226	10.0**
H262	0.0840	0.1899	0.4455	10.0**
H263	0.1953	0.1746	0.4588	10.0**
H271	-0.0404	0.2545	0.2764	10.0**
H272	-0.0816	0.1621	0.2552	10.0**
H273	-0.0479	0.1859	0.3486	10.0**
H281	0.0378	0.1785	0.0819	12.0**
H282	0.0624	0.0798	0.0760	12.0**
H283	-0.0286	0.1097	0.1220	12.0**

Table of Positional Parameters and Their Estimated Standard Deviations (cont.)

Atom	x	y	z	$B(A^2)$
H291	Ø.2868	Ø.1572	Ø.1131	12.Ø**
H292	Ø.3247	Ø.Ø718	Ø.1569	12.Ø**
H293	Ø.2348	Ø.Ø691	Ø.Ø923	12.Ø**

* -- Atoms refined with isotropic thermal parameters.
** -- Atoms included but not refined.
Anisotropically refined atoms are given in the form of the isotropic equivalent thermal parameter defined as:

$$(4/3) * [a^2*B(1,1) + b^2*B(2,2) + c^2*B(3,3) + ab(\cos\ gamma)*B(1,2) + ac(\cos\ beta)*B(1,3) + bc(\cos\ alpha)*B(2,3)]$$

Table I. (cont.)

Table Ia.

Table of General Temperature Factor Expressions - B's

Name	B(1,1)	B(2,2)	B(3,3)	B(1,2)	B(1,3)	B(2,3)	Beqv
VB1	2.696(7)	2.635(7)	2.871(7)	-0.075(8)	0.136(6)	0.035(8)	2.735(4)
MO1	2.69(2)	5.75(2)	3.00(2)	-0.77(2)	-0.17(1)	-0.06(2)	3.830(9)
SI1	4.81(7)	6.75(9)	3.91(6)	0.13(7)	-1.07(6)	-0.10(7)	5.21(4)
O1	3.1(1)	4.2(1)	6.3(2)	-0.2(1)	0.9(1)	-0.2(1)	4.50(8)
O2	5.9(2)	3.9(1)	3.3(1)	-0.3(1)	-1.0(1)	0.2(1)	4.45(7)
O3	9.3(3)	7.0(2)	9.1(3)	2.9(2)	0.9(2)	1.3(2)	8.4(1)
C1	5.7(3)	6.4(3)	5.1(3)	-2.7(2)	-1.5(2)	0.1(2)	5.8(1)
C2	3.0(2)	7.9(3)	3.8(2)	-1.1(2)	-0.5(2)	-1.1(2)	4.9(1)
C3	2.7(2)	16.1(5)	5.1(3)	-1.8(3)	-0.4(2)	-2.4(3)	8.0(2)
C4	6.8(3)	20.5(6)	4.8(3)	-7.9(3)	1.1(3)	-1.9(4)	10.6(2)
C5	11.2(4)	10.1(3)	5.6(3)	-8.0(3)	-2.5(3)	2.3(3)	9.1(2)
C6	23.6(9)	9.4(5)	9.2(5)	6.1(5)	-6.2(5)	-1.3(4)	14.4(3)
C7	6.5(4)	22.0(8)	6.1(4)	-2.6(4)	0.7(3)	3.8(4)	11.5(3)
C8	9.2(4)	10.8(4)	4.6(3)	-2.1(4)	-1.1(3)	-1.2(3)	8.3(2)
C10	4.0(2)	3.4(2)	4.4(2)	1.1(2)	-0.6(2)	-0.7(2)	4.0(1)
C11	3.6(2)	3.6(2)	5.6(3)	-0.0(2)	1.3(2)	-1.4(2)	4.2(1)
C12	5.8(3)	3.3(2)	3.6(2)	0.2(2)	0.3(2)	-0.6(2)	4.2(1)
C13	3.8(2)	3.1(2)	5.9(3)	0.0(2)	-0.9(2)	-1.2(2)	4.3(1)
C14	4.2(2)	2.8(2)	5.1(2)	0.3(2)	1.6(2)	0.1(2)	4.0(1)
C15	8.0(4)	6.4(3)	9.2(4)	3.7(3)	-3.6(3)	-2.6(3)	8.0(2)

Table Ia. (cont.)

Table of General Temperature Factor Expressions - B's (Continued)

Name	B(1,1)	B(2,2)	B(3,3)	B(1,2)	B(1,3)	B(2,3)	Beqv
C16	5.9(3)	5.2(3)	13.4(5)	-Ø.3(3)	4.2(3)	-2.8(3)	8.Ø(2)
C17	15.9(6)	6.5(3)	4.1(3)	Ø.3(4)	-Ø.4(4)	-1.5(3)	8.9(2)
C18	4.1(3)	5.8(3)	14.5(5)	Ø.1(2)	-1.5(3)	-3.8(3)	8.2(2)
C19	11.2(4)	4.Ø(3)	8.3(4)	Ø.7(3)	4.3(3)	1.3(3)	7.7(2)
C2Ø	3.4(2)	3.4(2)	6.1(3)	-Ø.7(2)	-Ø.Ø(2)	Ø.5(2)	4.3(1)
C21	7.2(3)	2.6(2)	3.9(2)	Ø.3(2)	-Ø.8(2)	Ø.4(2)	4.6(1)
C22	4.Ø(2)	3.Ø(2)	7.7(3)	Ø.5(2)	1.4(2)	1.7(2)	4.8(1)
C23	6.4(3)	4.1(2)	4.6(3)	-1.2(2)	-1.3(2)	1.7(2)	5.1(1)
C24	6.5(3)	3.3(2)	5.1(3)	-Ø.6(2)	2.5(2)	Ø.5(2)	4.9(1)
C25	5.7(3)	4.8(3)	19.6(7)	-1.2(3)	-3.6(4)	1.9(4)	1Ø.2(2)
C26	2Ø.2(7)	3.8(3)	5.5(3)	1.Ø(4)	2.Ø(4)	-Ø.2(3)	9.8(2)
C27	5.8(3)	5.3(3)	19.6(7)	1.6(3)	3.2(4)	4.3(4)	1Ø.2(2)
C28	17.5(6)	7.9(4)	8.7(4)	-4.2(4)	-7.7(4)	3.4(3)	11.7(2)
C29	17.Ø(5)	5.5(3)	12.Ø(4)	-1.1(4)	1Ø.4(3)	Ø.Ø(3)	11.1(2)
C3Ø	3.9(2)	3.Ø(2)	3.4(2)	-Ø.2(2)	-Ø.3(2)	-Ø.3(2)	3.4(1)
C31	3.4(2)	3.6(2)	3.6(2)	-Ø.Ø(2)	Ø.1(2)	Ø.1(2)	3.5(1)
C32	4.Ø(3)	7.2(3)	5.1(3)	1.4(2)	-Ø.2(2)	Ø.8(3)	5.5(1)

The form of the anisotropic thermal parameter is:

$$\exp[-Ø.25(h^2 a^{*2} B(1,1) + k^2 b^{*2} B(2,2) + l^2 c^{*2} B(3,3)' + 2hka^*b^*B(1,2) + 2hla^*c^*B(1,3) + 2klb^*c^*B(2,3))]$$, where a*,b*, and c* are reciprocal lattice constants.

Table II. $[(C_5Me_5)_2Ybbipy]^+[(C_5Me_5)_2YbCl_2]^-$

Table of Positional Parameters and Their Estimated Standard Deviations

Atom	x	y	z	$B(Å^2)$
YB1	0.55087(2)	-0.22087(1)	0.23286(1)	3.352(4)
YB2	0.06735(2)	0.28429(1)	0.26417(1)	3.302(4)
CL1	0.7467(1)	-0.1611(1)	0.32438(8)	5.80(3)
CL2	0.5014(1)	-0.38895(9)	0.30119(8)	6.01(3)
N1	0.1699(3)	0.3629(2)	0.3827(2)	3.59(7)
N2	-0.0034(3)	0.2058(2)	0.3837(2)	3.88(8)
C1	0.5467(4)	-0.2221(3)	0.0740(3)	4.2(1)
C2	0.5363(4)	-0.3238(3)	0.0951(3)	4.4(1)
C3	0.6520(4)	-0.3450(3)	0.1330(3)	4.6(1)
C4	0.7311(4)	-0.2555(3)	0.1366(3)	4.4(1)
C5	0.6663(4)	-0.1803(3)	0.1013(3)	4.2(1)
C6	0.4583(5)	-0.1770(4)	0.0136(3)	6.6(1)
C7	0.4271(5)	-0.3999(4)	0.0732(3)	6.6(1)
C8	0.6868(5)	-0.4461(4)	0.1574(4)	7.2(2)
C9	0.8679(4)	-0.2466(4)	0.1630(4)	6.9(1)
C10	0.7207(5)	-0.0742(4)	0.0880(4)	7.0(1)
C11	0.4148(4)	-0.0667(3)	0.2169(3)	4.3(1)
C12	0.3282(4)	-0.1521(3)	0.2193(3)	4.4(1)
C13	0.3393(4)	-0.1898(3)	0.2982(3)	4.9(1)
C14	0.4344(4)	-0.1309(3)	0.3445(3)	5.0(1)
C15	0.4807(4)	-0.0539(3)	0.2931(3)	4.5(1)
C16	0.4180(5)	0.0116(4)	0.1519(3)	6.6(1)
C17	0.2272(5)	-0.1876(4)	0.1563(4)	6.8(1)
C18	0.2527(5)	-0.2729(4)	0.3309(4)	7.6(2)
C19	0.4732(6)	-0.1432(5)	0.4324(3)	7.9(2)
C20	0.5737(5)	0.0337(4)	0.3185(4)	7.0(2)
C21	-0.0021(4)	0.4440(3)	0.1964(3)	4.2(1)
C22	-0.0676(4)	0.3628(3)	0.1496(3)	4.7(1)
C23	-0.1519(4)	0.3116(4)	0.2006(3)	4.8(1)
C24	-0.1422(4)	0.3624(3)	0.2766(3)	4.3(1)
C25	-0.0495(4)	0.4436(3)	0.2740(3)	4.2(1)
C26	0.0885(5)	0.5233(4)	0.1646(3)	6.0(1)
C27	-0.0666(6)	0.3480(4)	0.0594(3)	7.0(1)
C28	-0.2472(5)	0.2257(5)	0.1747(4)	7.5(2)
C29	-0.2276(5)	0.3433(4)	0.3442(3)	6.1(1)
C30	-0.0226(5)	0.5246(4)	0.3381(3)	5.7(1)
C31	0.2889(4)	0.2397(4)	0.2389(3)	5.7(1)
C32	0.2236(4)	0.2378(3)	0.1614(3)	5.0(1)
C33	0.1322(5)	0.1557(4)	0.1611(3)	5.5(1)
C34	0.1405(5)	0.1099(3)	0.2362(3)	5.5(1)
C35	0.2350(5)	0.1606(4)	0.2848(3)	5.9(1)
C36	0.4059(5)	0.3060(5)	0.2616(5)	9.7(2)

Table of Positional Parameters and Their Estimated Standard Deviations (cont.)

Atom	x	y	z	$B(A^2)$
C37	0.2611(6)	0.2995(4)	0.0905(4)	8.2(2)
C38	0.0508(6)	0.1118(5)	0.0883(4)	8.6(2)
C39	0.0706(7)	0.0113(4)	0.2573(4)	9.3(2)
C40	0.2815(6)	0.1274(5)	0.3681(4)	8.7(2)
C50	-0.0932(4)	0.1301(3)	0.3821(3)	5.0(1)
C51	-0.1349(5)	0.0853(4)	0.4507(3)	5.9(1)
C52	-0.0830(5)	0.1204(4)	0.5248(3)	6.3(1)
C53	0.0105(4)	0.1978(4)	0.5286(3)	5.1(1)
C54	0.0494(4)	0.2386(3)	0.4564(3)	3.69(9)
C55	0.1511(4)	0.3218(3)	0.4556(2)	3.44(9)
C56	0.2217(4)	0.3554(3)	0.5254(3)	4.4(1)
C57	0.3109(4)	0.4356(4)	0.5210(3)	5.0(1)
C58	0.3273(4)	0.4800(3)	0.4472(3)	4.9(1)
C59	0.2564(4)	0.4411(3)	0.3799(3)	4.3(1)

* -- Atoms refined with isotropic thermal parameters.
Anisotropically refined atoms are given in the form of the isotropic equivalent thermal parameter defined as:

$$(4/3) * [a^2*B(1,1) + b^2*B(2,2) + c^2*B(3,3) + ab(\cos\ \text{gamma})*B(1,2) + ac(\cos\ \text{beta})*B(1,3) + bc(\cos\ \text{alpha})*B(2,3)]$$

Table II. (cont.)

Table of Positional Parameters and Their Estimated Standard Deviations (cont.)

Atom	x	y	z	B(Å^2)
H61	0.4804	-0.1898	-0.0401	8.0**
H62	0.3761	-0.2060	0.0197	8.0**
H63	0.4628	-0.1068	0.0232	8.0**
H71	0.4367	-0.4299	0.0218	8.0**
H72	0.4230	-0.4500	0.1135	8.0**
H73	0.3527	-0.3678	0.0706	8.0**
H81	0.7208	-0.4770	0.1131	8.0**
H82	0.7466	-0.4392	0.2026	8.0**
H83	0.6150	-0.4862	0.1721	8.0**
H91	0.9136	-0.2626	0.1183	8.0**
H92	0.8938	-0.1801	0.1814	8.0**
H93	0.8823	-0.2916	0.2060	8.0**
H101	0.7594	-0.0712	0.0379	8.0**
H102	0.6563	-0.0310	0.0862	8.0**
H103	0.7804	-0.0539	0.1314	8.0**
H161	0.3592	0.0575	0.1615	8.0**
H162	0.4987	0.0463	0.1532	9.0**
H163	0.3981	-0.0198	0.1000	9.0**
H171	0.1565	-0.1526	0.1631	9.0**
H172	0.2553	-0.1754	0.1036	9.0**
H173	0.2056	-0.2573	0.1621	9.0**
H181	0.1833	-0.2454	0.3513	9.0**
H182	0.2250	-0.3199	0.2884	9.0**
H183	0.2957	-0.3055	0.3736	9.0**
H191	0.4235	-0.1069	0.4650	9.0**
H192	0.4628	-0.2120	0.4455	9.0**
H193	0.5580	-0.1184	0.4425	9.0**
H201	0.5315	0.0866	0.3385	9.0**
H202	0.6309	0.0137	0.3600	9.0**
H203	0.6172	0.0560	0.2729	9.0**
H261	0.0448	0.5757	0.1421	8.0**
H262	0.1453	0.5494	0.2079	8.0**
H263	0.1327	0.4951	0.1237	8.0**
H271	-0.1260	0.3862	0.0326	8.0**
H272	0.0137	0.3692	0.0426	8.0**
H273	-0.0868	0.2792	0.0458	8.0**
H281	-0.3210	0.2512	0.1530	8.0**
H282	-0.2154	0.1862	0.1343	8.0**
H283	-0.2650	0.1857	0.2205	8.0**
H291	-0.2975	0.3802	0.3351	8.0**
H292	-0.2546	0.2739	0.3455	8.0**
H293	-0.1845	0.3638	0.3948	8.0**

Table II. (cont.)

Table II. (cont.)

Table of Positional Parameters and Their Estimated Standard Deviations (cont.)

Atom	x	y	z	$B(A^2)$
H301	-0.0779	0.5746	0.3285	8.0**
H302	-0.0336	0.4969	0.3903	8.0**
H303	0.0606	0.5536	0.3361	8.0**
H361	0.4754	0.2740	0.2464	10.0**
H362	0.4034	0.3676	0.2341	10.0**
H363	0.4129	0.3183	0.3188	10.0**
H371	0.3193	0.2670	0.0619	10.0**
H372	0.1899	0.3075	0.0551	10.0**
H373	0.2979	0.3633	0.1096	10.0**
H381	0.0946	0.0664	0.0596	10.0**
H382	-0.0227	0.0773	0.1065	10.0**
H383	0.0294	0.1641	0.0532	10.0**
H391	0.1151	-0.0424	0.2413	10.0**
H392	0.0625	0.0093	0.3143	10.0**
H393	-0.0095	0.0051	0.2293	10.0**
H401	0.3425	0.0822	0.3623	10.0**
H402	0.3170	0.1841	0.3995	10.0**
H403	0.2141	0.0951	0.3948	10.0**
H501	-0.1300	0.1061	0.3307	7.0**
H511	-0.1984	0.0312	0.4469	7.0**
H521	-0.1113	0.0915	0.5734	7.0**
H531	0.0478	0.2228	0.5796	7.0**
H561	0.2091	0.3236	0.5758	7.0**
H571	0.3602	0.4598	0.5683	7.0**
H581	0.3864	0.5364	0.4428	7.0**
H591	0.2693	0.4710	0.3288	7.0**

* -- Atoms refined with isotropic thermal parameters.
** -- Atoms included but not refined.
Anisotropically refined atoms are given in the form of the isotropic equivalent thermal parameter defined as:

$$(4/3) * [a^2*B(1,1) + b^2*B(2,2) + c^2*B(3,3) + ab(\cos\ \text{gamma})*B(1,2) + ac(\cos\ \text{beta})*B(1,3) + bc(\cos\ \text{alpha})*B(2,3)]$$

Table of General Temperature Factor Expressions - B's

Name	B(1,1)	B(2,2)	B(3,3)	B(1,2)	B(1,3)	B(2,3)	Beqv
YB1	3.311(8)	3.608(8)	2.956(8)	0.024(7)	-0.149(6)	0.655(6)	3.326(4)
YB2	3.344(8)	3.517(8)	2.945(8)	0.294(7)	0.078(6)	0.361(6)	3.276(4)
CL1	4.83(5)	6.87(7)	5.17(6)	-0.12(5)	-1.75(5)	0.37(5)	5.76(3)
CL2	7.59(7)	4.74(5)	5.62(6)	-0.03(5)	0.91(5)	2.11(5)	5.99(3)
N1	3.5(1)	3.8(1)	3.3(1)	0.2(1)	-0.1(1)	0.5(1)	3.56(7)
N2	3.4(1)	4.4(2)	3.8(2)	0.1(1)	-0.1(1)	0.5(1)	3.89(8)
C1	4.0(2)	5.5(2)	3.2(2)	1.4(2)	0.0(2)	0.5(2)	4.2(1)
C2	3.3(2)	5.4(2)	4.3(2)	0.4(2)	0.3(2)	-0.4(2)	4.4(1)
C3	4.5(2)	4.8(2)	4.4(2)	1.5(2)	-0.1(2)	-0.0(2)	4.5(1)
C4	3.2(2)	6.0(2)	4.0(2)	0.9(2)	0.2(2)	-0.1(2)	4.4(1)
C5	4.2(2)	4.9(2)	3.7(2)	0.4(2)	1.0(2)	0.6(2)	4.2(1)
C6	7.0(3)	9.1(3)	3.9(2)	3.2(2)	-0.9(2)	1.2(2)	6.5(1)
C7	5.9(3)	7.0(3)	6.5(3)	-0.8(2)	0.2(2)	-2.3(2)	6.6(1)
C8	7.3(3)	6.0(3)	8.4(3)	2.9(2)	0.4(3)	0.2(3)	7.1(2)
C9	3.4(2)	9.1(3)	8.0(3)	0.9(2)	0.0(2)	-0.4(3)	6.8(2)
C10	7.0(3)	6.6(3)	7.4(3)	-0.5(2)	2.7(2)	1.5(2)	6.9(1)
C11	4.1(2)	3.8(2)	5.0(2)	1.0(2)	0.6(2)	0.3(2)	4.3(1)
C12	3.3(2)	4.7(2)	5.1(2)	0.5(2)	0.2(2)	-0.8(2)	4.4(1)
C13	4.3(2)	4.5(2)	5.8(2)	-0.9(2)	1.8(2)	-0.7(2)	4.9(1)
C14	5.4(2)	5.2(2)	4.4(2)	-0.1(2)	0.9(2)	-0.7(2)	5.0(1)
C15	4.3(2)	3.8(2)	5.3(2)	-0.1(2)	0.8(2)	-0.3(2)	4.5(1)

Table IIa.

Table of General Temperature Factor Expressions - B's (Continued)

Name	B(1,1)	B(2,2)	B(3,3)	B(1,2)	B(1,3)	B(2,3)	Beqv
C16	7.7(3)	6.Ø(2)	7.Ø(3)	2.6(2)	1.8(2)	2.1(2)	6.7(1)
C17	4.2(2)	7.7(3)	8.3(3)	1.1(2)	-Ø.3(2)	-2.3(3)	6.8(1)
C18	6.3(3)	6.1(3)	1Ø.5(4)	-1.3(2)	4.3(2)	Ø.3(3)	7.6(2)
C19	1Ø.5(4)	8.7(4)	4.3(3)	Ø.2(3)	Ø.7(3)	-Ø.1(3)	7.9(2)
C2Ø	5.4(3)	4.9(2)	1Ø.2(4)	-1.Ø(2)	Ø.3(3)	-Ø.7(3)	7.Ø(2)
C21	3.9(2)	4.4(2)	4.4(2)	Ø.9(2)	-Ø.2(2)	1.3(2)	4.2(1)
C22	4.7(2)	5.3(2)	3.8(2)	Ø.7(2)	-Ø.7(2)	Ø.6(2)	4.7(1)
C23	3.8(2)	5.6(2)	4.6(2)	-Ø.6(2)	-1.Ø(2)	Ø.8(2)	4.8(1)
C24	2.9(2)	5.2(2)	4.6(2)	Ø.8(2)	-Ø.Ø(2)	1.1(2)	4.2(1)
C25	4.Ø(2)	4.3(2)	4.5(2)	1.3(2)	-Ø.3(2)	Ø.6(2)	4.2(1)
C26	5.6(3)	5.2(2)	6.9(3)	Ø.Ø(2)	Ø.6(2)	2.Ø(2)	5.9(1)
C27	8.1(3)	9.Ø(3)	3.5(2)	1.Ø(3)	-1.Ø(2)	1.1(2)	6.9(2)
C28	5.5(3)	8.4(3)	7.8(3)	-1.8(3)	-1.4(3)	Ø.Ø(3)	7.5(2)
C29	4.4(2)	7.Ø(3)	7.1(3)	1.Ø(2)	1.7(2)	1.Ø(2)	6.1(1)
C3Ø	5.8(2)	5.3(2)	6.1(3)	1.4(2)	Ø.4(2)	-Ø.5(2)	5.7(1)
C31	4.2(2)	5.5(2)	7.7(3)	1.3(2)	1.4(2)	-1.5(2)	5.7(1)
C32	5.1(2)	5.3(2)	4.9(2)	Ø.9(2)	2.3(2)	-Ø.1(2)	5.Ø(1)
C33	5.8(2)	5.4(2)	5.4(2)	Ø.5(2)	1.4(2)	-Ø.9(2)	5.5(1)
C34	6.9(3)	4.1(2)	5.6(2)	Ø.9(2)	1.8(2)	Ø.1(2)	5.5(1)
C35	6.4(2)	5.4(2)	6.5(3)	2.8(2)	1.4(2)	Ø.7(2)	5.9(1)
C36	4.Ø(2)	9.8(4)	15.3(5)	Ø.8(3)	1.3(3)	-4.1(4)	9.7(2)

Table IIa. (cont.)

Table IIa. (cont.)

Table of General Temperature Factor Expressions - B's (Continued)

Name	B(1,1)	B(2,2)	B(3,3)	B(1,2)	B(1,3)	B(2,3)	Beqv
C37	9.7(3)	7.4(3)	8.3(3)	1.5(3)	5.1(2)	2.2(3)	8.2(2)
C38	10.2(4)	7.8(3)	7.5(3)	-0.2(3)	0.7(3)	-3.3(3)	8.6(2)
C39	12.9(4)	4.0(3)	11.4(4)	-0.2(3)	5.6(3)	0.2(3)	9.3(2)
C40	9.9(3)	10.2(3)	6.8(3)	6.0(2)	0.4(3)	1.5(3)	8.6(2)
C50	4.5(2)	5.0(2)	5.2(2)	-0.7(2)	-0.4(2)	0.7(2)	5.0(1)
C51	4.7(2)	5.7(2)	7.0(3)	-1.0(2)	0.3(2)	2.6(2)	5.9(1)
C52	5.9(3)	7.3(3)	5.1(2)	-1.1(2)	0.6(2)	2.7(2)	6.2(1)
C53	5.2(2)	5.7(2)	4.0(2)	-0.4(2)	0.3(2)	1.2(2)	5.0(1)
C54	3.6(2)	3.8(2)	3.7(2)	0.6(2)	0.2(2)	1.0(1)	3.66(9)
C55	3.0(2)	4.1(2)	3.3(2)	0.4(1)	-0.0(1)	0.5(1)	3.45(9)
C56	4.9(2)	5.1(2)	3.2(2)	0.7(2)	-0.0(2)	0.9(2)	4.4(1)
C57	4.9(2)	5.4(2)	4.3(2)	0.1(2)	-1.2(2)	0.1(2)	4.9(1)
C58	4.3(2)	5.2(2)	4.9(2)	-1.0(2)	-0.6(2)	0.7(2)	4.9(1)
C59	4.0(2)	4.4(2)	4.2(2)	-0.1(2)	0.0(2)	0.8(2)	4.2(1)

The form of the anisotropic thermal parameter is:

$$\exp[-0.25(h^2 a^{*2} B(1,1) + k^2 b^{*2} B(2,2) + l^2 c^{*2} B(3,3) + 2hka^*b^*B(1,2) + 2hla^*c^*B(1,3) + 2klb^*c^*B(2,3))]$$

, where a*,b*, and c* are reciprocal lattice constants.

Table III. 2,2'-bipyrimidine

Table of Positional Parameters and Their Estimated Standard Deviations

Atom	x	y	z	$B(A^2)$
N1	Ø.417Ø(3)	Ø.15441(7)	Ø.4233Ø(9)	2.14(2)
N2	Ø.6512(3)	-Ø.Ø2474(8)	Ø.32164(9)	2.Ø3(2)
C1	Ø.5194(3)	Ø.Ø3595(8)	Ø.4295(1)	1.6Ø(2)
C2	Ø.4531(3)	Ø.2164(1)	Ø.2965(1)	2.45(2)
C3	Ø.5911(3)	Ø.1645(1)	Ø.1792(1)	2.42(2)
C4	Ø.6851(3)	Ø.Ø419(1)	Ø.1973(1)	2.37(2)
H2	Ø.364(4)	Ø.299(1)	Ø.289(1)	3.1(3)*
H3	Ø.623(4)	Ø.212(1)	Ø.Ø94(1)	3.4(3)*
H4	Ø.783(4)	-Ø.ØØ2(1)	Ø.114(1)	3.1(3)*

* -- Atoms refined with isotropic thermal parameters.

Anisotropically refined atoms are given in the form of the isotropic equivalent thermal parameter defined as:

$(4/3) * [a^2*B(1,1) + b^2*B(2,2) + c^2*B(3,3) + ab(\cos \text{gamma})*B(1,2)$

$+ ac(\cos \text{beta})*B(1,3) + bc(\cos \text{alpha})*B(2,3)]$

H4	Ø.783(4)	-Ø.ØØ2(1)	Ø.114(1)	3.1(3)*

** -- Atoms included but not refined.

Table of General Temperature Factor Expressions - B's

Name	B(1,1)	B(2,2)	B(3,3)	B(1,2)	B(1,3)	B(2,3)	Beqv
N1	2.79(4)	1.54(3)	2.20(3)	0.12(3)	0.75(3)	0.14(2)	2.14(2)
N2	2.56(4)	1.89(3)	1.74(3)	0.07(3)	0.67(3)	-0.08(2)	2.03(2)
C1	1.69(4)	1.45(3)	1.63(3)	-0.18(3)	0.24(3)	-0.12(3)	1.60(2)
C2	2.90(4)	1.74(3)	2.76(4)	0.00(4)	0.68(3)	0.53(3)	2.45(2)
C3	2.48(4)	2.76(4)	2.04(4)	-0.32(4)	0.48(3)	0.81(3)	2.42(2)
C4	2.65(4)	2.74(4)	1.83(3)	0.03(4)	0.73(3)	0.05(3)	2.37(2)

The form of the anisotropic thermal parameter is:

$$\exp[-0.25(h^2 a^{*2} B(1,1) + k^2 b^{*2} B(2,2) + l^2 c^{*2} B(3,3) + 2hka^*b^*B(1,2) + 2hla^*c^*B(1,3) + 2klb^*c^*B(2,3))]$$

, where a*,b*, and c* are reciprocal lattice constants.

Table IIIa.

Table IV. $(C_5Me_5)_4Yb_3(\mu_2\text{-}C{\equiv}CPh)_4$

Table of Positional Parameters and Their Estimated Standard Deviations

Atom	x	y	z	B(Å^2)
YB1	Ø.13852(2)	Ø.1713Ø(3)	Ø.14861(1)	3.224(9)
YB2	Ø.36922(2)	Ø.32421(4)	Ø.36Ø64(1)	3.6Ø(1)
YB3	Ø.251Ø9(3)	Ø.25422(4)	Ø.25425(2)	5.24(1)
C1	Ø.21Ø7(5)	Ø.Ø986(8)	Ø.212Ø(3)	4.3(2)
C2	Ø.232Ø(5)	Ø.Ø323(8)	Ø.24Ø1(4)	4.2(2)
C3	Ø.25ØØ(5)	-Ø.Ø544(7)	Ø.2711(4)	4.Ø(2)
C4	Ø.3Ø9Ø(7)	-Ø.113(1)	Ø.2597(4)	7.1(3)
C5	Ø.3278(8)	-Ø.192(1)	Ø.2915(5)	9.4(4)
C6	Ø.2886(7)	-Ø.2149(9)	Ø.3318(4)	7.1(3)
C7	Ø.2334(7)	-Ø.1556(9)	Ø.3414(4)	7.2(3)
C8	Ø.2144(6)	-Ø.Ø781(8)	Ø.3136(4)	5.9(3)
C9	Ø.1832(5)	Ø.3263(7)	Ø.1799(4)	4.1(2)
C1Ø	Ø.1831(5)	Ø.4147(9)	Ø.1831(3)	5.Ø(3)
C11	Ø.1791(5)	Ø.5243(7)	Ø.1842(4)	4.4(2)
C12	Ø.1421(6)	Ø.5711(8)	Ø.2223(5)	5.8(3)
C13	Ø.1379(6)	Ø.6728(9)	Ø.2249(5)	6.8(3)
C14	Ø.1722(8)	Ø.726(1)	Ø.19Ø7(6)	9.4(4)
C15	Ø.2Ø81(8)	Ø.683(1)	Ø.1537(5)	9.1(4)
C16	Ø.2131(7)	Ø.5787(9)	Ø.1491(5)	7.Ø(3)
C17	Ø.3727(5)	Ø.3334(8)	Ø.271Ø(4)	4.3(2)
C18	Ø.3915(5)	Ø.3556(8)	Ø.2291(4)	4.3(2)
C19	Ø.4183(5)	Ø.3875(9)	Ø.1811(3)	4.9(3)
C2Ø	Ø.4669(7)	Ø.336(1)	Ø.1559(5)	8.2(4)
C21	Ø.4938(7)	Ø.371(1)	Ø.1112(5)	1Ø.9(5)
C22	Ø.4675(8)	Ø.454(1)	Ø.Ø918(5)	1Ø.9(5)
C23	Ø.4199(8)	Ø.5Ø8(1)	Ø.117Ø(5)	9.5(4)
C24	Ø.3941(7)	Ø.4799(9)	Ø.1614(4)	6.5(3)
C25	Ø.2523(5)	Ø.2443(7)	Ø.3486(4)	3.9(2)
C26	Ø.1969(5)	Ø.2Ø82(8)	Ø.3645(3)	4.4(2)
C27	Ø.1319(5)	Ø.1663(8)	Ø.3873(3)	4.6(2)
C28	Ø.1361(6)	Ø.Ø752(7)	Ø.4113(4)	5.2(3)
C29	Ø.Ø746(7)	Ø.Ø341(9)	Ø.433Ø(5)	6.7(3)
C3Ø	Ø.Ø1Ø1(7)	Ø.Ø85(1)	Ø.4279(5)	8.5(4)
C31	Ø.ØØ46(7)	Ø.169(1)	Ø.4Ø51(5)	9.3(5)
C32	Ø.Ø657(6)	Ø.211(1)	Ø.3846(4)	6.Ø(3)
C4Ø	Ø.Ø371(5)	Ø.213Ø(9)	Ø.2119(4)	5.Ø(3)
C41	Ø.Ø395(5)	Ø.1122(8)	Ø.2127(4)	4.6(3)
C42	Ø.Ø163(5)	Ø.Ø786(7)	Ø.165Ø(4)	4.4(2)
C43	-Ø.ØØ34(5)	Ø.1585(9)	Ø.1364(4)	4.9(3)
C44	Ø.Ø1Ø2(5)	Ø.2414(8)	Ø.1654(4)	4.6(3)
C45	Ø.Ø541(6)	Ø.Ø5Ø(1)	Ø.2566(5)	7.1(3)
C46	Ø.ØØ16(7)	-Ø.Ø263(9)	Ø.1522(6)	8.Ø(4)
C47	-Ø.Ø479(7)	Ø.161(1)	Ø.Ø878(5)	9.6(5)
C48	-Ø.ØØ58(7)	Ø.349(1)	Ø.1497(5)	7.7(4)

Table IV. (cont.)

Table of Positional Parameters and Their Estimated Standard Deviations (cont.)

Atom	x	y	z	$B(A^2)$
C49	Ø.Ø516(6)	Ø.281(1)	Ø.2566(4)	6.5(3)
C5Ø	Ø.2566(5)	Ø.1475(9)	Ø.Ø975(4)	5.4(3)
C51	Ø.2159(6)	Ø.Ø636(8)	Ø.Ø9ØØ(4)	5.6(3)
C52	Ø.1538(6)	Ø.Ø859(8)	Ø.Ø626(3)	5.2(3)
C53	Ø.1558(7)	Ø.1853(9)	Ø.Ø532(4)	6.2(3)
C54	Ø.2195(7)	Ø.2219(9)	Ø.Ø742(4)	6.3(3)
C55	Ø.1ØØ1(8)	Ø.Ø11(1)	Ø.Ø397(5)	1Ø.5(4)
C56	Ø.1Ø67(9)	Ø.243(1)	Ø.Ø189(5)	11.4(5)
C57	Ø.249(1)	Ø.324(1)	Ø.Ø675(6)	12.4(5)
C58	Ø.33Ø7(7)	Ø.15Ø(1)	Ø.1234(5)	1Ø.8(5)
C59	Ø.2381(8)	-Ø.Ø39(1)	Ø.1Ø63(5)	8.6(4)
C6Ø	Ø.376Ø(7)	Ø.5148(9)	Ø.3539(4)	6.9(3)
C61	Ø.4Ø21(7)	Ø.4976(9)	Ø.4ØØ2(5)	7.1(3)
C62	Ø.3484(8)	Ø.4612(9)	Ø.429Ø(5)	7.9(4)
C63	Ø.2837(6)	Ø.4538(8)	Ø.4Ø29(5)	7.Ø(3)
C64	Ø.2954(7)	Ø.4893(8)	Ø.354Ø(4)	8.2(3)
C65	Ø.412(1)	Ø.561(1)	Ø.31Ø3(6)	23.5(7)
C66	Ø.4779(9)	Ø.533(1)	Ø.4194(9)	2Ø.5(8)
C67	Ø.361(1)	Ø.442(2)	Ø.4872(6)	17.2(8)
C68	Ø.2163(8)	Ø.421(1)	Ø.4331(7)	15.2(5)
C69	Ø.2314(9)	Ø.492(1)	Ø.32Ø1(7)	23.9(5)
C7Ø	Ø.4948(6)	Ø.2598(9)	Ø.3958(5)	7.2(3)
C71	Ø.4886(5)	Ø.2261(9)	Ø.348Ø(4)	5.8(3)
C72	Ø.4322(6)	Ø.1576(8)	Ø.3451(5)	6.8(3)
C73	Ø.4Ø61(6)	Ø.151(1)	Ø.3928(5)	9.Ø(4)
C74	Ø.4437(7)	Ø.216(1)	Ø.423Ø(4)	9.3(4)
C75	Ø.434(1)	Ø.213(2)	Ø.4791(6)	22.7(6)
C76	Ø.351Ø(8)	Ø.Ø71(1)	Ø.4Ø63(8)	19.6(6)
C77	Ø.4156(9)	Ø.Ø96(1)	Ø.2985(6)	15.Ø(5)
C78	Ø.5452(7)	Ø.255(1)	Ø.3Ø45(6)	13.5(5)
C79	Ø.5557(7)	Ø.322(1)	Ø.4181(8)	18.7(6)
C8Ø	Ø.765(1)	Ø.217(1)	Ø.Ø226(6)	12.Ø(6)
C81	Ø.693(1)	Ø.238(1)	Ø.Ø3Ø7(5)	12.9(6)
C82	Ø.669(1)	Ø.335(1)	Ø.Ø16Ø(6)	12.7(6)
C83	Ø.72ØØ(9)	Ø.399(1)	-Ø.ØØ41(5)	9.7(5)
C84	Ø.785(1)	Ø.367(1)	-Ø.Ø1Ø6(6)	12.2(6)
C85	Ø.8Ø7(1)	Ø.274(2)	Ø.ØØ3Ø(6)	12.7(6)

Anisotropically refined atoms are given in the form of the isotropic equivalent thermal parameter defined as:

$$(4/3) * [a^2*B(1,1) + b^2*B(2,2) + c^2*B(3,3) + ab(\cos\ \text{gamma})*B(1,2)$$

$$+ ac(\cos\ \text{beta})*B(1,3) + bc(\cos\ \text{alpha})*B(2,3)]$$

Table IV. (cont.)

Table of Positional Parameters and Their Estimated Standard Deviations (cont.)

Atom	x	y	z	B(Å^2)
H41	0.3362	-0.1015	0.2303	9.1**
H51	0.3693	-0.2302	0.2844	11.2**
H61	0.2992	-0.2707	0.3520	9.0**
H71	0.2056	-0.1685	0.3702	9.1**
H81	0.1747	-0.0379	0.3237	7.9**
H121	0.1187	0.5326	0.2469	7.7**
H131	0.1115	0.7047	0.2504	8.7**
H141	0.1716	0.7960	0.1923	11.7**
H151	0.2308	0.7223	0.1295	11.1**
H161	0.2386	0.5493	0.1225	8.9**
H201	0.4839	0.2747	0.1683	10.0**
H211	0.5299	0.3380	0.0939	13.1**
H221	0.4817	0.4779	0.0602	13.6**
H231	0.4035	0.5692	0.1039	11.6**
H241	0.3607	0.5203	0.1791	8.4**
H281	0.1812	0.0409	0.4126	7.1**
H291	0.0769	-0.0261	0.4508	8.6**
H301	-0.0331	0.0582	0.4412	10.4**
H311	-0.0405	0.2034	0.4026	11.1**
H321	0.0616	0.2726	0.3679	7.9**
H451	0.0101	0.0390	0.2737	9.0**
H452	0.0741	-0.0108	0.2463	9.0**
H453	0.0878	0.0828	0.2781	9.0**
H461	-0.0465	-0.0427	0.1619	10.0**
H462	0.0062	-0.0354	0.1175	10.0**
H463	0.0354	-0.0671	0.1696	10.0**
H471	-0.0980	0.1546	0.0954	11.6**
H472	-0.0399	0.2219	0.0717	11.6**
H473	-0.0334	0.1085	0.0672	11.6**
H481	-0.0545	0.3656	0.1581	9.6**
H482	0.0268	0.3921	0.1669	9.6**
H483	0.0002	0.3559	0.1149	9.6**
H491	0.0084	0.2869	0.2754	8.5**
H492	0.0890	0.2532	0.2772	8.5**
H493	0.0662	0.3434	0.2452	8.5**
H551	0.1180	-0.0095	0.0083	12.6**
H552	0.0967	-0.0438	0.0612	12.6**
H553	0.0544	0.0413	0.0354	12.6**
H561	0.1245	0.2360	-0.0142	13.4**
H562	0.0594	0.2166	0.0205	13.4**
H563	0.1076	0.3090	0.0285	13.4**
H571	0.2762	0.3253	0.0374	14.4**
H572	0.2089	0.3683	0.0639	14.4**
H573	0.2781	0.3409	0.0947	14.4**

Table of Positional Parameters and Their Estimated Standard Deviations (cont.)

Atom	x	y	z	B(Å^2)
H581	Ø.3667	Ø.1399	Ø.ØØ92	12.7**
H582	Ø.3366	Ø.212Ø	Ø.1386	12.7**
H583	Ø.3324	Ø.Ø994	Ø.1475	12.7**
H591	Ø.2656	-Ø.Ø686	Ø.ØØØ9	1Ø.4**
H592	Ø.2659	-Ø.Ø349	Ø.1361	1Ø.4**
H593	Ø.1953	-Ø.Ø768	Ø.1118	1Ø.4**

** -- Atoms included but not refined.

Table IV. (cont.)

Table of General Temperature Factor Expressions - B's

Name	B(1,1)	B(2,2)	B(3,3)	B(1,2)	B(1,3)	B(2,3)	Beqv
YB1	3.67(2)	3.28(2)	2.72(2)	-Ø.ØØ8(2)	Ø.Ø3(1)	Ø.12(2)	3.224(9)
YB2	3.52(2)	4.Ø7(2)	3.2Ø(2)	-Ø.21(2)	-Ø.Ø1(2)	Ø.Ø2(2)	3.6Ø(1)
YB3	5.98(2)	5.93(2)	3.75(2)	-1.67(2)	-1.23(2)	Ø.3Ø(2)	5.24(1)
C1	4.2(5)	4.7(5)	4.Ø(4)	1.Ø(5)	Ø.Ø(4)	Ø.3(4)	4.3(2)
C2	3.7(5)	4.9(5)	4.Ø(5)	1.Ø(4)	Ø.8(4)	-Ø.5(4)	4.2(2)
C3	4.6(5)	3.4(4)	4.2(4)	1.2(4)	-1.Ø(4)	-Ø.7(4)	4.Ø(2)
C4	8.1(7)	6.7(7)	6.6(6)	2.3(6)	1.3(6)	Ø.7(6)	7.1(3)
C5	11.1(8)	8.7(8)	8.5(8)	5.9(7)	Ø.Ø(7)	Ø.4(7)	9.4(4)
C6	9.4(8)	5.8(6)	6.1(6)	2.6(6)	Ø.7(6)	2.8(5)	7.1(3)
C7	7.1(7)	8.Ø(7)	6.5(6)	2.2(6)	2.1(5)	4.3(5)	7.2(3)
C8	7.2(6)	5.4(6)	5.3(5)	1.4(6)	1.4(5)	1.6(5)	5.9(3)
C9	5.Ø(5)	2.7(4)	4.7(5)	Ø.Ø(4)	-Ø.3(4)	-Ø.3(4)	4.1(2)
C1Ø	4.1(5)	7.9(7)	3.Ø(4)	-Ø.3(5)	-Ø.3(4)	Ø.9(5)	5.Ø(3)
C11	5.2(5)	2.6(4)	5.3(5)	-Ø.4(4)	-2.1(4)	-Ø.2(4)	4.4(2)
C12	5.4(6)	3.4(5)	8.4(7)	Ø.4(5)	-Ø.2(5)	-1.Ø(5)	5.8(3)
C13	5.6(6)	5.8(6)	8.9(7)	1.9(6)	-Ø.1(6)	Ø.3(6)	6.8(3)
C14	9.5(9)	7.9(8)	1Ø.9(9)	1.1(8)	-Ø.6(8)	-3.7(8)	9.4(4)
C15	1Ø.9(9)	6.Ø(7)	1Ø.3(9)	-2.4(7)	-Ø.9(8)	3.Ø(7)	9.1(4)
C16	7.7(7)	5.3(7)	8.1(7)	-1.Ø(6)	2.2(6)	1.8(6)	7.Ø(3)
C17	3.9(4)	4.8(5)	4.1(4)	Ø.Ø(5)	Ø.1(4)	Ø.7(5)	4.3(2)
C18	4.5(5)	4.5(5)	3.9(4)	-Ø.6(4)	Ø.2(4)	-Ø.2(4)	4.3(2)

Table IVa.

Table of General Temperature Factor Expressions - B's (Continued)

Name	B(1,1)	B(2,2)	B(3,3)	B(1,2)	B(1,3)	B(2,3)	Beqv
C19	4.6(5)	6.7(6)	3.4(4)	-1.4(5)	Ø.1(4)	-Ø.9(5)	4.9(3)
C2Ø	8.2(7)	11(1)	5.5(6)	-2.5(8)	2.Ø(6)	-Ø.7(7)	8.2(4)
C21	8.8(8)	18(1)	5.7(6)	-4.3(9)	4.4(5)	-1.8(8)	1Ø.9(5)
C22	12(1)	16(1)	4.8(6)	-6.5(9)	-Ø.4(7)	2.8(7)	1Ø.9(5)
C23	13(1)	1Ø.6(9)	4.7(6)	-5.Ø(8)	-1.Ø(7)	Ø.5(7)	9.5(4)
C24	8.9(8)	5.6(6)	4.9(5)	-1.7(6)	-Ø.Ø(6)	1.9(5)	6.5(3)
C25	3.6(4)	3.9(5)	4.2(4)	Ø.3(4)	-Ø.1(4)	-Ø.1(4)	3.9(2)
C26	4.3(5)	5.7(6)	3.2(4)	1.Ø(5)	Ø.3(4)	-Ø.3(4)	4.4(2)
C27	4.5(5)	6.3(6)	3.1(4)	-1.4(5)	Ø.3(4)	-1.6(4)	4.6(2)
C28	6.4(6)	2.9(5)	6.2(6)	-Ø.9(5)	Ø.9(5)	-1.Ø(5)	5.2(3)
C29	7.3(7)	5.8(6)	7.Ø(6)	-2.7(6)	2.Ø(6)	Ø.2(6)	6.7(3)
C3Ø	6.4(6)	12(1)	7.Ø(7)	-4.5(7)	2.7(5)	-Ø.3(7)	8.5(4)
C31	6.4(7)	17(1)	5.Ø(6)	-Ø.8(9)	Ø.4(6)	-Ø.3(8)	9.3(5)
C32	4.1(5)	9.4(8)	4.4(5)	Ø.3(6)	Ø.4(4)	Ø.2(6)	6.Ø(3)
C4Ø	3.1(4)	7.2(7)	4.6(5)	-Ø.2(5)	Ø.4(4)	Ø.2(5)	5.Ø(3)
C41	3.7(5)	5.3(6)	4.9(5)	Ø.Ø(5)	1.2(4)	1.Ø(5)	4.6(3)
C42	4.1(5)	3.Ø(5)	6.1(5)	Ø.2(4)	-Ø.2(4)	Ø.5(4)	4.4(2)
C43	3.7(4)	7.Ø(7)	4.1(5)	Ø.4(5)	-Ø.8(4)	-Ø.2(5)	4.9(3)
C44	4.2(5)	4.5(5)	5.1(5)	Ø.5(4)	Ø.5(4)	1.6(4)	4.6(3)
C45	4.7(6)	8.8(8)	7.8(7)	Ø.6(6)	1.8(5)	3.1(6)	7.1(3)
C46	6.8(7)	3.8(6)	13(1)	-1.3(6)	2.5(7)	-1.8(7)	8.Ø(4)

Table IVa. (cont.)

Table of General Temperature Factor Expressions - B's (Continued)

Name	B(1,1)	B(2,2)	B(3,3)	B(1,2)	B(1,3)	B(2,3)	Beqv
C47	5.3(6)	17(1)	6.3(7)	-1.1(9)	-1.4(5)	Ø.9(9)	9.6(5)
C48	6.3(6)	8.5(8)	8.2(7)	2.7(6)	-Ø.Ø(6)	1.8(7)	7.7(4)
C49	6.7(6)	8.3(8)	4.7(5)	-1.1(6)	2.5(5)	-1.6(5)	6.5(3)
C5Ø	3.9(5)	7.8(7)	4.5(5)	-1.1(5)	1.1(4)	-1.7(5)	5.4(3)
C51	7.5(7)	5.1(6)	4.1(5)	1.Ø(6)	1.7(5)	Ø.3(5)	5.6(3)
C52	6.Ø(6)	6.4(6)	3.2(4)	-1.2(5)	Ø.8(4)	-2.Ø(4)	5.2(3)
C53	8.4(7)	6.1(6)	4.1(5)	3.4(6)	Ø.4(5)	Ø.8(5)	6.2(3)
C54	9.4(7)	4.7(6)	5.Ø(5)	-Ø.5(6)	4.1(5)	Ø.Ø(5)	6.3(3)
C55	9.2(8)	13.4(9)	9.Ø(7)	-4.7(7)	1.Ø(7)	-7.7(6)	1Ø.5(4)
C56	13(1)	15(1)	5.7(7)	6(1)	2.3(7)	3.7(8)	11.4(5)
C57	21(1)	4.1(7)	12.2(9)	-3.5(8)	1Ø.1(8)	-1.5(7)	12.4(5)
C58	7.1(7)	18(1)	7.8(8)	-3.3(9)	1.4(7)	-4.3(9)	1Ø.8(5)
C59	11.1(9)	8.6(9)	6.1(7)	2.3(8)	1.9(7)	-Ø.5(7)	8.6(4)
C6Ø	11.3(9)	3.9(6)	5.5(6)	Ø.3(6)	2.6(6)	-Ø.5(5)	6.9(3)
C61	7.6(7)	4.9(6)	8.7(7)	-Ø.7(6)	-1.5(6)	-1.6(6)	7.1(3)
C62	13(1)	3.6(6)	6.8(7)	-Ø.1(7)	2.2(7)	-1.2(5)	7.9(4)
C63	6.2(6)	3.9(5)	1Ø.8(8)	-Ø.7(5)	1.6(6)	-3.7(5)	7.Ø(3)
C64	11.7(7)	5.Ø(6)	7.5(6)	4.8(5)	-6.1(5)	-3.2(5)	8.2(3)
C65	48(2)	2.9(7)	2Ø.5(9)	4(1)	26.3(9)	3.2(7)	23.5(7)
C66	1Ø(1)	13(1)	38(2)	-1(1)	-8(1)	-1(1)	2Ø.5(8)
C67	33(2)	14(1)	4.7(7)	6(2)	-2(1)	-1.9(9)	17.2(8)

Table IVa. (cont.)

Table IVa. (cont.)

Table of General Temperature Factor Expressions - B's (Continued)

Name	B(1,1)	B(2,2)	B(3,3)	B(1,2)	B(1,3)	B(2,3)	Beqv
C68	13.Ø(8)	8.1(9)	25(1)	-3.2(8)	15.Ø(7)	-5.9(9)	15.2(5)
C69	27.8(9)	16.Ø(9)	27(1)	19.Ø(6)	-23.(7)	-13.(9)	23.9(5)
C7Ø	6.1(6)	6.1(7)	9.3(7)	1.1(6)	-3.5(5)	-2.5(6)	7.2(3)
C71	4.3(5)	6.3(6)	6.7(6)	2.1(5)	1.6(5)	2.8(5)	5.8(3)
C72	6.2(6)	3.5(5)	1Ø.6(8)	1.Ø(5)	-3.Ø(6)	Ø.5(6)	6.8(3)
C73	5.2(6)	9.Ø(7)	13.Ø(8)	1.9(6)	3.3(6)	7.7(6)	9.Ø(4)
C74	1Ø.4(8)	13.2(9)	4.4(6)	6.8(7)	Ø.7(6)	2.7(6)	9.3(4)
C75	35(2)	28(1)	4.8(7)	26(1)	4.Ø(9)	5.5(8)	22.7(6)
C76	6.4(8)	13.5(8)	39(2)	Ø.6(7)	5(1)	19.6(8)	19.6(6)
C77	18(1)	9.3(8)	17(1)	8.3(8)	-11.(8)	-7.4(8)	15.Ø(5)
C78	6.5(7)	2Ø(1)	14(1)	4.2(9)	5.2(7)	1Ø.6(9)	13.5(5)
C79	8.9(7)	9(1)	38(2)	1.9(8)	-14.(8)	-8(1)	18.7(6)
C8Ø	18(1)	1Ø(1)	7.8(8)	4(1)	-2.7(9)	-1.6(9)	12.Ø(6)
C81	2Ø(1)	13(1)	6.Ø(8)	-9(1)	-Ø.Ø(9)	-1.3(8)	12.9(6)
C82	16(1)	12(1)	1Ø(1)	-2(1)	2(1)	-3(1)	12.7(6)
C83	12(1)	9.1(9)	7.7(8)	2.7(9)	2.Ø(8)	-1.2(8)	9.7(5)
C84	16(1)	12(1)	8.1(9)	2(1)	1.7(9)	-1.2(9)	12.2(6)
C85	13(1)	16(2)	9(1)	4(1)	Ø.6(9)	-2(1)	12.7(6)

The form of the anisotropic thermal parameter is:

$$\exp[-Ø.25(h^2 a^{*2} B(1,1) + k^2 b^{*2} B(2,2) + l^2 c^{*2} B(3,3) + 2hka^*b^*B(1,2) + 2hla^*c^*B(1,3) + 2klb^*c^*B(2,3))]$$ where a*,b*, and c* are reciprocal lattice constants.

Table V. $(C_5Me_5)_2Eu_2(\mu_2\text{-}C{\equiv}CPh)_2(THF)_4$

Table of Positional Parameters and Their Estimated Standard Deviations

Atom	x	y	z	B(Å^2)
EU1	Ø.ØØ3Ø1(2)	Ø.Ø5139(3)	Ø.ØØ98Ø4(2)	3.648(8)
O1	Ø.1ØØØ(3)	Ø.1693(4)	Ø.12Ø3(4)	6.2(2)
O2	-Ø.Ø71Ø(4)	Ø.2Ø11(4)	Ø.ØØ99Ø(4)	6.8(2)
C1	Ø.1Ø39(5)	-Ø.Ø198(5)	Ø.ØØ46(5)	4.4(2)
C2	Ø.1717(5)	-Ø.Ø311(5)	Ø.Ø1ØØ(4)	4.2(2)
C3	Ø.254Ø(4)	-Ø.Ø43Ø(5)	Ø.Ø188(4)	4.2(2)
C4	Ø.3Ø11(5)	-Ø.Ø597(7)	-Ø.Ø369(6)	7.6(3)
C5	Ø.383Ø(6)	-Ø.Ø7Ø3(8)	-Ø.Ø264(6)	8.5(4)
C6	Ø.4116(6)	-Ø.Ø611(7)	Ø.Ø393(7)	8.1(3)
C7	Ø.3663(6)	-Ø.Ø463(7)	Ø.Ø964(6)	7.9(3)
C8	Ø.2875(5)	-Ø.Ø354(7)	Ø.Ø854(5)	6.2(3)
C11	Ø.Ø288(5)	-Ø.Ø894(6)	Ø.1925(5)	4.7(2)
C12	-Ø.Ø488(5)	-Ø.Ø938(6)	Ø.1729(5)	4.8(2)
C13	-Ø.Ø885(4)	-Ø.Ø239(6)	Ø.2Ø53(5)	4.9(2)
C14	-Ø.Ø335(5)	Ø.Ø258(6)	Ø.2426(5)	4.6(2)
C15	Ø.Ø377(5)	-Ø.Ø148(6)	Ø.2352(4)	4.6(2)
C16	Ø.Ø937(6)	-Ø.1531(7)	Ø.1716(6)	8.Ø(3)
C17	-Ø.Ø828(7)	-Ø.1651(8)	Ø.129Ø(6)	8.8(3)
C18	-Ø.1746(5)	-Ø.ØØ86(8)	Ø.2Ø13(6)	7.9(3)
C19	-Ø.Ø489(7)	Ø.1Ø36(8)	Ø.2873(6)	7.5(3)
C2Ø	Ø.1137(6)	Ø.ØØ99(9)	Ø.2698(6)	8.4(4)
C21	Ø.11Ø1(6)	Ø.2279(8)	Ø.1788(6)	8.3(4)
C22	Ø.1763(6)	Ø.1882(7)	Ø.Ø792(6)	7.3(3)
C23	Ø.2359(6)	Ø.2156(9)	Ø.1281(8)	1Ø.1(4)
C24	Ø.1962(6)	Ø.2448(8)	Ø.1935(7)	9.8(4)
C31	-Ø.Ø636(8)	Ø.251Ø(9)	Ø.Ø338(8)	11.8(5)
C32	-Ø.12ØØ(7)	Ø.3148(9)	Ø.Ø34(1)	18.2(6)
C33	-Ø.1719(8)	Ø.293(1)	Ø.ØØ3(1)	16.9(7)
C34	-Ø.1389(8)	Ø.23Ø(1)	Ø.1331(8)	14.8(5)

* -- Atoms refined with isotropic thermal parameters.
Anisotropically refined atoms are given in the form of the isotropic equivalent thermal parameter defined as:

$$(4/3) * [a^2*B(1,1) + b^2*B(2,2) + c^2*B(3,3) + ab(\cos\gamma)*B(1,2) + ac(\cos\beta)*B(1,3) + bc(\cos\alpha)*B(2,3)]$$

Table of Positional Parameters and Their Estimated Standard Deviations (cont.)

Atom	x	y	z	B(Å^2)
H41	Ø.2799	-Ø.Ø645	-Ø.Ø836	8.Ø**
H51	Ø.4161	-Ø.Ø836	-Ø.Ø654	8.Ø**
H61	Ø.466Ø	-Ø.Ø652	Ø.Ø46Ø	8.Ø**
H71	Ø.3878	-Ø.Ø433	Ø.1431	8.Ø**
H81	Ø.2554	-Ø.Ø223	Ø.1251	8.Ø**
H161	Ø.Ø974	-Ø.1974	Ø.2Ø66	8.Ø**
H162	Ø.Ø821	-Ø.1782	Ø.1265	8.Ø**
H163	Ø.1416	-Ø.123Ø	Ø.1687	8.Ø**
H171	-Ø.Ø985	-Ø.2111	Ø.1593	8.Ø**
H172	-Ø.1264	-Ø.1438	Ø.1Ø35	8.Ø**
H173	-Ø.Ø45Ø	-Ø.1856	Ø.Ø961	8.Ø**
H181	-Ø.1994	-Ø.Ø369	Ø.24Ø1	8.Ø**
H182	-Ø.1848	Ø.Ø518	Ø.2Ø38	8.Ø**
H183	-Ø.1941	-Ø.Ø3Ø9	Ø.1576	8.Ø**
H191	-Ø.Ø6Ø4	Ø.Ø861	Ø.3347	8.Ø**
H192	-Ø.ØØ44	Ø.1398	Ø.2875	8.Ø**
H193	-Ø.Ø917	Ø.1345	Ø.2682	8.Ø**
H2Ø1	Ø.1174	-Ø.Ø169	Ø.3153	8.Ø**
H2Ø2	Ø.1554	-Ø.ØØ88	Ø.24Ø6	8.Ø**
H2Ø3	Ø.116Ø	Ø.Ø71Ø	Ø.2752	8.Ø**
H211	Ø.Ø861	Ø.2Ø29	Ø.2195	1Ø.Ø**
H212	Ø.Ø845	Ø.28Ø4	Ø.1669	1Ø.Ø**
H221	Ø.1656	Ø.2331	Ø.Ø459	1Ø.Ø**
H222	Ø.1926	Ø.1379	Ø.Ø542	1Ø.Ø**
H231	Ø.265Ø	Ø.2617	Ø.1Ø8Ø	1Ø.Ø**
H232	Ø.2696	Ø.1686	Ø.1387	1Ø.Ø**
H241	Ø.2Ø53	Ø.3Ø47	Ø.2Ø15	1Ø.Ø**
H242	Ø.2133	Ø.2126	Ø.2337	1Ø.Ø**

* -- Atoms refined with isotropic thermal parameters.
** -- Atoms included but not refined.
Anisotropically refined atoms are given in the form of the isotropic equivalent thermal parameter defined as:

$$(4/3) * [a^2*B(1,1) + b^2*B(2,2) + c^2*B(3,3) + ab(\cos\ \text{gamma})*B(1,2) + ac(\cos\ \text{beta})*B(1,3) + bc(\cos\ \text{alpha})*B(2,3)]$$

Table V. (cont.)

Table of General Temperature Factor Expressions - B's

Name	B(1,1)	B(2,2)	B(3,3)	B(1,2)	B(1,3)	B(2,3)	Beqv
EU1	3.5Ø(2)	4.22(2)	3.23(2)	-Ø.17(3)	Ø.13(2)	Ø.Ø2(2)	3.648(8)
O1	6.Ø(3)	6.Ø(3)	6.4(4)	-1.9(3)	Ø.3(3)	-1.7(3)	6.2(2)
O2	6.6(3)	5.6(3)	8.4(5)	1.6(3)	-Ø.8(4)	-Ø.5(4)	6.8(2)
C1	3.5(4)	5.3(6)	4.5(4)	Ø.2(3)	-Ø.2(4)	Ø.1(5)	4.4(2)
C2	3.8(4)	5.Ø(5)	3.7(4)	Ø.2(3)	-Ø.1(3)	-Ø.8(4)	4.2(2)
C3	3.1(3)	4.7(4)	4.8(4)	Ø.Ø(4)	-Ø.3(4)	Ø.9(4)	4.2(2)
C4	4.2(4)	12.6(8)	5.9(6)	3.1(5)	Ø.3(4)	2.4(6)	7.6(3)
C5	6.3(6)	12.3(9)	6.9(7)	1.7(6)	2.2(5)	2.5(6)	8.5(4)
C6	4.7(5)	9.9(8)	9.8(8)	1.1(6)	Ø.1(6)	2.9(6)	8.1(3)
C7	5.9(5)	8.1(7)	9.8(8)	-Ø.7(5)	-3.3(5)	-Ø.4(7)	7.9(3)
C8	4.7(4)	6.5(6)	7.4(7)	Ø.7(4)	-1.Ø(4)	-1.3(5)	6.2(3)
C11	4.7(4)	5.1(4)	4.3(4)	Ø.6(4)	1.2(4)	1.4(4)	4.7(2)
C12	5.3(5)	5.5(5)	3.6(4)	-1.2(4)	-Ø.3(4)	1.3(4)	4.8(2)
C13	3.7(4)	6.8(5)	4.2(4)	Ø.4(4)	Ø.7(4)	1.4(4)	4.9(2)
C14	5.7(4)	4.7(5)	3.4(4)	Ø.2(4)	Ø.9(4)	Ø.3(4)	4.6(2)
C15	3.9(4)	6.1(5)	3.7(4)	-Ø.6(4)	-Ø.4(3)	1.8(4)	4.6(2)
C16	7.3(6)	7.1(6)	9.5(7)	2.3(5)	Ø.4(6)	4.6(5)	8.Ø(3)
C17	1Ø.8(7)	1Ø.1(7)	5.6(6)	-5.1(6)	Ø.5(6)	1.5(6)	8.8(3)
C18	4.6(5)	12.Ø(8)	7.1(6)	Ø.2(6)	1.8(5)	2.3(7)	7.9(3)
C19	8.4(6)	8.4(7)	5.8(6)	-Ø.7(6)	2.Ø(6)	Ø.3(6)	7.5(3)

Table Va.

Table of General Temperature Factor Expressions - B's (Continued)

Name	B(1,1)	B(2,2)	B(3,3)	B(1,2)	B(1,3)	B(2,3)	Beqv
C2Ø	6.6(6)	12.9(9)	5.7(7)	-1.8(7)	-1.8(5)	1.4(7)	8.4(4)
C21	8.7(7)	9.3(8)	6.9(7)	-2.4(6)	2.2(5)	-Ø.4(6)	8.3(4)
C22	6.3(5)	7.6(7)	7.9(7)	-1.7(5)	1.4(5)	-Ø.6(6)	7.3(3)
C23	6.1(6)	1Ø.7(9)	13.6(9)	-1.5(6)	-1.Ø(7)	-4.1(7)	1Ø.1(4)
C24	9.7(7)	9.6(7)	1Ø.2(8)	-3.1(7)	-3.2(7)	-1.4(7)	9.8(4)
C31	12.6(9)	8.3(7)	15(1)	Ø.5(8)	3.2(9)	4.6(8)	11.8(5)
C32	6.4(7)	16(1)	33(2)	3.4(7)	1(1)	13(1)	18.2(6)
C33	9.2(7)	16(1)	25(2)	7.3(7)	1(1)	7(1)	16.9(7)
C34	15.3(9)	19(1)	1Ø.Ø(9)	11.3(8)	4.6(8)	3(1)	14.8(5)

The form of the anisotropic thermal parameter is:

$\exp[-Ø.25(h^2 a^{*2} B(1,1) + k^2 b^{*2} B(2,2) + l^2 c^{*2} B(3,3)' + 2hka^*b^*B(1,2) + 2hla^*c^*B(1,3)$

$+ 2klb^*c^*B(2,3))]$, where a*,b*, and c* are reciprocal lattice constants.

Table Va. (cont.)

Table VI. $\{[(Me_3Si)_2N]_2Yb\}_2$

Table of Positional Parameters and Their Estimated Standard Deviations

Atom	x	y	z	$B(A^2)$
YB1	Ø.14117(2)	Ø.45535(2)	Ø.29Ø97(1)	2.433(5)
YB2	Ø.3Ø5Ø2(2)	Ø.24259(2)	Ø.21182(1)	2.16Ø(4)
SI1	Ø.5813(1)	Ø.118Ø(1)	Ø.Ø9814(6)	2.73(3)
SI2	Ø.3242(1)	Ø.Ø262(1)	Ø.16153(6)	2.58(3)
SI3	Ø.4738(1)	Ø.1628(1)	Ø.34924(6)	2.71(3)
SI4	Ø.14ØØ(1)	Ø.2Ø62(1)	Ø.38473(6)	2.5Ø(3)
SI5	-Ø.ØØ81(1)	Ø.4548(1)	Ø.14431(6)	2.41(3)
SI6	Ø.2631(1)	Ø.5491(1)	Ø.13953(6)	2.59(3)
SI7	-Ø.Ø357(2)	Ø.6961(1)	Ø.32175(6)	2.76(3)
SI8	Ø.2925(2)	Ø.5973(1)	Ø.38376(7)	3.73(3)
N1	Ø.4333(4)	Ø.1178(3)	Ø.1516(2)	2.37(8)
N2	Ø.2754(4)	Ø.24Ø2(3)	Ø.3293(2)	2.13(8)
N3	Ø.1597(4)	Ø.4571(3)	Ø.1793(2)	2.ØØ(8)
N4	Ø.1518(4)	Ø.6Ø11(3)	Ø.3332(2)	2.62(9)
C1	Ø.7156(6)	Ø.1947(6)	Ø.1158(3)	6.1(2)
C2	Ø.7141(7)	-Ø.Ø3Ø9(5)	Ø.Ø971(3)	5.1(2)
C3	Ø.5ØØ7(6)	Ø.1961(5)	Ø.Ø152(2)	3.9(1)
C4	Ø.2263(6)	Ø.Ø262(4)	Ø.ØØ88(2)	3.9(1)
C5	Ø.1568(5)	Ø.Ø763(4)	Ø.2153(2)	3.4(1)
C6	Ø.43ØØ(6)	-Ø.13Ø4(4)	Ø.2Ø4Ø(3)	4.4(1)
C7	Ø.516Ø(6)	Ø.ØØØ6(5)	Ø.3713(3)	4.5(1)
C8	Ø.5952(5)	Ø.192Ø(5)	Ø.2771(3)	4.4(1)
C9	Ø.5633(6)	Ø.1998(5)	Ø.4125(3)	4.6(1)
C1Ø	Ø.2159(6)	Ø.1496(5)	Ø.4692(2)	4.3(1)
C11	-Ø.Ø321(6)	Ø.3426(4)	Ø.384Ø(2)	3.6(1)
C12	Ø.Ø493(6)	Ø.Ø983(4)	Ø.3725(2)	3.6(1)
C13	-Ø.1183(5)	Ø.38Ø9(4)	Ø.2Ø85(2)	3.2(1)
C14	Ø.Ø47Ø(6)	Ø.3677(4)	Ø.ØØ49(2)	3.5(1)
C15	-Ø.1537(6)	Ø.5973(4)	Ø.1Ø21(2)	3.8(1)
C16	Ø.1541(7)	Ø.7Ø53(5)	Ø.1234(5)	8.7(3)
C17	Ø.339Ø(9)	Ø.5214(6)	Ø.ØØ39(3)	11.9(2)
C18	Ø.4318(7)	Ø.53Ø8(6)	Ø.19Ø1(4)	1Ø.9(2)
C19	-Ø.1488(6)	Ø.6519(4)	Ø.2685(3)	3.7(1)
C2Ø	-Ø.1516(7)	Ø.6955(5)	Ø.3943(3)	5.3(2)
C21	-Ø.Ø548(6)	Ø.8523(4)	Ø.28Ø1(3)	4.4(1)
C22	Ø.2746(8)	Ø.7427(5)	Ø.3959(3)	7.5(2)
C23	Ø.4985(6)	Ø.5436(6)	Ø.3532(3)	6.Ø(2)
C24	Ø.2852(7)	Ø.4965(6)	Ø.4637(3)	6.4(2)

Anisotropically refined atoms are given in the form of the isotropic equivalent thermal parameter defined as:

$(4/3) * [a^2*B(1,1) + b^2*B(2,2) + c^2*B(3,3) + ab(\cos\ gamma)*B(1,2)$

$+ ac(\cos\ beta)*B(1,3) + bc(\cos\ alpha)*B(2,3)]$

Table of Positional Parameters and Their Estimated Standard Deviations (cont.)

Atom	x	y	z	B(Å^2)
H11	0.7970	0.1923	0.0859	7.2**
H12	0.6563	0.2720	0.1144	7.2**
H13	0.7634	0.1541	0.1574	7.2**
H21	0.7929	-0.0245	0.0666	6.0**
H22	0.7640	-0.0717	0.1379	6.0**
H23	0.6522	-0.0735	0.0866	6.0**
H31	0.5861	0.1940	-0.0125	5.0**
H32	0.4334	0.1584	0.0041	5.0**
H33	0.4408	0.2747	0.0133	5.0**
H41	0.1691	-0.0279	0.0997	5.0**
H42	0.1561	0.1023	0.0701	5.0**
H43	0.3060	0.0043	0.0596	5.0**
H51	0.0915	0.0276	0.2222	5.0**
H52	0.2004	0.0725	0.2545	5.0**
H53	0.0942	0.1550	0.1955	5.0**
H61	0.3607	-0.1747	0.2070	5.5**
H62	0.5205	-0.1595	0.1802	5.5**
H63	0.4651	-0.1351	0.2447	5.5**
H71	0.6269	-0.0370	0.3816	5.4**
H72	0.4563	-0.0218	0.4067	5.4**
H73	0.4882	-0.0206	0.3364	5.4**
H81	0.7045	0.1496	0.2879	5.3**
H82	0.5608	0.1675	0.2448	5.3**
H83	0.5815	0.2731	0.2628	5.3**
H91	0.6719	0.1523	0.4201	5.5**
H92	0.5559	0.2794	0.3996	5.5**
H93	0.5071	0.1841	0.4506	5.5**
H101	0.1344	0.1328	0.4961	5.3**
H102	0.3043	0.0792	0.4739	5.3**
H103	0.2504	0.2058	0.4803	5.3**
H111	-0.1060	0.3237	0.4144	5.0**
H112	0.0071	0.3983	0.3938	5.0**
H113	-0.0826	0.3747	0.3429	5.0**
H121	-0.0228	0.0850	0.4052	5.0**
H122	-0.0053	0.1277	0.3326	5.0**
H123	0.1314	0.0265	0.3740	5.0**
H131	-0.2122	0.3786	0.1907	5.0**
H132	-0.0527	0.3039	0.2280	5.0**
H133	-0.1476	0.4239	0.2392	5.0**
H141	-0.0466	0.3675	0.0663	5.0**
H142	0.1079	0.4016	0.0528	5.0**
H143	0.1091	0.2895	0.1055	5.0**
H151	-0.2400	0.5835	0.0854	5.0**
H152	-0.1928	0.6426	0.1313	5.0**

Table VI. (cont.)

Table VI. (cont.)

Table of Positional Parameters and Their Estimated Standard Deviations (cont.)

Atom	x	y	z	B(Å^2)
H153	-Ø.1Ø31	Ø.6376	Ø.Ø689	5.Ø**
H161	Ø.2172	Ø.7512	Ø.1Ø14	9.5**
H162	Ø.Ø588	Ø.7253	Ø.Ø981	9.5**
H163	Ø.1221	Ø.7258	Ø.1623	9.5**
H171	Ø.3956	Ø.5736	Ø.Ø432	12.1**
H172	Ø.4Ø99	Ø.4427	Ø.Ø7Ø9	12.1**
H173	Ø.253Ø	Ø.5311	Ø.Ø362	12.1**
H181	Ø.4925	Ø.58Ø7	Ø.17Ø3	1Ø.9**
H182	Ø.3953	Ø.5493	Ø.2297	1Ø.9**
H183	Ø.5Ø22	Ø.4515	Ø.2Ø13	1Ø.9**
H191	-Ø.2549	Ø.7Ø43	Ø.2616	5.Ø**
H192	-Ø.Ø981	Ø.6538	Ø.2294	5.Ø**
H193	-Ø.1513	Ø.5747	Ø.2884	5.Ø**
H2Ø1	-Ø.2555	Ø.7511	Ø.3834	6.2**
H2Ø2	-Ø.1614	Ø.6199	Ø.4119	6.2**
H2Ø3	-Ø.1ØØØ	Ø.7154	Ø.4236	6.2**
H211	-Ø.1656	Ø.8982	Ø.2763	5.3**
H212	-Ø.ØØØ1	Ø.881Ø	Ø.3Ø43	5.3**
H213	-Ø.Ø13Ø	Ø.8576	Ø.2394	5.3**
H221	Ø.3569	Ø.7332	Ø.4248	8.4**
H222	Ø.2836	Ø.7952	Ø.3567	8.4**
H223	Ø.1738	Ø.7727	Ø.4131	8.4**
H231	Ø.5761	Ø.5422	Ø.382Ø	7.1**
H232	Ø.5186	Ø.4669	Ø.3492	7.1**
H233	Ø.5Ø7Ø	Ø.5945	Ø.3129	7.1**
H241	Ø.3652	Ø.496Ø	Ø.4913	7.4**
H242	Ø.1838	Ø.5225	Ø.48Ø9	7.4**
H243	Ø.3Ø49	Ø.4197	Ø.46Ø2	7.4**

** -- Atoms included but not refined.

Table of General Temperature Factor Expressions - B's

Name	B(1,1)	B(2,2)	B(3,3)	B(1,2)	B(1,3)	B(2,3)	Beqv
YB1	3.185(8)	1.796(7)	1.895(7)	-Ø.117(6)	Ø.Ø47(7)	-Ø.627(6)	2.433(5)
YB2	2.532(7)	1.8ØØ(7)	1.926(7)	-Ø.262(5)	Ø.121(6)	-Ø.673(6)	2.16Ø(4)
SI1	2.29(4)	3.58(5)	2.58(5)	-Ø.82(4)	Ø.44(4)	-1.46(4)	2.73(3)
SI2	2.89(5)	1.98(4)	3.ØØ(5)	-Ø.67(3)	Ø.Ø4(4)	-Ø.99(4)	2.58(3)
SI3	2.42(5)	2.77(5)	2.6Ø(5)	-Ø.13(4)	-Ø.59(4)	-Ø.88(4)	2.71(3)
SI4	2.8Ø(5)	2.32(5)	2.Ø3(5)	-Ø.49(4)	Ø.32(4)	-Ø.49(4)	2.5Ø(3)
SI5	2.39(4)	2.4Ø(4)	2.2Ø(5)	-Ø.53(3)	-Ø.4Ø(4)	-Ø.46(4)	2.41(3)
SI6	2.75(5)	2.44(5)	2.57(5)	-Ø.87(4)	Ø.81(4)	-Ø.74(4)	2.59(3)
SI7	3.41(5)	1.9Ø(4)	2.92(5)	-Ø.75(4)	Ø.97(4)	-Ø.87(4)	2.76(3)
SI8	4.52(5)	3.9Ø(5)	3.36(6)	-2.33(4)	-Ø.47(5)	-Ø.65(4)	3.73(3)
N1	2.2(1)	2.5(1)	2.5(1)	-Ø.6(1)	Ø.3(1)	-1.3(1)	2.37(8)
N2	2.4(1)	1.9(1)	1.8(1)	-Ø.4(1)	Ø.Ø(1)	-Ø.5(1)	2.13(8)
N3	2.3(1)	1.9(1)	1.5(1)	-Ø.4(1)	-Ø.Ø(1)	-Ø.3(1)	2.ØØ(8)
N4	2.7(1)	2.4(1)	2.8(2)	-Ø.8(1)	Ø.2(1)	-Ø.8(1)	2.62(9)
C1	5.1(2)	11.1(3)	4.9(2)	-5.3(2)	2.7(2)	-4.3(2)	6.1(2)
C2	4.Ø(3)	5.5(3)	4.2(2)	Ø.9(2)	Ø.7(2)	-1.8(2)	5.1(2)
C3	4.3(2)	4.4(2)	2.8(2)	-1.5(2)	Ø.5(2)	-Ø.9(2)	3.9(1)
C4	4.3(2)	4.Ø(2)	4.5(2)	-1.8(1)	-Ø.2(2)	-2.1(2)	3.9(1)
C5	3.5(2)	2.9(2)	3.8(2)	-1.3(1)	Ø.8(2)	-Ø.8(2)	3.4(1)
C6	4.3(2)	2.8(2)	6.1(3)	-1.3(2)	-Ø.4(2)	-Ø.9(2)	4.4(1)
C7	4.4(2)	3.1(2)	4.9(3)	Ø.4(2)	-Ø.9(2)	-1.2(2)	4.5(1)
C8	2.Ø(2)	6.4(3)	4.9(3)	-1.4(2)	-Ø.Ø(2)	-1.7(2)	4.4(1)

Table VIa.

Table of General Temperature Factor Expressions - B's (Continued)

Name	B(1,1)	B(2,2)	B(3,3)	B(1,2)	B(1,3)	B(2,3)	Beqv
C9	3.7(2)	5.4(2)	4.6(2)	-1.Ø(2)	-1.1(2)	-1.7(2)	4.6(1)
C1Ø	5.1(2)	4.9(2)	2.4(2)	-1.Ø(2)	Ø.4(2)	-Ø.9(2)	4.3(1)
C11	3.2(2)	3.5(2)	3.6(2)	-Ø.6(2)	1.2(2)	-Ø.9(2)	3.6(1)
C12	4.1(2)	3.4(2)	3.7(2)	-1.9(1)	1.4(2)	-Ø.9(2)	3.6(1)
C13	3.Ø(2)	3.6(2)	3.7(2)	-1.6(1)	Ø.5(2)	-1.4(2)	3.2(1)
C14	4.3(2)	3.4(2)	2.9(2)	-1.3(1)	-Ø.7(2)	-Ø.7(2)	3.5(1)
C15	3.7(2)	3.7(2)	3.4(2)	-Ø.2(2)	-Ø.9(2)	-Ø.7(2)	3.8(1)
C16	4.8(3)	3.3(2)	17.Ø(7)	-2.Ø(2)	2.1(4)	-Ø.6(4)	8.7(3)
C17	2Ø.9(4)	13.1(3)	1Ø.4(3)	-14.(2)	12.3(3)	-9.Ø(2)	11.9(2)
C18	7.6(2)	1Ø.8(4)	13.1(6)	-7.2(2)	-5.5(3)	4.5(4)	1Ø.9(2)
C19	2.9(2)	2.9(2)	4.8(3)	-Ø.4(2)	-Ø.1(2)	-Ø.8(2)	3.7(1)
C2Ø	7.2(3)	3.6(2)	5.1(3)	-1.5(2)	2.8(2)	-2.Ø(2)	5.3(2)
C21	5.7(2)	2.7(2)	4.9(3)	-1.7(2)	Ø.8(2)	-Ø.8(2)	4.4(1)
C22	1Ø.2(3)	6.Ø(2)	8.Ø(3)	-3.9(2)	-2.7(3)	-2.4(2)	7.5(2)
C23	4.Ø(2)	7.7(3)	5.9(3)	-2.8(2)	-Ø.9(2)	Ø.2(3)	6.Ø(2)
C24	7.6(3)	8.5(3)	3.6(3)	-4.3(2)	-1.3(2)	Ø.1(2)	6.4(2)

The form of the anisotropic thermal parameter is:

$\exp[-Ø.25(h^2 a^{*2} B(1,1) + k^2 b^{*2} B(2,2) + l^2 c^{*2} B(3,3) + 2hka^*b^*B(1,2) + 2hla^*c^*B(1,3) + 2klb^*c^*B(2,3))]$, where a*,b*, and c* are reciprocal lattice constants.

Table VIa. (cont.)

Table VII. $(C_5Me_5)Yb[N(SiMe_3)_2]_2$

Table of Positional Parameters and Their Estimated Standard Deviations

Atom	x	y	z	$B(A^2)$
YB1	Ø.ØØ342(1)	Ø.Ø7913(1)	Ø.1ØØ13(2)	1.664(6)
SI1	-Ø.11472(9)	-Ø.Ø891(1)	Ø.Ø953(1)	1.74(3)
SI2	-Ø.16492(9)	Ø.Ø476(1)	-Ø.Ø446(1)	1.8Ø(3)
N1	-Ø.Ø977(3)	-Ø.Ø157(2)	Ø.ØØ91(3)	1.5(1)
C11	-Ø.Ø914(4)	-Ø.Ø467(4)	Ø.2161(4)	2.8(1)
C12	-Ø.Ø451(4)	-Ø.18Ø2(4)	Ø.Ø773(4)	2.4(1)
C13	-Ø.2155(4)	-Ø.1333(4)	Ø.1Ø63(5)	2.9(1)
C21	-Ø.1728(4)	Ø.15ØØ(4)	Ø.Ø183(5)	2.8(1)
C22	-Ø.1334(4)	Ø.Ø722(4)	-Ø.1677(4)	3.Ø(1)
C23	-Ø.2675(3)	Ø.ØØ64(4)	-Ø.Ø542(5)	3.2(2)
C3Ø	Ø.Ø2Ø2(3)	Ø.1314(4)	Ø.2847(4)	2.2(1)
C31	Ø.Ø919(3)	Ø.1511(4)	Ø.243Ø(4)	2.3(1)
C32	Ø.ØØØ6(3)	Ø.215Ø(4)	Ø.1756(4)	2.3(1)
C33	-Ø.ØØØ8(3)	Ø.2354(4)	Ø.1757(4)	2.Ø(1)
C34	-Ø.Ø379(4)	Ø.1828(3)	Ø.245Ø(4)	1.9(1)
C35	Ø.ØØ9Ø(4)	Ø.Ø767(4)	Ø.3717(6)	3.4(2)
C36	Ø.1716(4)	Ø.1235(4)	Ø.2773(5)	4.3(2)
C37	Ø.1443(4)	Ø.2611(4)	Ø.1254(5)	3.7(2)
C38	-Ø.Ø385(4)	Ø.3Ø63(4)	Ø.1243(5)	3.1(1)
C39	-Ø.1215(3)	Ø.19Ø8(4)	Ø.2787(5)	2.8(1)

Anisotropically refined atoms are given in the form of the isotropic equivalent thermal parameter defined as:

$$(4/3) * [a^2*B(1,1) + b^2*B(2,2) + c^2*B(3,3) + ab(\cos\ \text{gamma})*B(1,2) + ac(\cos\ \text{beta})*B(1,3) + bc(\cos\ \text{alpha})*B(2,3)]$$

Table VII. (cont.)

Table of Positional Parameters and Their Estimated Standard Deviations (cont.)

Atom	x	y	z	B(Å^2)
C100	0.0308	0.1831	0.2248	4.0**
H111	-0.0997	-0.0872	0.2650	4.0**
H112	-0.0358	-0.0306	0.2202	4.0**
H113	-0.1210	0.0021	0.2308	4.0**
H121	-0.0886	-0.1982	0.0382	3.3**
H122	-0.0652	-0.1646	0.1375	3.3**
H123	-0.0108	-0.2272	0.0852	3.3**
H131	-0.2157	-0.1739	0.1576	4.0**
H132	-0.2517	-0.0912	0.1200	4.0**
H133	-0.2291	-0.1617	0.0496	4.0**
H211	-0.2108	0.1856	-0.0112	4.0**
H212	-0.1891	0.1419	0.0834	4.0**
H213	-0.1236	0.1786	0.0193	4.0**
H221	-0.1714	0.1091	-0.1974	4.0**
H222	-0.0841	0.1020	-0.1668	4.0**
H223	-0.1282	0.0240	-0.2046	4.0**
H231	-0.3016	0.0452	-0.0851	4.0**
H232	-0.2688	-0.0451	-0.0899	4.0**
H233	-0.2891	-0.0055	0.0075	4.0**
H351	0.0193	0.1093	0.4270	4.6**
H352	-0.0417	0.0557	0.3726	4.6**
H353	0.0466	0.0322	0.3691	4.6**
H361	0.1912	0.1565	0.3266	5.2**
H362	0.1723	0.0655	0.2964	5.2**
H363	0.2096	0.1270	0.2242	5.2**
H371	0.1643	0.3062	0.1617	4.6**
H372	0.1880	0.2237	0.1116	4.6**
H373	0.1268	0.2826	0.0650	4.6**
H381	-0.0362	0.3571	0.1618	4.0**
H382	-0.0159	0.3162	0.0651	4.0**
H383	-0.0945	0.2948	0.1153	4.0**
H391	-0.1238	0.2303	0.3311	3.6**
H392	-0.1547	0.2100	0.2303	3.6**
H393	-0.1402	0.1384	0.3023	3.6**

** -- Atoms included but not refined.

Table of General Temperature Factor Expressions - B's

Name	B(1,1)	B(2,2)	B(3,3)	B(1,2)	B(1,3)	B(2,3)	Beqv
YB1	1.7Ø(1)	1.63(1)	1.67(1)	-Ø.254(9)	Ø.16(1)	-Ø.526(9)	1.664(6)
SI1	2.Ø7(6)	1.5Ø(6)	1.66(7)	-Ø.Ø7(6)	Ø.16(6)	Ø.1Ø(6)	1.74(3)
SI2	1.79(6)	1.75(6)	1.85(7)	Ø.14(6)	-Ø.37(6)	Ø.Ø5(6)	1.8Ø(3)
N1	1.5(2)	1.3(2)	1.6(2)	-Ø.1(2)	Ø.1(2)	Ø.3(2)	1.5(1)
C11	4.6(3)	1.7(2)	2.2(3)	Ø.2(3)	Ø.5(3)	Ø.1(2)	2.8(1)
C12	3.1(3)	2.2(3)	2.Ø(3)	Ø.7(2)	-Ø.5(2)	-Ø.3(2)	2.4(1)
C13	2.9(3)	2.6(3)	3.2(3)	-Ø.8(2)	1.Ø(3)	Ø.4(3)	2.9(1)
C21	2.5(3)	2.4(3)	3.4(3)	Ø.8(2)	-Ø.3(3)	-Ø.2(3)	2.8(1)
C22	4.4(3)	2.4(3)	2.1(3)	-Ø.1(3)	-Ø.4(3)	Ø.Ø(3)	3.Ø(1)
C23	2.3(3)	3.2(3)	4.1(3)	-Ø.3(3)	-1.1(3)	Ø.4(3)	3.2(2)
C3Ø	3.2(3)	1.7(3)	1.7(3)	-Ø.2(2)	-Ø.4(2)	-Ø.6(2)	2.2(1)
C31	1.5(2)	2.7(2)	2.6(3)	-Ø.1(2)	-Ø.2(2)	-1.7(2)	2.3(1)
C32	2.3(2)	2.2(2)	2.4(3)	-1.1(2)	Ø.6(2)	-1.5(2)	2.3(1)
C33	2.4(2)	1.9(2)	1.9(2)	-Ø.4(2)	-Ø.3(2)	-Ø.4(2)	2.Ø(1)
C34	2.2(2)	1.8(2)	1.8(3)	-Ø.2(2)	-Ø.2(2)	-Ø.6(2)	1.9(1)
C35	4.7(4)	3.Ø(3)	2.5(3)	-Ø.3(3)	-1.4(3)	-Ø.6(2)	3.4(2)
C36	3.1(3)	3.8(3)	6.1(4)	Ø.9(3)	-1.8(3)	-2.7(3)	4.3(2)
C37	3.9(3)	4.Ø(3)	3.2(3)	-1.8(3)	1.3(3)	-1.7(3)	3.7(2)

Table VIIa.

Table VIIa. (cont.)

Table of General Temperature Factor Expressions - B's (Continued)

Name	B(1,1)	B(2,2)	B(3,3)	B(1,2)	B(1,3)	B(2,3)	Beqv
C38	4.6(3)	1.8(3)	3.Ø(3)	-Ø.3(3)	-Ø.2(3)	-Ø.4(3)	3.1(1)
C39	2.1(2)	3.Ø(3)	3.4(3)	-Ø.2(2)	Ø.8(2)	-1.Ø(3)	2.8(1)

The form of the anisotropic thermal parameter is:

$$\exp[-Ø.25(h^2 a^{*2} B(1,1) + k^2 b^{*2} B(2,2) + l^2 c^{*2} B(3,3) + 2hka^*b^*B(1,2) + 2hla^*c^*B(1,3) + 2klb^*c^*B(2,3))]$$

, where a*,b*, and c* are reciprocal lattice constants.

Table VIII. $[(Me_3Si)_2N]_2Yb(AlMe_3)_2$

Table of Positional Parameters and Their Estimated Standard Deviations

Atom	x	y	z	$B(A^2)$
YB1	Ø.19426(1)	Ø.31799(1)	Ø.21184(1)	2.Ø22(3)
SI1	Ø.48996(8)	Ø.31Ø51(6)	Ø.32464(6)	2.Ø7(2)
SI2	Ø.24218(8)	Ø.2228Ø(6)	Ø.ØØØ1Ø(6)	2.13(2)
SI3	Ø.25322(8)	Ø.Ø1849(6)	Ø.2Ø474(6)	2.21(2)
SI4	Ø.26263(8)	Ø.27Ø76(6)	Ø.5Ø3Ø4(6)	2.13(2)
AL1	Ø.24712(9)	Ø.49111(6)	Ø.29736(7)	2.2Ø(2)
AL2	-Ø.ØØ36Ø(8)	Ø.18Ø55(6)	Ø.18Ø44(6)	2.Ø2(2)
N1	Ø.3164(2)	Ø.3342(2)	Ø.3621(2)	1.72(5)
N2	Ø.191Ø(2)	Ø.1577(2)	Ø.14Ø9(2)	1.82(5)
C1	Ø.3268(4)	Ø.5539(3)	Ø.14Ø1(3)	3.59(8)
C2	Ø.Ø489(3)	Ø.4839(2)	Ø.2746(3)	3.12(7)
C3	Ø.2727(4)	Ø.5861(3)	Ø.3794(3)	3.5Ø(7)
C4	-Ø.1276(3)	Ø.ØØØØ(3)	Ø.1631(3)	3.48(8)
C5	-Ø.Ø596(3)	Ø.34Ø1(3)	Ø.Ø927(2)	2.94(7)
C6	-Ø.Ø1Ø8(3)	Ø.1822(2)	Ø.335Ø(2)	2.73(7)
C11	Ø.5683(3)	Ø.1735(3)	Ø.4121(3)	3.11(7)
C12	Ø.5Ø76(3)	Ø.3Ø53(2)	Ø.1823(2)	2.82(7)
C13	Ø.5996(3)	Ø.4192(3)	Ø.3258(3)	3.2Ø(7)
C21	Ø.2557(3)	Ø.3768(2)	-Ø.Ø354(2)	2.89(7)
C22	Ø.4171(4)	Ø.1767(3)	-Ø.Ø441(3)	3.55(8)
C23	Ø.122Ø(4)	Ø.2Ø48(3)	-Ø.Ø9Ø8(2)	3.21(7)
C31	Ø.4372(3)	Ø.ØØ7Ø(3)	Ø.2299(3)	3.47(8)
C32	Ø.1637(4)	-Ø.Ø525(3)	Ø.3435(3)	3.5Ø(8)
C33	Ø.2285(3)	-Ø.Ø676(2)	Ø.1228(3)	3.21(7)
C41	Ø.Ø86Ø(3)	Ø.32Ø1(3)	Ø.5381(2)	3.41(8)
C42	Ø.3744(4)	Ø.3Ø17(3)	Ø.5926(2)	3.34(7)
C43	Ø.26Ø2(3)	Ø.1162(3)	Ø.5461(3)	3.13(7)

Anisotropically refined atoms are given in the form of the isotropic equivalent thermal parameter defined as:

$$(4/3) * [a^2*B(1,1) + b^2*B(2,2) + c^2*B(3,3) + ab(\cos\ gamma)*B(1,2) + ac(\cos\ beta)*B(1,3) + bc(\cos\ alpha)*B(2,3)]$$

Table VIII. (cont.)

Table of Positional Parameters and Their Estimated Standard Deviations (cont.)

Atom	x	y	z	B(Å^2)
H1	0.0000	0.5430	0.2930	4.0**
H2	0.0000	0.4160	0.3125	4.0**
H3	0.0293	0.5000	0.2090	4.0**
H4	-0.0820	0.2500	0.3555	3.7**
H5	-0.0547	0.1250	0.3750	3.7**
H6	0.0547	0.1875	0.3750	3.7**
H11	0.2947	0.6294	0.1075	4.6**
H12	0.4239	0.5497	0.1383	4.6**
H13	0.3004	0.5118	0.1007	4.6**
H31	0.2363	0.6595	0.3417	4.5**
H32	0.2272	0.5568	0.4512	4.5**
H33	0.3677	0.5880	0.3847	4.5**
H41	-0.2188	0.0996	0.1848	4.5**
H42	-0.1208	0.0869	0.0880	4.5**
H43	-0.1034	0.0054	0.2079	4.5**
H51	-0.1542	0.3538	0.1102	3.9**
H52	-0.0081	0.3884	0.1105	3.9**
H53	-0.0431	0.3532	0.0162	3.9**
H111	0.6615	0.1670	0.3868	4.1**
H112	0.5613	0.1690	0.4867	4.1**
H113	0.5211	0.1148	0.4079	4.1**
H121	0.6017	0.2924	0.1613	3.8**
H122	0.4575	0.2465	0.1822	3.8**
H123	0.4741	0.3742	0.1316	3.8**
H131	0.6919	0.4017	0.3048	4.2**
H132	0.5702	0.4898	0.2752	4.2**
H133	0.5928	0.4212	0.3979	4.2**
H211	0.2835	0.4110	-0.1117	3.9**
H212	0.1695	0.4091	-0.0189	3.9**
H213	0.3214	0.3875	0.0067	3.9**
H221	0.4369	0.2159	-0.1211	4.6**
H222	0.4823	0.1928	-0.0049	4.6**
H223	0.4213	0.0991	-0.0291	4.6**
H231	0.1542	0.2414	-0.1657	4.2**
H232	0.1164	0.1275	-0.0758	4.2**
H233	0.0339	0.2362	-0.0766	4.2**
H311	0.4657	-0.0694	0.2644	4.4**
H312	0.4904	0.0384	0.1616	4.4**
H313	0.4489	0.0460	0.2766	4.4**
H321	0.2005	-0.1269	0.3742	4.5**
H322	0.1751	-0.0134	0.3902	4.5**
H323	0.0688	-0.0530	0.3365	4.5**

Table of Positional Parameters and Their Estimated Standard Deviations (cont.)

Atom	x	y	z	B(Å^2)
H331	0.2629	-0.1420	0.1595	4.2**
H332	0.1338	-0.0673	0.1156	4.2**
H333	0.2760	-0.0374	0.0518	4.2**
H411	0.0613	0.2837	0.6145	4.4**
H412	0.0827	0.3984	0.5202	4.4**
H413	0.0244	0.3032	0.4967	4.4**
H421	0.3423	0.2664	0.6677	4.3**
H422	0.4656	0.2749	0.5802	4.3**
H423	0.3722	0.3803	0.5745	4.3**
H431	0.2773	0.0820	0.5000	4.1**
H432	0.3249	0.0847	0.5994	4.1**
H433	0.1710	0.0967	0.5805	4.1**

** -- Atoms included but not refined.

Table VIII. (cont.)

Table of General Temperature Factor Expressions - B's

Name	B(1,1)	B(2,2)	B(3,3)	B(1,2)	B(1,3)	B(2,3)	Beqv
YB1	1.969(5)	2.100(5)	2.322(5)	0.021(4)	-0.555(4)	-1.106(3)	2.022(3)
SI1	1.66(3)	2.46(3)	2.09(3)	-0.09(2)	-0.30(2)	-0.82(2)	2.07(2)
SI2	2.34(3)	2.28(3)	1.66(2)	-0.00(2)	-0.11(2)	-0.66(2)	2.13(2)
SI3	2.59(3)	1.79(3)	2.29(3)	0.06(2)	-0.60(2)	-0.72(2)	2.21(2)
SI4	2.19(3)	2.41(3)	1.77(3)	-0.21(2)	-0.20(2)	-0.72(2)	2.13(2)
AL1	2.52(3)	1.79(3)	2.47(3)	0.08(3)	-0.71(3)	-0.87(2)	2.20(2)
AL2	1.83(3)	2.34(3)	2.01(3)	-0.28(3)	-0.21(3)	-0.89(2)	2.02(2)
N1	1.66(8)	1.76(7)	1.81(7)	-0.07(7)	-0.23(7)	-0.71(6)	1.72(5)
N2	1.79(9)	1.94(8)	1.70(7)	-0.10(7)	-0.19(7)	-0.62(6)	1.82(5)
C1	4.4(2)	2.8(1)	3.2(1)	0.1(1)	-0.7(1)	-0.5(1)	3.59(8)
C2	3.2(1)	2.6(1)	4.0(1)	0.5(1)	-1.6(1)	-1.54(8)	3.12(7)
C3	3.7(1)	3.1(1)	4.4(1)	-0.1(1)	-0.9(1)	-2.09(9)	3.50(7)
C4	3.1(1)	4.5(1)	3.3(1)	-1.1(1)	-0.4(1)	-1.64(9)	3.48(8)
C5	2.3(1)	3.5(1)	3.1(1)	0.6(1)	-0.7(1)	-1.32(9)	2.94(7)
C6	2.8(1)	3.4(1)	2.1(1)	-0.9(1)	0.09(9)	-1.06(8)	2.73(7)
C11	2.1(1)	3.4(1)	3.6(1)	0.8(1)	-0.8(1)	-1.1(1)	3.11(7)
C12	2.4(1)	3.4(1)	2.7(1)	0.0(1)	0.1(1)	-1.35(8)	2.82(7)
C13	2.6(1)	3.7(1)	3.2(1)	-1.0(1)	-0.1(1)	-1.11(9)	3.20(7)
C21	3.1(1)	2.7(1)	2.4(1)	-0.3(1)	-0.3(1)	-0.27(9)	2.89(7)
C22	3.6(1)	3.9(1)	2.9(1)	0.3(1)	0.4(1)	-1.2(1)	3.55(8)
C23	4.1(1)	3.7(1)	2.1(1)	-0.3(1)	-0.7(1)	-1.21(9)	3.21(7)

Table VIIIa.

Table of General Temperature Factor Expressions - B's (Continued)

Name	B(1,1)	B(2,2)	B(3,3)	B(1,2)	B(1,3)	B(2,3)	Beqv
C31	3.5(1)	2.7(1)	4.3(1)	Ø.7(1)	-1.8(1)	-1.2(1)	3.47(8)
C32	4.7(2)	2.3(1)	2.9(1)	-Ø.3(1)	-Ø.6(1)	-Ø.2(1)	3.5Ø(8)
C33	3.7(1)	2.6(1)	3.7(1)	Ø.Ø(1)	-Ø.7(1)	-1.52(8)	3.21(7)
C41	3.4(1)	4.2(1)	2.7(1)	-Ø.1(1)	Ø.4(1)	-1.55(9)	3.41(8)
C42	3.9(1)	3.9(1)	2.3(1)	-Ø.4(1)	-Ø.7(1)	-1.11(9)	3.34(7)
C43	3.4(1)	2.5(1)	3.Ø(1)	-Ø.3(1)	-Ø.6(1)	-Ø.29(9)	3.13(7)

The form of the anisotropic thermal parameter is:

$$\exp[-Ø.25(h^2 a^{*2} B(1,1) + k^2 b^{*2} B(2,2) + l^2 c^{*2} B(3,3)' + 2hka^*b^*B(1,2) + 2hla^*c^*B(1,3) + 2klb^*c^*B(2,3))]$$, where a*,b*, and c* are reciprocal lattice constants.

Table VIIIa. (cont.)

Table IX. $[(C_5Me_5)_2Yb]_2bipm$

Table of Positional Parameters and Their Estimated Standard Deviations

Atom	x	y	z	B(Å^2)
YB1	Ø.173Ø9(2)	Ø.22394(2)	Ø.Ø7229(1)	2.786(5)
YB2	Ø.46732(3)	Ø.1Ø98Ø(2)	Ø.62872(1)	3.568(6)
N1	-Ø.ØØ35(5)	Ø.1654(4)	Ø.ØØ45(2)	3.1(1)
N2	Ø.1457(5)	Ø.Ø149(4)	Ø.Ø5Ø2(2)	3.2(1)
N3	Ø.5865(6)	Ø.1427(5)	Ø.5414(2)	4.2(1)
N4	Ø.3769(5)	-Ø.Ø476(5)	Ø.5577(2)	3.6(1)
C1	-Ø.Ø749(6)	Ø.2323(5)	-Ø.Ø187(3)	3.8(1)
C2	-Ø.1843(6)	Ø.1872(6)	-Ø.Ø58Ø(3)	4.6(2)
C5	Ø.2776(7)	-Ø.14Ø1(7)	Ø.5637(3)	4.6(2)
C4	-Ø.Ø36Ø(5)	Ø.Ø374(5)	-Ø.Ø113(3)	2.7(1)
C7	Ø.687Ø(7)	Ø.2324(6)	Ø.531Ø(3)	5.Ø(2)
C6	Ø.7614(8)	Ø.2366(7)	Ø.4796(3)	5.5(2)
C3	Ø.2135(6)	-Ø.Ø597(5)	Ø.Ø715(3)	4.Ø(1)
C8	Ø.4482(6)	-Ø.Ø465(5)	Ø.5Ø43(3)	3.4(1)
C1Ø	Ø.2869(7)	Ø.3ØØ8(6)	-Ø.Ø268(3)	4.3(2)
C11	Ø.2982(7)	Ø.4Ø18(6)	Ø.Ø131(4)	5.8(2)
C12	Ø.3863(8)	Ø.3888(8)	Ø.Ø616(4)	7.3(2)
C13	Ø.4198(7)	Ø.2748(8)	Ø.Ø482(4)	5.8(2)
C14	Ø.36Ø9(6)	Ø.2241(6)	-Ø.ØØ46(3)	4.3(2)
C15	Ø.215(1)	Ø.284(1)	-Ø.Ø875(4)	8.6(3)
C16	Ø.243(1)	Ø.5159(8)	Ø.ØØ27(6)	13.2(3)
C17	Ø.452(1)	Ø.496(1)	Ø.1Ø73(5)	15.6(4)
C18	Ø.5173(9)	Ø.222(1)	Ø.Ø867(5)	11.7(3)
C19	Ø.3859(9)	Ø.1Ø78(8)	-Ø.Ø374(5)	8.5(2)
C2Ø	-Ø.Ø198(2)	Ø.2449(2)	Ø.1442(2)	3.2(2)*
C21	Ø.Ø223(2)	Ø.1383(2)	Ø.1592(2)	2.9(2)*
C22	Ø.15Ø5(2)	Ø.175Ø(2)	Ø.1844(2)	3.5(2)*
C23	Ø.187Ø(2)	Ø.3Ø44(2)	Ø.1855(2)	3.8(3)*
C24	Ø.Ø832(2)	Ø.3474(1)	Ø.159Ø(2)	4.Ø(3)*
C25	-Ø.1547(3)	Ø.2496(6)	Ø.1233(3)	6.7(4)*
C26	-Ø.Ø597(5)	Ø.Ø1Ø7(3)	Ø.1546(6)	5.5(3)*
C27	Ø.2249(4)	Ø.Ø931(3)	Ø.2137(2)	6.5(4)*
C28	Ø.3Ø18(3)	Ø.382Ø(5)	Ø.22ØØ(2)	8.Ø(5)*
C29	Ø.Ø737(6)	Ø.4788(2)	Ø.1583(6)	7.2(4)*
C3Ø	Ø.2577(3)	Ø.1886(3)	Ø.58936(8)	5.Ø(3)*
C31	Ø.3638(3)	Ø.2915(2)	Ø.59235(8)	4.4(3)*
C32	Ø.4ØØØ(3)	Ø.3216(2)	Ø.65412(9)	4.6(3)*
C33	Ø.3145(3)	Ø.2385(3)	Ø.68928(7)	4.1(3)*
C34	Ø.2286(2)	Ø.1546(2)	Ø.64917(9)	4.1(3)*
C35	Ø.1768(5)	Ø.1372(7)	Ø.534Ø(1)	5.8(4)*

Table of Positional Parameters and Their Estimated Standard Deviations (cont.)

Atom	x	y	z	B(Å^2)
C36	Ø.4141(8)	Ø.3665(4)	Ø.54Ø3(1)	6.8(4)*
C37	Ø.4991(5)	Ø.4313(3)	Ø.6785(3)	6.5(4)*
C38	Ø.2977(9)	Ø.2534(9)	Ø.7562(1)	6.5(4)*
C39	Ø.1158(4)	Ø.Ø578(4)	Ø.6675(3)	6.3(4)*
C4Ø	Ø.6593(2)	Ø.1159(2)	Ø.71Ø6(1)	4.7(3)*
C41	Ø.5442(2)	Ø.Ø549(2)	Ø.73843(9)	4.Ø(3)*
C42	Ø.4961(2)	-Ø.Ø577(2)	Ø.7Ø5Ø(1)	4.1(3)*
C43	Ø.5854(2)	-Ø.Ø695(2)	Ø.6586(1)	4.4(3)*
C44	Ø.6856(2)	Ø.Ø384(2)	Ø.6616(1)	5.4(3)*
C45	Ø.7484(5)	Ø.2324(3)	Ø.7344(3)	6.8(4)*
C46	Ø.4941(5)	Ø.Ø936(6)	Ø.7978(1)	6.6(4)*
C47	Ø.3802(4)	-Ø.1534(4)	Ø.721Ø(3)	6.7(4)*
C48	Ø.5854(8)	-Ø.1841(3)	Ø.62Ø3(2)	5.7(3)*
C49	Ø.8Ø97(3)	Ø.Ø564(8)	Ø.6269(2)	6.1(4)*
C5Ø	-Ø.1128(3)	Ø.6566(2)	Ø.6Ø83(1)	9.6(6)*
C51	Ø.Ø1Ø7(3)	Ø.4976(2)	Ø.6Ø76(1)	9.4(6)*
C52	Ø.Ø721(3)	Ø.5482(2)	Ø.6622(1)	8.5(5)*
C53	Ø.Ø399(3)	Ø.6523(2)	Ø.69Ø3(1)	8.1(5)*
C54	-Ø.Ø49Ø(3)	Ø.7Ø9Ø(2)	Ø.6622(1)	9.1(6)*
C55	-Ø.Ø831(3)	Ø.55Ø9(2)	Ø.581Ø(1)	7.7(5)*
C2Ø1	Ø.Ø137(2)	Ø.3Ø73(2)	Ø.1457(2)	3.5(2)*
C211	-Ø.Ø153(2)	Ø.1794(2)	Ø.1527(2)	4.3(3)*
C221	Ø.Ø951(2)	Ø.1491(2)	Ø.18Ø2(2)	4.5(3)*
C231	Ø.192Ø(2)	Ø.2583(2)	Ø.19Ø5(2)	3.6(2)*
C241	Ø.1395(2)	Ø.3567(2)	Ø.1715(2)	3.5(2)*
C251	-Ø.Ø793(3)	Ø.38Ø3(3)	Ø.1234(3)	8.6(5)*
C261	-Ø.14Ø7(3)	Ø.Ø912(4)	Ø.1349(4)	7.8(5)*
C271	Ø.1Ø18(7)	Ø.Ø265(2)	Ø.2Ø2Ø(3)	8.2(5)*
C281	Ø.3149(3)	Ø.271Ø(7)	Ø.2276(2)	6.7(4)*
C291	Ø.1926(8)	Ø.4895(2)	Ø.1887(4)	7.3(4)*
C3Ø1	Ø.2628(2)	Ø.1852(3)	Ø.6Ø179(8)	4.1(3)*
C311	Ø.3682(3)	Ø.2715(3)	Ø.57933(7)	4.2(3)*
C321	Ø.4433(2)	Ø.335Ø(2)	Ø.62949(9)	4.3(3)*
C331	Ø.3842(3)	Ø.2879(3)	Ø.68293(7)	4.1(3)*
C341	Ø.2736(2)	Ø.1941(3)	Ø.6658Ø(8)	3.9(3)*
C351	Ø.1527(4)	Ø.1Ø66(5)	Ø.5646(2)	6.3(4)*
C361	Ø.384(1)	Ø.3Ø47(6)	Ø.5149(1)	5.4(3)*
C371	Ø.5552(4)	Ø.4434(3)	Ø.6272(4)	6.2(4)*
C381	Ø.4194(9)	Ø.3418(6)	Ø.7458(1)	5.9(4)*
C391	Ø.1794(4)	Ø.123Ø(5)	Ø.7Ø79(2)	6.5(4)*

Table IX. (cont.)

Table IX. (cont.)

Table of Positional Parameters and Their Estimated Standard Deviations (cont.)

Atom	x	y	z	$B(A^2)$
C401	0.6790(2)	0.1225(2)	0.6896(1)	4.2(3)*
C411	0.5808(3)	0.1073(2)	0.73380(9)	4.2(3)*
C421	0.4991(2)	-0.0108(2)	0.7228(1)	3.8(3)*
C431	0.5485(3)	-0.0694(2)	0.6726(1)	3.9(3)*
C441	0.6609(2)	0.0123(2)	0.6527(1)	4.1(3)*
C451	0.7918(4)	0.2302(3)	0.6877(4)	5.7(3)*
C461	0.5811(9)	0.1898(4)	0.7894(1)	6.4(4)*
C471	0.3871(3)	-0.0682(6)	0.7605(2)	6.3(4)*
C481	0.5031(9)	-0.2007(3)	0.6504(3)	5.7(4)*
C491	0.7490(4)	-0.0146(6)	0.6034(2)	5.5(3)*
C501	0.1381(3)	0.4486(2)	0.6513(1)	11.8(8)*
C511	-0.0280(2)	0.5217(2)	0.5967(1)	8.1(5)*
C521	-0.0220(2)	0.6163(2)	0.64120(9)	10.8(7)*
C531	0.0637(2)	0.6268(2)	0.6909(1)	11.1(7)*
C541	0.1411(3)	0.5408(2)	0.6968(1)	10.7(7)*
C551	0.0514(2)	0.4373(2)	0.6020(1)	12.3(8)*
C561	-0.1012(3)	0.7109(3)	0.6337(2)	15(1)*

* -- Atoms refined with isotropic thermal parameters.

Anisotropically refined atoms are given in the form of the isotropic equivalent thermal parameter defined as:

$$(4/3) * [a^2 * B(1,1) + b^2 * B(2,2) + c^2 * B(3,3) + ab(\cos \text{gamma}) * B(1,2) + ac(\cos \text{beta}) * B(1,3) + bc(\cos \text{alpha}) * B(2,3)]$$

C561	-0.1012(3)	0.7109(3)	0.6337(2)	15(1)*

** -- Atoms included but not refined.

Table of General Temperature Factor Expressions - B's

Name	B(1,1)	B(2,2)	B(3,3)	B(1,2)	B(1,3)	B(2,3)	Beqv
YB1	2.75(1)	2.211(9)	3.29(1)	Ø.355(8)	-Ø.243(9)	Ø.Ø37(9)	2.786(5)
YB2	4.33(1)	3.74(1)	2.47(1)	Ø.56(1)	Ø.Ø2(1)	Ø.Ø2(1)	3.568(6)
N1	3.3(2)	2.3(2)	3.8(2)	Ø.8(2)	-Ø.6(2)	-Ø.1(2)	3.1(1)
N2	3.1(2)	2.4(2)	4.Ø(2)	Ø.8(2)	-Ø.8(2)	-Ø.2(2)	3.2(1)
N3	5.2(3)	4.Ø(2)	2.9(2)	-Ø.2(2)	Ø.4(2)	Ø.Ø(2)	4.2(1)
N4	4.Ø(2)	3.6(2)	2.9(2)	-Ø.1(2)	Ø.2(2)	Ø.4(2)	3.6(1)
C1	4.3(3)	2.6(2)	4.8(3)	1.3(2)	-Ø.8(3)	Ø.1(2)	3.8(1)
C2	4.3(3)	3.6(3)	6.2(4)	1.5(2)	-2.Ø(3)	-Ø.2(3)	4.6(2)
C5	4.6(3)	5.1(3)	3.7(3)	Ø.3(3)	Ø.4(3)	Ø.6(3)	4.6(2)
C4	2.5(2)	2.4(2)	3.2(2)	Ø.5(2)	-Ø.2(2)	-Ø.1(2)	2.7(1)
C7	5.7(4)	3.7(3)	4.2(3)	-1.7(3)	Ø.3(3)	-Ø.6(3)	5.Ø(2)
C6	6.3(4)	5.3(4)	4.Ø(3)	-Ø.6(3)	Ø.4(3)	-Ø.5(3)	5.5(2)
C3	4.2(3)	3.1(2)	4.8(3)	1.3(2)	-1.3(3)	-Ø.1(2)	4.Ø(1)
C8	4.Ø(3)	3.6(3)	2.4(2)	Ø.3(2)	Ø.Ø(2)	Ø.Ø(2)	3.4(1)
C1Ø	3.7(3)	4.3(3)	4.5(3)	Ø.1(2)	Ø.5(3)	Ø.8(3)	4.3(2)
C11	6.7(3)	2.4(2)	8.8(4)	1.1(2)	4.3(3)	1.7(3)	5.8(2)
C12	5.8(4)	8.Ø(5)	5.3(4)	-3.8(4)	2.1(3)	-2.1(3)	7.3(2)
C13	2.8(3)	8.2(4)	6.3(4)	Ø.6(3)	Ø.2(3)	2.2(3)	5.8(2)
C14	4.2(3)	3.4(3)	5.6(3)	1.3(2)	1.2(3)	Ø.5(3)	4.3(2)
C15	7.8(5)	12.4(7)	4.5(4)	-Ø.9(5)	-Ø.6(4)	2.4(4)	8.6(3)

Table IXa.

Table IXa. (cont.)

Table of General Temperature Factor Expressions - B's (Continued)

Name	B(1,1)	B(2,2)	B(3,3)	B(1,2)	B(1,3)	B(2,3)	Beqv
C16	16.7(6)	4.9(3)	2Ø.5(9)	6.6(3)	1Ø.9(6)	5.1(5)	13.2(3)
C17	14.7(7)	15.4(7)	9.6(6)	-1Ø1(5)	6.1(5)	-6.3(6)	15.6(4)
C18	3.9(4)	2Ø.5(9)	11.1(6)	2.1(5)	-1.1(4)	8.Ø(5)	11.7(3)
C19	1Ø.1(5)	4.8(4)	11.2(6)	2.7(3)	5.8(4)	Ø.1(4)	8.5(2)

The form of the anisotropic thermal parameter is:

$$\exp[-Ø.25(h^2 a^{*2} B(1,1) + k^2 b^{*2} B(2,2) + l^2 c^{*2} B(3,3)' + 2hka^*b^*B(1,2) + 2hla^*c^*B(1,3) + 2klb^*c^*B(2,3))]$$, where a*,b*, and c* are reciprocal lattice constants.

TECHNICAL INFORMATION DEPARTMENT
LAWRENCE BERKELEY LABORATORY
UNIVERSITY OF CALIFORNIA
BERKELEY, CALIFORNIA 94720